



Università
Ca'Foscari
Venezia

**Scuola Dottorale di Ateneo
(Graduate School)**

**Research Doctorate in Chemical Sciences
Cycle XXVIII
Academic Year 2015/2016**

Title

**SYNTHESIS AND CHARACTERIZATION OF NOVEL LIGANDS AND
APPLICATION OF THEIR TRANSITION METAL COMPLEXES AS
CATALYSTS OR ANTICANCER AGENTS**

SETTORE SCIENTIFICO DISCIPLINARE DI AFFERENZA: CHIM/04
Ph.D. Thesis of Md. Mahbubul Alam, Matricola 956023

**Ph.D. Coordinator
Prof. Maurizio Selva**

**Ph.D. Supervisor
Prof. Valentina Beghetto**

**Co-Supervisor
Prof. Alberto Scrivanti**

TABLE OF CONTENTS

CHAPTER 1

1 Introduction	1
1.1 Introduction to Pd-catalyzed carbonylation	1
1.1.1 Catalysis: Definition, consideration, and classification	1
1.1.2 Green chemistry	3
1.1.3 Fine chemicals	3
1.1.4 The Agrochemicals	4
1.1.5 The aryloxy-propanoic acids	6
1.1.6 Drent's Catalyst	15
1.2 Innovative aspect of ligand synthesis in homogeneous catalysis	17
1.3 Introduction to triazole ligand synthesis and transition metal complex catalyzed hydrogenation and hydroformylation reactions	25
1.3.1 The triazole: Synthesis and application in pharmaceuticals	25
1.3.2 Click Reaction	30
1.3.3 Synthesis of triazole ligands	30
1.3.4 Biphasic hydrogenation	34
1.3.5 Biphasic hydroformylations	39
1.4 Introduction to anticancer activity of ruthenium triazole complex	42

CHAPTER 2

2. Scope of the Thesis	47
------------------------	----

CHAPTER 3

3. The development of an innovative process for the stereoselective synthesis of agrochemical intermediates	54
3.1 Results and discussion	55
3.1.1 Synthesis of 2-(6-methyl)(diphenylphosphine)pyridine	57
3.1.2 Methoxycarbonylation of (trimethylsilyl)acetylene	58
3.1.3 Hydroxycarbonylation of (trimethylsilyl)acetylene	73
3.2 Experimental section	76
3.2.1 Purification of reagents and solvents	76

3.2.2 Instrumentation used for carbonylation reaction	76
3.2.3 Instrumentation used for analysis	77
3.2.4 Stereoselective synthesis of 2-substituted acrylic derivatives <i>via</i> carbonylation reaction	77
3.3 Conclusion	92
CHAPTER 4	
The synthesis of new water-soluble triazole ligands by click chemistry (CuAAC)	93
4.1 Results and discussion	96
4.1.1 Synthesis and characterization of triazole ligands	96
4.1.2 Synthesis and characterization of ruthenium-triazole complexes	108
4.1.3 Synthesis and characterization of Pd-triazole and Co-triazole complexes	115
4.1.4 Biphasic catalysis: hydrogenations and hydroformylation	119
4.2 Experimental section	131
4.2.1 General methods	131
4.2.2 Synthesis of pyridyl-triazole ligands	131
4.2.3 Synthesis of methyl(thio)ethyl-triazole ligands	143
4.2.4 Synthesis of metal-triazole complexes	157
4.2.5 Biphasic hydrogenation of C=C and C=O double bonds	176
4.2.6 Biphasic hydrofomylation of styrene	179
4.3 Conclusion	181
CHAPTER 5	
Application of ruthenium-pyridyl triazole complexes as antimetastatic and anticancer agent against human cancer cell	182
5.1 Results and discussion	182
5.2 Experimental section	185
5.2.1 Material and Methods	185
5.2.1.1 Experiments with Cultured Human Cells	185
5.2.1.2 Cell Cultures	185
5.2.1.3 MTT Assay	185
5.2.1.4 Tumor cell invasion assays	188

5.3	Conclusion	188
6.0	Acknowledgements	189
7.0	References	190
8.0	Abstract	196
8.0	Curriculum Vitae	199

1. INTRODUCTION

1.1 Introduction to Pd-catalyzed carbonylation

1.1.1 Catalysis: Definition, consideration and classification

The people were using catalysis in their daily lives without knowing that this processes was involved such as fermentation of wines.

Catalysis is the process of chemical transformation influenced by a catalyst. The term catalysis comes from the Greek word *kata* and *lyein*. *Kata* mean down and *lyien* mean loosen. The Swedish chemist Jons Berzelius in 1836 described the meaning of catalysis as the driving force provided by catalyst responsible for chemical transformation from one step to another [1]. Friedrich Wilhelm Ostwald (Noble prize winner in 1909), a German chemist stated that a catalyst accelerates a chemical reaction without affecting the position of the equilibrium. He described catalysis in terms of physical chemistry. In a chemical reaction, a catalyst lowers the activation energy compared to the corresponding uncatalyzed reaction.

1.1.1.1 Typical considerations for a catalyst

The following parameters must be considered for the choise of a typical catalyst:

- **Activity:** Activity of a catalyst is the measure of the influence of a catalyst on the chemical reaction rate. The activity depends on the chemical and physical parameters such as, concentration, temperature, and pressure.

- **Turnover number (TON):** The turnover number (TON) defined as the number of moles of substrate that a mole of catalyst can convert before becoming inactivated. An ideal catalyst would have an infinite turnover number in this sense, because it wouldn't ever be disactivated, but in actual practice one often sees turnover numbers which go from 100 up to 40 million. For homogeneous catalysis, TON can be mathematically expressed as
$$\text{TON} = \text{Number of moles of substrate reacted} / \text{number of moles of active catalyst}$$

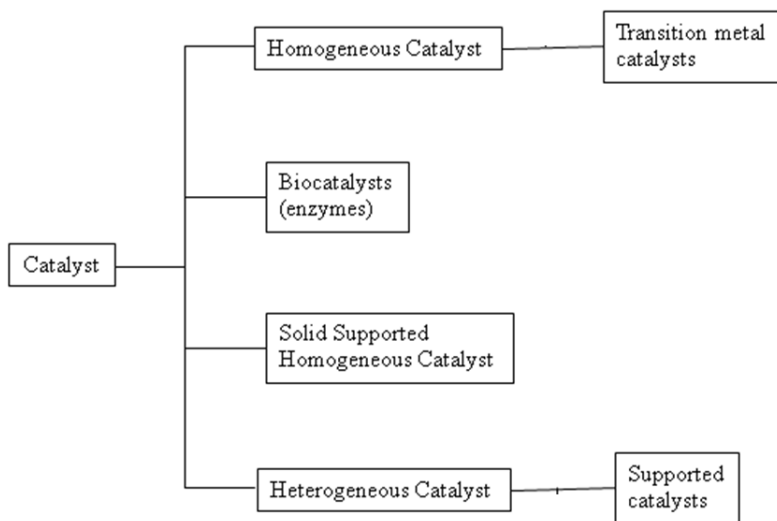
- **Turnover frequency (TOF):** Turnover frequency (TOF) defined as the ratio of turnover number per unit time. More precise mathematical expression of TOF are as follows:

$$\text{TOF} = (\text{number of moles substrate reacted}) / (\text{number of moles of active catalyst})(\text{unit time})$$

- **Selectivity:** The selectivity of a reaction describes the ratio of the quantity of desired product per quantity of undesired product or more simply the selectivity of a chemical reaction is defined as the number of moles of desired product per the number of moles of undesired product.
- **Stability:** The stability defines the lifetime of a catalyst in which it maintains its properties during a chemical reaction.

1.1.1.2 Classification of catalysts [1]

Catalysts are divided into heterogeneous and homogeneous, according to whether a catalyst exists in the same phase as the substrate or not. There are also some forms such as biocatalysis which is a type of heterogeneous catalysis catalyzed by enzyme. The classification of catalysts are shown below (Scheme 1.1).



Scheme 1.1 Classification of catalysts.

1.1.1.2.1 Homogeneous catalysis

Homogeneous catalysis is a type of catalysis in which the catalyst and all reagents are in the same phase. Homogeneous catalysts are generally chemical compounds or metal complexes which are soluble in reaction medium. Examples of homogeneous catalysis are the palladium catalyzed Suzuki–Miyaura coupling reaction between aryl halides and boronic acids [2],

Heck reaction between alkenes and aryl halides in presence of transition metal complex [3] etc.

1.1.1.2 Heterogeneous catalysis

Heterogeneous catalysis refers to processes in which the catalyst is in a different phase with respect to the reactants. Generally, solid catalysts are used with either liquid or gaseous reactants. A typical heterogeneous catalyst contains three components: an active catalytic phase usually a transition metals (or their oxides, sulfides, carbides, etc.), normally dispersed into the pores of the support or on its surface, promoters and the support [4]. The function of promoters depends on their nature: the texture promoters are used to facilitate the preparation and dispersion of the active phase and to maintain it in a well-dispersed state during the reaction conditions. The chemical promoters are additives that improve activity or selectivity of the catalytic phase. The role of the support is to facilitate the dispersion of the active catalytic phase and to stabilize it; indeed the heterogeneous catalysis is often affected by leaching of metal from support due to the reaction conditions. Reabsorption of metallic particles on the support may occur but very often after an aggregation and change of particle size [5]. There are many types of supports, characterized by different surface area, pore volume and pore diameters.

1.1.2 Green chemistry

Rachel Carson, a leading innovator of environmental protection reported her “Silent Spring,” in 1962 helped explicit the public’s awareness to pesticides and their ties to environmental pollution. In 1991, Paul Anastas introduced a new concept concerning chemistry termed as green chemistry.

Green chemistry referred to as the replacement of toxic substances and dangerous process. The main goal of green chemistry is to minimize the use of hazardous reagents and maximize the efficiency of any chemical reaction. The philosophy of green chemistry is to achieve a more sustainable development with the lowest environmental impact [6].

1.1.3 Fine chemicals

The three segmentations of the universe of chemicals are commodities, fine chemicals, and specialty chemicals. Fine chemicals are complex, single, pure chemical substances made to high specifications at relatively low volumes and high price typically in multi-purpose, batch chemical (or biotech) plants. It lies/fits between the commodities and specialty chemicals. In the present days "fine chemical" refers to the branch of molecular sciences, which is engaged in production of chemical substances which have defined molecular characteristics, intended mostly devoted to the pharmaceutical, biopharmaceutical, agrochemical, fragrance and flavor industry. From the early part of twentieth century, there is an increasing demand of fine chemicals from the market. Due to legislation restrictions and environmental concern regarding drawbacks and side effects of massive employment of chemicals in agriculture there is increasing quest for the research of new molecules and synthetic strategies to be used in order to control pests with decreased environmental impact.

1.1.4 The Agrochemicals

The agrochemicals are main products among fine chemicals. The term agrochemical means natural or synthetic chemicals used in agriculture. Depending on the type of target organism or pest, the agrochemicals are subdivided into four main categories: herbicides, insecticides, fungicides and plant growth regulators. At present most of the pesticides are of synthetic origin. There are only a few examples of natural pesticides such as the ryanodine (I) obtained from *Ryania Speciosa*, pyrethrin (II) obtained from the flowers of *Chrysanthemum Cineriaefolium*, the rotenone (III) extracted from the roots of tropical plants *Derris Elliptica* (leguminous family), Nicotine (IV) (Figure 1.1) [7]. Ryanodine, pyrethrin and rotenone all act as insecticides where nicotine is used as fungicides.

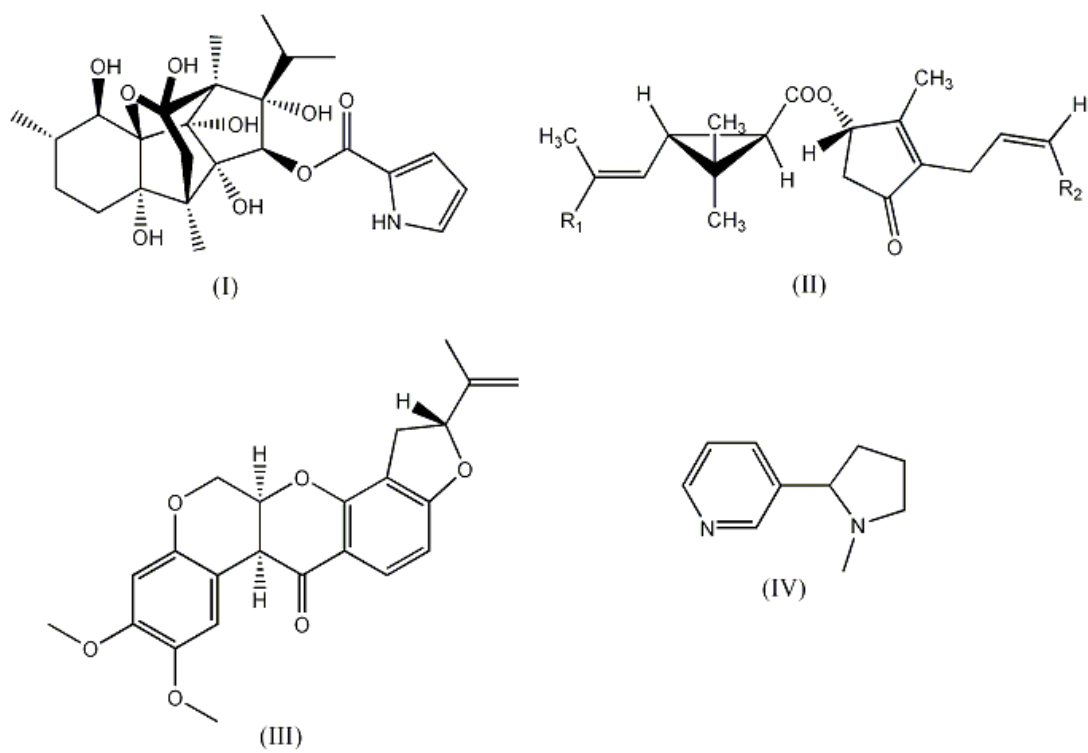


Figure 1.1 Structure of naturally occurring agrochemicals.

The most commonly used agrochemicals are herbicides. Herbicides are classified according to their chemical structure and mode of action. According to chemical structure the herbicides are grouped as: urea derivatives that inhibit photosynthesis (diuron, V), triazine (atrazine, VI), carbamates (VII) and derivatives of phenoxyacetic acid (Figure 1.2). The 2,4-dichlorophenoxyacetic acid is the first example of laboratory synthesized herbicide (VIII) which was used as biological weapon in second world war.

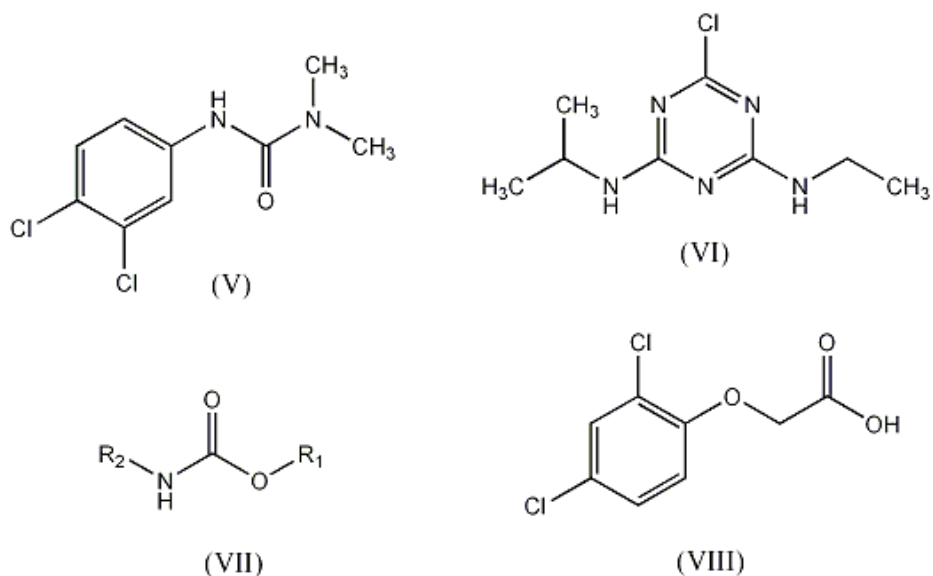


Figure 1.2 Structure of the diuron (V), atrazine (VI), carbamates (VII) and 2,4-dichlorophenoxyacetic acid (VIII).

1.1.5 The aryloxy-propanoic acids

The use of synthetic agrochemicals have several advantages like higher crop quality and yield, a small number of agricultural producers provides food for the much larger nonagricultural population. But due to legislation restrictions and environmental concern regarding drawbacks and side effects of massive employment of chemicals in agriculture there is increasing quest for the research of new molecules and synthetic strategies to be used in order to control pests with decreased environmental impact.

Optically active aryloxy-propanoic acids are widely used as important building blocks for asymmetric synthesis of agrochemicals and pharmaceuticals [8]. 2-aryloxypropanoic acid and its methyl ester derivatives (Figure 1.3) have been advanced as herbicides and plant growth regulators. They display the herbicidal activity by inhibiting the acetyl-CoA carboxylase in plant chloroplasts [9].

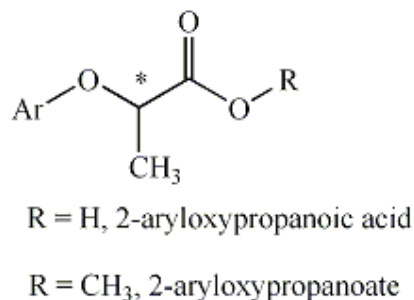


Figure 1.3 Structure of 2-aryloxypropanoic acid and 2-aryloxypropanoate.

The α -derivatives of aryloxy-phenoxy-propionic acid are the most important class of herbicides which selectively attack a specific family of plants, the Gramineae or grass family, without concern of potential crop injury (Figure 1.4) [10]. The origin of the selectivity of these herbicides results from their ability to inhibit the enzyme responsible for Gramineae's growth [11].

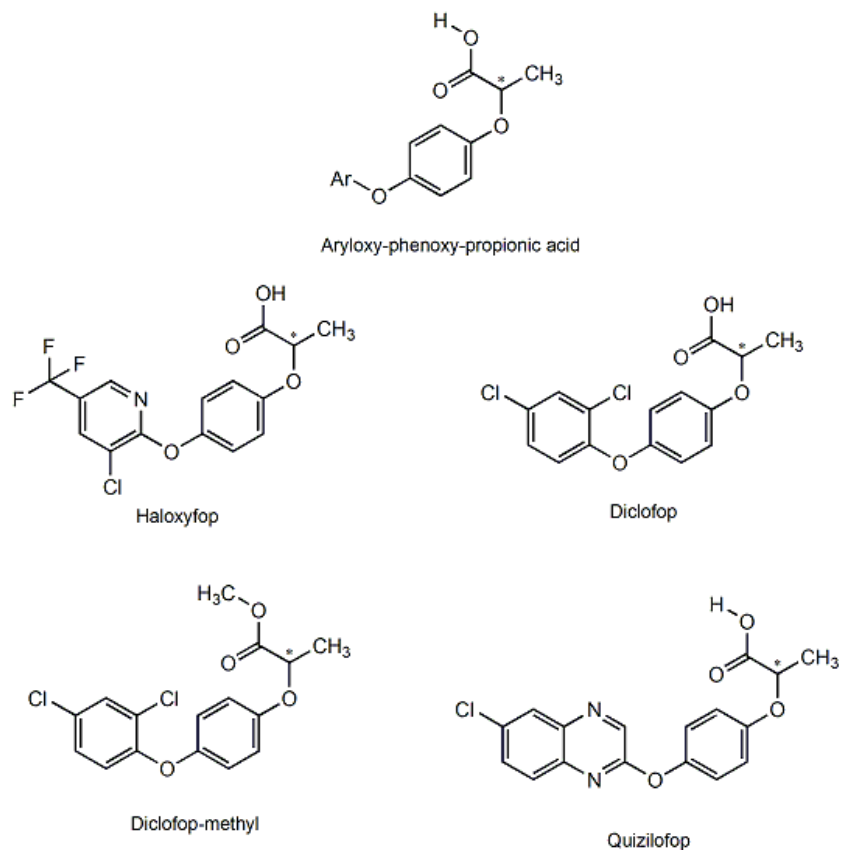
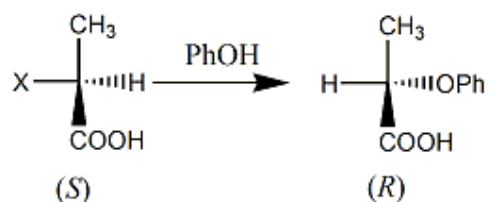


Figure 1.4 Chemical structure of aryloxy-phenoxy-propionic acid derivatives.

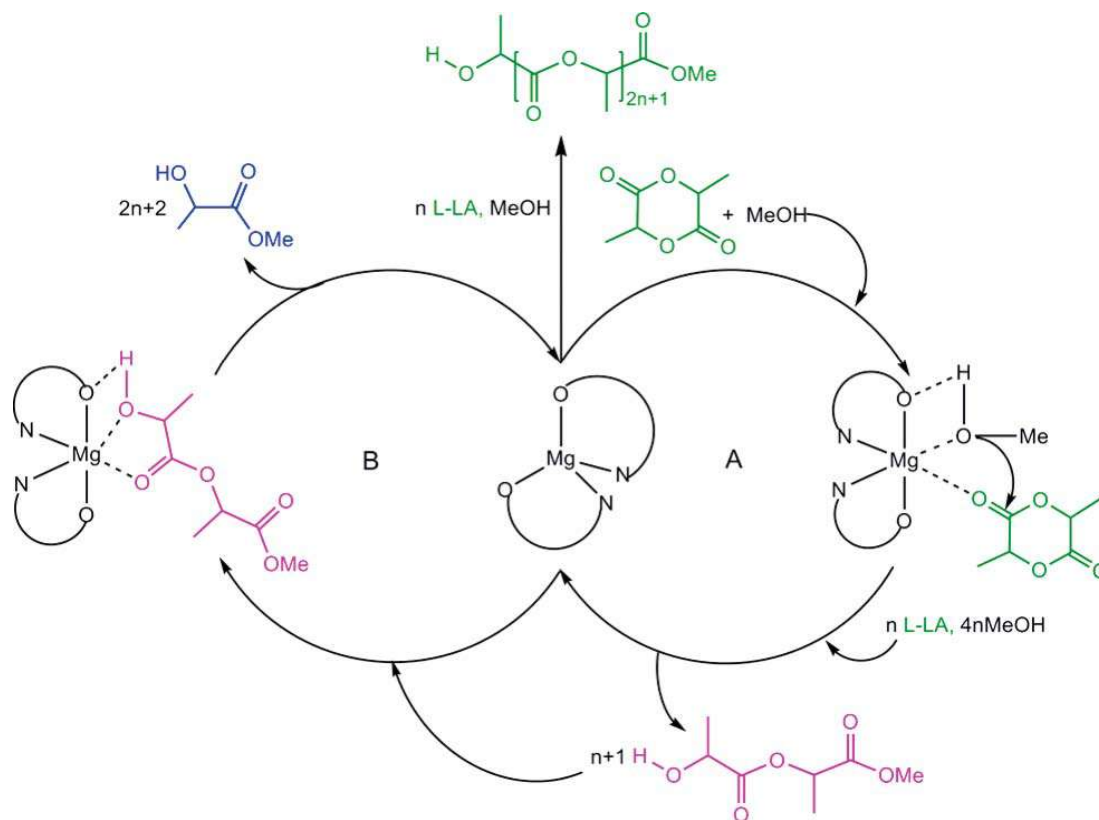
It is interesting to point out that enantiomers of 2-arylpropanoic acids are widely used for many different applications. In fact, (*S*)-enantiomers are the biologically active species in many different nonsteroidal anti-inflammatory drugs (NSAIDs), while (*R*)-enantiomers of 2-aryloxypropanoic acids are used as herbicides; in addition, (*R*)-2-(4-chlorophenoxy)propanoic acid is an anti-cholesterol. Thus the preparation of optically pure enantiomers are extremely important. The main objective of this project is to develop synthetic route for enantiomerically enriched α -aryloxypropanoic acid herbicides. There exist several methods involving this synthesis of chiral herbicides, including modification of chiral intermediates, biocatalysis and asymmetric hydrogenation.

Nowadays, an important procedure involves the nucleophilic substitution of α -halogenated propanoic acid by phenol with inversion of configuration (Scheme 1.2).



Scheme 1.2 Nucleophilic substitution of α -halogenated propanoic acid by phenol.

Many reports are available for the selective synthesis from chiral intermediates. For example, G.M. Gauchi reports the synthesis of chiral aryloxyphenoxypropionic acids by intermediate synthesis of (*R*)- or (*S*)-lactic acid alkylester[**12**]. This procedure usually requires a multistep synthesis, a stoichiometric amount of metal complex, long reaction times and high temperatures [14]. Recently A. Grala has reported the chemoselective alcoholysis of lactide Alkyl-(*S,S*)-O-lactyllactate (Scheme 1.3) mediated by a magnesium catalyst with mild reaction conditions yielding (*R*)- or (*S*)-lactic acid alkylester in high yields and moderate to good enantiomeric excess (e.e.%) up to 98 % [15]. The mechanism of the alcoholysis reaction is as following (Scheme 1.3)-

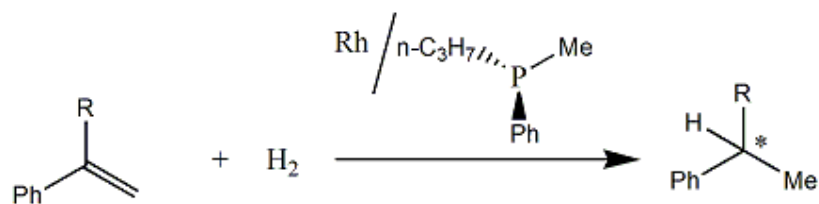


Scheme 1.3 Proposed mechanism for the alcoholysis and polymerization of *L*-lactide.

The enantiomerically enriched (*R*)- or (*S*)-aryloxypropionic acid may also be achieved via biocatalysts. For example, Sih *et al.* hydrolyzed 2-(chlorophenoxy)-propanoate to obtain enantiomerically enriched aryloxypropionic acids using lipase [12]. Fukui and his co-workers reported the enantioselective esterification (Scheme 1.2) of 2-(4-chlorophenoxy)propanoic acid with celite-adsorbed lipase OF 360 from *Candida cylindracea* [13]. This procedure produced optically pure 2-(4-chlorophenoxy)propanoic acid though the extent is limited due to a long reaction time of 63 days.

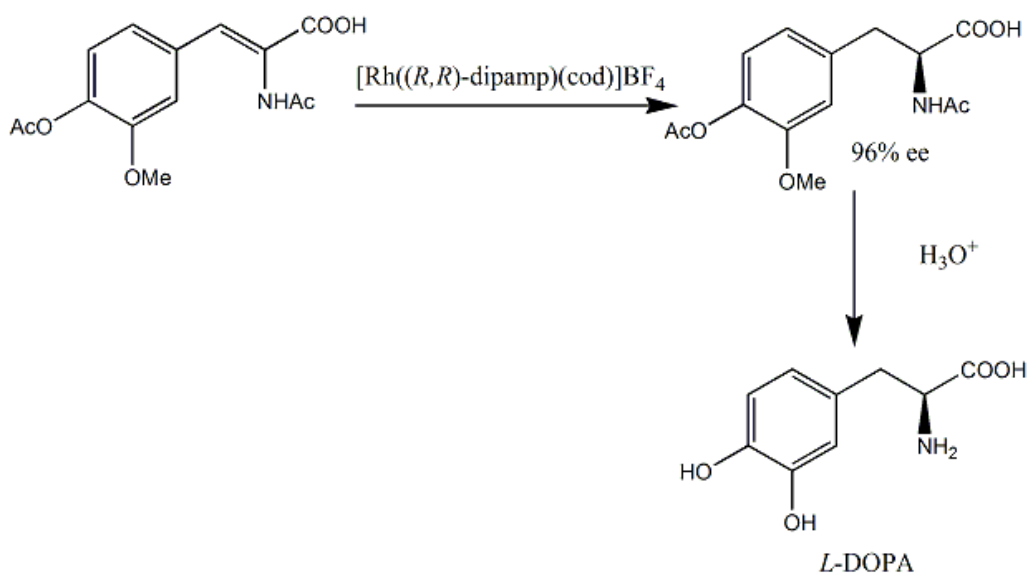
Asymmetric hydrogenation is the most efficient and practical method for the preparation of chiral compounds [16]. The increasing demand for enantiomerically pure pharmaceuticals, agrochemicals and fine chemicals encouraged chemists for the development of asymmetric catalysis.

During the last few decades of the 20th century, significant attention was devoted to the discovery of new asymmetric catalysts. In 1968, William Knowles and his co-workers reported the first example of asymmetric hydrogenation using a homogeneous rhodium catalyst with low enantiomeric excess (Scheme 1.4).



Scheme 1.4 First example of homogeneous asymmetric hydrogenation.

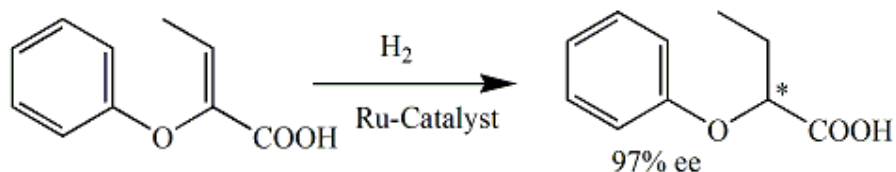
The asymmetric hydrogenation of α,β -unsaturated carbonyl compounds was used as a very efficient approach to the enantioselective synthesis of acids having a chiral carbon in α position with respect to the carboxyl group. As an example, in 1998, Knowles prepared (*S*)-3-(3,4-dihydroxyphenyl)alanine (*L*-DOPA) drug used for the treatment of Parkinson's disease. *L*-DOPA, is produced by the asymmetric hydrogenation of acetamidocinnamic acid followed by the hydrolysis of 2-acetamido-3-phenylpropanoic acid. This was the first example of an industrial scale asymmetric catalysis (Scheme 1.5) [17].



Scheme 1.5 Preparation of (*S*)-3-(3,4-dihydroxyphenyl)alanine (*L*-DOPA).

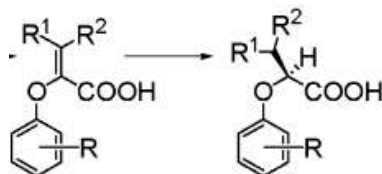
Maligres *et al.* reported the highly enantioselective (e.e. > 90%, yield 100%) asymmetric hydrogenation of α -phenoxybutenoic acid (Scheme 1.6) using ruthenium catalyst [20]. Hydrogenation reactions were conducted using *in situ* catalyst made by mixing [(*p*-

cymene)RuCl₂]₂ with commercially available biophosphine ligands (ex. (*S*)-synphos, (*S*)-BINAP, (+)-TMBTP etc.) in MeOH. The triethylamine was used as a base. The highest enantioselective (e.e. 99%, yield 100%) product was obtained when the reaction was carried out with (+)-TMBTP.



Scheme 1.6 Asymmetric hydrogenation of α -phenoxybutenoic.

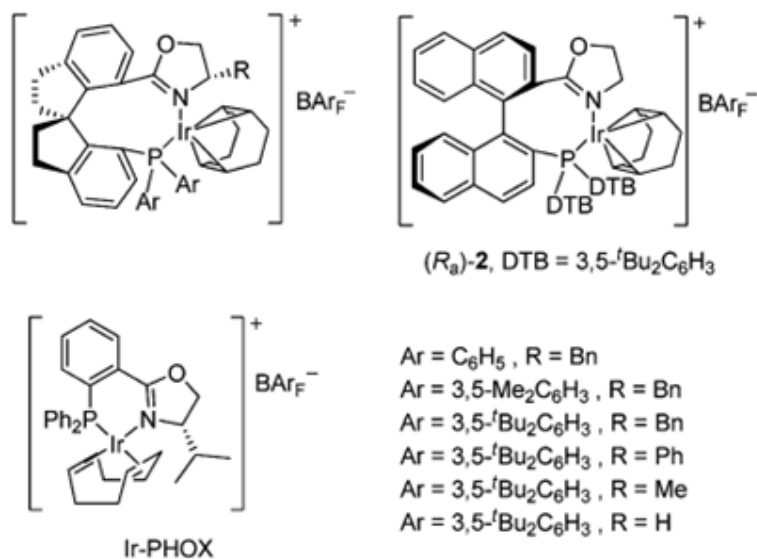
In their extended work, the asymmetric hydrogenation of α -aryloxy unsaturated acids with R¹ = H, Me or nC₅H₁₁ and R² = H or Me were hydrogenated using 20 mol % [(*S*)-BINAP]RuCl₂ as preformed catalyst giving corresponding R-aryloxy acids with >99% conversion and moderate to high yields. Substrates with a trisubstituted olefin gave moderate to high enantioselectivity, while with tetrasubstituted olefin showed relatively lower enantioselectivity in the hydrogenation.



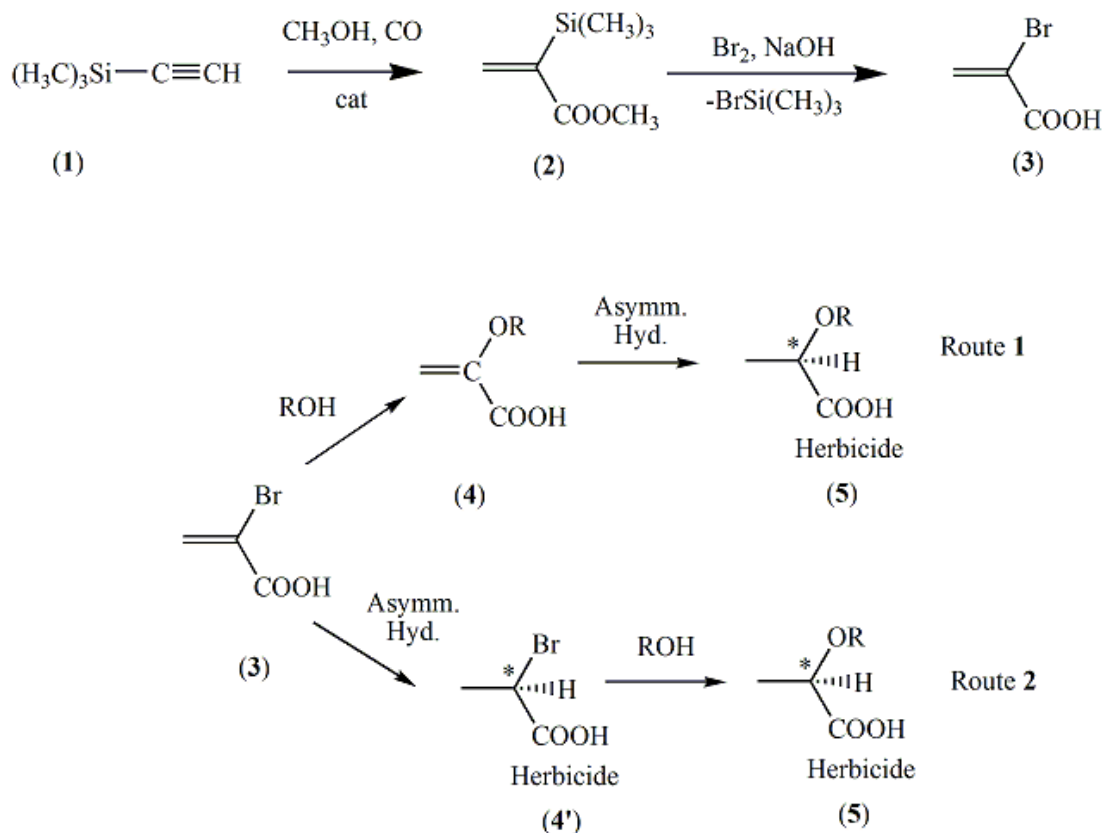
The enantioselectivity were largely influenced by the substitution on the aryl group, including ortho and meta substituents. When the reactions were carried out using only 1 mol % catalyst, there are no effects on the conversion and selectivity. Interestingly, it is observed that the phenol impurities are increased in the presence of bulky group in the ortho-position and in the more electron-deficient aryl ethers.

In the proposed scheme 1.7 (proposed scheme, route 1), the asymmetric hydrogenation [20] of product (4) results in the formation of chiral 2-aryloxypropanoic acid or its alkyl ester herbicides. In case of Maligres *et al.*, the asymmetric hydrogenation of α -aryloxy unsaturated acid using [(*S*)-BINAP]RuCl₂ in MeOH produced moderate to high enantioselective products

(yield. 98%). The reaction conversion and enantioselectivity are largely depends on the % mol catalyst employed, the internal structure (alkyl substitutes) aryl group.



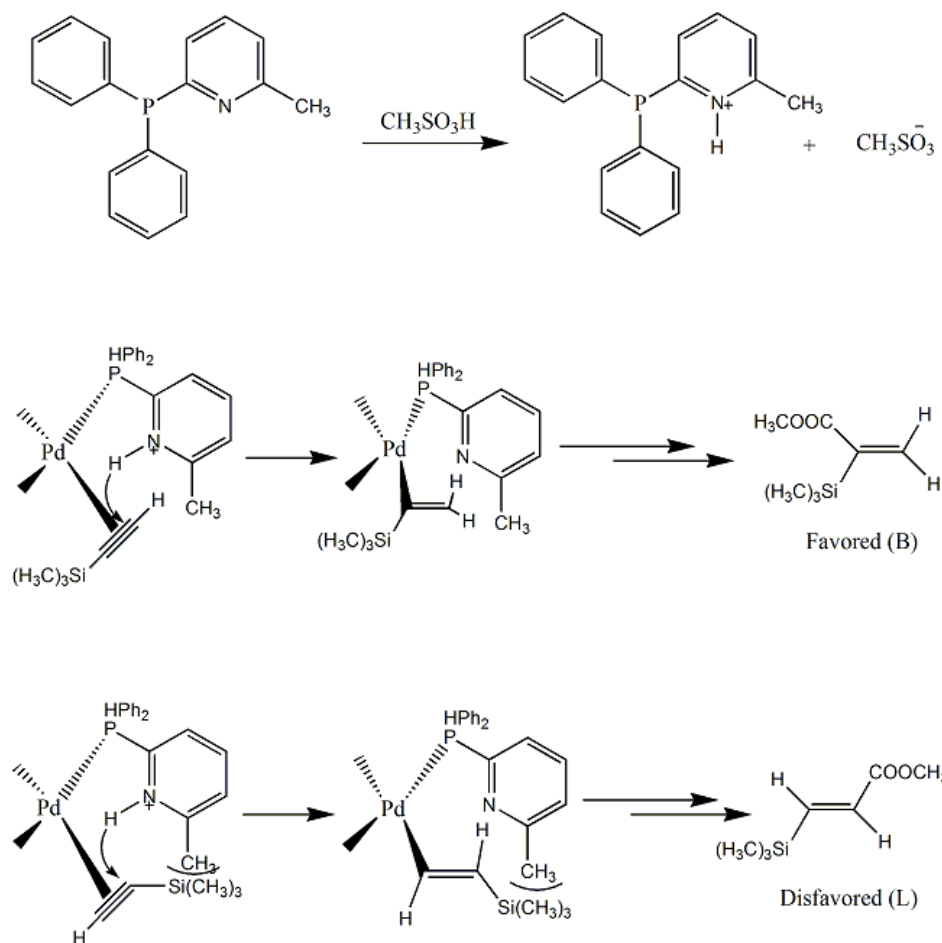
In our case, the asymmetric hydrogenation of 2-bromoacrylic acid (**3**) or 2-alkoxyacrylic acid (**4**) will be carried out using preformed [(S)-BINAP]RuCl₂ catalyst or iridium complexes reported by Shen Li *et al.* [8]



Scheme 1.7 Proposed synthetic scheme for enantiomerically enriched herbicides

The main advantages of our proposed synthetic scheme includes:-

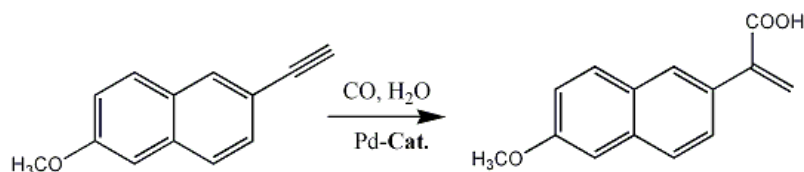
- (1) The stereo selective preparation of the 2-bromoacrylic acid is started from a easily available, cheap starting material, (trimethylsilyl) acetylene. The preparation is carried by carbonylation reaction using the well known 'Drent's catalytic system ($\text{Pd}(\text{OAc})_2/\text{P}/\text{CH}_3\text{SO}_3\text{H}$)'.
- (2) The stereoselectivity of the carbonylation reaction is achieved by changing the phosphine ligand in the catalytic system. The highly steric phosphine in the catalytic system enhanced the branched selectivity of the carbonylation reaction. This result can be explained by considering the mechanism of intermediate formation given below-



(3) The alcoholysis of synthesized 2-bromoacrylic acid produces the corresponding alkoxy acid, which is converted into chiral herbicides by asymmetric hydrogenation (route 1).

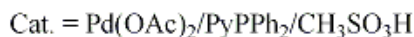
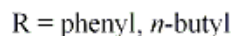
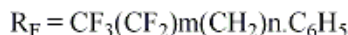
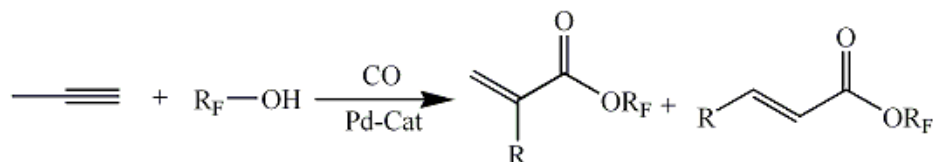
(4) Alternatively, the synthesized 2-bromoacrylic acid functions as the intermediate for the preparation of α -halogenated propanoic acid, which is then converted into the chiral herbicides by asymmetric hydrogenation (route 2).

Our research group has long been interested in the development of alternative enantioselective catalytic routes for the synthesis of enantiomerically enriched and pure fragrances, pharmaceuticals, etc. For examples, Matteoli *et al.* reported the alternative stereoselective synthesis of (*R*)- and (*S*)-Rosaphen via asymmetric catalytic hydrogenation of 2-methyl-5-phenylpentanoic acid (ee up to 99%) in the presence of an *in situ* prepared ruthenium catalyst containing the chiral ferrocenyl phosphine, Mandyphos-4 [26]. A. Scrivanti *et al.* prepared the hydroxycarbonylation of 2-(6-methoxy-2-naphthyl)ethyne using Drent's catalyst giving 95 % of 2-(6-methoxy-2-naphthyl)propenoic acid, a naproxen precursor (Scheme 1.8) [25].



Scheme 1.8 Synthesis of 2-(6-methoxy-2-naphthyl)propenoic acid.

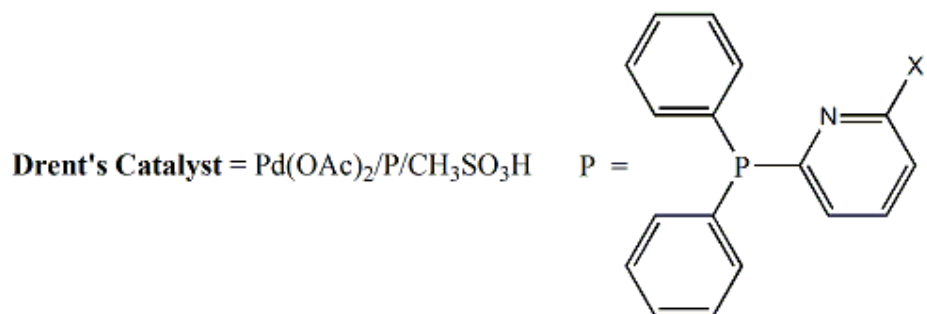
Recently, our group reported the synthesis of fluorinated acrylates using similar catalytic system. The carbonylation reaction of alkyne with fluorinated alcohol is a versatile and easy synthetic strategy to produce fluorinated acrylates (Scheme 1.9), an important intermediate of for fluorinated polymers employed for the protection of artistic materials.



Scheme 1.9 Synthesis of fluorinated acrylates.

1.1.6 Drent's Catalyst

Many forms of palladium complex containing phosphine ligand are used in the carbonylation reaction of alkyne [21]. The palladium carbonylation reaction greatly influence by the structure of the phosphine ligand. In the early 1990's E. Drent's *et al.* established a catalytic system by mixture of palladium acetate, methanesulphonic acid and 2-(diphenylphosphino)pyridine in proper ratio (Figure 1.5) [22].



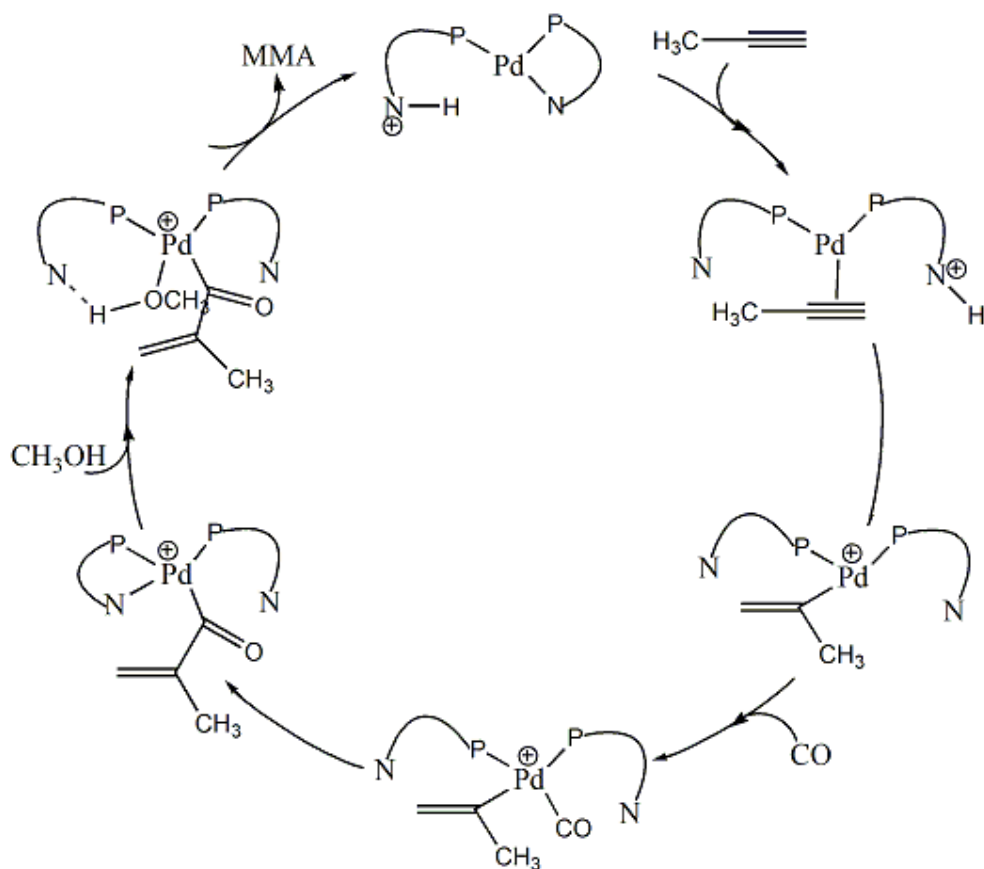
X = H, P = (Diphenylphosphino)pyridine

X = CH₃, P = 2-(6-methyl)(diphenylphosphino)pyridine

Figure 1.5 Drent's catalyst.

They studied the methoxycarbonylation of propyne by substituting the phosphine, 2-(diphenylphosphino)pyridine with triphenylphosphine. The lower TOF value indicates that the pyridine ring of 2-(diphenylphosphino)pyridine plays a key role in the Drent's catalytic system. Furthermore, the increase of TOF and the selectivity towards the methyl methacrylate upon the substitution of 2-(diphenylphosphino)pyridine with 2-(6-methyl)(diphenylphosphino)pyridine support the above argument.

The mechanism of methoxycarbonylation reaction provided by Drent followed the intermolecular proton transfer from a protonated pyridyl ligand. The pyridine nitrogen transfers the proton from methanesulphonic acid to the coordinated alkyne. The transfer can be in two ways (Scheme 1.10): i) the proton transfer from pyridine nitrogen (**1**) to the palladium center to form hydride complex (**2**), from which it transferred into the coordinated alkyne, or ii) the proton is directly transferred from the pyridine nitrogen into the coordinated alkyne. The same vinyl intermediate (**3**) is formed in both cases. Currently there is no evidence to accept or reject any one of the two concepts, but it is no doubt that the pyridine nitrogen plays a key role in the carbonylation reaction [22, 27]. Subsequent studies [27] have shown that the catalytic cycle starts with the transfer of a proton from the 2-(diphenylphosphino)pyridine into the coordinated alkyne (Scheme 1.10). Computational studies by L. Crawford *et al* support the arguments [28].



Scheme 1.10 Proposed mechanism of carbonylation via proton transfer followed by CO insertion and protonolysis.

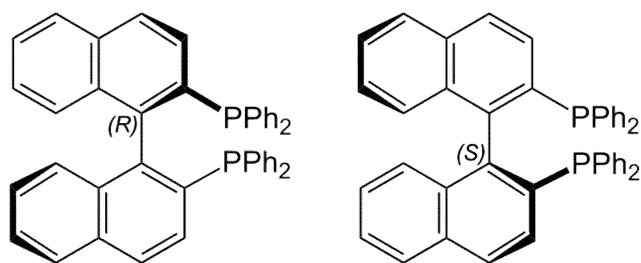
Besides carbonylation reactions, the Drent's catalyst also used in the copolymerization ethylene/methyl acrylate. The polymerization reaction is carried out by using sulfonic acid substituted triphenylphosphine in the catalytic system.

Considering the above mentioned facts, we propose that this newly developed route demands the priority over the previously methods for yielding the target herbicides

1.2 Innovative aspect of ligand synthesis in homogeneous catalysis

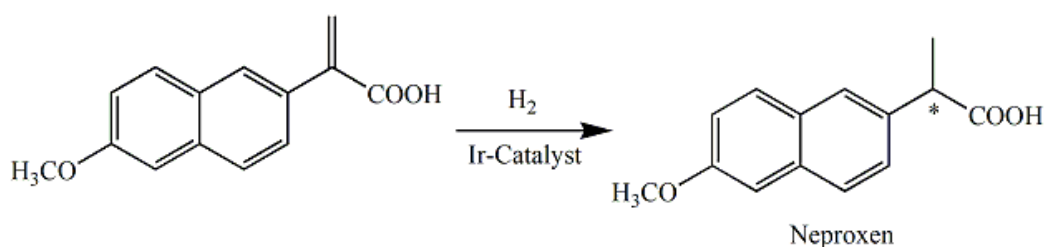
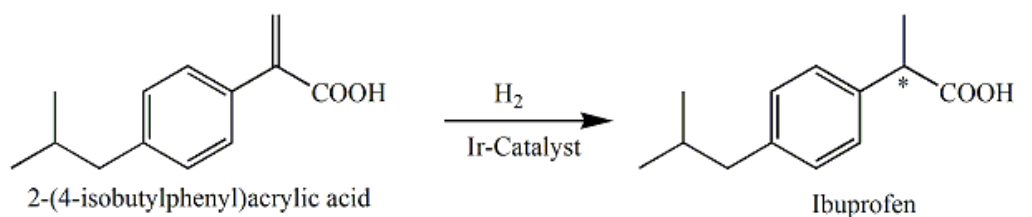
Transition-metal-catalyzed reactions have become powerful tools in the production of pharmaceuticals and fine chemicals. In the past decades, enantioselective catalysis, especially chiral catalysts hold an increasing role for building chirality. Enantioselective synthesis is

defined as the chemical reaction, where the enantiomeric product formation is favorable over distereomeric product. This type of reaction usually catalyzed by chiral transition metal complex. The most fascinating enantioselective synthesis is asymmetric hydrogenation to reduce variety of functional group. For example, the asymmetric hydrogenation of α -substituted acrylic acid derivatives in the presence of Ir or Ru catalyst allowing to obtain optically pure propionic acids. Ryōji Noyori introduced the use of Ru-BINAP asymmetric catalyst that could be used to hydrogenate several important types of substrates. The *R*- and *S*- structure of the BINAP ligand are presented below-.



BINAP ligand.

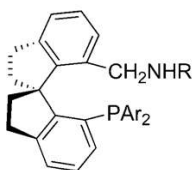
The method has employed for industrial production of many useful optically active compounds such as pharmaceutical ingredients, agrochemicals, and flavors [18]. In 2012, Shou-Fei Zhu *et al.* synthesized two important non-steroidal anti-inflammatory drugs ibuprofen (e.e. 99%, yield 98%) and naproxen (e.e. 98%, yield 99%) by asymmetric hydrogenation of the corresponding α -arylacrylic acids using Ir-catalyst (Scheme 1.11).



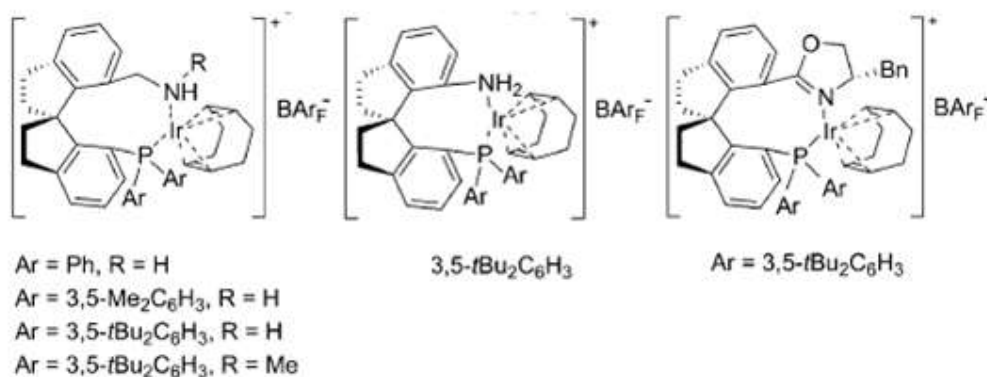
Scheme 1.11 Synthesis of ibuprofen (I) and naproxen (II) by asymmetric hydrogenation.

The iridium catalyst containing chiral spiro aminophosphine ligands displayed excellent activity and enantioselectivity for the asymmetric hydrogenation of α -(4-isobutylphenyl)acrylic acid.[19]. The catalysis were carried out in MeOH using 0.5 equivalent amount of base (Cs_2CO_3 or Na_2CO_3 or Et_3N) in ambient temperature at 6 atm. pressure. 0.1 mol% of catalyst within 10 minutes gave the complete conversion with high TOF values ($6000\ h^{-1}$) and excellent enantioselectivity (98% ee). Iridium catalysts with less bulky P-aryl groups exhibited slightly lower activity and enantioselectivity. Though the hydrogenation reaction was not completed after 18 h, the catalyst which has an N-methyl group displayed excellent enantioselectivity.

The structure of the ligand and Ir-catalyst are as follows



Ligand (R = H or Me)

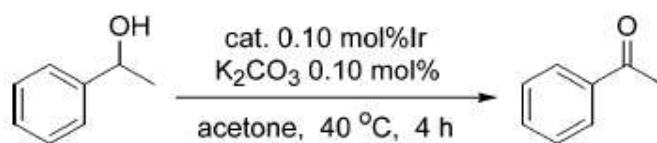


Catalyst

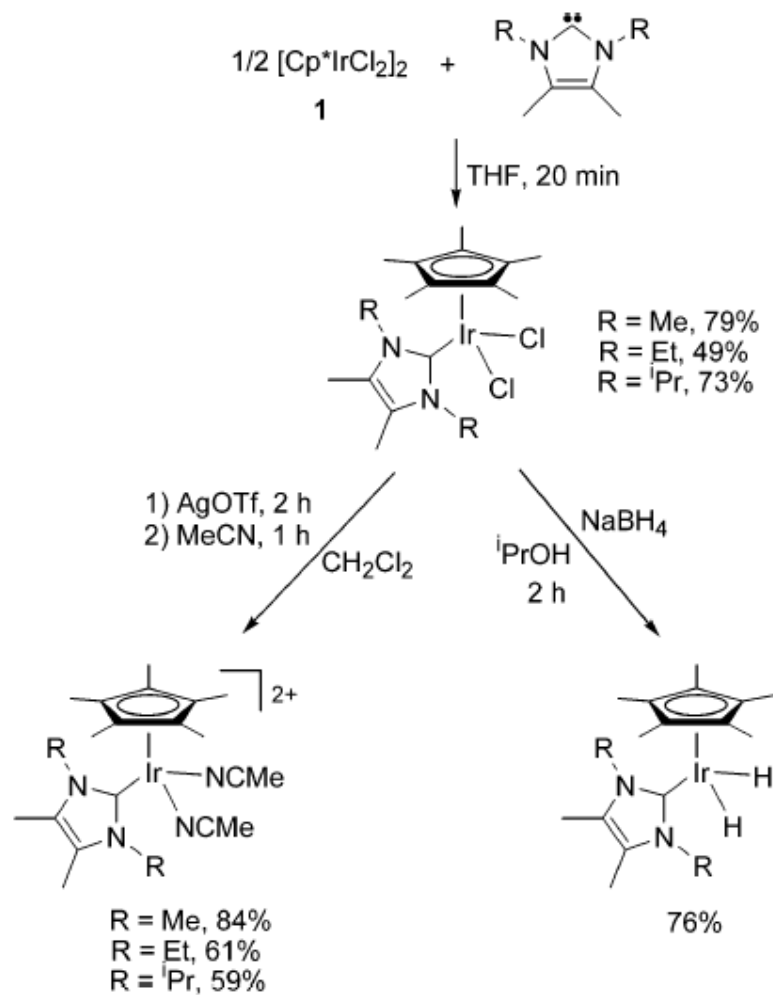
Beside asymmetric catalysis, the transition metal complex containing variety of organic ligands are being employed widely in the catalysis of numerous chemical reactions including:

1) N-Heterocyclic carbenes (NHC) employed in oxidation of alcohols:

N-Heterocyclic carbenes (NHC) is an important class of ligand used in homogeneous catalysis for many reactions. Metal complexes containing NHC ligands are employed in the oxidation of alcohols such as air stable CpIr(imidazol-2-ylidene)Cl₂ complex used in the oxidation of 1-phenylethanol to acetophenone in acetone [54-56].

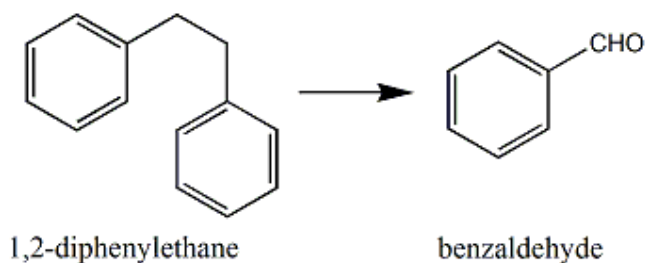


The reaction of [Cp*IrCl₂]₂ (**1**) with 2 equiv of the imidazol-2-ylidene (NHC) ligands in THF gave Cp*Ir(L)-Cl₂ (L, NHC ligand) as air-stable crystals. The synthetic scheme of the catalyst is shown below-

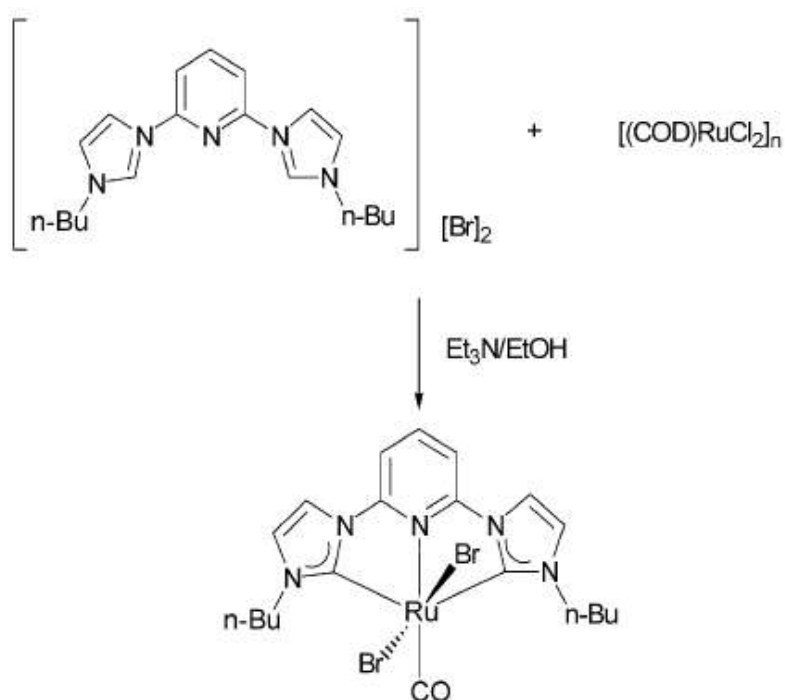


Further treatment of $\text{Cp}^*\text{Ir(L)-Cl}_2$ with 2 equiv of AgOTf followed by acetonitrile gave the dicationic complexes $[\text{Cp}^*\text{Ir(L)(MeCN)}_2]^{2+}$. The percentage of yield depends on the substituent R. The dihydrido complex $\text{Cp}^*\text{Ir(L)H}_2$ complex can be obtained by the treatment of $\text{Cp}^*\text{Ir(L)-Cl}_2$ with NaBH_4 in PrOH.

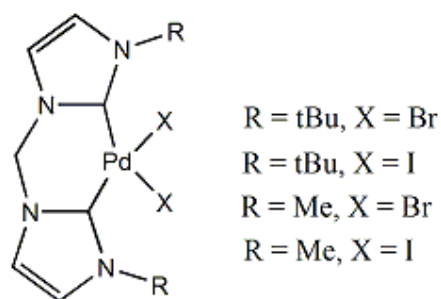
Ruthenium-NHC such as $\text{Ru-(2,6-bis(butylimidazol-2-ylidene)-pyridine)(CO)Br}_2$ is used in oxidative cleavage of alkenes [57]. For example, the oxidative cleavage of 1,2-diphenylethane gave 55% conversion in 24 hours.



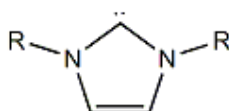
The reaction was carried out 1 mol% catalyst with 1.25 mol NaIO₄ in 1.0 mL CDCl₃/0.1 mL H₂O solution. The catalyst is prepared by the reflux (12 hours) of [(COD)RuCl₂]_n and 2,6-bis(1-*n*-butylimidazolium-3-yl)pyridine bromide in ethanol in the presence of NEt₃ gave 25% of Ru(CNC)(CO)Br₂.



Palladium-NHC complex is employed for the oxidation of methane [58]. The complex catalyzes the conversion of methane into methyl ester. The structures of the highly thermal stable palladium complexes are as follows

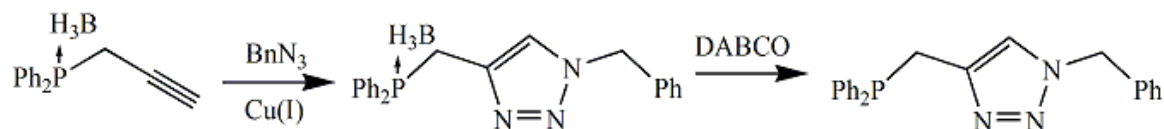


Beside oxidation reactions, carbene ligands are used in combination with palladium in Heck reaction [59], Hiyama reaction [60], allylic alkylation [61], etc. The general structure of NHC ligands is as follows:



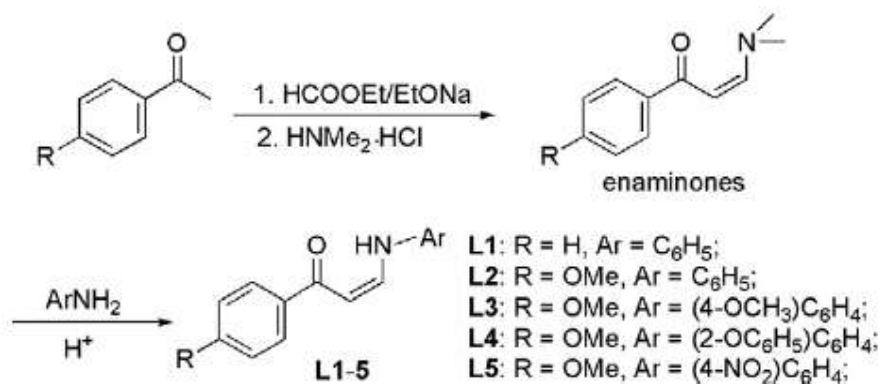
2) Catalysis of both organic and aqueous phase carbon-carbon bond formation coupling reaction:

R.J. Detz *et al.* synthesized a triazole-phosphine bidentate ligand for palladium catalyzed Suzuki-coupling reactions (Scheme 1.12) [48].

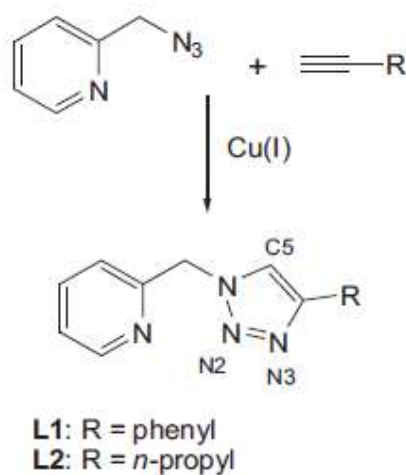


Scheme 1.12 Synthesis of triazole-phosphine ligand.

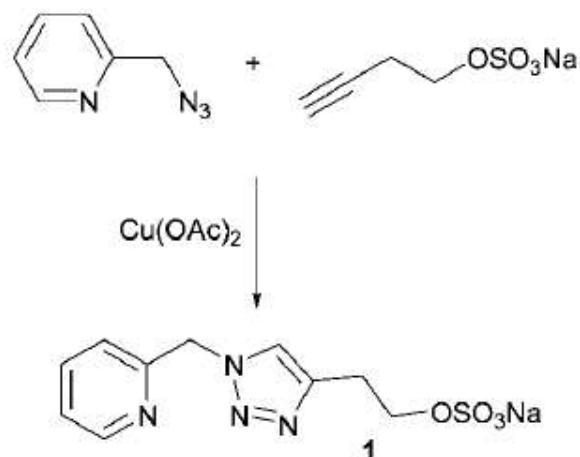
There are several phosphine ligands are used in the cross coupling reaction [51-53]. These ligands are highly efficient but their use is limited due to toxic properties. In contrast, among the phosphine free ligands, Z. Z. Zhou and co workers synthesized and successfully employed a series of β -ketoamine ligands in Suzuki cross-coupling of aryl bromides with phenylboronic acid in aerobic condition. The *in situ* palladium catalyst of these ligands are highly active in cross-coupling reaction [2].



Amadio *et al* reported the synthesized triazole ligands for palladium catalyzed Suzuki-coupling reactions by azide-alkyne cycloaddition reaction [44]. The general synthetic scheme as follows:



The preformed palladium complex of L2 was tested against Suzuki-coupling reaction and found more active than that of L1 under same conditions. Latter on our group synthesized the water soluble ligand for the same cross coupling reaction. The ligand is highly active in aqueous phase reaction The synthetic procedure is exactly same as for L1/L2.



The structure and properties of the ligands are not only effective in the preparation of active homogeneous catalyst but also plays an important role in catalyst separation catalysis. For example, a number of synthetic and commercially available water soluble ligands are successfully used by Paganelli *et al* in the biphasic hydrogenation and hydrofomylation reaction [74, 75].

The pre requisite condition for designing ligand for development of metal complex includes the possibility of binding donor group with metal center with availability of lone pair electron, special arrangement of the appended groups ($-\text{OSO}_3\text{Na}$) and carbon chain around the donor groups of extent of coordinate bond formation with the central metal atom. Considering the application of the ligand in catalysis we focused our synthetic route with referred literature and some now innovative feedback.

1.3 Introduction to triazole ligand synthesis and transition metal complex catalyzed hydrogenation and hydroformylation reactions

1.3.1 Triazole, its synthesis and application in catalysis

Triazoles are a class of organic heterocyclic compounds containing a five membered ring structure having two carbon atoms and three nitrogen atoms at one adjacent positions. The triazoles are the isosters of imidazoles in which the carbon atom of imidazole is replaced by nitrogen atom. Triazoles are a white to yellow solid compound with characteristic odor, soluble in water and alcohols. The isomeric structure of 1,2,3-triazole and 1,2,4-triazole are shown in Figure 1.6.

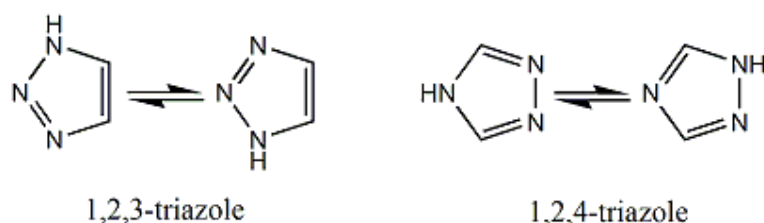
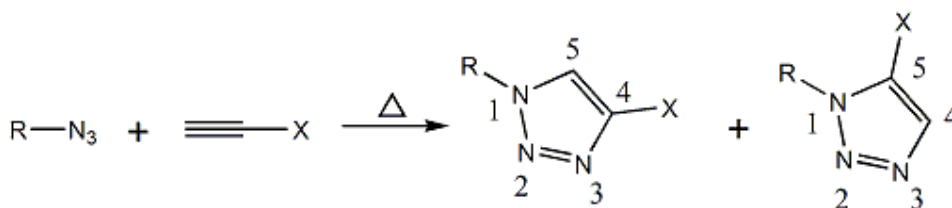


Figure 1.6 Isomeric structure of 1,2,3-triazole and 1,2,4-triazole.

There are several methods reported in literature for the synthesis of triazoles [35-37]. In the early part of the 20th century Huisgen discovered 1,3-dipolar cycloaddition reaction between azides and terminal alkynes (Scheme 1.13). 1,3-dipolar cycloaddition reaction is a general protocol for the synthesis of five membered heterocycles. The cycloaddition reaction undergoes between the substance containing dipolarophile (1,3-dipolar) resonance structure and a multiple bond system.

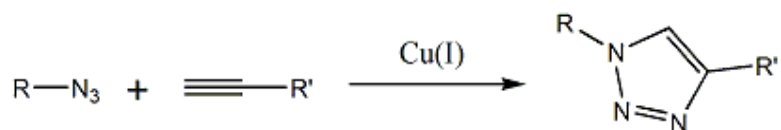


Scheme 1.13 Azide-alkyne 1,3-dipolar cycloaddition reaction (Huisgen reaction).

The Huisgen reaction is a highly exothermic reaction. The requirement of high activation energy lowers the reaction rate even at high temperature. This thermal reaction always produces a mixture of 1,4- and 1,5-disubstituted regioisomers. This drawback comes from the two different types of interaction between the highest occupied molecular orbital of azide and lowest unoccupied molecular orbital of multiple bond [38].

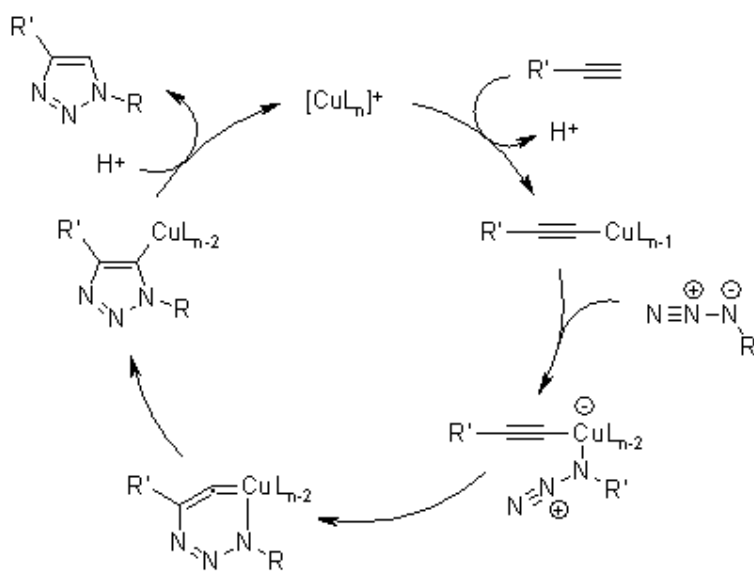
In 2001, Sharpless and co-workers developed click chemistry [39]. The click reaction encompasses many of advantages: reactions are modular, stereospecific, high yielding, and produce only non-offensive by-products. Moreover, the click reaction requires mild reaction conditions, readily available starting materials and reagents, the use of no solvent or easily removable solvent [40]. After development of the click reaction, the synthetic chemists turned their attention to the classical 1,3-dipolar cycloaddition reaction, which did not fall into the click reaction. The development of copper(I)-catalyzed azide-alkyne cycloaddition

(CuAAC) leads to the formation of 1,4-disubstituted specific regio-isomer instead of a mixture of 1,4- and 1,5- regio-isomers (Scheme 1.14) [36]. This reaction obeyed the criteria of click reaction at room temperature and very short time. The reaction is usually carried out using a mixture of $\text{CuSO}_4 \cdot 5\text{H}_2\text{O}$ and a reducing agent sodium ascorbate or $\text{Cu}(\text{OAc})_2 \cdot \text{H}_2\text{O}$ as catalyst. A mixture of *tert*-BuOH and H_2O is used as solvent.



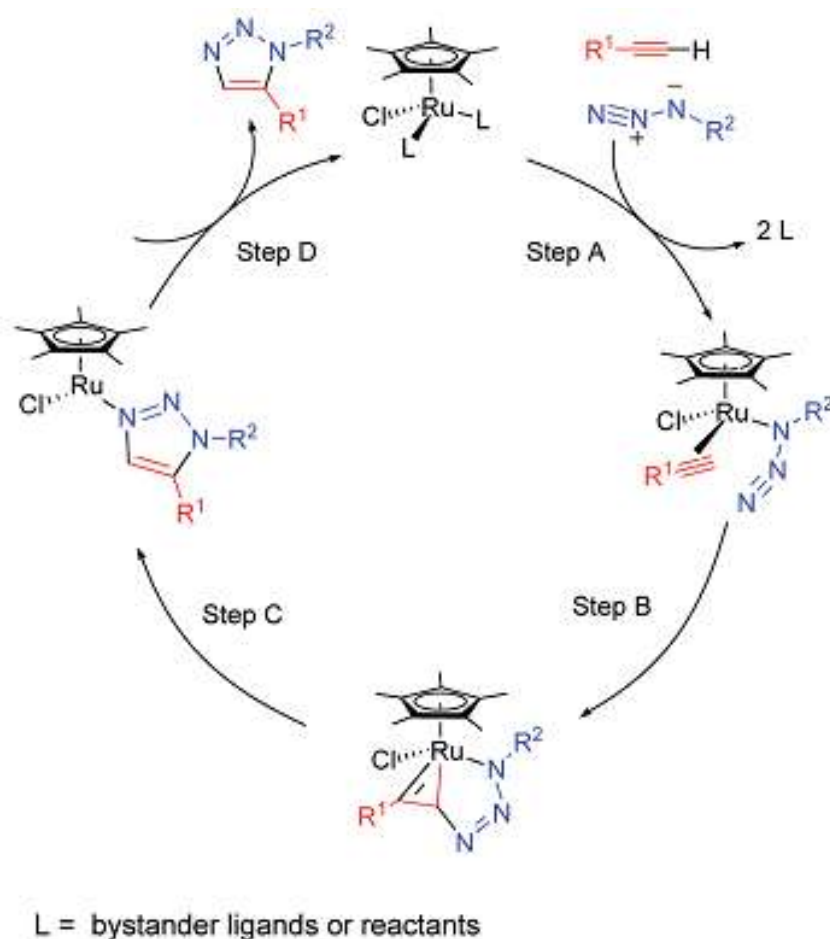
Scheme 1.14 Copper(I)-catalyzed azide-alkyne cycloaddition reaction.

The well accepted mechanism of this reaction was reported by F. Himo *et al.* [36]. The most common experimental procedures involve the *in-situ* generation of Cu(I) by the reduction of CuSO_4 with sodium ascorbate in aqueous medium. [33]. In some cases, however, the reaction can be carried without sodium ascorbate, using $\text{Cu}(\text{OAc})_2 \cdot \text{H}_2\text{O}$. The solvent *tert*-BuOH is used to reduce the Cu(II) to Cu(I): the advantage of this approach lies in an easier purification of triazole product [41]. The terminal alkyne formed copper alkylide by replacing a ligand from the copper(I)-species. After which the azide displaces another ligand and binds to the copper. Then, an unusual six-membered copper(III) metallacycle is formed. Ring contraction to a triazolyl-copper derivative is followed by protonolysis that produces the triazole and closes the catalytic cycle. The mechanism of the copper-catalyzed azide-alkyne cycloaddition (CuAAC) is reported in Scheme 1.15 [36].



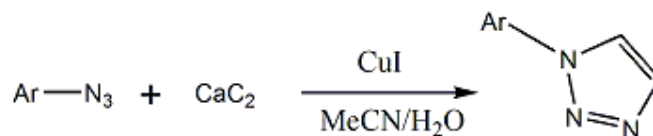
Scheme 1.15 Catalytic cycle of azide-alkyne cycloaddition reaction catalyzed by Cu(I).

B.C. Boren and co-workers demonstrated the ruthenium catalyzed azide-alkyne cycloaddition reaction. Interestingly, the observed regioselectivity was reversed when compared with related copper(I)-catalysis. In ruthenium-catalyzed cycloaddition reaction, the participation of both terminal and internal alkyne discarded the hypothesis of formation of ruthenium alkylides like copper alkylide formation in copper catalyzed cycloaddition reaction. Instead, an activated complex is formed (Step A of Scheme 1.16) by replacement of bidentate ligand from ruthenium catalyst, which takes part in the oxidative coupling (Step B of Scheme 1.16) of azide and alkyne to form ruthenacycle. The ruthenacycle intermediate then undergoes reductive elimination (Step C of Scheme 1.16) releasing the triazole product and regenerating the catalyst (Step D of Scheme 1.16). [37].



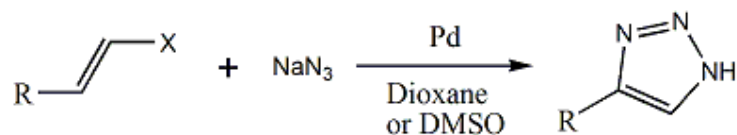
Scheme 1.16 Ruthenium catalyzed cycle of azide-alkyne cycloaddition reaction.

Among other modern developed synthetic methods, the synthesis of mono-substituted 1,2,3-triazoles (Scheme 1.17) may be achieved by i) copper(I)-catalyzed 1,3-dipolar cycloaddition reaction of aryl-azide with calcium carbide. The calcium carbide is used as a source of acetylene which in turn forms copper-acetylenide complex. This reaction is carried out in a mixture of MeCN-H₂O. [42].



Scheme 1.17 Copper(I)-catalyzed 1,3-dipolar cycloaddition reaction between aryl-azide and calcium carbide.

ii) the palladium catalyzed synthesis of 1*H*-triazoles by the reaction between alkenyl halides and sodium azide (Scheme 1.18). Dimethylsulfoxide is used as solvent for aliphatic halides whereas dioxane for aromatic halides [43].



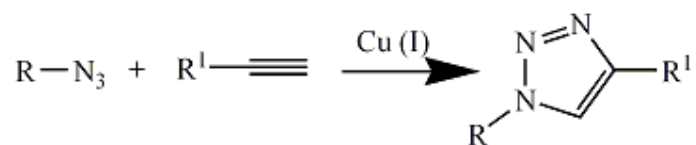
Scheme 1.18 Copper(I)-catalyzed reaction between alkenyl halide and sodium azide.

1.3.2 Click Reaction

The click chemistry was first introduced by Barry Sharpless in 1999 [44]. In 2001 he defined click chemistry as modular, wide scope reactions, which gives very high yields and atom efficiency, employs readily available starting material and reagents, allows simple product isolation and the use of green solvents which are easily removed. The copper(I)-catalyzed azide-alkyne cycloaddition (CuAAC) is the most important class of click reactions for the synthesis 1,2,3-triazoles. This reaction generally forms 1,4-substituted products regioselectively [36]. In azide-alkyne click reaction, both azide and terminal alkynes are easy to introduce, extremely stable at standard conditions. They both permit the use of oxygen, water, and biological molecules, allow the condition of organic synthesis and living systems reaction (ex. hydrolysis). [39]. Accordingly, this reaction has been used in a variety of research areas including the synthesis of biomolecules, polymers, and dendrimers, the modification of surfaces etc [40].

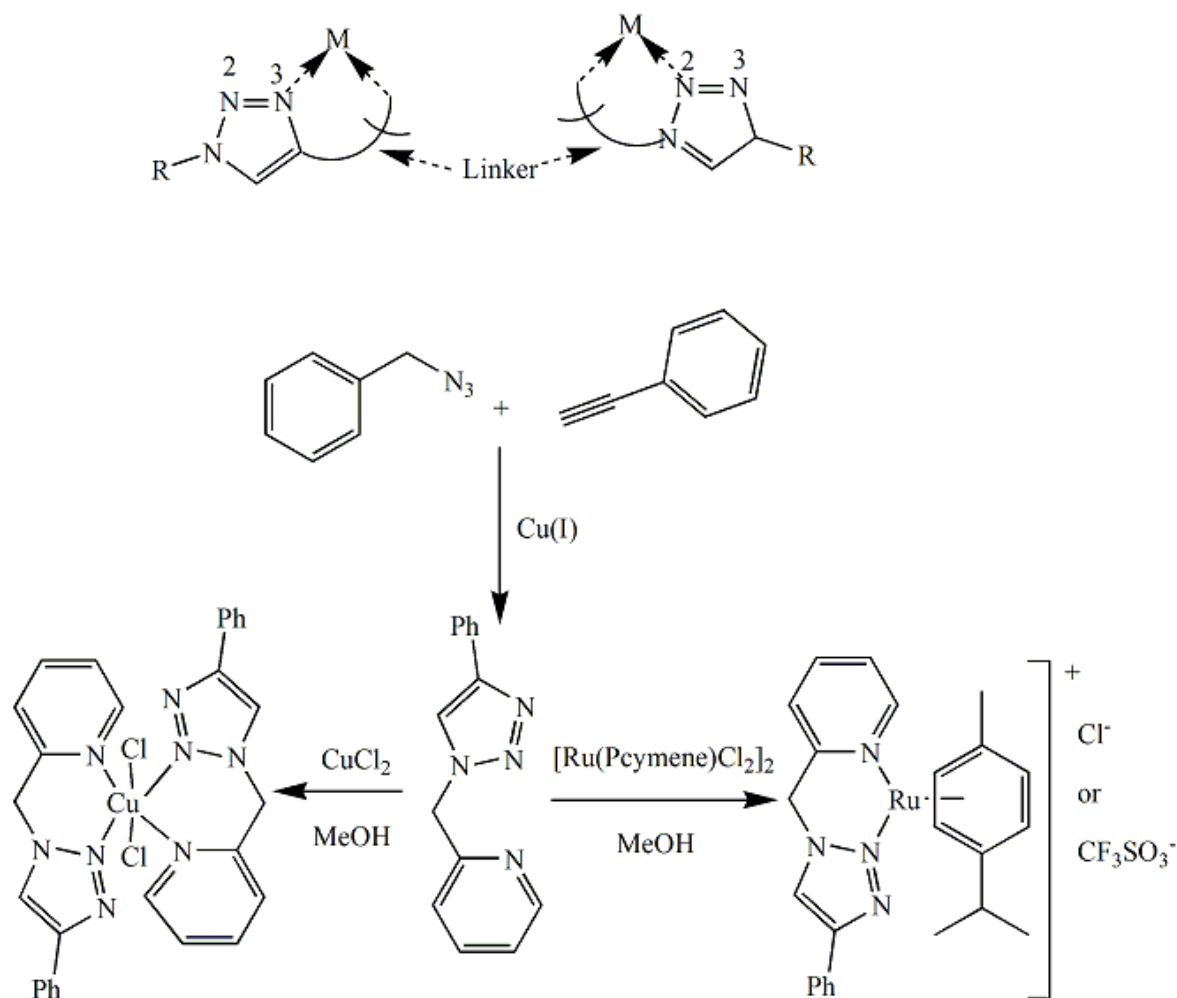
1.3.3 Synthesis of triazole ligands

Among the several synthetic methods, the copper(I)-catalyzed azide-alkyne cycloaddition reaction is one of the most emerging because of its modular properties, includes all the advantages of click reactions (Scheme 1.19). [35, 47].



Scheme 1.19 Copper(I)-catalyzed azide-alkyne cycloaddition reaction.

The important application of this type of chemistry is the synthesis of novel triazole ligands for coordination chemistry [48]. There are several studies which report the synthesis of 1,2,3-triazole ligands and their coordination behavior in the presence of transition metals. Urankar *et al.* synthesized a series of triazole ligands and studied their chelation to Pt(II), Pd(II), Cu(II), Ru(II), and Ag(I) (Scheme 1.20) [45].



Scheme 1.20 Synthesis of triazole ligands and Cu(II) and Ru(II) complexes.

Later on he reported the synthesis and anticancer activities of ruthenium-triazole complexes against human cancer cell mentioning the effects of aquation of the complexes (Figure 1.7) [49].

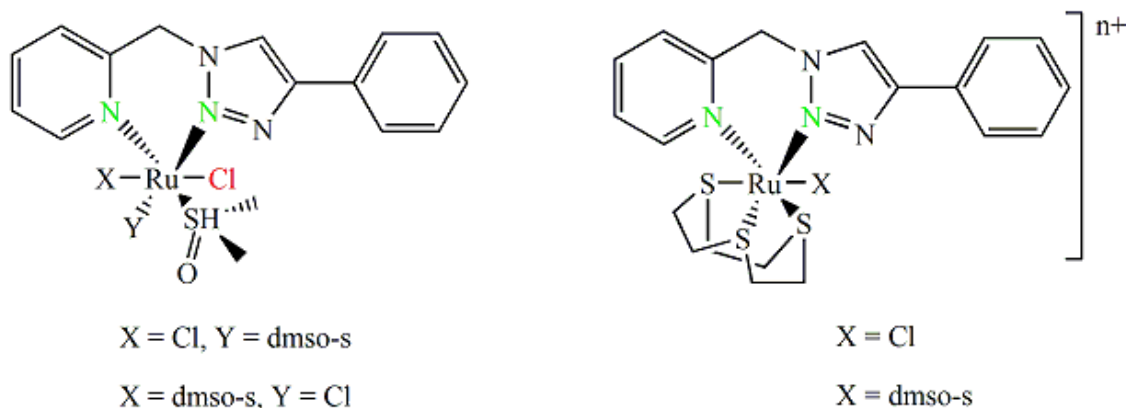
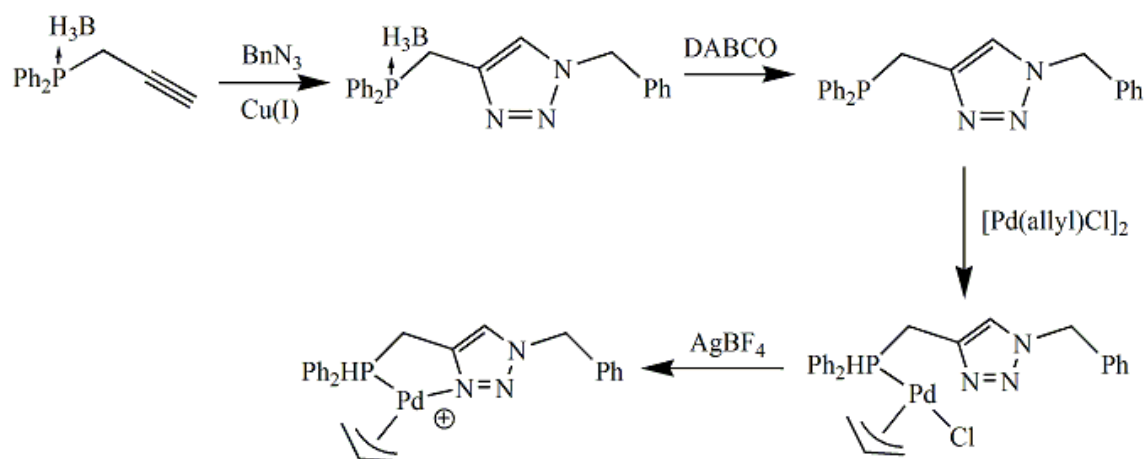


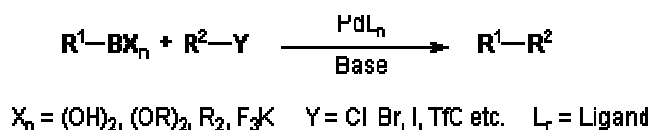
Figure 1.7 Ruthenium-triazole anti-cancer agents.

Among transition metal complexes, palladium-triazole complexes are widely employed as catalysts in cross-coupling reaction, a very powerful and versatile tool for organic synthesis. R.J. Detz *et al.* synthesized a triazole-phosphine bidentate ligand for palladium catalyzed Suzuki-coupling reactions (Scheme 1.21) [50].



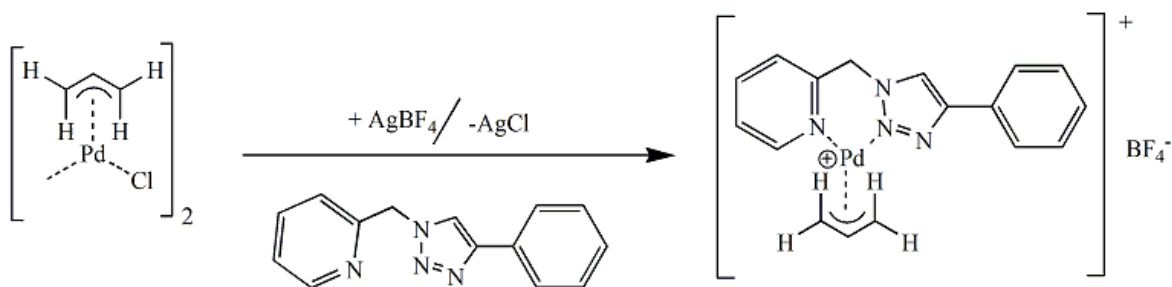
Scheme 1.21 Synthesis of triazole-phosphine ligand and its palladium complex.

By taking the advantages of copper(I)-catalyzed azide-alkyne cycloaddition click reaction, our group has long been involved in the synthesis of triazole ligands and their application in homogeneous catalysis. For example, in 2011 our group reported the synthesis, characterization and catalytic activity of palladium-triazole complexes for Suzuki-Miyaura coupling. Suzuki-Miyaura reaction is a coupling reaction between organic boron compounds and organic halides. This is a simple and versatile C-C bond formation reaction can be extended to various substrates and therefore finds wide application for the synthesis of pharmaceuticals and total synthesis of complex natural products (Scheme 1.22)



Scheme 1.22 Suzuki coupling reaction.

The palladium-allyl complex (Scheme 1.23) containing 2-pyridyl-1,2,3-triazole bidentate ligand displayed good activity in the reaction of aryl bromide with phenyl boronic acid [62].



Scheme 1.23 Preparation of palladium-allyl complex containing 2-pyridyl-1,2,3-triazole ligand.

Latter on we prepared a water-soluble 2-pyridyl-1,2,3-triazole ligand (Figure 1.8) and the *in-situ* catalyst preparation with a 1:1 mixture of ligand and $[\text{Pd}(\eta^3\text{-C}_3\text{H}_5)\text{Cl}]_2$ which provides an efficient catalytic system for the Suzuki-Miyaura (S-M) coupling reactions. The S-M coupling reaction of phenylboronic acid with aryl bromide has been carried out in water phase. Water is used as an important alternative to organic solvents usually employed in coupling reaction because it is nontoxic and inexpensive. The use of water as the solvent in

catalysis allows the additional advantages: prompt catalyst separation and reuse in recycle experiments, and easy recovery of the product by extraction or filtration with an appropriate organic solvent.[63].

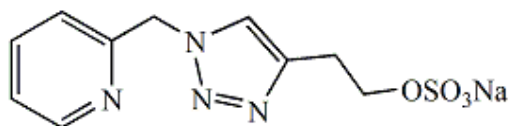


Figure 1.8 Structure of water-soluble ligand.

The success of this aqueous phase reaction encouraged us to perform water/organic phase catalysis of some other industrially important reactions such as biphasic hydrogenations and biphasic hydroformylations.

1.3.4 Biphasic hydrogenation

Hydrogenation is a chemical reaction between molecular hydrogen and a compound, ordinarily in the presence of a catalyst. In organic hydrogenation reactions a hydrogen adds to a double or triple bond. Nearly all organic compounds containing multiple bonds between two atoms can react with hydrogen in the presence of a catalyst. The catalysts most commonly used for hydrogenation reactions are both heterogeneous and homogeneous. Hydrogenation reactions are of great industrial importance. The typical examples of homogeneous catalysts for hydrogenation reaction are Wilkinson or Crabtree's catalyst.

In the 1960s, G. Wilkinson developed a highly active rhodium catalyst called Wilkinson catalyst, $\text{RhCl}(\text{PPh}_3)_3$ for the hydrogenation of alkenes [64]. R.H. Crabtree synthesized an iridium based catalyst for the hydrogenation of mono-, di-, tri-, and tetra-substituted substrates [65]. The structure of Wilkinson and Crabtree's catalysts are given below (Figure 1.9)

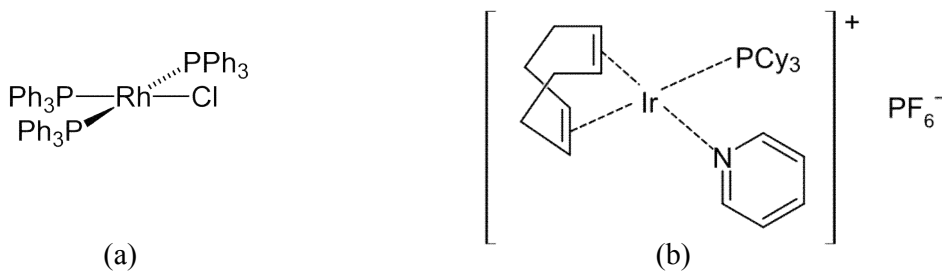
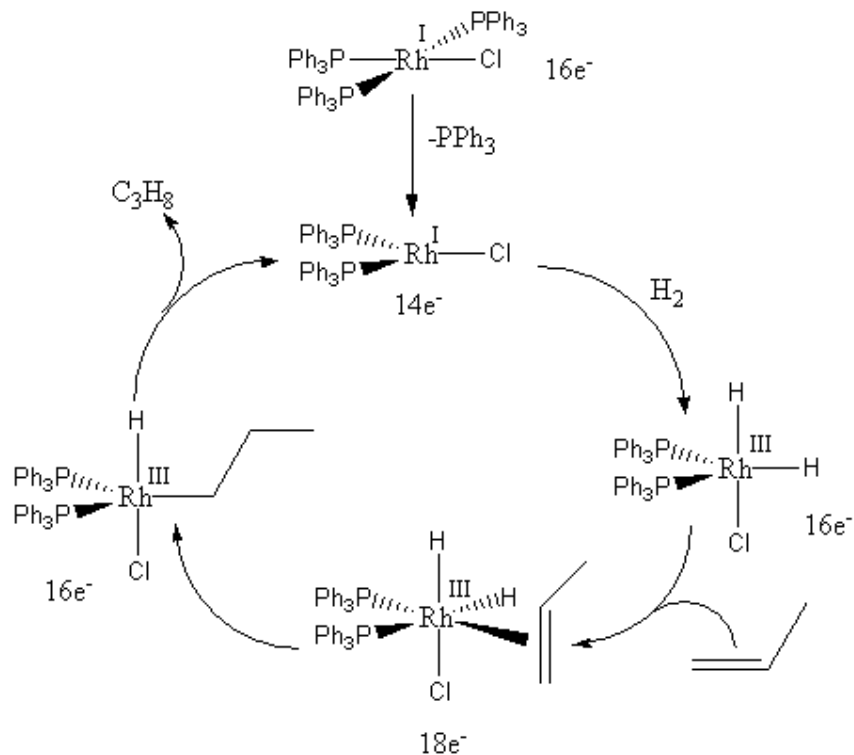


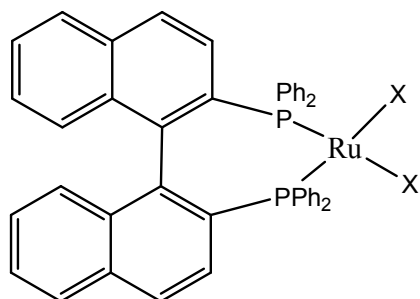
Figure 1.9 Chemical structure of (a) Wilkinson catalyst, and (b) Crabtree's catalyst.

The mechanism of the hydrogenation of Wilkinson catalyst is shown in Scheme 1.24. The catalysis is carried by the dissociation of phosphine ligand followed by the oxidative addition of hydrogen. The alkane product is formed by the alkene coordination, internal insertion, and reductive elimination, respectively[66].

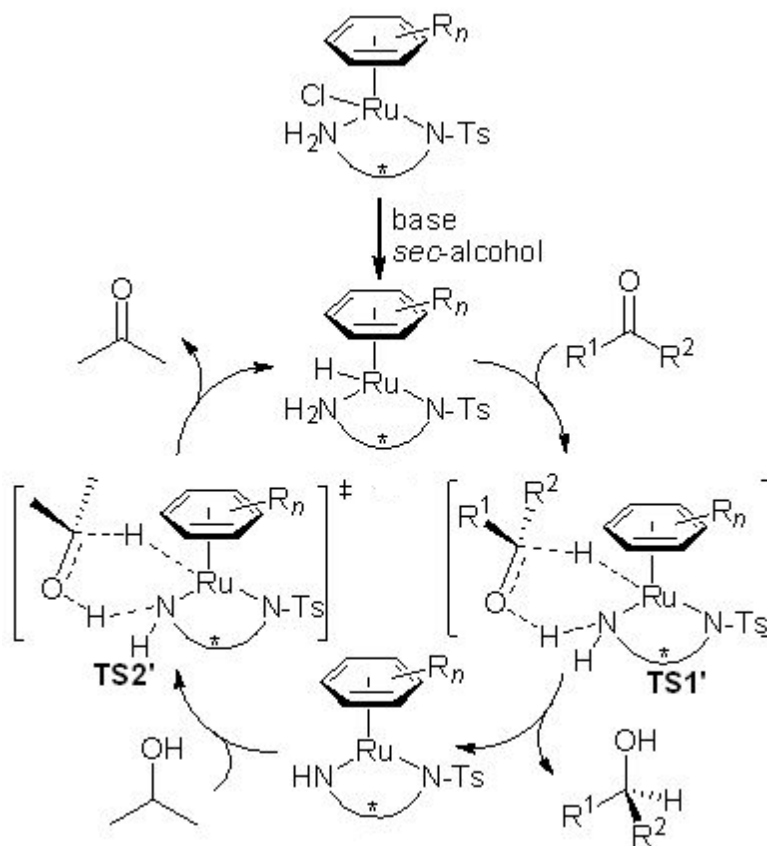


Scheme 1.24 Hydrogenation of propene with Wilkinson catalyst.

The ruthenium organometallic complex is widely used as catalyst for hydrogenation reaction. Ryoji Noyori developed the Ru-BINAP catalyst for asymmetric hydrogenation of ketones with high selectivity in the homogeneous phase[67]. The structure complex is given below:



Bogdan Štefane and Franc Požgan reported the catalysis for the hydrogenation of ketones using a tetra-coordinated ruthenium catalyst [68] (Scheme 1.25).



Scheme 1.25 Mechanism of hydrogenation of ketone catalyzed by a tetra-coordinated ruthenium complex.

The efficiency (selectivity and activity) of the homogeneous hydrogenation reaction largely depends on the nature of the ligands and substrates. The success of homogeneous catalysis in industrial applications is limited because of difficult catalyst separation and reuse. To overcome this issue, the use of biphasic catalysis is at present of great interest because the catalyst is confined in one of the two-phases and the product is in the other phase allowing for a prompt recovery of the product and an easy recycle of the catalyst. Phase separation contributes to the protection of both the substrates/products and the catalyst against side reactions (degradation), thereby resulting in an increased selectivity and less byproducts. In particular, the development of water soluble catalysts for aqueous/organic biphasic reactions

is increasingly attractive [69-70]. The use of water-soluble catalyst in biphasic homogeneous catalysis is in line with the fundamental principles of green chemistry. This provides an inexpensive answer to the challenge of preserving resources, making the process more environmentally friendly.

Nowadays water-soluble catalysts are increasingly employed either in water or in water/organic solvent biphasic system. The most commonly employed catalysts in water/organic phase biphasic systems are metal complexes modified with water soluble phosphines, such as TPPTS (Figure 1.10) (triphenylphosphine-3,3',3''-trisulfonic acid trisodium salt) which, for instance, is employed in the renowned OXEA (former Ruhrchemie/Rhône-Poulenc) hydroformylation process [71-73].

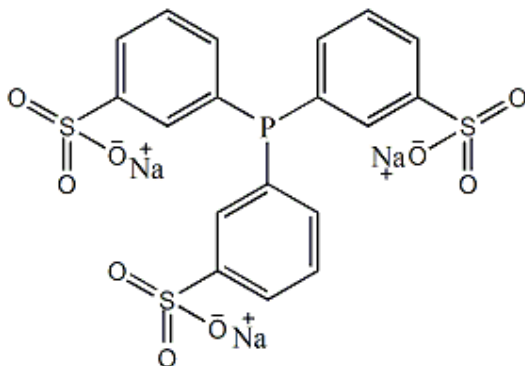


Figure 1.10 Structure of triphenylphosphine-3,3',3''-trisulfonic acid trisodium salt.

In recent years, new species bearing different hydrophilic groups such as -COOH, -OH, and amino acids have been used as ligands in combination with transition metal species in order to obtain catalysts active in water. For example, S. Paganelli *et al.* tested the catalytic activity of a system prepared by *in situ* mixing of water soluble thioligands (*L*)-Cysteine and (*S*)-Captopril (Figure 1.11) with [Rh(CO)₂(acac)] and [Ir(COD)Cl]₂ in the aqueous biphasic hydrogenation of 2-cyclohexen-1-one, *trans*-cinnamaldehyde and [3-(1,3-benzodioxol-5-yl)-2-methylpropenal] [74].

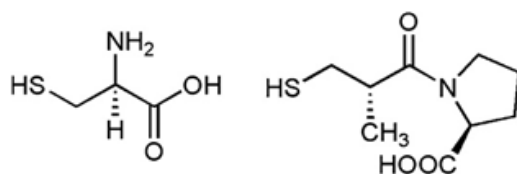
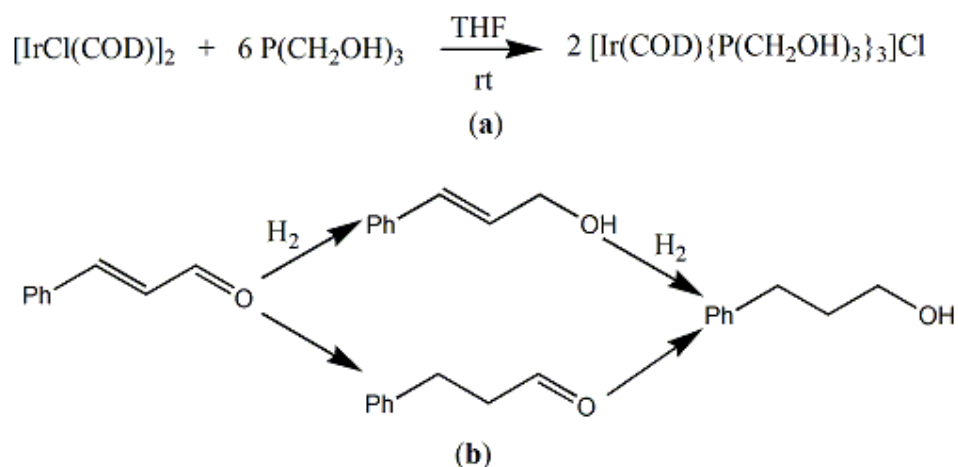


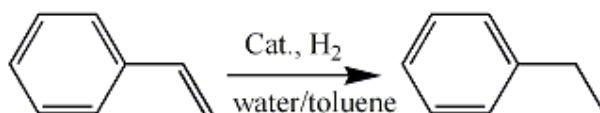
Figure 1.11 Water soluble ligands (*L*)-Cysteine and (*S*)-Captopril.

A. Fukuoka and his co-workers performed the biphasic hydrogenation of cinnamaldehyde catalyzed by Ir and Rh preformed catalysts containing a highly water-soluble tris(hydroxymethyl)phosphine, $P(CH_2OH)_3$ ligand (Scheme 1.26)[75].



Scheme 1.26 (a) Synthesis of the catalyst, (b) biphasic hydrogenation of cinnamaldehyde.

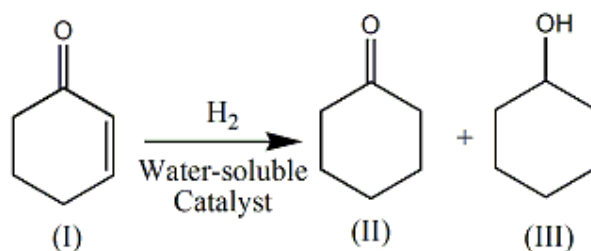
The hydrogenation of styrene produced ethylbenzene (Scheme 1.27). Styrene is widely used as a standard to test the activity of many catalytic systems.



Scheme 1.27 Hydrogenation of styrene.

In contrast, the hydrogenation 2-cyclohexen-1-one (Scheme 1.28) is an important reaction in the chemical industry. The most important product formed by this reaction is

cyclohexanone(II), which is a key intermediate for the production of caprolactam for nylon 6 and of adipic acid for nylon [76].

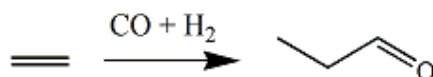


Scheme 1.28 Hydrogenation of 2-cyclohexen-1-one.

1.3.5 Biphasic hydroformylations

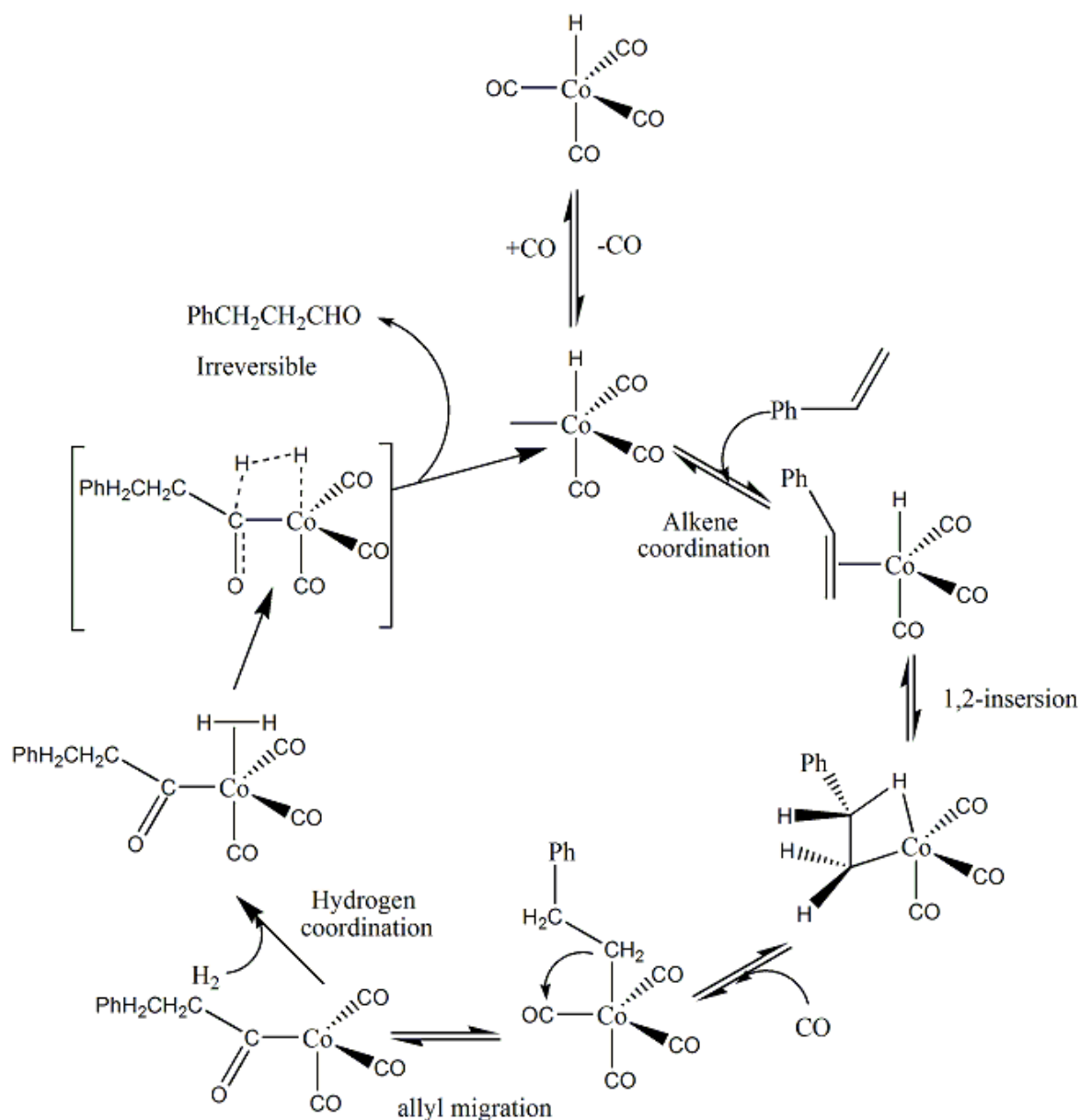
Hydroformylation also known as oxo synthesis or oxo process, is a general reaction in which the introduction of both hydrogen and formyl group into the olefin bonds is carried out. This industrial process catalyzed by homogeneous catalysts is widely used for the synthesis of aldehydes from alkenes [77].

Hydroformylation was first discovered by Otto Roelen in 1938 during an investigation on the origin of oxygenated products occurring in cobalt catalyzed Fischer-Tropsch reactions. Roelen's observation that the reaction of ethylene with H₂ and CO produced propanal, marked the beginning of hydroformylation (Scheme 1.29). [78-79].



Scheme 1.29 Synthesis of propionic aldehyde through hydroformylation of ethylene.

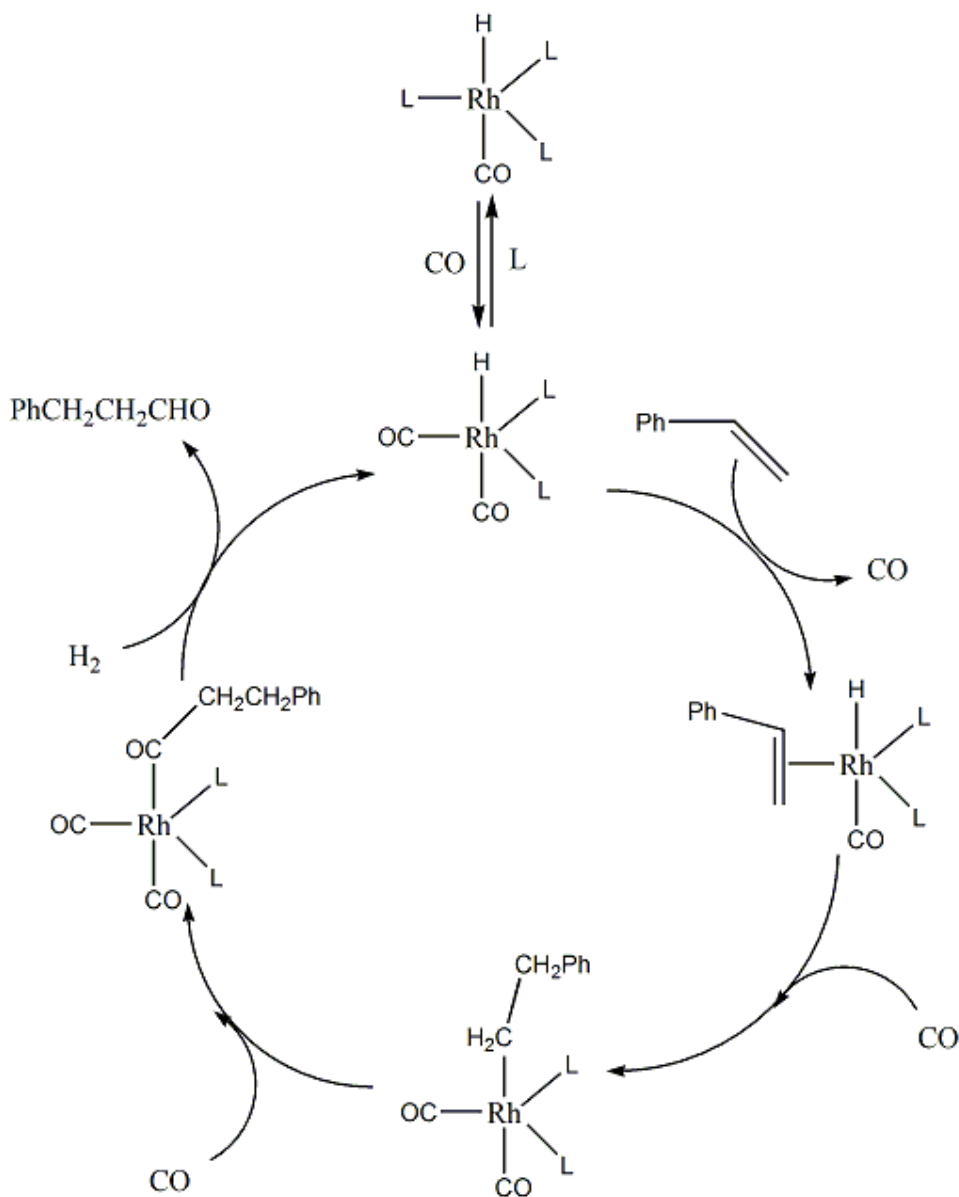
Roelen's original hydroformylation involved the use of cobalt salts Co₂(CO)₈ that, under H₂/CO pressure, produce HCo(CO)₄ as the active catalyst. In 1960 and 1961 Heck and Breslow proposed the accepted general mechanism for hydroformylation [80-81] (Scheme 1.30).



Scheme 1.30 General mechanism for alkene hydroformylation reaction catalyzed by CoH(CO)_4 .

In the 1958's, the rhodium catalyzed hydroformylation is started. The initial catalyst were RhCl_3 or $\text{Rh/Al}_2\text{O}_3$. In the 1960s, G. Wilkinson and his co-workers developed highly active rhodium catalyst, *trans*- $\text{RhX(CO)(PR}_3)_2$, ($\text{X} = \text{halogen}$, $\text{R} = \text{aryl}$) for the hydroformylation of alkenes [82]. The first Wilkinson catalyst, $\text{RhCl(PPh}_3)_3$ is highly active for hydrogenation but the chloride ion acts as inhibitor of hydroformylations [83]. Therefore, the formation of hydrido-species is carried out by replacing chloride ligand by H^- upon the addition of hydrogen chloride acceptor. The hydrido-species then exchange a phenyl ligand by CO to

form active catalytic species, $\text{RhH}(\text{CO})_2(\text{PPh}_3)_2$. The catalytic cycle by a generic rhodium catalyst, $[\text{RhH}(\text{CO})_2(\text{PPh}_3)_2]$ is given below (Scheme 1.31)



Scheme 1.31 General mechanism for alkene hydroformylation reactions catalyzed by $[\text{RhH}(\text{CO})\text{L}_3]$. Where, $\text{L} = \text{PPh}_3$.

There are many different approaches which aim to make effective hydroformylations. Particularly, water-organic biphasic methods have been employed for preferential catalyst separation [84-85]. In association, the use of water as a solvent makes considerable interest

from an environmental and economical points of view. The organometallic complexes containing water soluble ligands could be the best tool for biphasic systems. [86-87]

In the past, the biphasic hydroformylation of olefine using highly water-soluble rhodium polyethylene glycolate catalyst were reported by Uwe Ritter *et. al.*, [88]. The use of *in situ* catalysts prepared by mixing $\text{Rh}(\text{CO})_2(\text{acac})$ and naturally available water-soluble ligand was reported by S. Paganelli [84-85]. The biphasic hydroformylation of styrene with $\text{Rh}(\text{CO})_2(\text{acac})$ -*L*-tryptophan experienced difficulties in catalyst separations even the ligand is water soluble. The complete leaching of catalyst into organic phase indicates the weak metal-ligand coordination in the aqueous phase. However, rhodium coordinated with thiolic ligands showed effective hydroformylations [89] indicating the greater interaction of sulphure containing ligands with “soft” metal rhodium.

1 4 Introduction to anticancer activity of ruthenium triazole complex

Chemists have been considered with the synthesis of triazoles especially 1,2,3-triazole containing molecules because of their important biological activities. In fact, the properties possessed by 1,2,3-triazoles make them pharmaceutically important molecules. These triazoles have high dipole moment and are able to give rise to hydrogen bond formation as well as to dipole-dipole and π stacking interactions which permit the easy binding to the biological targets and improve their solubility [29]. The search for biologically active and potential pharmaceuticals containing 1,2,3-triazole moieties is still going on. For examples, the structure of anticancer compound carboxyamidotriazole (CAI) [30], β -lactum antibiotic tazobactam and cefatrizine [31] are shown in Figure 1.12.

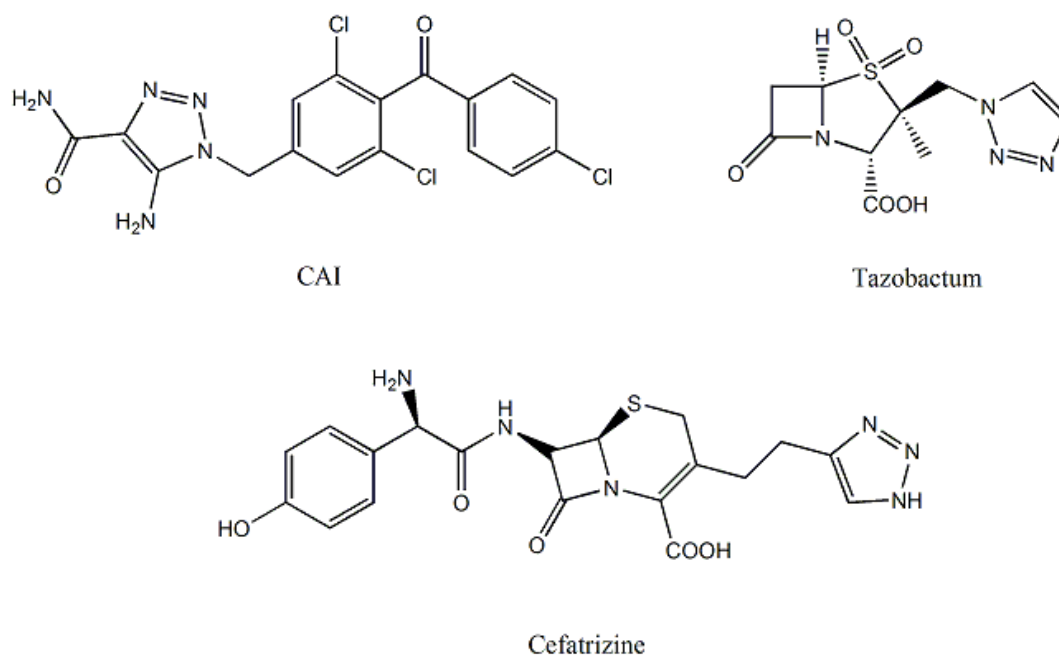


Figure 1.12 Structure of the potential pharmaceutical based on 1,2,3-triazoles.

The heterocyclic compounds containing triazole moiety widen the range of therapeutically interesting drugs including anti-inflammatory, sedatives, antimicrobial and antifungal activity.

Some important triazole based drugs available for clinical uses are shown in the Table 1.1. [32]. These anti-inflammatory active molecules comprise benzoxazolinone based 1,2,3-triazoles (**1**) [33] and bis-heterocycles encompassing 2-mercapto benzothiazole and 1,2,3-triazoles (**2**) (Figure 1.13) [34].

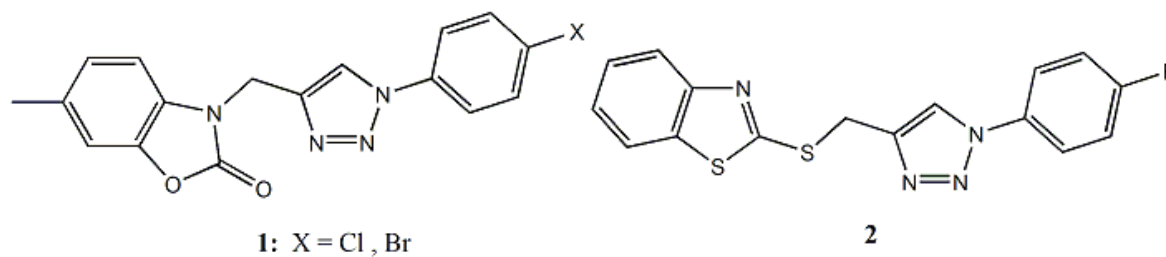
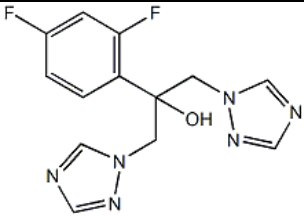
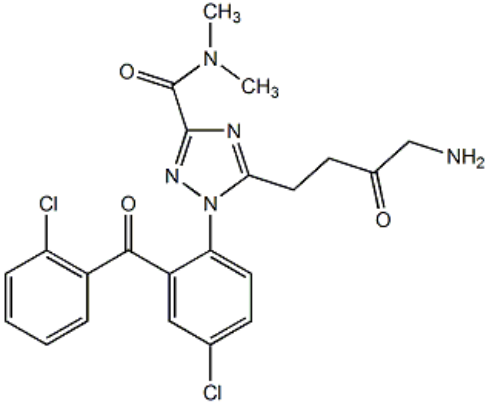
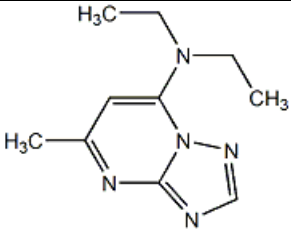
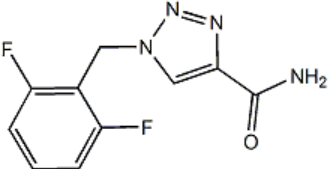
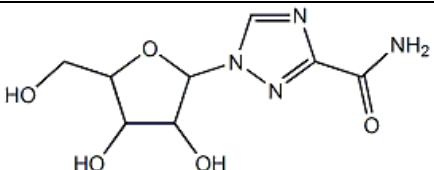


Figure 1.13 Examples of anti-inflammatory active molecules containing 1,2,3-triazole moiety.

Some important triazole based drugs available for clinical uses are shown in the Table 1.1. [32].

Table 1.1. Triazole based drugs

Drugs	Structure	Therapeutic uses
Fluconazole		Antifungal
Rilmazafone		Anxiolytic
Trapidil		Antihypertensive Vasodilator
Rufinamide		Antiepileptic
Ribavirin		Antiviral

During 1960's, American scientist Barnet Rosenberg identified that the electro-generated platinum (II) species stop the growth of *E. coli*. This observation encourage inorganic

chemists to test anticancer activity of *cis*-[Pt(NH₃)₂(Cl)₂] known as cisplatin which was first prepared by Michele Peyrone in 1845. In 1978 cisplatin reached the clinical approve and became the most widely used anticancer drug. Since the discovery of cisplatin, thousands of other metal complexes have been synthesized and screened for antitumor activity. However, only other 2 complexes reached the clinical approval, namely carboplatin (1993) and oxaliplatin (2003)(Figure 1.14).

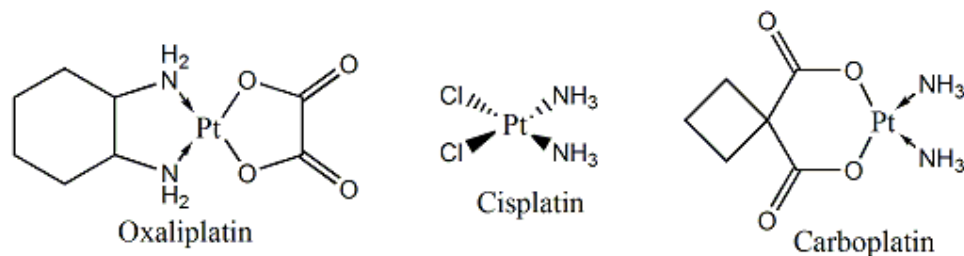


Figure 1.14 Structure of oxaliplatin, cisplatin, and carboplatin.

Although these heavy metal agents are active against a variety of cancers, their use is associated with severe side effects and is limited by primary and acquired resistance to this agent. These complexes damages the DNA, kill the cell by cross-linking with the DNA and disrupted replication and transaction. The cross-linking ability is not selective only for cancer cell but also the healthy cell. That's why sometime the use of these drug as bad or worse than the disease [91]. This has led to an ongoing quest for the discovery of non-platinum metals that may extend the spectrum of activity of metal-based drugs. Among these, ruthenium (Ru) appears to be the most promising. Indeed, in recent years ruthenium-based molecules have emerged as promising antitumor and antimetastatic agents with potential uses in platinum-resistant tumors or as alternatives to platinum. Ruthenium compounds possess unique biochemical features thus allowing them to accumulate preferentially in neoplastic cells and to convert to their active state only after entering tumor cells. The first property seems to correlate with its ability to interact with transferrin. It has been proposed that transferrin–ruthenium complexes are actively transported into neoplastic tissues containing high transferrin receptor densities. The latter, conversely, depends on its ability to be selectively reduced where there is a lower oxygen content and higher acidity compared to normal tissues, such as in hypoxic tumors. A lot of ruthenium complexes have been tested for their anticancer properties without knowing their mode action. The two ruthenium complexes

appeared clinical trial are NAMI-A and KP1019 (Figure 1.15) [92] Both of these complexes have similar structure with Ru^{3+} oxidation state and coordinated with chloride and heterocyclic ligand. But the mode of action of these ruthenium drug is different. KP1019 is a potential primary anticancer drug where NAMI-A acts as antimetastatic agents.

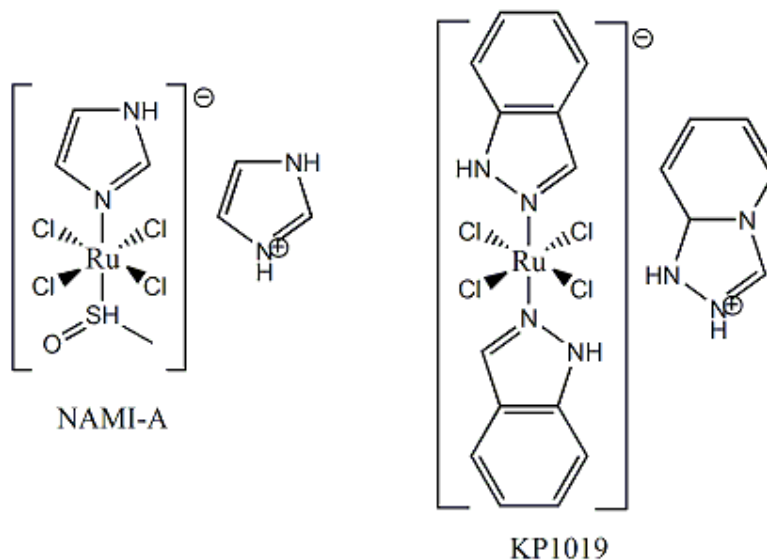


Figure 1.15 Structure of NAMI-A and KP1019.

P. J. Sadler reported a new class of Ru-arene complexes were found to have cytotoxic effect on various human cancer cell [93]. According to our literature review only few ruthenium-triazole complexes are tested for anticancer properties. I. Bratsos et al. synthesized the Ru-triazole ligand complexes (Figure 1.16) and tested against human epithelial cell (HEp-2) and human lung cancer cell (A-549) [47]. These metal complexes displayed a good cytotoxic activity .

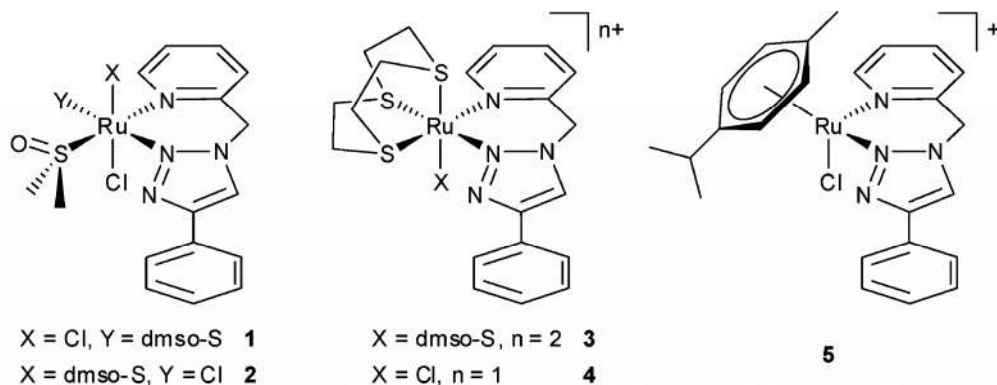


Figure 1.16 Structure of some Ru-triazole ligand complexes.

The potentiality of these complexes is greatly influenced by the nature of ligands. The introduction of water-soluble part into triazole ligands might have positive effects to leave non chelating ligand (-Cl) and make available site for DNA. These has led to an interest for the discovery of ruthenium-water soluble triazole ligand anticancer drug. Since our group has long been involved in the synthesis of triazole ligand for homogeneous catalysis, we synthesized some water soluble triazole ligands and tested the anticancer and antimetastatic properties of their ruthenium complexes (Figure 1.17). The target cell lines are A431 (human cervical carcinoma cell), BxPC3 (pancreatic cancer cell), A549 (human lung cancer cell), HCT-15 (colon cancer cell).

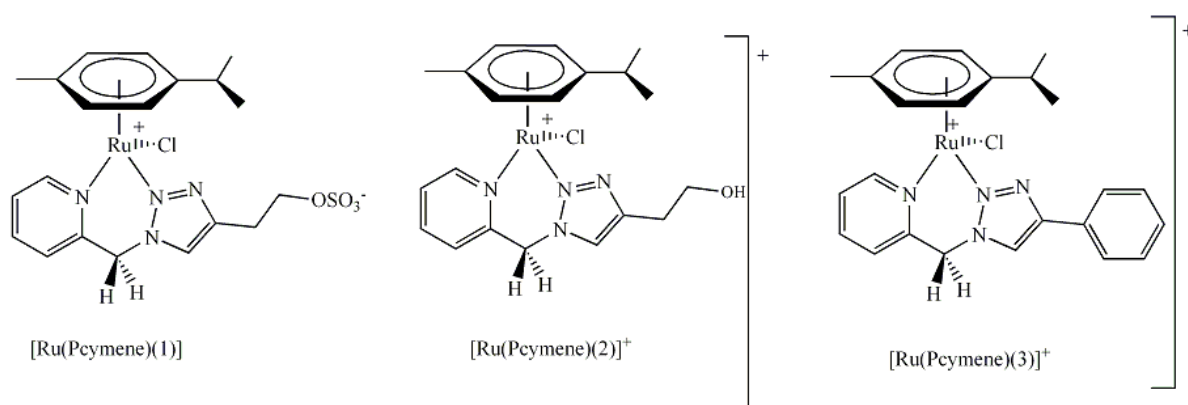
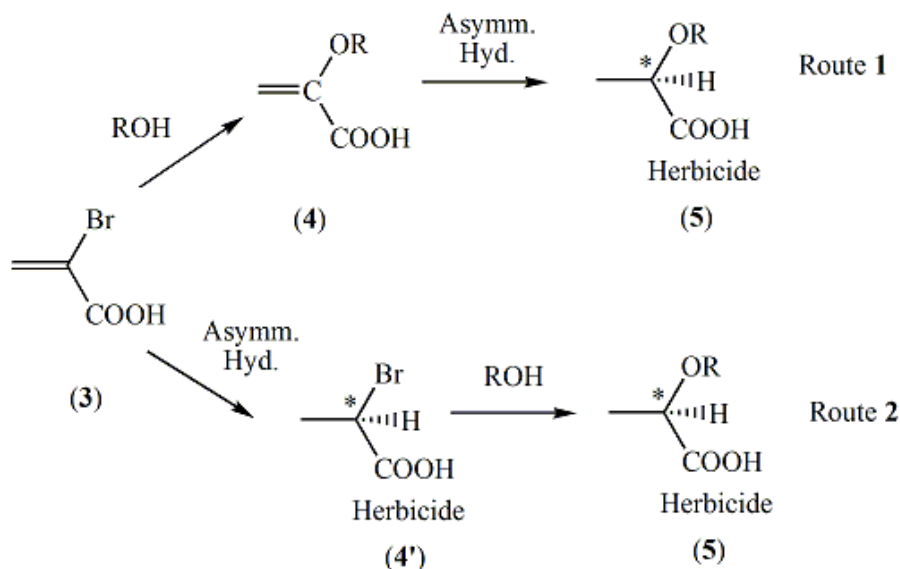
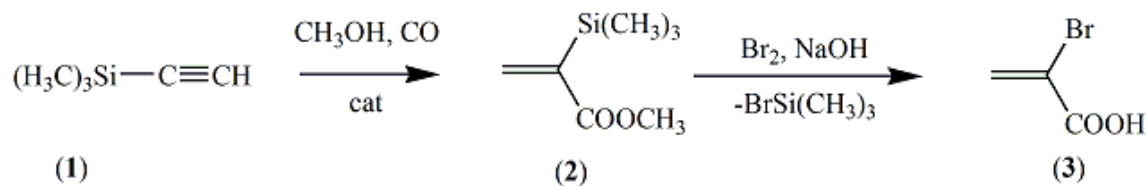


Figure 1.17 Chemical structure of Ru-triazole complexes used as anticancer and anti metastatic agents against human cancer cell.

2. SCOPE OF THE THESIS

The purposes of this thesis work are as follows:

1. Development of alternative methods for the stereoselective synthesis of agrochemical intermediates. The stereoselective preparation of 2-bromoacrylic acid and its methyl ester derivatives as important intermediates for the synthesis of enantiomerically enriched aryloxypropionic herbicides has been carried out (Scheme 2.1). In this research work, the proposed scheme for the enantioselective synthesis of (*R*)- and (*S*)-aryloxyphenoxypionic acids is based on a multi step strategy reported in Scheme 2.1.

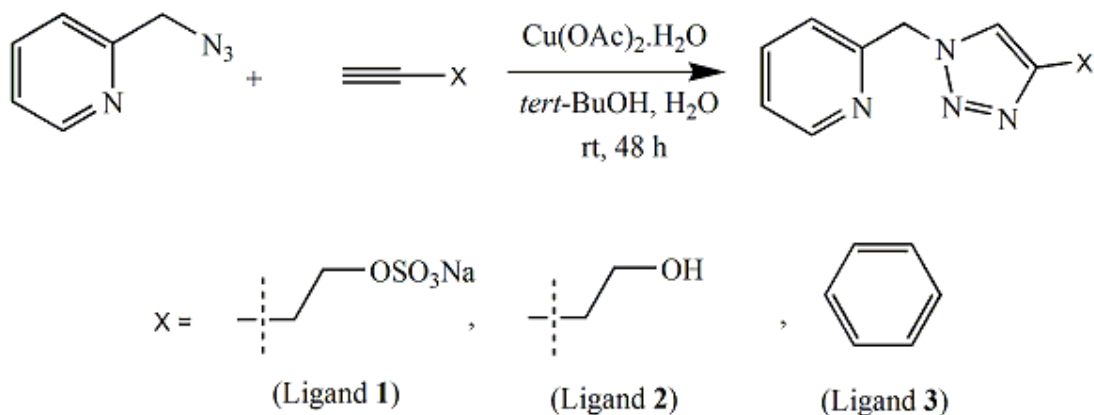


Scheme 2.1 Proposed synthetic scheme for enantiomerically enriched herbicides.

The first step of proposed synthetic scheme (Route 1) is the carbonylation of trimethylsilylacetylene, a relatively inexpensive and easily available reagent using Drent's catalyst [22]. This reaction may yield both linear and branched isomer but only branched isomer is prochiral. The second step is bromodesilylation of branched isomer [23], the third step involves the reaction between vinyl α -bromide bearing an activating group adjacent to the sp^2 -carbon with phenol or alcohol in K_2CO_3 -acetone medium [24] produced branched-substituted product (4) and finally the asymmetric hydrogenation [20] of product (4) to give the chiral 2-aryloxypropanoic acid or its methyl ester. The synthesis of enantiomerically enriched herbicides can be carried out by asymmetric hydrogenation of (3) followed by nucleophilic substitution reaction (Route 2).

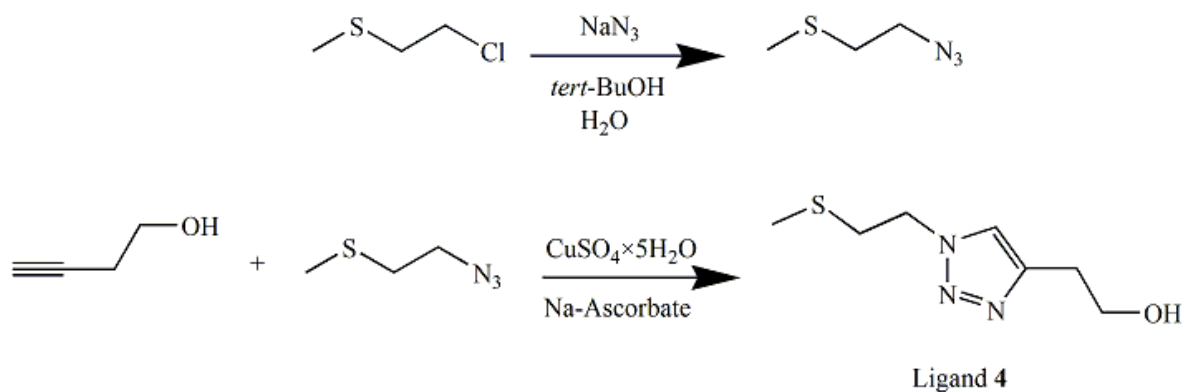
2. The synthesis of a series of new water-soluble triazole ligands using copper(I)-catalyzed azide-alkyne cycloaddition (CuAAC) reaction was tested. By changing the substituents in triazole moiety the ligand structure will be modified to modulate the properties. The

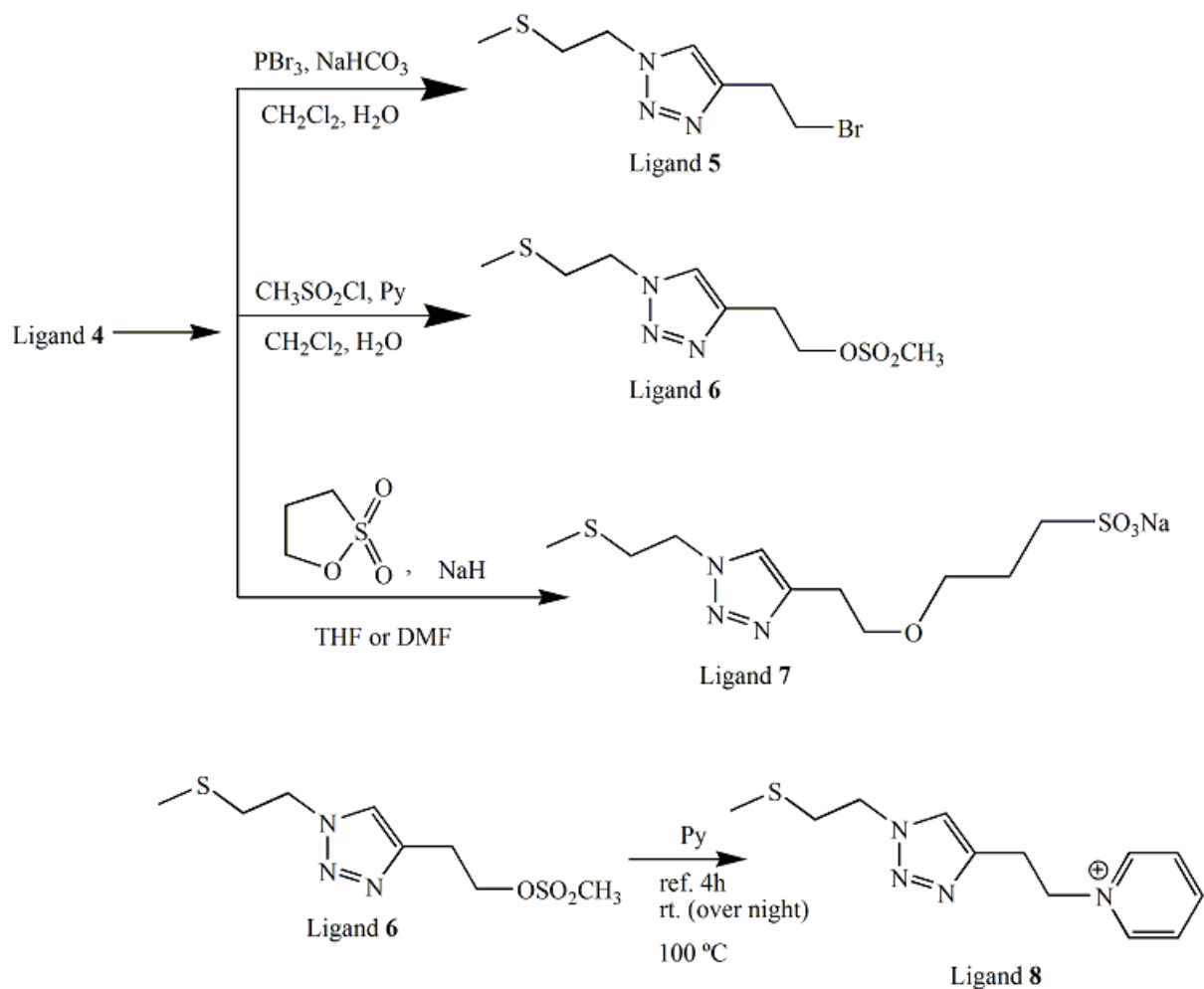
synthesized ligands will include pyridyl-triazole (Scheme 2.2) and methyl(thio)ethyl-triazole ligands (Scheme 2.3). The catalyst used for pyridyl-triazole ligand synthesis is $\text{Cu}(\text{OAc})_2$ while for methyl(thio)ethyl-triazole ligands the catalyst is a mixture of CuSO_4 and Na-ascorbate in *tert*-BuOH/ H_2O (4:1) as solvent.



Scheme 2.2 Synthesis of pyridyl-triazole ligands (**1**, **2**, and **3**).

The short synapses of the synthesized methyl(thio)ethyl-triazoles are shown below (Scheme 2.4). The characterization of the synthesized ligands will be carried out by NMR spectroscopy.





Scheme 2.3 Synthesis of methyl(thio)ethyl-triazole ligands (4, 5, 6, 7 and 8).

3. The synthesis of triazole-transition metal complexes using standard protocol. For this at first we will synthesis precursor metal complexes such as $[\text{Ru}(p\text{-cymene})\text{Cl}_2]_2$, $[\text{Rh}(\text{COD})\text{Cl}]_2$, and $[\text{Pd}(\eta^3\text{-C}_3\text{H}_5)\text{Cl}]_2$ (Figure 2.1).

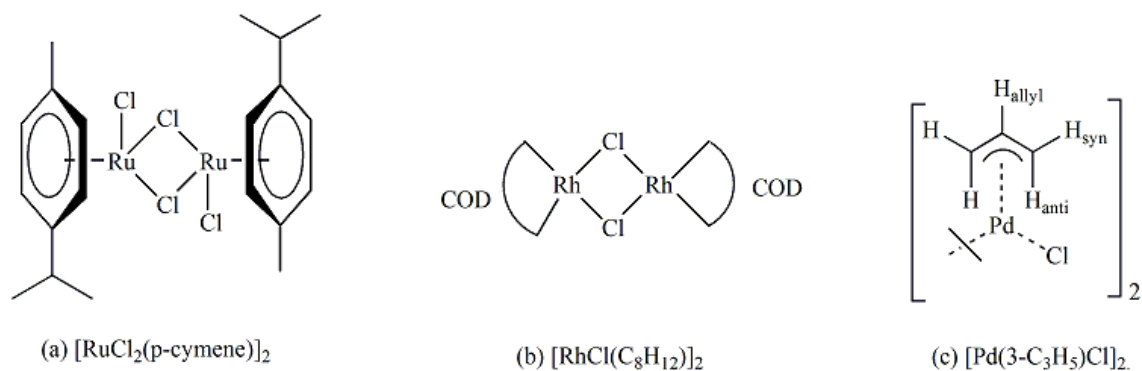


Figure 2.1 Structure of precursor metal precursors: (a) $[\text{Ru}(\eta^6\text{-cymene})\text{Cl}_2]_2$, (b) $[\text{Rh}(\text{COD})\text{Cl}]_2$, and (c) $[\text{Pd}(\eta^3\text{-C}_3\text{H}_5)\text{Cl}]_2$.

These metal precursors will be employed for the synthesis of $[\text{RuCl}(\eta^6\text{-p-cymene})(\text{ligand } \mathbf{1})]$, $[\text{RuCl}(\eta^6\text{-p-cymene})(\text{ligand } \mathbf{2})]\text{Cl}$, $[\text{RuCl}(\eta^6\text{-p-cymene})(\text{ligand } \mathbf{3})]\text{Cl}$, and (d) $[\text{Pd}(\eta^3\text{-C}_3\text{H}_5)(\text{ligand } \mathbf{8})](\text{CH}_3\text{SO}_3)_2$ according to synthetic protocol. The structure of the synthesized metal-triazole complexes are given below (Figure 2.2). These complexes will be characterized by FT-IR, NMR, and ESI-MS spectroscopy.

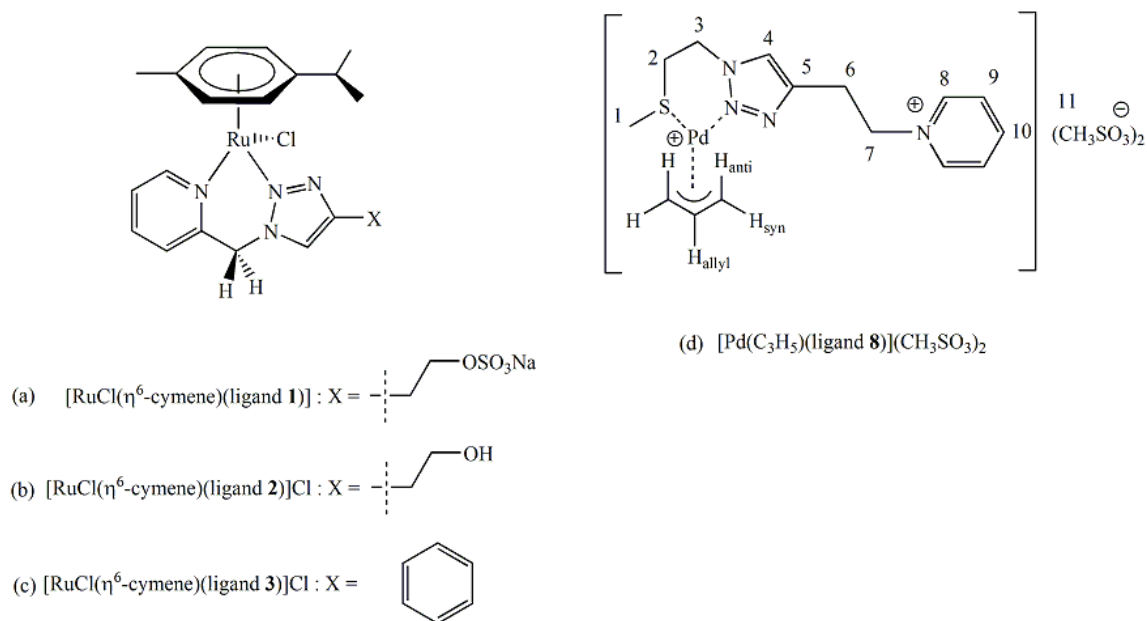
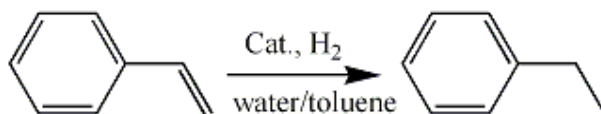
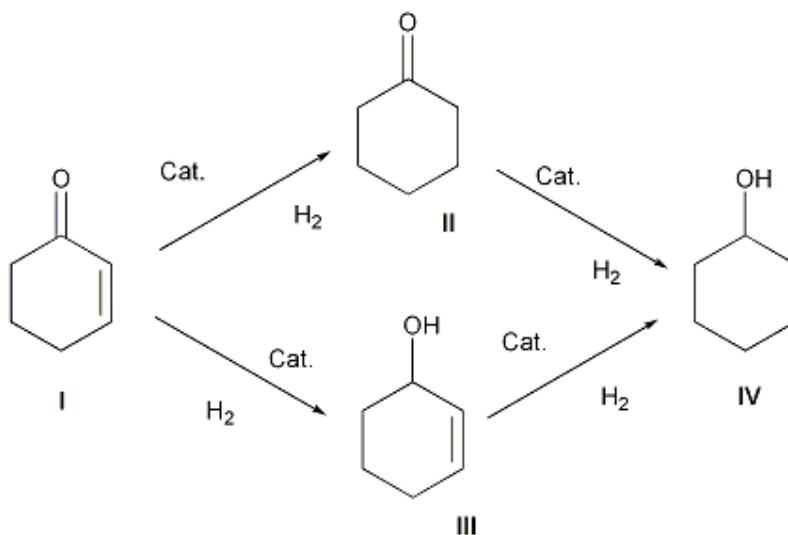


Figure 2.2 Structure of metal-triazole complexes: (a) $[\text{RuCl}(\eta^6\text{-cymene})(\text{ligand } \mathbf{1})]$, (b) $[\text{RuCl}(\eta^6\text{-cymene})(\text{ligand } \mathbf{2})]\text{Cl}$, (c) $[\text{RuCl}(\eta^6\text{-cymene})(\text{ligand } \mathbf{3})]\text{Cl}$ and (d) $[\text{Pd}(\eta^3\text{-C}_3\text{H}_5)(\text{ligand } \mathbf{8})](\text{CH}_3\text{SO}_3)_2$.

Application of the metal-triazole complexes in homogeneous catalysis either performed or *in-situ* (Scheme 2.4 & 2.5) will be tested, particularly in Suzuki-Miyaura reaction, biphasic hydrogenation and hydroformylation reaction in order to study the easy preparation of catalyst, adaptability towards different substrates, selectivity towards interesting product and the possibility of efficient recycling. Comparison of the activity of these catalysts with previously reported (other commercially available) catalyst will be reported.

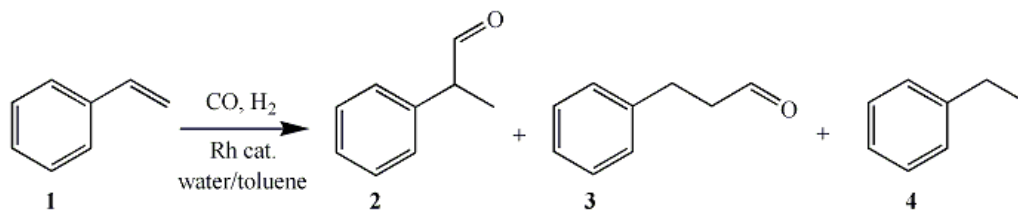


(a) Hydrogenation of styrene.



(b) Hydrogenation of 2-cyclohex-1-ene.

Scheme 2.4 Biphasic hydrogenation of styrene and 2-cyclohex-1-ene.



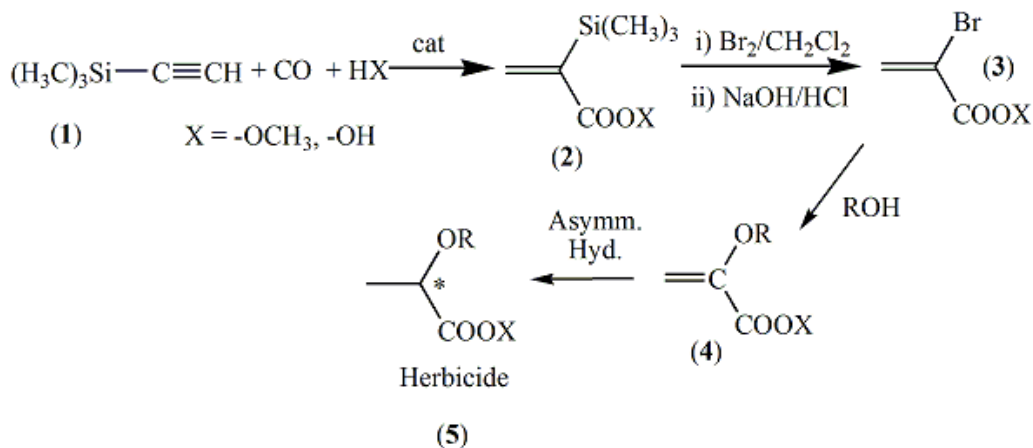
Scheme 2.5 Biphasic hydroformylation of styrene.

4. The application of synthesized transition metal complexes as anticancer and antimetastatic agents against human cancer cells such as cervical cancer cell, pancreatic cancer cell, human lung cancer cell, colon cancer cell etc will be investigated.

THE DEVELOPMENT OF AN INNOVATIVE PROCESS FOR THE STEREOSELECTIVE SYNTHESIS OF AGROCHEMICAL INTERMEDIATES

The palladium catalyzed carbonylation of terminal alkynes is a strong tool for the synthesis of important intermediates such as α,β -unsaturated carboxylic acids [119-120]. It is interesting to point out that enantiomers of 2-arylpropanoic acids are widely used for many different applications. In fact (*S*)-enantiomers are the biologically active species in many different nonsteroidal anti-inflammatory drugs (NSAIDs), while (*R*)-enantiomers of 2-aryloxypropanoic acids are utilized as herbicide [10]; in addition, (*R*)-2-(4-chlorophenoxy)propanoic acid is an anti-cholesterol [121-122]. Thus the preparation of optically pure enantiomers is extremely important.

In our present thesis work, Chapter 3 outlined the development of the alternative method for the synthesis of 2-bromoacrylic acid and its methyl ester derivatives, important intermediates for the synthesis of enantiomerically enriched aryloxypropionic compounds employed as herbicides, pharmaceuticals, etc. (Scheme 3.1).



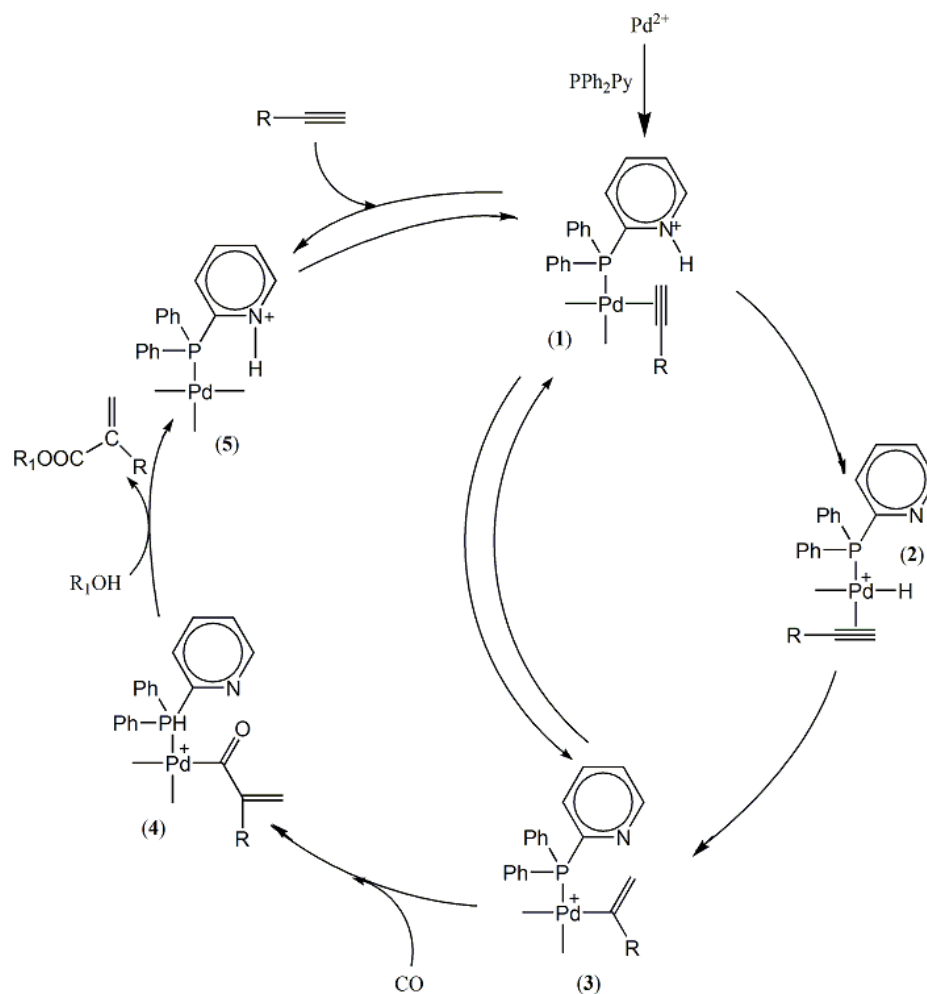
Scheme 3.1 Synthetic scheme for enantiomerically enriched herbicides.

2-(trimethylsilyl)acrylic acid and its methyl esters have been synthesized *via* carbonylation of commercially available trimethylsilylacetylene, in the presence of the readily available catalytic system obtained *in situ* from $\text{Pd}(\text{OCOCH}_3)_2/\text{CH}_3\text{SO}_3\text{H}/2$ -(6-methyl)(diphenylphosphine)pyridine [22].

The carbonylation reaction may give both branched and linear products. The branched isomer is of our interest. Reactions were carried out at 60-80 °C; methoxycarbonylation reactions allow to obtain methyl 2-(trimethylsilyl)acrylate in good conversions (ca. 93%) and with a branched/linear ratio 95/5, whereas hydroxycarbonylation reactions give 2-(trimethylsilyl)acrylic acid with lower conversions and selectivities (ca. 53%, and 93/7 respectively). We studied the effects of various reaction parameters (for example, phosphine/catalyst, acid/catalyst, pressure, temperature, and reaction time) on the conversion and selectivity of the carbonylation reaction. Methyl 2,3-dibromo-2-(trimethylsilyl)propanoate is easily achieved by reaction of methyl 2-(trimethylsilyl)acrylate with bromine in dry dichloromethane [23]. The bromodesilylation of 2-(trimethylsilyl)acrylate followed by acid-base treatment gives 2-bromoacrylic acid (**3**) in good yield (ca. 90%).

3.1 RESULTS AND DISCUSSION

In the early 1990's, E. Drent *et al.* developed a homogeneous palladium catalyst for the carbonylation of terminal alkynes, prepared by mixing palladium acetate ($\text{Pd}(\text{OCOCH}_3)_2$), methanesulphonic acid ($\text{CH}_3\text{SO}_3\text{H}$) and 2-(diphenylphosphino)pyridine (PPh_2Py). They studied the methoxycarbonylation of propyne obtaining a high value of TOF (40000 h^{-1}) and good selectivity towards the branched isomer, methyl methacrylate (98.9%) [22]. By substituting the 2-(diphenylphosphino)pyridine with triphenylphosphine in the catalytic system, they obtained comparatively lower TOF values (10 h^{-1}) and only moderated selectivity towards the branched methyl methacrylate (89%). This result indicates that the pyridine ring of 2-(diphenylphosphino)pyridine plays a key role in the Drent's catalytic system.



Scheme 3.2 Mechanism of the formation of vinyl intermediate followed by proton transfer.

The pyridine nitrogen transfers the proton from methanesulphonic acid to the coordinated alkyne. The transfer can be in two ways (Scheme 3.2): i) the proton transfer from pyridine nitrogen (1) to the palladium center to form hydride complex (2), from which it transferred into the coordinated alkyne, or ii) the proton is directly transferred from the pyridine nitrogen into the coordinated alkyne. The same vinyl intermediate (3) is formed in both cases. Currently there is no evidence to accept or reject any one of the two concepts, but it is no doubt that the pyridine nitrogen plays a key role in the carbonylation reaction [22, 27]. Computational studies by L. Crawford *et al.* suggest that the catalytic cycle starts with the transfer of proton from 2-(diphenylphosphino)pyridine into the coordinated alkyne [28].

Furthermore, it is observed that if the 2-(diphenylphosphino)pyridine is substituted with 2-(6-methyl)(diphenylphosphino)pyridine, the TOF reaches values up to 50000 h⁻¹ and the selectivity towards the methyl methacrylate further increases to 99.95% [94]. The chemical structure of the three phosphines employed in the carbonylation reaction are shown below (Figure 3.1).

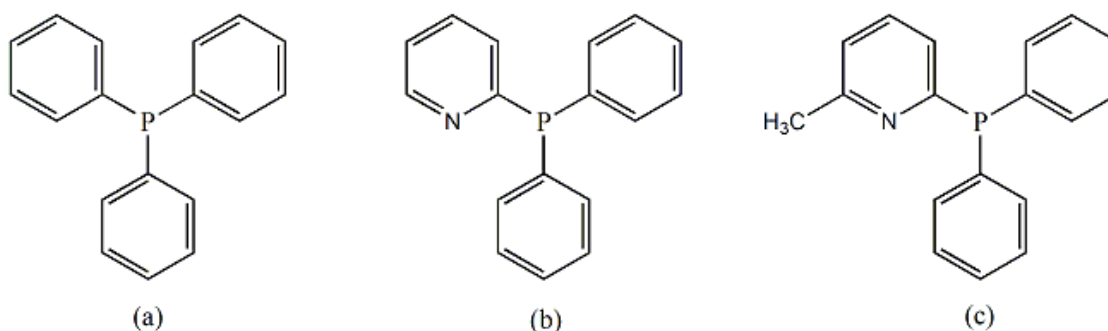
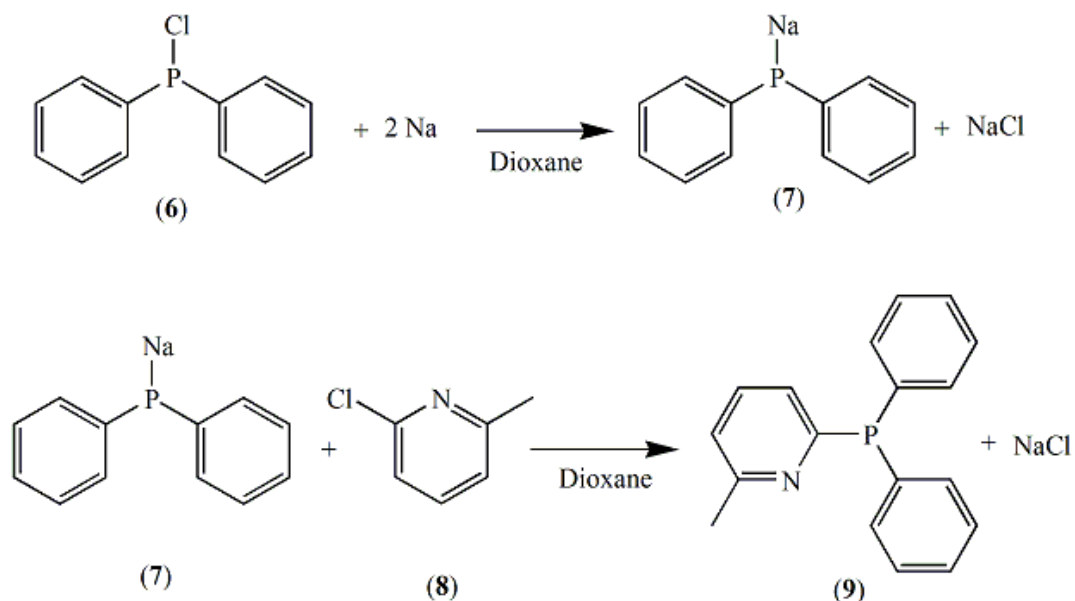


Figure 3.1 Chemical structure of (a) triphenylphosphine, (b) 2-(diphenylphosphino)pyridine, and (c) 2-(6-methyl)(diphenylphosphino)pyridine.

From the above considerations, we decided to employ both (b) and (c) for the methoxycarbonylation of (trimethylsilyl)acetylene.

3.1.1 Synthesis of 2-(6-methyl)(diphenylphosphine)pyridine

While (b) is commercially available, the synthesis of 2-(6-methyl)(diphenylphosphino)pyridine (c) was carried out according to the methodology described in the Thesis of L. Piovesan [95]. The synthesis consists of two reactions. In the first one, chlorodiphenylphosphine (**6**) is allowed to react with metallic sodium in anhydrous dioxane under inert atmosphere. After overnight reflux at 110 °C, a yellow solution of sodium diphenylphosphide (**7**) is formed.



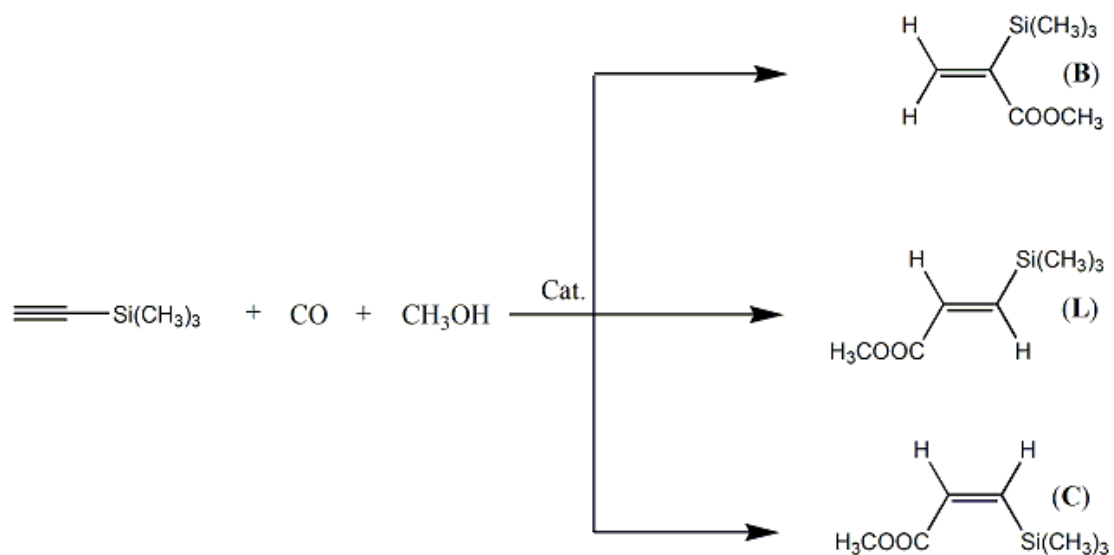
Scheme 3.3 Synthesis of 2-(6-methyl)(diphenylphosphine)pyridine.

In the second reaction, sodium diphenylphosphide replaces the chloride of 2-chloro-6-methylpyridine (**8**) by nucleophilic substitution reaction (Scheme 3.3). The reaction is carried out in anhydrous dioxane. After complete evaporation of solvent the white crude solid is extracted with diethyl ether/THF/water. Recrystallization of organic layer from methanol and water gives needle like white crystal of title product (**9**) in 65% yield. The product was characterized by melting point (81 °C), ¹H NMR (Figure 3.9), ¹³C NMR (Figure 3.10), and ³¹P NMR (Figure 3.11) spectroscopy (see the experimental section 3.2.2).

3.1.2 Methoxycarbonylation of (trimethylsilyl)acetylene

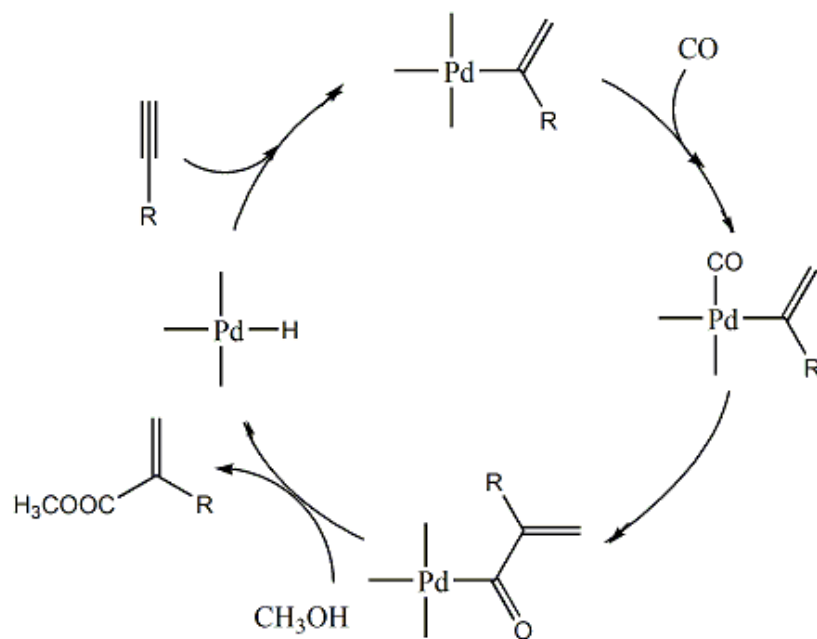
The carbonylation (both methoxy- and hydroxy-) reactions were carried out according to the procedure reported by A. Scrivanti *et al.*[27].

According to the reaction Scheme 3.4, we should obtained three isomers from the methoxycarbonylation of (trimethylsilyl)acetylene: the branched isomer (**B**) which is of our interest and the two linear *trans* and *cis* isomers (**L**) and (**C**). However, employing Drent's catalytic system only the branched (**B**) and the linear *trans* isomers-(**L**) form.



Scheme 3.4 Tentative methoxycarbonylations of (trimethylsilyl)acetylene using Drent's catalyst.

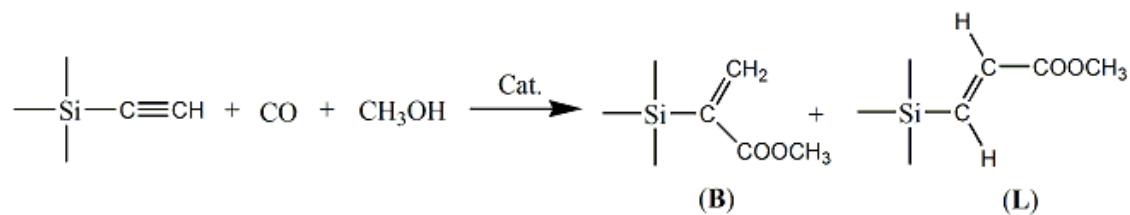
The formation of the products can be explained by the mechanism of the reaction (Scheme 3.5) that essentially involves three steps: 1) the formation of vinyl complex via addition of proton to the terminal alkyne coordinated to the palladium center; 2) the internal insertion of CO into the Pd-carbon bond of vinyl complex, leading to the formation of an acyl-palladium complex, and which in the third step is converted into the ester by alcoholysis thus regenerating the hydride [27, 96-98].



Scheme 3.5 Proposed mechanism for the methoxycarbonylation of terminal alkyne.

3.1.2.1 Methoxycarbonylation of (trimethylsilyl)acetylene in presence of the catalytic system $\text{Pd}(\text{OCOCH}_3)_2/\text{CH}_3\text{SO}_3\text{H}/2$ -(diphenylphosphino)pyridine(PPh_2Py).

In some preliminary experiments (Entry 1, Table 3.1), the methoxycarbonylations of (trimethylsilyl)acetylene was carried out using a mixture of dichloromethane/methanol (10/2 mL) in presence of the catalytic system $\text{Pd}(\text{OCOCH}_3)_2/\text{CH}_3\text{SO}_3\text{H}/2$ -(diphenylphosphino)pyridine at 80 °C for 24 hours (Scheme 3.6).



Cat. = $\text{Pd}(\text{OCOCH}_3)_2/\text{CH}_3\text{SO}_3\text{H}/2$ -(diphenylphosphino)pyridine

Scheme 3.6 Methoxycarbonylation of (trimethylsilyl)acetylene using $\text{Pd}(\text{OCOCH}_3)_2/\text{CH}_3\text{SO}_3\text{H}/2$ -(diphenylphosphino)pyridine.

A first experiment was carried out at $P(\text{CO}) = 20$ atm in the presence of a catalyst having formulation: $\text{Pd}/\text{H}^+/\text{PPh}_2\text{Py} = 1/20/20$. Working with a substrate/palladium molar ratio of 1000, after 24h the alkyne conversion reached 62%. The gas chromatographic analysis indicates that the product is a 61/39 mixture of methyl 2-(trimethylsilyl)acrylate (**B**) and methyl 3-(trimethylsilyl)acrylate (**L**), respectively. In a second experiment, the pressure was increased to 40 atmosphere and the $\text{CH}_3\text{SO}_3\text{H}/\text{Pd}$ and $\text{PPh}_2\text{Py}/\text{Pd}$ ratio were decreased to 10. The reaction allowed to obtained 68% conversion with 50/50 mixture of branched and linear product (substrate/palladium = 500, Entry 2, Table 3.1). A third experiment (Entry 3, Table 3.1) was carried out at 40 atmosphere of CO using a $\text{Pd}/\text{PPh}_2\text{Py}/\text{CH}_3\text{SO}_3\text{H}$ ratio of 1/20/20. The substrate conversion was of 70 % with a 57/43 isomer (**B/L**) ratio.

Table 3.1 Methoxycarbonylation of (trimethylsilyl)acetylene in presence of catalytic system $\text{Pd}(\text{OCOCH}_3)_2/\text{CH}_3\text{SO}_3\text{H}/\text{PPh}_2\text{Py}$.

Entry	Sub/Pd	$\text{PPh}_2\text{Py}/\text{Pd}$	H^+/Pd	$P(\text{CO})$ atm.	Conv. (%)	^a B (%)	^a L (%)
1	1000	20	20	20	62	61	39
2	500	10	10	40	68	50	50
3	500	20	20	40	70	57	43

Reaction Conditions: (Trimethylsilyl)acetylene = 10.3 mmol; 2-(diphenylphosphino)pyridine = 0.206 mmol; $\text{CH}_2\text{Cl}_2 = 10.0$ mL; $\text{CH}_3\text{OH} = 2.0$ mL; $T = 80$ °C; $t = 24$ h. ^aSelectivity.

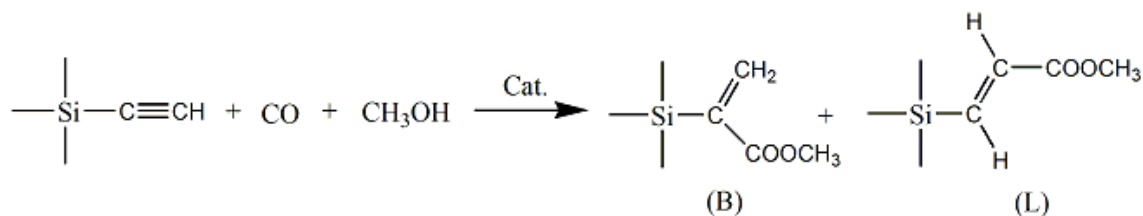
B = methyl 2-(trimethylsilyl)acrylate; **L** = methyl 3-(trimethylsilyl)acrylate

From these data, it appears that complete conversion was not attained even in the presence of high catalyst loads (Entry 2 & 3). Therefore, it appears that the substrate is very deactivated probably owing to the high steric hindrance of the (trimethylsilyl)acetylene group.

3.1.2.2 Methoxycarbonylation of (trimethylsilyl)acetylene in presence of catalytic system $\text{Pd}(\text{OCOCH}_3)_2/\text{CH}_3\text{SO}_3\text{H}/2$ -(6-methyl)(diphenylphosphino)pyridine.

In order to increase the conversion as well as the selectivity towards branched isomer, we decided to test the catalytic system $\text{Pd}(\text{OCOCH}_3)_2/\text{CH}_3\text{SO}_3\text{H}/2$ -(6-Methyl)(diphenylphosphino)pyridine in the methoxycarbonylation of (trimethylsilyl)acetylene (Scheme 3.7). In fact, it is reported in the literature [22] that the

methoxycarbonylation of propyne using this catalytic system produced 99.95% of branched methyl methacrylate with a TOF values of 50000 h⁻¹. But the same reaction under same condition using 2-(diphenylphosphino)pyridine instead of 2-(6-Methyl)(diphenylphosphino)pyridine gave 98% selectivity with TOF values of 40000 h⁻¹.



Cat. = Pd(OCOCH₃)₂/CH₃SO₃H/2-(6-Methyl)(diphenylphosphino)pyridine

Scheme 3.7 Methoxycarbonylation of (trimethylsilyl)acetylene using Pd(OCOCH₃)₂/CH₃SO₃H/2-(6-Methyl)(diphenylphosphino)pyridine.

In order to optimize the conversion and selectivity towards branched isomer, numerous tests have been performed by varying the reaction conditions. Each test was performed by varying only one parameter, in order to properly attribute the effects of variations. Particularly, the effects due to reaction time, temperature, CO pressure, substrate/palladium, acid/phosphine, and phosphine/palladium ratio were studied. In every methoxycarbonylation reaction, methanol was used both as the reagent and the solvent. The reaction mixtures were analyzed by gas chromatography. The ester obtained was purified by column chromatography and characterized by ¹H NMR (Figure 3.12), ¹³C NMR (Figure 3.13), and DEPT 135 (Figure 3.14) NMR spectroscopy (see the experimental section).

3.1.2.2.1 Influence of 2-(6-methyl)(diphenylphosphino)pyridine/Pd(OCOCH₃)₂ ratio

A series of methoxycarbonylation reaction was carried out by varying only phosphine/catalyst (Pd(OCOCH₃)₂) ratio. All other conditions were maintained constant (substrate/Pd(OCOCH₃)₂ = 1000, acid/phosphine = 1, P(CO) = 30 atm, temperature = 60 °C, reaction time = 3 hours). The results obtained are summarized in Table 3.2. The graphical representation of the result is shown in Figure 3.2.

Table 3.2 Methoxycarbonylation of (trimethylsilyl)acetylene: influence of phosphine/palladium ratio

Entry	Phosphine/Pd	Acid/Pd	Conversion ^a (%)	Selectivity ^{a,b} (%)
1	10	10	86	95
2	20	20	87	96
3	30	30	96	98

Reaction conditions: (Trimethylsilyl)acetylene = 10.3 mmol; substrate/palladium = 1000; P(CO) = 30 atm.; T = 60 °C; t = 3 h.

^aConversion and selectivity were determined by gas chromatography.

^bRegioselectivity towards branched isomer.

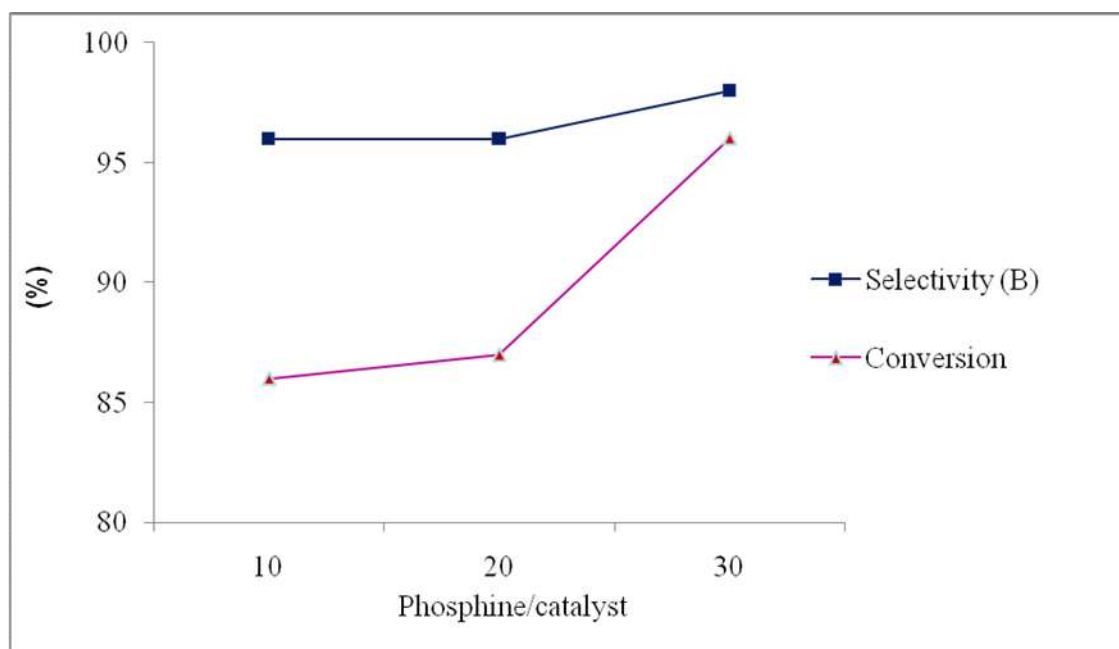


Figure 3.2 Methoxycarbonylation of (trimethylsilyl)acetylene: trend of conversion and selectivity in function of the phosphine/palladium ratio.

It can be noted that the conversion and selectivity towards branched isomer increases on increasing the phosphine/palladium ratio. In particular, the reaction (Entry 3, Table 3.2) at phosphine/ palladium = 30 allowed to obtain 96% of conversion with almost total selectivity (98%) towards the branched isomer. For the formation of the species active in catalysis, it is necessary to coordinate the phosphine to the palladium center [22]. The increased conversion

upon the increase of the phosphine/palladium ratio, may be due to the fact that in presence of the large excess of phosphine, the formation of Pd-phosphine bond is favored over the formation of Pd-CO bond and hence gives higher concentrations of the active complex which take part in catalysis.

We have chosen the maximum value of phosphine/palladium = 30, because further increase of the phosphine/palladium ratio decreases the conversion. This result is consistent with the literature reported by A. Scrivanti *et al.* [99]. The decrease can be explained by assuming that, for high values of phosphine/palladium ratio (higher than 30), the excess phosphine prevent the coordination of alkyne into the palladium center causing a decrease of the reaction rate.

Considering these results, a set of methoxycarbonylation reaction has been carried out with a substrate/palladium = 4000, and the phosphine/palladium ratio varying from 10 to 30. The other parameters were unchanged (acid/phosphine = 1, P(CO) = 30 atm, temperature = 60 °C, reaction time = 3 hours). The results obtained are collected in Table 3.3 and graphically presented in Figure 3.3.

Table 3.3 Methoxycarbonylation of (trimethylsilyl)acetylene: influence of phosphine/palladium ratio

Entry	Phosphine/Pd	Acid/Pd	Conversion ^a (%)	Selectivity ^{a,b} (%)
1	10	10	53	92
2	20	20	66	94
3	30	30	73	95

Reaction conditions: (Trimethylsilyl)acetylene = 10.3 mmol; substrate/catalyst = 4000; P(CO) = 30 atm.; T = 60 °C; t = 3 h. ^aConversion and selectivity were determined by gas chromatography. ^bRegioselectivity towards branched isomer.

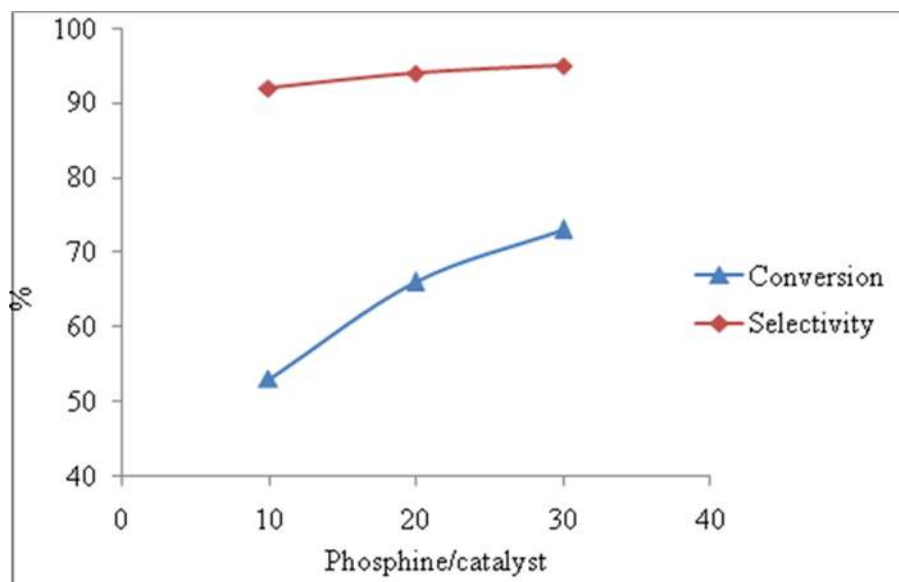


Figure 3.3 Methoxycarbonylation of (trimethylsilyl)acetylene: trend of conversion and selectivity in function of the phosphine/catalyst ratio.

Compared to the previous results, it is observed that the trend of conversion and selectivity (depending on the phosphine/ palladium ratio) remains unchanged. It can be noticed that the selectivity decreases only slightly. These results are very good, because with high substrate/catalyst ratio (4000), using phosphine/palladium =30 (Entry 3, Table 3.3), it was possible to obtain about 3200 catalytic cycles in 3 hours with an excellent selectivity towards the branched isomer.

3.1.2.2.2 Influence of $CH_3SO_3H/2$ -(6-methyl)(diphenylphosphino)pyridine ratio

A set of methoxycarbonylation reaction has been carried out by varying only the acid/phosphine ratio. All other conditions were kept constant (substrate/ $Pd(OCOCH_3)_2$ = 4000, phosphine/ palladium = 30, $P(CO)$ = 30 atm, temperature = 60 °C, reaction time = 3 hours). The values of acid/phosphine ratio were varied between 0.5 and 2. The results obtained are summarized in Table 3.4 and graphically represented in Figure 3.4, respectively.

Table 3.4 Methoxycarbonylation of (trimethylsilyl)acetylene: influence of acid/phosphine ratio

Entry	Acid/Phosphine	Conversion ^a (%)	Selectivity ^{a,b} (%)
1	0.5	17	94
2	1	73	95
3	2	52	92

Reaction conditions: (Trimethylsilyl)acetylene = 10.3 mmol; substrate/palladium = 4000; phosphine/palladium = 30; P(CO) = 30 atm.; T = 60 °C; t = 3 h.

^aConversion and selectivity were determined by gas chromatography.

^bRegioselectivity towards branched isomer.

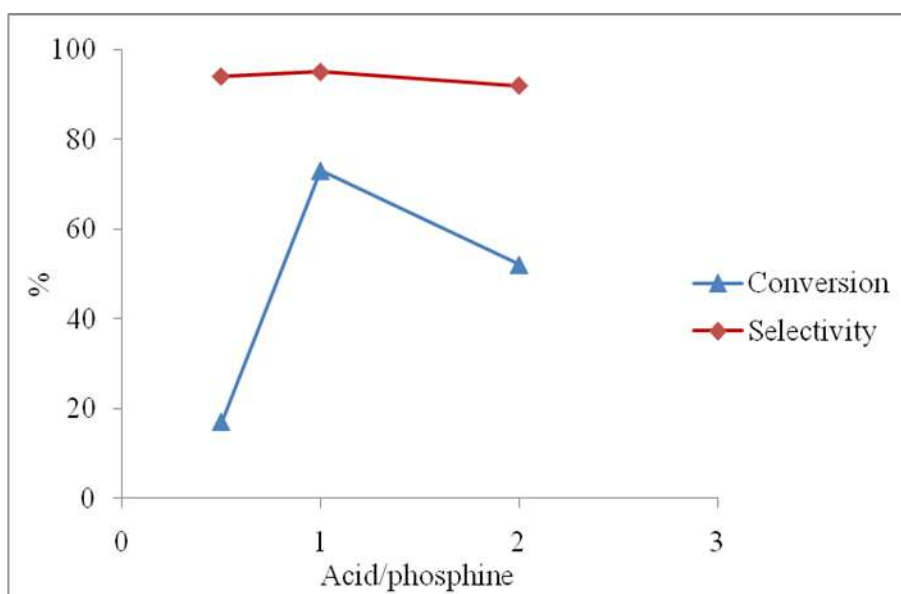


Figure 3.4 Methoxycarbonylation of (trimethylsilyl)acetylene: trend of conversion and selectivity in function of the acid/phosphine ratio.

From the Table 3.4, it can be seen that the maximum conversion was attained at unit acid/phosphine ratio. A decrease (Entry 1) or increase (Entry 3) of acid/phosphine ratio brings to a decrease of conversion. This means that the best conversion was achieved when the high value of phosphine/catalyst ratio (30) is supported by an unit acid/catalyst ratio. This behavior can be explained by assuming that, at lower acid/phosphine ratio i.e., in the presence of an excess phosphine with respect to acid, a higher amount of phosphine does not protonate in the reaction medium and remains strongly bound to the palladium and does not allow the

coordination of the substrate, thus lowering the reaction conversion [99]. In any case, the selectivity of the reaction changes very little with respect to the acid/phosphine ratio.

It is worth to note that when the reaction was carried out at higher than 1 acid/phosphine ratio, it was observed the formation of palladium black, therefore lowering of substrate conversion is also to ascribe to a scarce longevity of the catalyst.

The experiment 3 of Table 3.4 (acid/phosphine equal to 2) was repeated with the addition of dimethylaniline as a promoter, in agreement with the effect reported by Drent for the carbonylation of propyne [100]. The mechanism of the role of promoter has not yet been clarified, but a possible hypothesis is that it prevents the formation of nanoparticles even if this aspect has never been investigated. In the first reaction (Entry 2, Table 3.5), we used a promoter/acid ratio = 2. In the second reaction (Entry 3, Table 3.5), the promoter was added so as to have a relationship promoter/acid = 5. The results obtained are gathered in Table 3.5 and graphically represented in Figure 3.5, respectively.

Table 3.5 Methoxycarbonylation of (trimethylsilyl)acetylene: influence of promoter/acid ratio

Entry	Promoter/acid	Conversion ^a (%)	Selectivity ^{a,b} (%)
1	0	52	92
2	2	64	94
3	5	33	92

Reaction conditions: (Trimethylsilyl)acetylene = 10.3 mmol; substrate/palladium = 4000; phosphine/catalyst = 30; Phosphine = 30; acid/phosphine = 2; P(CO) = 30 atm.; T = 60 °C; t = 3 h.

^aConversion and selectivity were determined by gas chromatography.

^bRegioselectivity towards branched isomer.

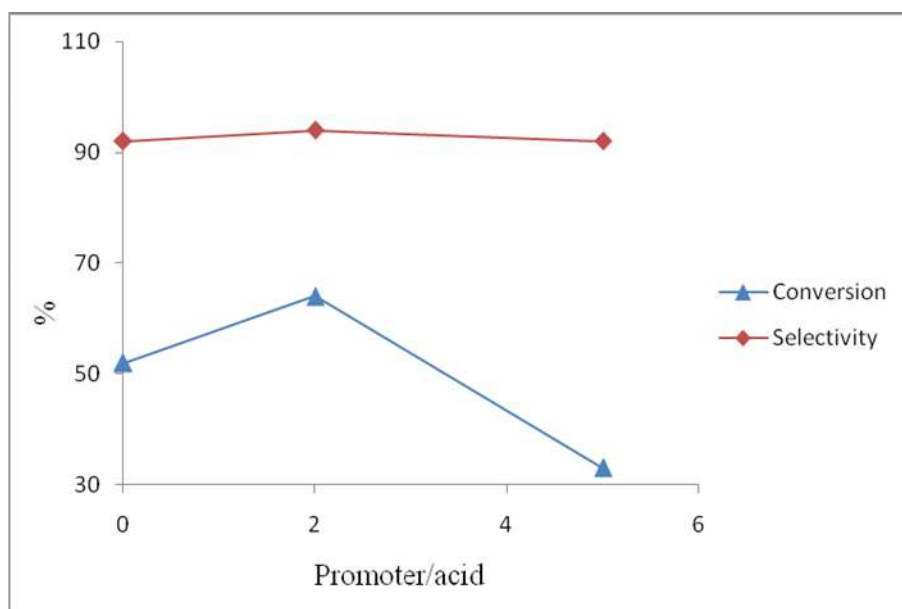


Figure 3.5 Methoxycarbonylation of (trimethylsilyl)acetylene: trend of conversion and selectivity in function of the promoter/acid ratio.

The use of promoter in our case does not seem to bring useful improvements to the catalysis.

3.1.2.2.3 Influence of the reaction temperature

To study the effect of temperature on the methoxycarbonylation of (trimethylsilyl)acetylene, we have carried out a set of experiments by varying the temperature from 50 to 80 °C. All other conditions were kept constant (substrate/palladium = 4000, phosphine/palladium = 30, acid/phosphine = 1, P(CO) = 30 atm., t = 3 h). The results obtained are reported in Table 3.6 and graphically presented in Figure 3.6, respectively.

Table 3.6 Methoxycarbonylation of (trimethylsilyl)acetylene: influence of temperature

Entry	Temperature (°C)	Conversion ^a (%)	Selectivity ^{a,b} (%)
1	50	50	95
2	60	73	95
3	70	82	94
4	80	90	93

Reaction conditions: (Trimethylsilyl)acetylene = 10.3 mmol; substrate/palladium = 4000; phosphine/palladium = 30; acid/phosphine = 1; P(CO) = 30 atm.; t = 3 h. ^aConversion and selectivity were determined by gas chromatography. ^bRegioselectivity towards branched isomer.

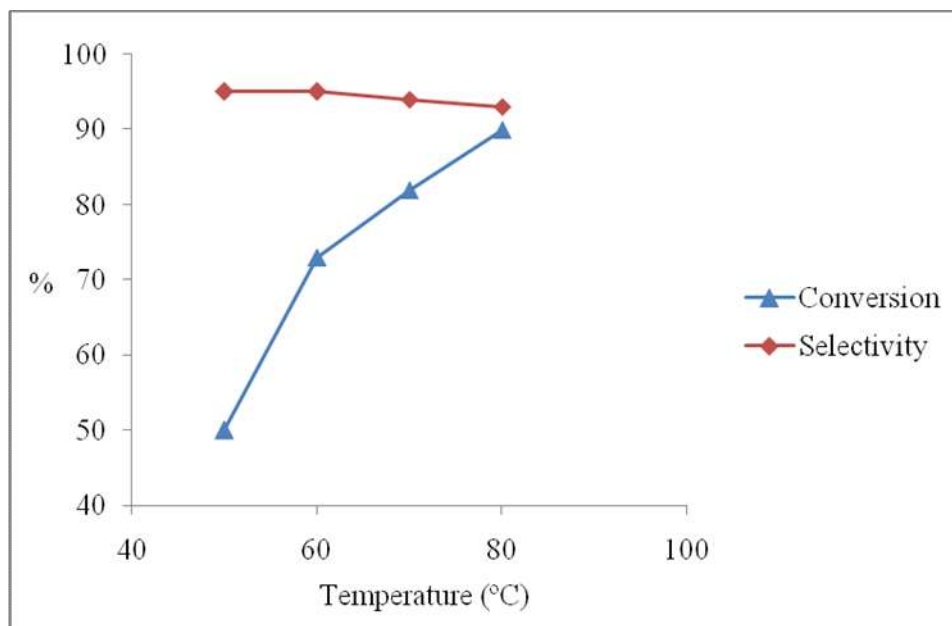


Figure 3.6 Methoxycarbonylation of (trimethylsilyl)acetylene: trend of conversion and selectivity in function of the temperature.

From the data presented in the Figure 3.6, it can be noticed that an increase of temperature results favorably in an increase of conversion but this is accompanied by a small decrease in selectivity. The best results (conversion = 82%, selectivity = 94%) were obtained in the reaction carried out at 70 °C (Entry 3, Table 3.6).

3.1.2.2.4 Influence of CO pressure

In order to study the effect of carbon monoxide pressure on the conversion and selectivity of methoxycarbonylation of (trimethylsilyl)acetylene, we have carried out some experiments by varying the CO pressure from 20 to 40 atm. All other conditions were kept constant (substrate/palladium = 4000, phosphine/palladium = 30, acid/phosphine = 1, T = 60 °C, atm,

t = 3 h). The results obtained are reported in Table 3.7 and graphically presented in Figure 3.7, respectively.

Table 3.7 Methoxycarbonylation of (trimethylsilyl)acetylene: influence of CO pressure

Entry	P(CO) atm.	Conversion ^a (%)	Selectivity ^{a,b} (%)
1	15	55	93
2	20	80	95
3	30	73	95
4	40	60	94

Reaction conditions: (Trimethylsilyl)acetylene = 10.3 mmol; substrate/palladium = 4000; phosphine/palladium = 30; acid/phosphine = 1; T = 60 °C; t = 3 h.

^aConversion and selectivity were determined by gas chromatography.

^bRegioselectivity towards branched isomer.

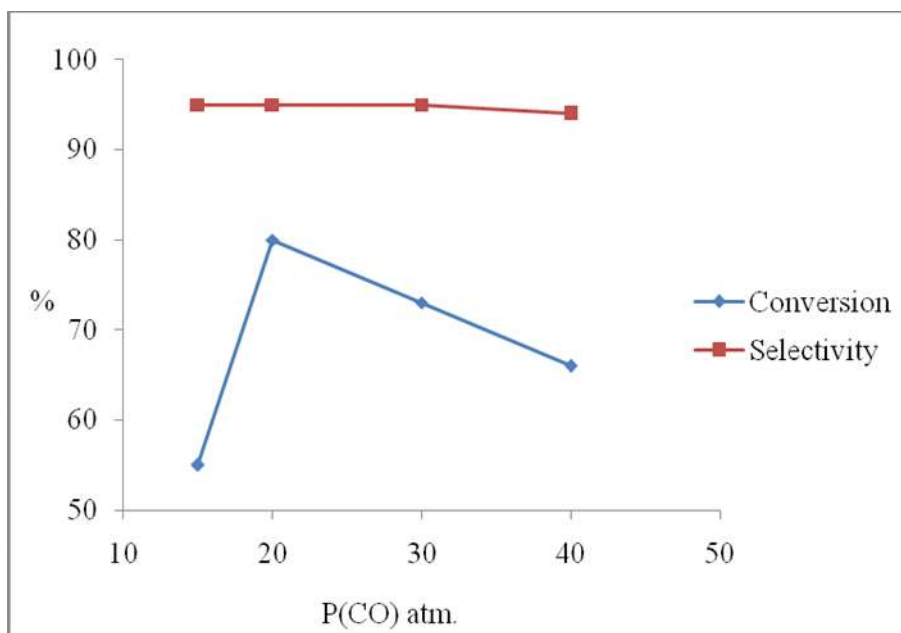


Figure 3.7 Methoxycarbonylation of (trimethylsilyl)acetylene: trend of conversion and selectivity in function of the CO pressure.

From the data presented in the Table 3.7, it can be noticed that the conversion of the reaction is higher with lower values (Entry 2) of CO pressure. This result can be explained by

admitting that above certain pressure, the CO competes with the alkyne substrate for coordination site of the palladium and consequently slows down the reaction rate.

3.1.2.2.5 Influence of reaction time

To investigate the effect of reaction time, some experiment were carried out by varying the reaction time. All other conditions were kept constant (substrate/catalyst = 1000, phosphine/palladium = 20, phosphine/acid = 1, temperature = 60 °C, p(CO) = 30 atm.). The results obtained are reported in Table 3.8 and represented in Figure 3.8, respectively.

Table 3.8 Methoxycarbonylation of (trimethylsilyl)acetylene: influence of reaction time

Entry	t(h)	Conversion ^a (%)	Selectivity ^{a,b} (%)
1	3	87	96
2	6	93	96
3	24	95	96

Reaction conditions: (Trimethylsilyl)acetylene = 10.3 mmol; substrate/palladium = 1000; phosphine/palladium = 20; acid/phosphine = 1; T = 60 °C.

^aConversion and selectivity were determined by gas chromatography.

^bRegioselectivity towards branched isomer.

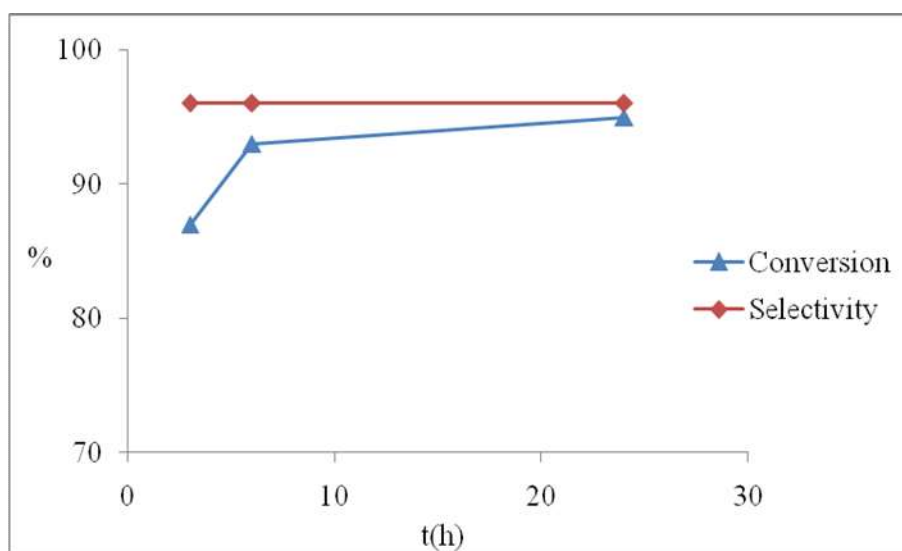
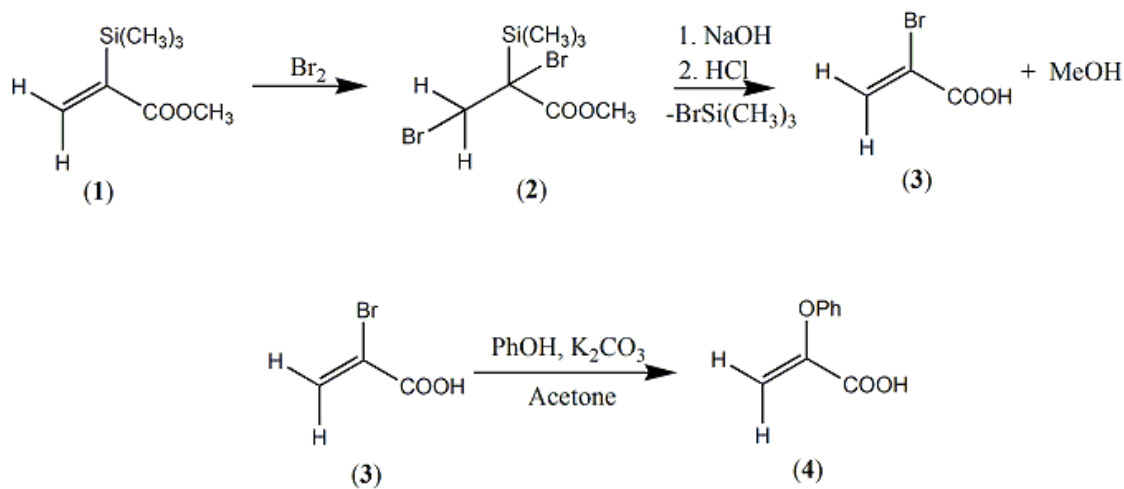


Figure 3.8 Methoxycarbonylation of (trimethylsilyl)acetylene: trend of conversion and selectivity in function of reaction time.

From the data presented in Table 3.8, it can be seen that, the conversion of the reaction increases by increasing the time, while the selectivity remains constant. This result indicates that albeit the catalyst retains its activity, the reaction slows down as the substrate is consumed.

3.1.2.3 Bromodesilylation of methyl 2-(trimethylsilyl)acrylate

A method for the synthesis of enantiomerically enriched α -aryloxipropanoic acid involves the nucleophilic substitution of 2-bromoacrylic acid with phenol (from **3** to **4** in Scheme 3.8) in presence of potassium carbonate and acetone [8, 23, 24]. In turn, the 2-bromoacrylic acid (**3**) can be prepared by the bromodesilylation of methyl 2-(trimethylsilyl)acrylate (**1**) followed by a treatment with a base (NaOH) (Scheme 3.5). The base treatment removes the bromo trimethylsilyl group ($-\text{BrSi}(\text{CH}_3)_3$) and hydrolyzes the ester group into the corresponding acid.



Scheme 3.8 Synthetic scheme of 2-bromoacrylic acid (**3**) starting from methyl 2-(trimethylsilyl)acrylate(**1**).

A lot of works report the halodesilylation of vinylsilanes bearing alkyl substituents but not with carboxyl groups, such as the methyl 2-(trimethylsilyl)acrylate [23]. In our previous work, no result was obtained when we conducted the iododesilylation of methyl 2-(trimethylsilyl)acrylate [80]. Accordingly, we attempted to conduct the reaction using bromine, as the literature reports that the bromine is more reactive than iodine [23, 101].

A CH_2Cl_2 solution of Br_2 was added to a CH_2Cl_2 solution of methyl 2-(trimethylsilyl)acrylate. The bromine-addition intermediate methyl 2,3-dibromo-2-(trimethylsilyl)propanoate was obtained in 96% yield. It was characterized by ^1H NMR (Figure 3.15) and ^{13}C NMR (Figure 3.16) spectroscopy (see the experimental section). To remove the bromotrimethylsilyl group and obtain the vinylbromide, we have treated (**2**) with weak bases such as NaHCO_3 and NaHSO_4 , but they are ineffective, in any case no bromodesilylation was observed. Even, the addition of a methanol solution of NaOMe (in excess of 10%) did not allow to obtain the desired vinylbromide. On the contrary, the use of aqueous stronger bases, such as aqueous solutions of NaOH (5%) or Na_2CO_3 (in the ratio 4:1), caused not only the elimination of bromotrimethylsilyl ($-\text{BrSi}(\text{CH}_3)_3$) group, but also the hydrolysis of ester group to give the corresponding acid (**3**, Scheme 3.5) which was characterized by means of ^1H NMR (Figure 3.17, see experimental section) spectroscopy.

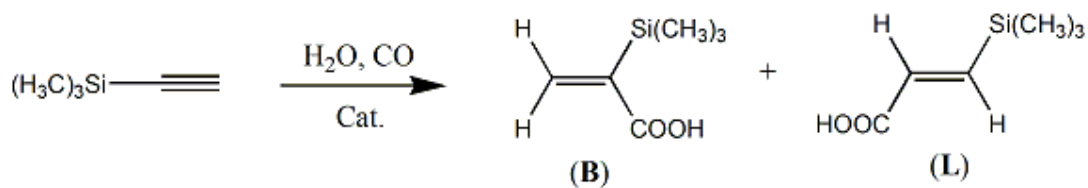
Although we were not able to cleanly bromodesilylate ester (**2**), it is interesting to note that our procedure is very advantageous because in a single step the trimethylsilyl group is eliminated and the ester is transfer into corresponding acid.

In a last experiment to obtain methyl 2-bromoacrylate, an acetonitrile solution of (**2**) was refluxed for 18 hours, but the treatment did not lead to a satisfactory result. It was decided to use this procedure, since A. G. Brook *et al.* reported the effective elimination of bromotrimethylsilyl group from 1,2-dibromo-(2-trimethylsilyl)alkanes by simply heating in polar solvent (acetonitrile for 12 days and dimethyl sulfoxide for 20 hours). [102].

3.1.3 Hydroxycarbonylation of (trimethylsilyl)acetylene

Considering the good results (conversion and selectivity) obtained in the methoxycarbonylation of (trimethylsilyl)acetylene using the catalytic system $\text{Pd}(\text{OCOCH}_3)_2/\text{CH}_3\text{SO}_3\text{H}/2$ -(6-methyl) (diphenylphosphino)pyridine, we decided to investigate the hydroxycarbonylation of the same substrate using the same catalytic system. In fact, since the ultimate goal is the synthesis of 2-bromoacrylic acid (**3**, scheme 3.8), the hydroxycarbonylation is preferable to methoxycarbonylation, because it allows to obtain the acid directly.

Like methoxycarbonylation, the hydroxycarbonylation of (trimethylsilyl)acetylene can lead to the formation of three isomers: one branched isomer and two linear isomers. But because of the *cis* stereochemistry of the addition of alkyne into the palladium center, we obtained only the branched and the *trans* linear isomers (Scheme 3.9).



Scheme 3.9 Reaction scheme for the hydroxycarbonylation of (trimethylsilyl)acetylene.

Preliminary tests did not furnish good results. In fact, the hydroxycarbonylation in THF using a substrate/palladium ratio of 500, high reaction temperature (80 °C), a long time (24h), the conversion does not exceed 50%. In order to increase the conversion and selectivity towards branched isomer, some experiments have been carried out by changing the reaction conditions. Each experiment was carried out by changing only one parameter at a time, in order to properly attribute the possible variations. In particular, the following parameters were varied: solvent, temperature, and acid/phosphine ratio.

3.1.3.1 Influence of solvent

First, some hydroxycarbonylation reactions have been carried out in some different solvents. The choice of solvent is not easy, because it is necessary to find a polar organic solvent capable of solubilizing both the organic substrate and water. Reactions were carried out in THF and acetone.

In THF (Entry 1 of Table 3.9), the reaction proceeds affording as the only products the branched and linear acids. The reaction is much slower than the methoxycarbonylation so that substrate conversion is only 50% after 24 hours. The **B/L** isomer ratio is 93 %. In acetone, the reaction is almost unchanged, but the conversion is slightly higher than 55 %.

When the hydroxycarbonylation was carried out in isopropanol, the conversion increases up to 77%. But the reaction is limited by the formation of significant amount (42 %) of the isopropyl ester. With *tert*-butanol as the solvent the conversion is lower but very low ester formation is observed. This behavior can be explained by admitting that the bulkier *tert*-butanol attacks the carbonyl group less readily than isopropanol. The results are summarized in Table 3.9.

Table 3.9 Hydroxycarbonylation of (trimethylsilyl)acetylene: influence of solvents

Entry	Solvent	Conversion ^a (%)	TOF ^b	Product Composition ^a		Branched Isomer ^a (%)
				Acid	Ester	
1	THF	49	10	100	0	93
2	Isopropanol	77	16	58	42	99
3	<i>Tert</i> -butanol	57	12	92	8	95
4	Acetone	55	11	100	0	93

Reaction conditions: (Trimethylsilyl)acetylene = 10.3 mmol; substrate/palladium = 500; phosphine/palladium = 20; acid/phosphine = 2; P(CO) = 30 atm.; T = 80 °C; t = 24 h.

^aConversion and selectivity were determined by gas chromatography. ^bMoles of substrate carboxylated/moles of catalyst per hour.

Acetone appears to be a solvent better than THF, but in no case substrate conversion was complete.

3.1.3.2 Influence of CH₃SO₃H/2-(6-methyl)(diphenylphosphino)pyridine ratio

Aiming at improving the reaction, some experiments were carried out in acetone and THF at different CH₃SO₃H/2-(6-methyl)(diphenylphosphino)pyridine ratio. The results obtained are collected in the Table 3.10.

Table 3.10 Hydroxycarbonylation of (trimethylsilyl)acetylene: influence of CH₃SO₃H/2-(6-methyl) (diphenylphosphino)pyridine ratio

Entry	T(°C)	Solvent	Acid/P	P/Pd.	Acid/Pd	Conversion ^a	Selectivity ^{a,b}
						(%)	(%)
1	80	Acetone	1	30	30	43	93
2	80	"	2	20	40	55	93
3	100	"	2	20	40	33	100
4	80	THF	1	20	20	42	92
5	80	"	2	20	40	49	92

Reaction conditions: (Trimethylsilyl)acetylene = 10.3 mmol; substrate/palladium = 500; P(CO) = 30 atm.; T = 80 °C; t = 24 h. ^aConversion and selectivity were determined by gas chromatography. ^bRegioselectivity to the branched isomer.

From the Table 3.10, it can be seen that the conversion of hydroxycarbonylation of (trimethylsilyl)acetylene increases on increasing the CH₃SO₃H/2-(6-methyl) (diphenylphosphino)pyridine ratio. On the contrary, the regioselectivity is not affected.

3.1.3.3 Influence of temperature

From the Entry 2 of Table 3.10, it can be seen that the conversion of the hydroxycarbonylation reaction decreases on increasing temperature. When the reaction was carried out at 100 °C, a large amount of Pd black precipitate is formed. This behavior can be explained by admitting that at high temperatures and in excess acid, extensive decomposition of the catalyst is occurred. On the contrary, the regioselectivity toward the branched isomer increases to 100%.

3.2 EXPERIMENTAL SECTION

3.2.1 Purification of reagents and solvents

The reagents and solvents with high degree of purity were purchased directly from the market and used without further purification. In case where it is necessary to handle the reaction in absence of oxygen and water, solvents and reagents were distilled and dried according to the procedure reported in the literature [103]. The carbonylation reactions were carried out in an inert atmosphere using a special type Schlenk technique.

3.2.2 Instrumentation used for carbonylation reaction

The carbonylation reactions were carried out in a AISI 316 stainless steel autoclave, having a capacity of 150 mL and provided with an external jacket of insulation. The stirring of the mixture is maintained by magnetic external stirrer. The temperature was controlled by

thermostat. The circulation of ethylene glycol able to maintain the reaction temperature within $\pm 1^\circ\text{C}$ throughout the reaction time.

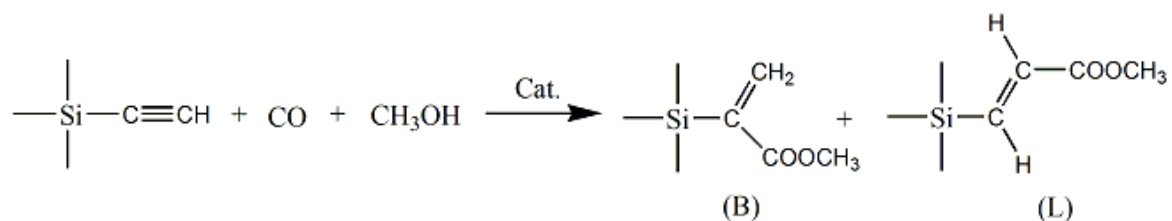
3.2.3 Instrumentation used for analysis

^1H NMR, ^{13}C NMR and ^{31}P NMR spectra were measured on Bruker Avance-300 spectrometer. Infrared spectra were recorded on a Perkin Elmer Spectrum One FT-IR in KBr pellet in the range of $4000\text{--}400\text{ cm}^{-1}$. Gas chromatographic analysis were performed on a Agilent Technologies 6850 gas chromatograph fitted with an HP-5 column ($30\text{m} \times 0.32\text{ }\mu\text{m} \times 0.25\text{ }\mu\text{m}$). In case where it is needed the gas chromatographic analysis were performed employing a FFAP capillary column heated at a rate of 10°C per min from an initial temperature of 30°C to 200°C .

3.2.4 Stereoselective synthesis of 2-substituted acrylic derivatives *via* carbonylation reaction

The carbonylation (both methoxy- and hydroxy-) reactions were carried out according to the procedure reported by A. Scrivanti *et al.* [27].

3.2.4.1 Methoxycarbonylation of (trimethylsilyl)acetylene in the presence of the catalytic system $\text{Pd}(\text{OCOCH}_3)_2/\text{CH}_3\text{SO}_3\text{H}/2\text{-(diphenylphosphino)pyridine}$

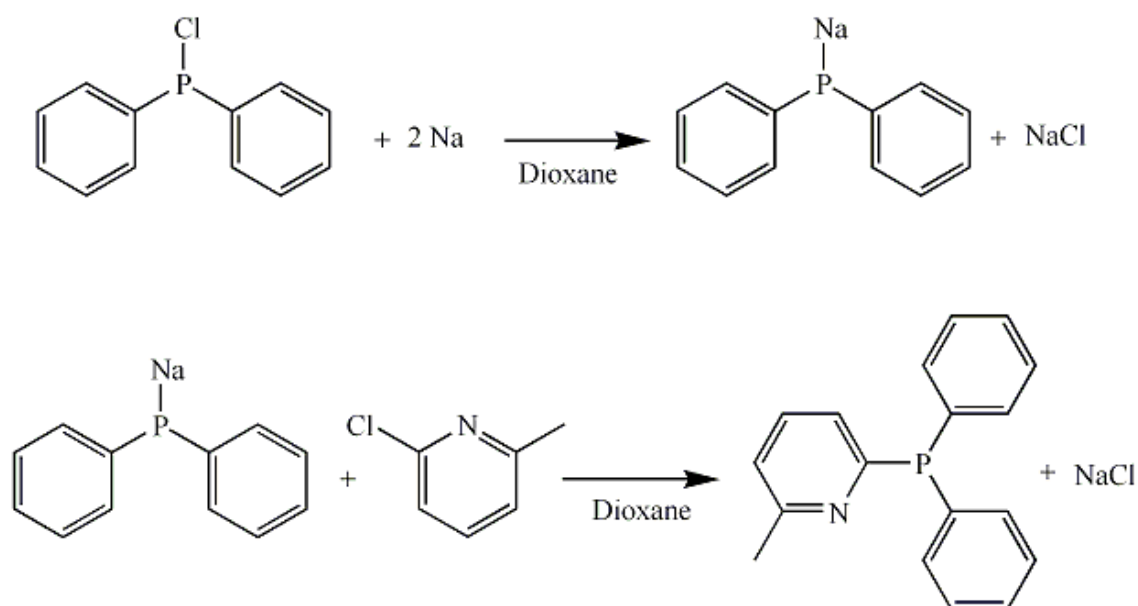


$$\text{Cat.} = \text{Pd}(\text{OCOCH}_3)_2/\text{CH}_3\text{SO}_3\text{H}/2\text{-(diphenylphosphino)pyridine}$$

As an example the experimental details relevant to Entry 1 of Table 3.1 (see results and discussion). In a Schlenk tube, we introduced 10.0 mL of anhydrous dichloromethane and 2.0 mL of anhydrous methanol. 2.32 mg (0.0103 mmol) of $\text{Pd}(\text{OCOCH}_3)_2$, 54.23 mg (0.206 mmol) of 2-(diphenylphosphino)pyridine, 1.01g (10.3 mol, 1.45 mL)

(trimethylsilyl)acetylene, and 13.4 μL (0.206 mmol) of methanesulfonic acid were successively added to the tube. After careful vacuum (using liquid nitrogen trap), the solution transferred into previously cleaned autoclave by *cannula*. The autoclave was pressurized with 20 atm of CO. The reaction mixture was allowed to react for 24 hours at 80 $^{\circ}\text{C}$ under stirring. The reaction was cooled and the gas was carefully released. A small amount of black precipitate was appeared and filtered off.

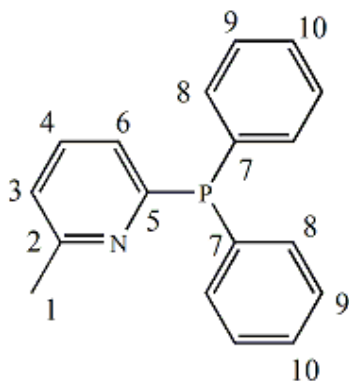
3.2.4.2. Synthesis of 2-(6-methyl)(diphenylphosphine)pyridine



Scheme 3.10 Synthesis of 2-(6-methyl)(diphenylphosphine)pyridine.

The synthesis of 2-(6-methyl)(diphenylphosphine)pyridine (scheme 10) was carried out according to the methodology described by L. Piovesan [95]. In a 100.0 mL two-necked round bottom flask, 1.385 g (60.21 mmol) of metallic sodium was put under inert atmosphere. In another 250.0 mL two-necked round bottom flask, chlorodiphenylphosphine (5.4 mL, 6.64 g, 30.11 mmol) was dissolved in 40 mL of anhydrous dioxane. The chlorodiphenylphosphine solution was then transferred into the first flask by *cannula*. After overnight reflux at 110 $^{\circ}\text{C}$, the reaction mixture was cooled at room temperature. 2-chloro-6-methylpyridine (3.40 mL, 3.90 g, 30.11 mmol) was added and the resulting solution, stirred at

room temperature for 24 hours and then reflux at 106 °C for 4 hours under inert atmosphere. The careful evaporation of solvent by vacuum gave a crude white solid which was dissolved in a mixture of solvent of 140 mL diethyl ether, 10 mL THF, and 80 mL of water. The organic layer was extracted, dried with MgSO₄, and concentrated. Hot recrystallization (solvent mixture CH₃OH (47.0 mL) and H₂O(3.0 mL)) gave desired 2-(6-methyl)(diphenylphosphine) pyridine as white crystal (65%) which was characterized by ¹H NMR (Figure 3.9), ¹³C NMR(Figure 3.10), and ³¹P NMR spectroscopy (Figure 3.11).



2-(6-methyl)(diphenylphosphine) pyridine

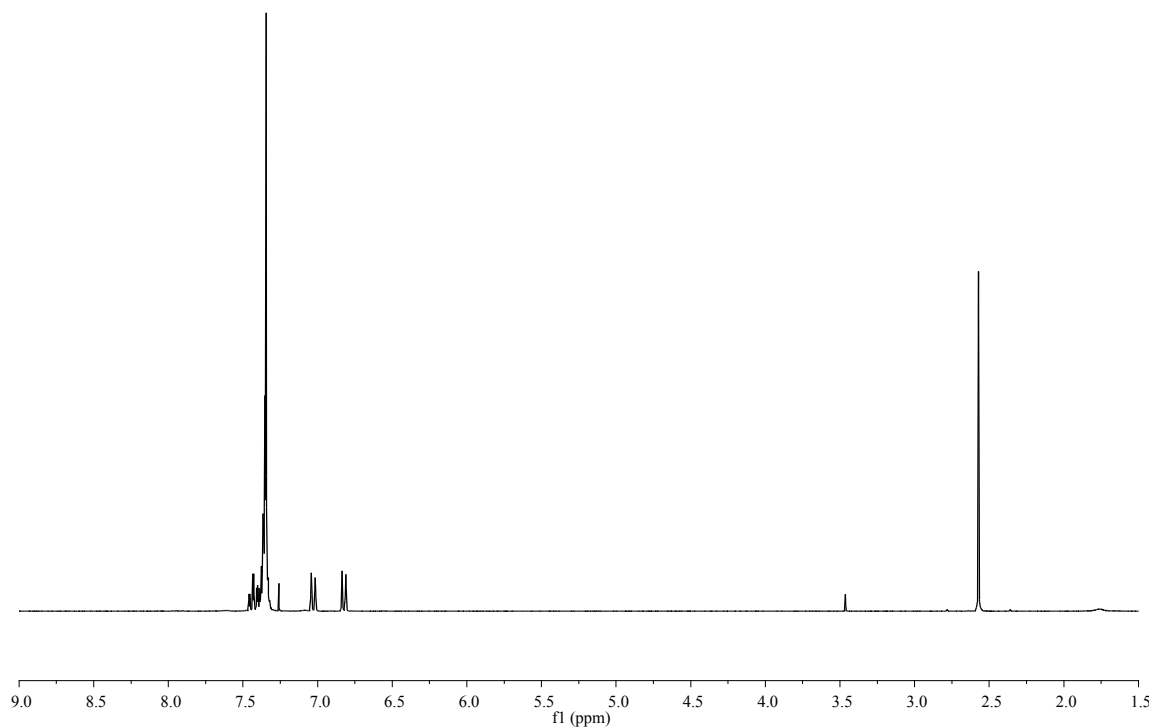
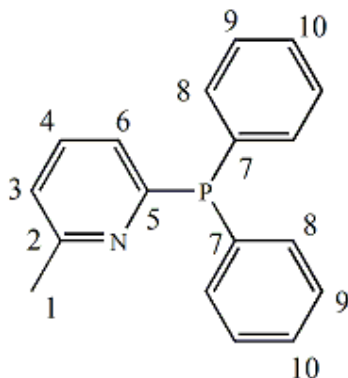


Figure 3.9 ¹H NMR spectrum of 2-(6-methyl)(diphenylphosphine)pyridine in CDCl₃.

¹H NMR (300 MHz, CDCl₃, 298 K): δ 7.46-7.43 (m, 1H(4)), 7.41-7.28 (m, 10H(8,9,10)), 7.03 (d, 1H(6), *J* = 7.4 Hz), 6.83 (d, 1H(3), *J* = 7.7 Hz), 2.57 (s, 3H(1)) ppm.



¹³C of 2-(6-methyl)(diphenylphosphine)pyridine

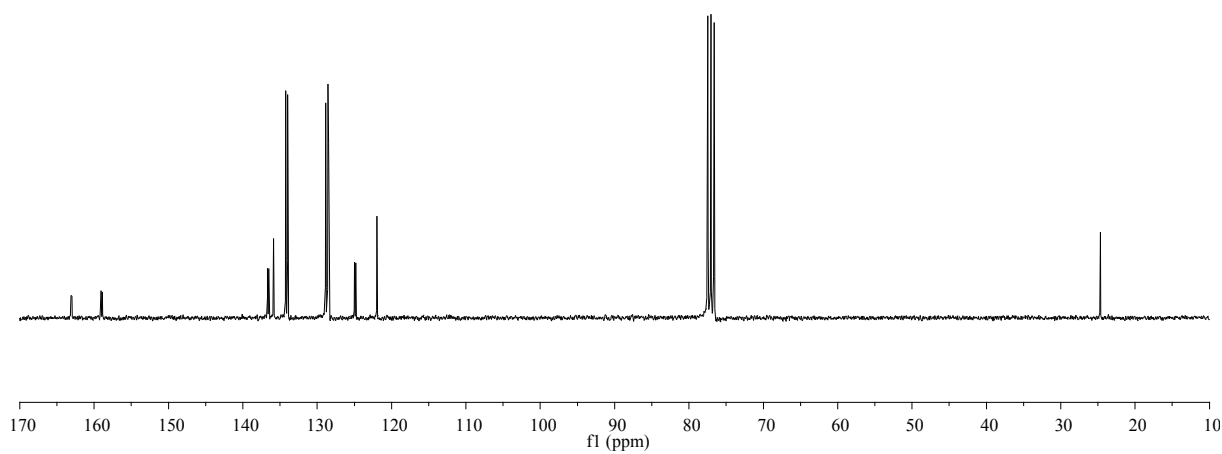
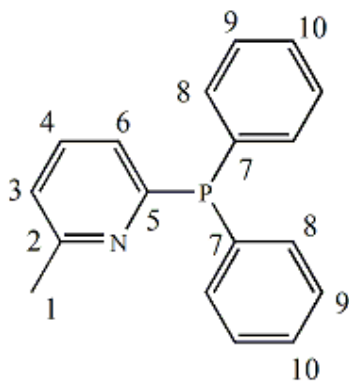


Figure 3.10 ¹³C NMR spectrum of 2-(6-methyl)(diphenylphosphine)pyridine in CDCl₃.

¹³C NMR (300 MHz, CDCl₃, 298 K): 163.16(C5), 159.10(C2), 135.98(C4), 134.22(C8), 128.98(C10), 128.64(C9), 125.02(C7), 122.07(C3), 24.78(C1) ppm.



^{31}P 2-(6-methyl)(diphenylphosphine)pyridine

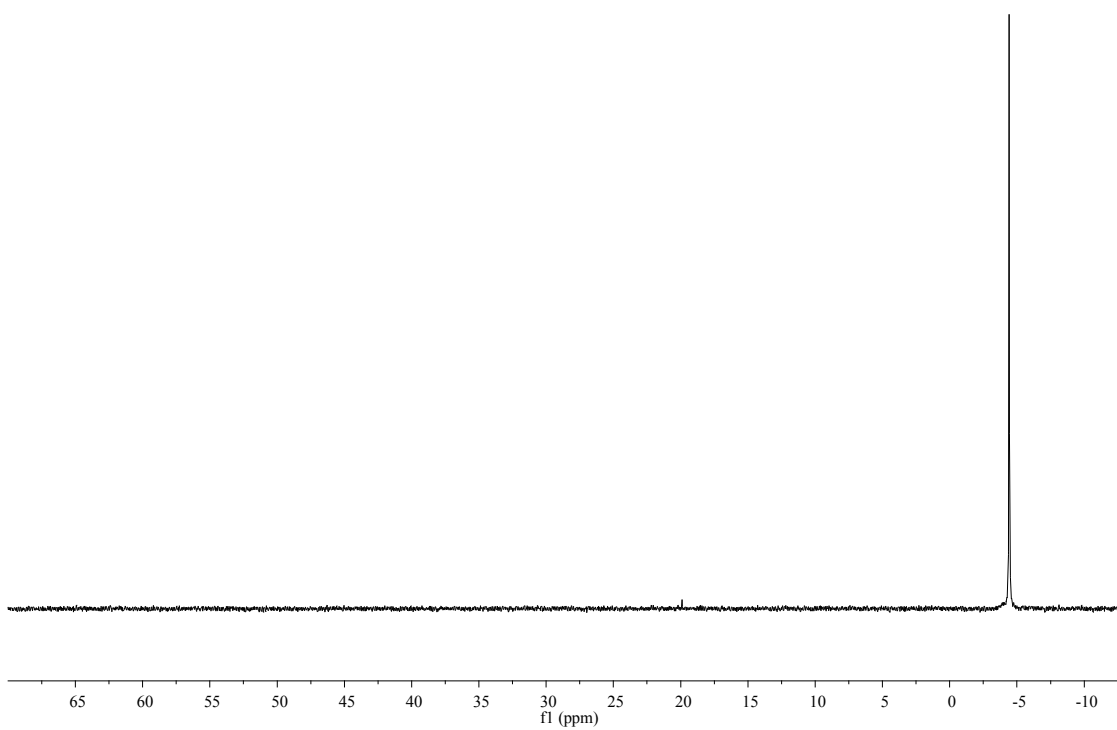
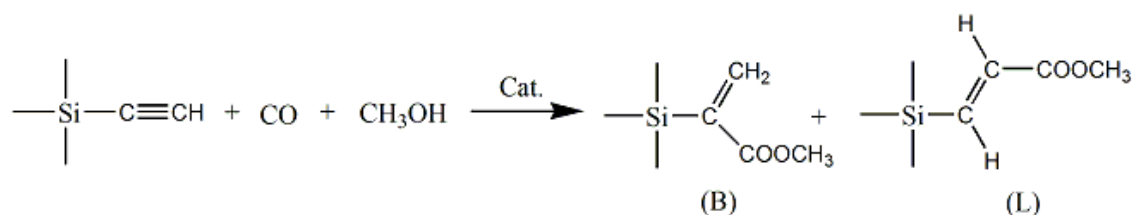


Figure 3.11 ^{31}P NMR spectrum of 2-(6-methyl)(diphenylphosphine)pyridine in CDCl_3 . (One singlet at -4.41 ppm)

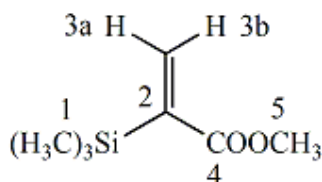
3.2.4.3 Methoxycarbonylation of (trimethylsilyl)acetylene in the presence of the catalytic system $\text{Pd}(\text{OCOCH}_3)_2/\text{CH}_3\text{SO}_3\text{H}/2\text{-}(6\text{-methyl})(\text{diphenylphosphino})\text{pyridine}$



Cat. = $\text{Pd}(\text{OCOCH}_3)_2/\text{CH}_3\text{SO}_3\text{H}/2\text{-}(6\text{-Methyl})(\text{diphenylphosphino})\text{pyridine}$

Considering the Entry 2 of Table 3.2 (see results and discussion), 10.0 mL of anhydrous MeOH were introduced in a Schlenk flask containing a magnetic bar. 2.32 mg (0.0103 mmol) of $\text{Pd}(\text{OCOCH}_3)_2$ and 57.4 mg (0.206 mmol) of 2-(6-methyl)(diphenylphosphino)pyridine were added to the flask under stirring. The reaction was degassed and then 1.45 mL (10.3 mmol) of (trimethylsilyl)acetylene and 13.4 μL (0.206 mmol) of methanesulfonic acid were added under inert atmosphere. The resulting solution was transferred to the autoclave by *cannula*. The autoclave was pressurized with 20 atm of CO. After 3 hours of stirring at 60 °C, the reactor was cooled and the residual gas vented off. The substrate conversion and selectivity of the reaction were determined by gaschromatography.

Crude mixture obtained from the methoxycarbonylation of (trimethylsilyl)acetylene was filtered off, and solvent was removed by controlled evaporation. The brown oil obtained was extracted with toluene. The resulting solution was evaporated under reduced pressure. The purification by column chromatography using 1:1 mixture of ethyl acetate and hexane gave the title compound (44%) which was characterized by ^1H NMR (Figure 3.12), ^{13}C NMR (Figure 3.13), and DEPT 135 (Figure 3.14) spectroscopy.



Methyl 2-(trimethylsilyl)acrylate

Methyl-2-(trimethylsilyl)acrylate

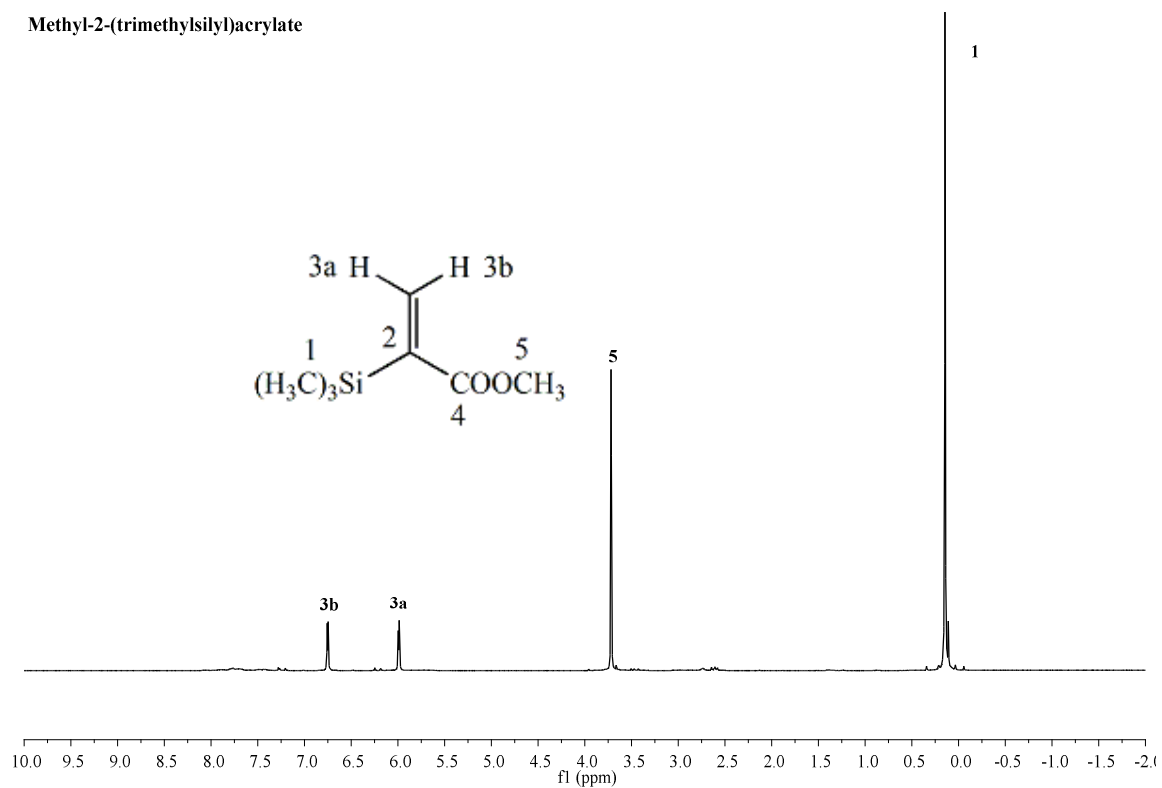


Figure 3.12 ^1H NMR spectrum of methyl 2-(trimethylsilyl)acrylate in CDCl_3 .

^1H NMR (300 MHz, CDCl_3 , 298 K): δ 6.75 (d, 1H(3b), $J = 3.0$ Hz), 5.99 (d, 1H(3a), $J = 3.0$ Hz), 3.71 (s, 3H(5)), 0.14 (s, 9H(1)) ppm.

Methyl 2-(trimethylsilyl)acrylate

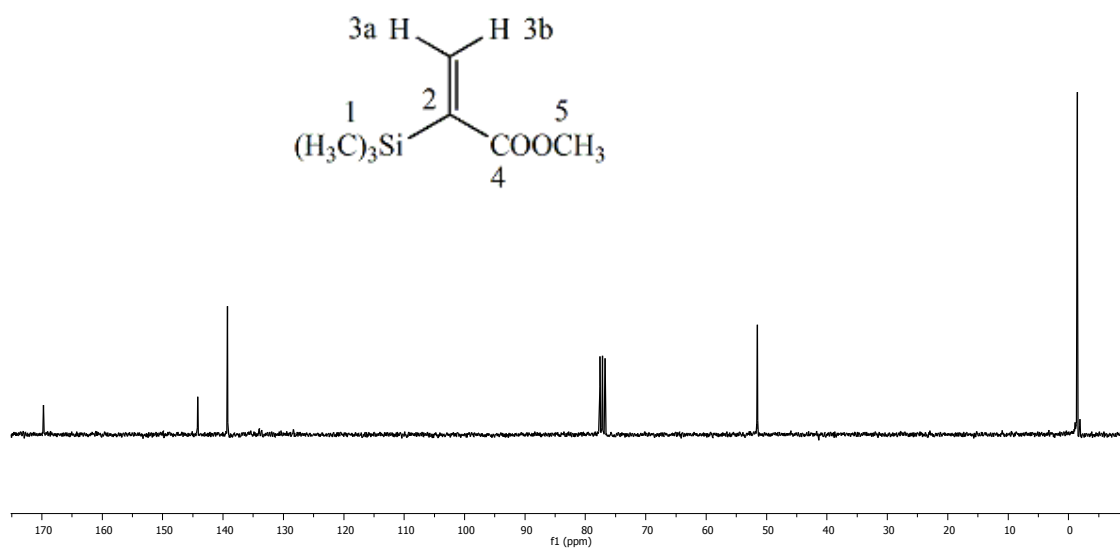


Figure 3.13 ^{13}C NMR spectrum of methyl 2-(trimethylsilyl)acrylate in CDCl_3 .

^{13}C NMR (300 MHz, CDCl_3 , 298 K): δ 169.71 (C4), 144.18 (C2), 139.25 (C3), 51.51 (5), -1.46 (C1) ppm.

Methyl 2-(trimethylsilyl)acrylate

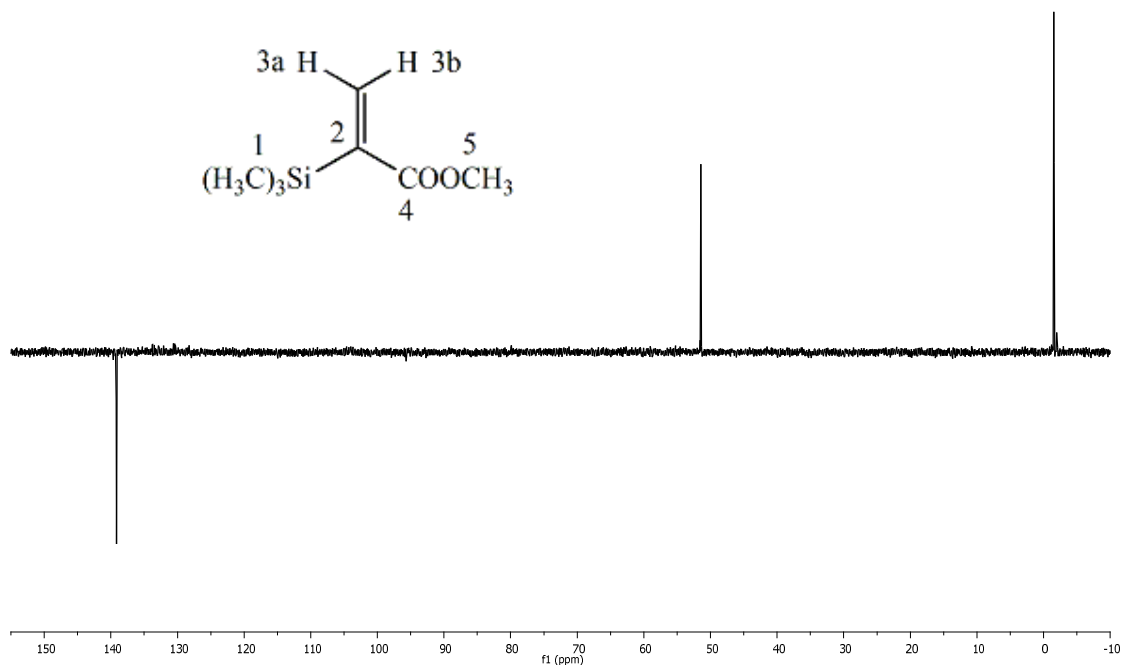
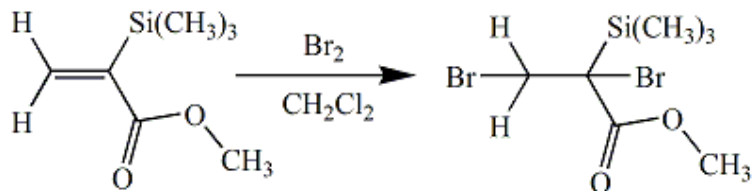


Figure 3.14 DEPT 135 spectrum of methyl 2-(trimethylsilyl)acrylate in CDCl_3 .

DEPT NMR spectrum of methyl 2-(trimethylsilyl)acrylate support the structure determination by ^1H NMR and ^{13}C NMR spectra. In the DEPT spectrum, two positive phase indicates C1 and C5 whereas the one negative phase indicates C3.

3.2.4.4 Synthesis of methyl 2,3-dibromo-2-(trimethylsilyl)propanoate



In a 50.0 mL two-necked round bottom flask (equipped with magnetic stirrer, bubble condenser and connected to the vacuum/argon line), 640 mg (4.1 mmol) of methyl 2-(trimethylsilyl)acrylate was put under inert atmosphere. 12.0 mL of anhydrous dichloromethane were added to the reaction vessel. A solution of 0.21 mL (4.1 mmol)

bromine in 6.0 mL anhydrous dichloromethane was dropwise added to the reaction vessel under inert atmosphere. A yellow color changes into red. The reaction mixture was heated to reflux for 4 hours and then left under stirring at room temperature overnight. The reaction was monitored by gaschromatography. After completion of the reaction, the removal of solvent under reduced pressure gave the title compound (93%) as a brown liquid which was characterized by ^1H NMR (Figure 3.15) and ^{13}C NMR (Figure 3.16) spectroscopy.

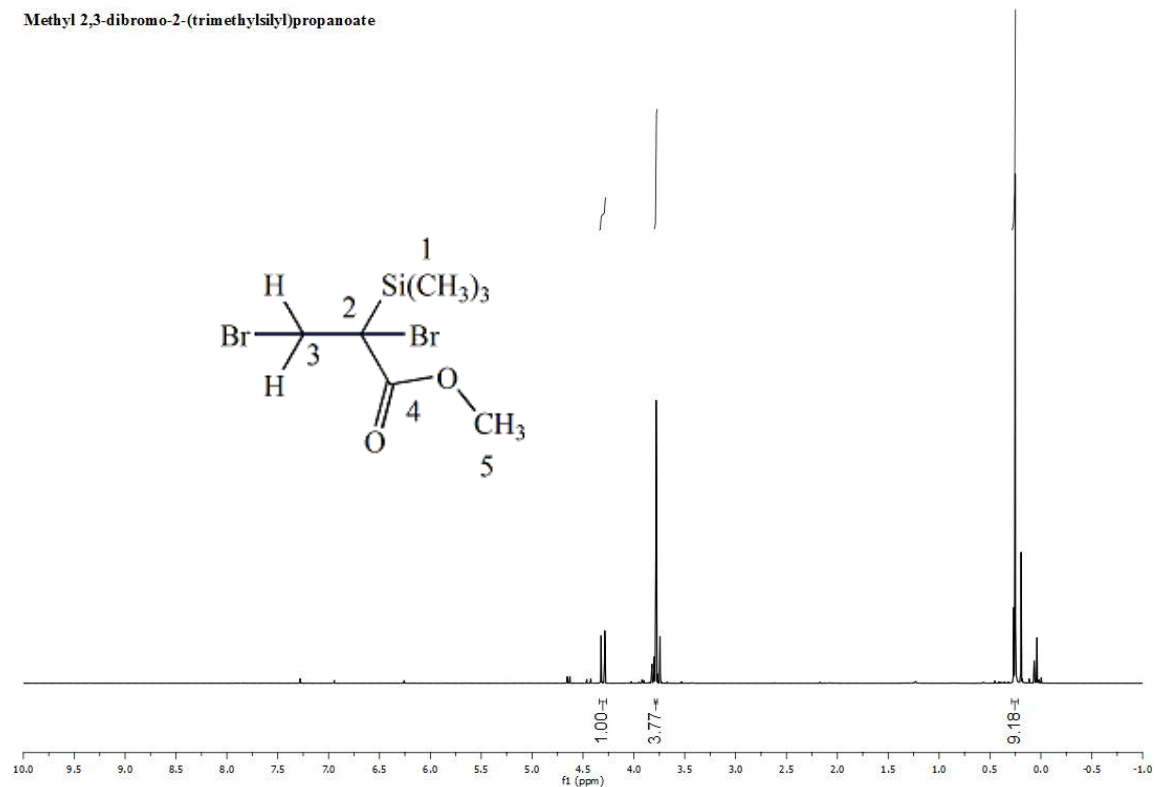


Figure 3.15 ^1H NMR spectrum of methyl 2,3-dibromo-2-(trimethylsilyl)propanoate in CDCl_3 .

^1H NMR (200 MHz, CDCl_3 , 298K): δ 4.31 (d, 1H(3), $J = 10.8$ Hz), 3.76 (d, 1H(3), $J = 10.8$ Hz), 3.78 (s, 3H(5); 0.25 (s, 9H(1)) ppm.

Methyl 2,3-dibromo-2-(trimethylsilyl)propanoate

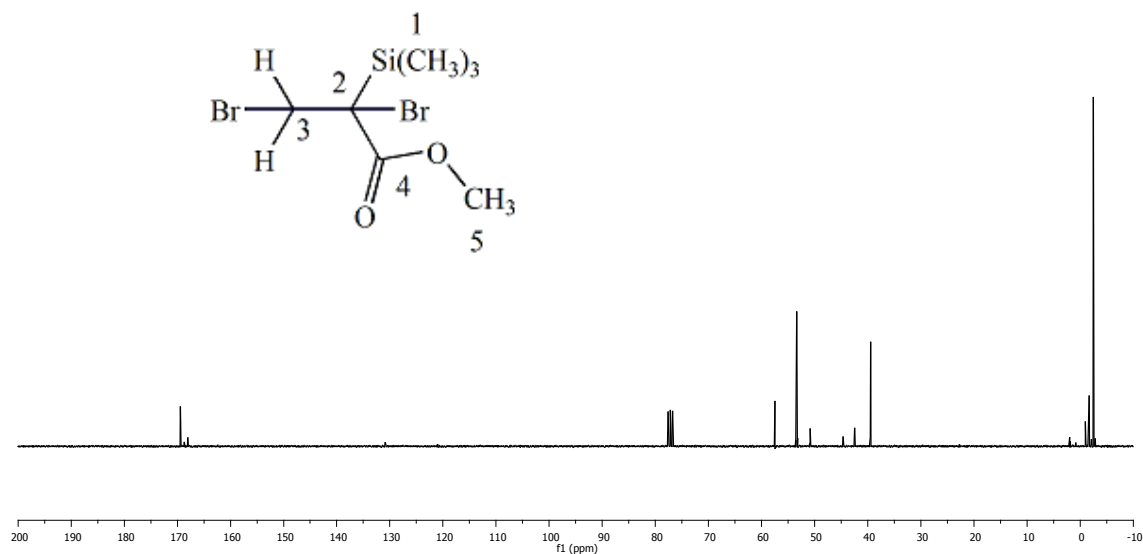
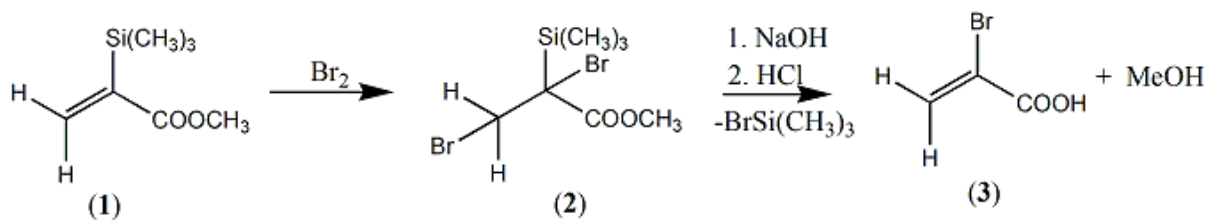


Figure 3.16 ^{13}C NMR spectrum of methyl 2,3-dibromo-2-(trimethylsilyl)propanoate in CDCl_3 .

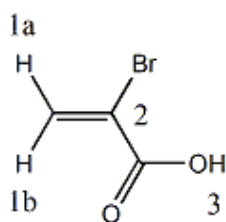
^{13}C NMR (300 MHz, CDCl_3 , 298 K): δ 169.45 (C4), 57.32 (C5); 53.11 (C2), 39.13 (C3), -2.81 (C1) ppm.

3.2.4.5 Synthesis of 2-bromoacrylic acid



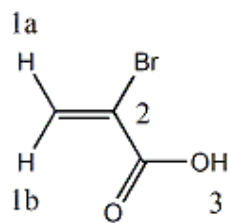
The synthesis of 2-bromoacrylic acid *via* bromodesilylation of methyl 2-(trimethylsilyl)acrylate was carried out according to the method described by L. Piovesan [95].

In a 50.0 mL two-necked round bottom flask (equipped with magnetic stirrer, bubble condenser and connected to the vacuum/argon line), 400 mg (2.5 mmol) of methyl 2-(trimethylsilyl)acrylate was put under inert atmosphere. 5.0 mL of anhydrous dichloromethane were added to the reaction vessel. A solution of 0.13 mL (2.5 mmol) bromine in 8.0 mL anhydrous dichloromethane was dropwise added to reaction vessel under nitrogen atmosphere. A yellow color changes into red. The reaction mixture was heated to reflux for 4 hours. An aqueous solution (5.0 mL) of 10% NaOH was added to the reaction mixture and left under stirring at room temperature overnight. After removing all the solvent, the crude was dissolved in H₂O, acidified with HCl and then extracted with diethyl ether. The evaporation of diethyl ether giving 2-bromoacrylic acid in 37% yield. The title compound (orange solid) was characterized by ¹H NMR (Figure 3.17) and ¹³C NMR (Figure 3.18) spectroscopy.



2-bromoacrylic acid

2-bromoacrylic acid



2-bromoacrylic acid

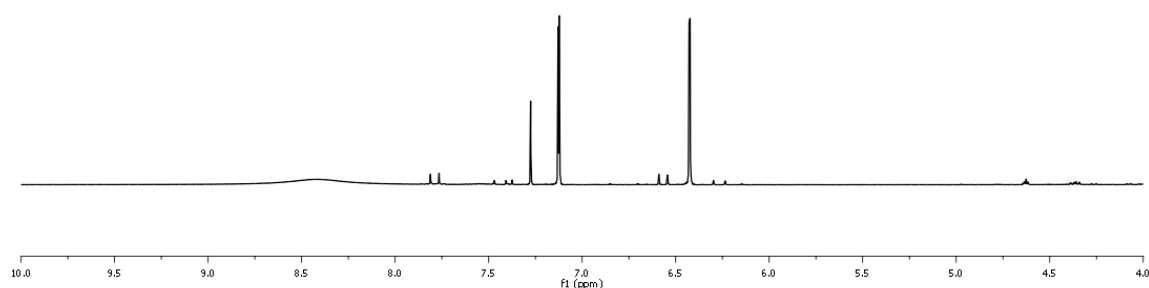


Figure 3.17 ¹H NMR spectrum of 2-bromoacrylic acid in CDCl₃.

¹H NMR (300 MHz, CDCl₃, 298K): δ 7.10 (s, 1H(1b)), 6.40 (s, 1H(1a)) ppm.

The small signals appeared from the starting carboxylated product i.e., methyl 2-(trimethylsilyl)acrylate . The purification of this starting material still need more affords.

2-bromoacrylic acid

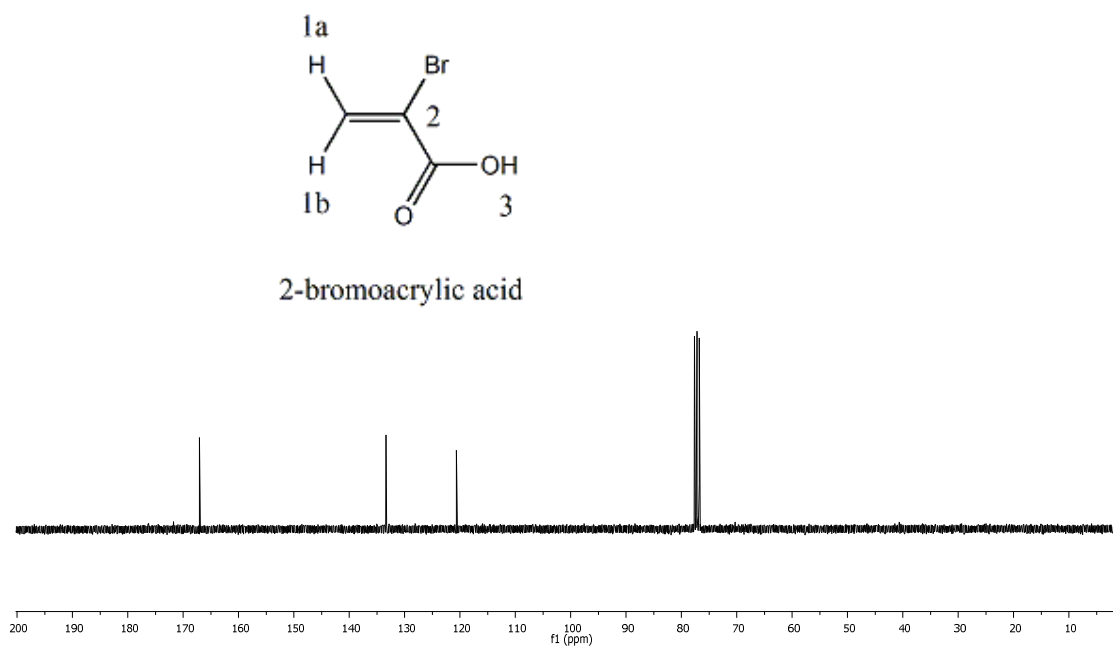
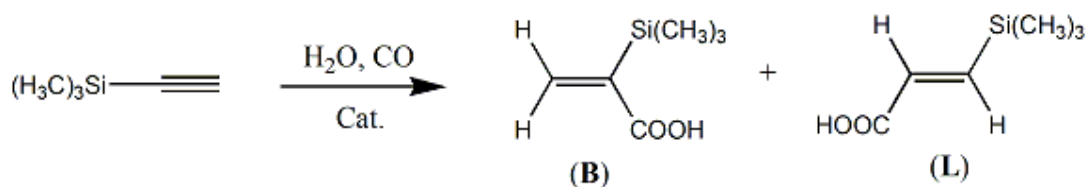


Figure 3.18 ¹³C NMR spectrum of 2-bromoacrylic acid in CDCl₃.

¹³C NMR (300 MHz, CDCl₃, 298 K): δ 167.01 (C3), 133.49 (C1); 120.74 (C2) ppm.

3.2.4.6 Hydroxycarbonylation of (trimethylsilyl)acetylene in the presence of the catalytic system Pd(OCOCH₃)₂/CH₃SO₃H/2-(6-methyl)(diphenylphosphino)pyridine



Cat. = Pd(OCOCH₃)₂/CH₃SO₃H/2-(6-Methyl)(diphenylphosphino)pyridine

Considering the Entry 1 of Table 3.9 (see results and discussion), 10.0 mL of THF and 2.0 mL of H₂O were introduced in a Schlenk flask containing a magnetic bar. 4.62 mg (0.0206 mmol) of Pd(OCOCH₃)₂ and 114.8 mg (0.412 mmol) of 2-(6-

methyl)(diphenylphosphino)pyridine were added under stirring. The solution was degassed. 1.01 g (10.3 mmol) of (trimethylsilyl)acetylene and 53.6 μL (0.824 mmol) of methanesulfonic acid were added to the solution under inert atmosphere. The resulting solution was transferred by *cannula*, under N_2 flux, into the autoclave which was then pressurized with 30 atm of CO. After 24 hours stirring at 80°C, the reactor was cooled and the residual gas vented off. The substrate conversion was determined by gaschromatography. The light yellow crude mixture was filtered off, the volume of filtrate reduced by controlled evaporation, and extracted with diethyl ether. After complete evaporation, we obtained light yellow product which was characterized by ^1H NMR spectroscopy.

2-(trimethylsilyl)acrylic acid

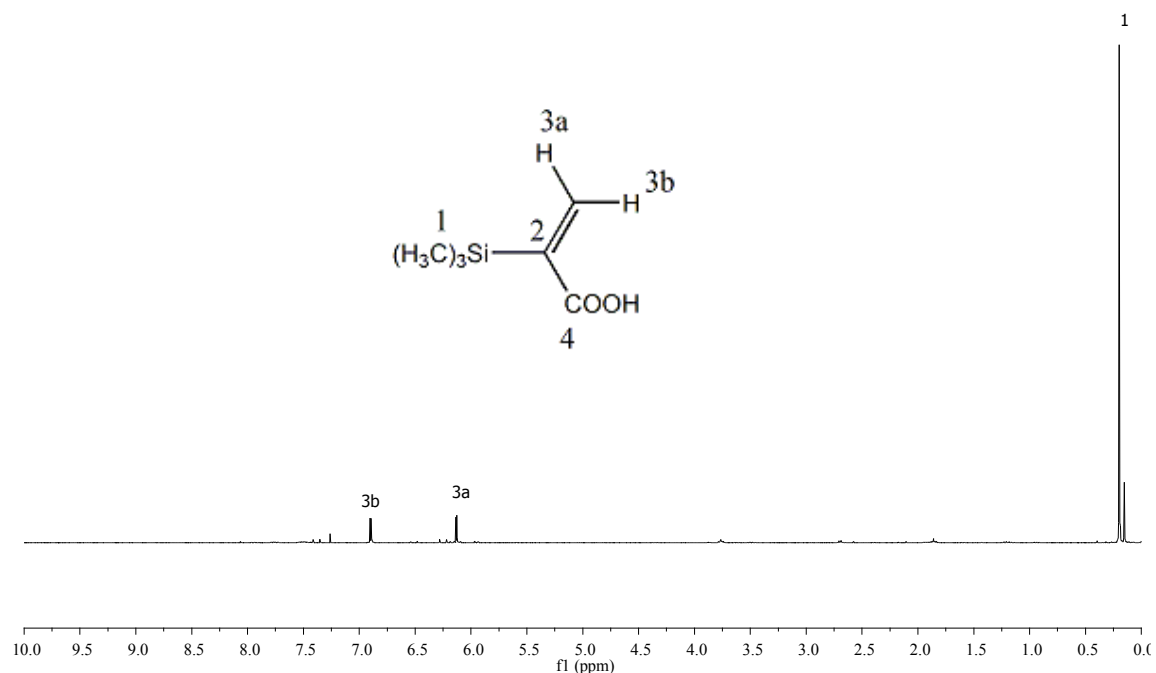


Figure 3.19 ^1H NMR spectrum of 2-(trimethylsilyl)acrylic acid in CDCl_3 .

^1H NMR (300 MHz, CDCl_3 , 298K): δ 6.89 (d, 1H(3b), $J = 2.8$ Hz), 6.13(d, 1H(3a), $J = 2.8$ Hz), 0.20 (s, 9H(1)) ppm.

CDCl_3 is acidic in nature. Therefore, the proton of 2-bromoacrylic acid exchange exchanged with deuterated solvent and the peak is invisible.

3.3 CONCLUSION

In this chapter, we studied the activities of the catalytic system $\text{Pd}(\text{CH}_3\text{COO})_2/\text{CH}_3\text{SO}_3\text{H}/2$ -(6-methyl)(diphenylphosphine)pyridine in the carbonylation of (trimethylsilyl)acetylene. We performed both methoxycarbonylation and hydroxycarbonylation by changing the reaction conditions to optimize the better conversion and selectivity towards branched isomer. The branched isomer is of our interest because it is used for the synthesis of intermediate of enantiomerically enriched α -aryloxypropanoic acid which employed as herbicides.

In methoxycarbonylation reaction, we obtained high values of conversion (73%) and selectivity (95%) toward branched isomer even under mild conditions (substrate/palladium = 4000, phosphine/palladium = 30, acid/phosphine = 1, $P(\text{CO}) = 20$ atm., $T = 60$ °C, and $t = 3$ h). In particular, it has been observed that the conversion and selectivity decreases on increasing the substrate/palladium ratio. The higher phosphine/palladium ratio increases both the conversion and selectivity. The best conversion is obtained with unit acid/phosphine ratio. In any case the regioselectivity changes very little with respect to acid/phosphine ratio. The conversion increases on decreasing the CO pressure to a certain value (20 atm.). Further decrease in pressure (15 atm.) decreases the conversion. Increase of reaction temperature increases the conversion with slight decrease of selectivity. An increase of reaction time to 24 hours, we obtained almost quantitative yield. On the contrary, the hydroxycarbonylation reaction of (trimethylsilyl)acetylene does not provide us equal satisfactory result as methoxycarbonylation reaction. We obtained only 55% conversion. Solvent is the most influencing parameters. The best results were obtained using THF or acetone as solvent. When the reaction is carried out by doubling the acid/phosphine ratio, the conversion increases and the selectivity remains almost constant. Furthermore, it was observe that an increase of reaction temperature from 80 to 100 °C in a condition with excess of acid causing a sharp decrease in conversion and an increase in selectivity.

We also performed the bromodesilylation of branched isomer obtained from methoxycarbonylation reaction. The bromination of methyl 2-(trimethylsilyl)acrylate followed by the elimination of bromotrimethylsilyl group using strong base ($\text{NaOH}/\text{Na}_2\text{CO}_3$) gives us 2-bromoacrylic acid, an important intermediate for the synthesis of α -aryloxypropanoic acid.

THE SYNTHESIS OF NEW WATER-SOLUBLE TRIAZOLE LIGANDS BY CLICK CHEMISTRY (CuAAC)

Triazoles are important heterocyclic organic compounds characterized by five member ring structure. Many organic molecules containing 1,2,3-triazole moieties are employed as the biologically active molecules for pharmaceuticals [30-31]. For examples, carboxyamidotriazole (CAI) is used as anticancer agents. The bidentate ligands containing a triazole core are attractive compounds also for transition metal complex. Many different synthetic approaches are reported for the preparation of triazoles. Of them, the copper(I) catalyzed azide-alkyne cycloaddition reaction is most widely used because of its unique properties. The cycloaddition reaction is highly representative example of click reactions [36]. In this chapter, we report the synthesis of a series of triazole ligands by click azide-alkyne cycloaddition reaction. The synthesized ligands are subdivided into two categories: pyridyl-triazole and methyl(thio)ethyl-triazole ligands (Table 4.0).

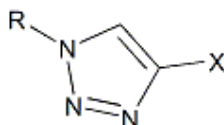


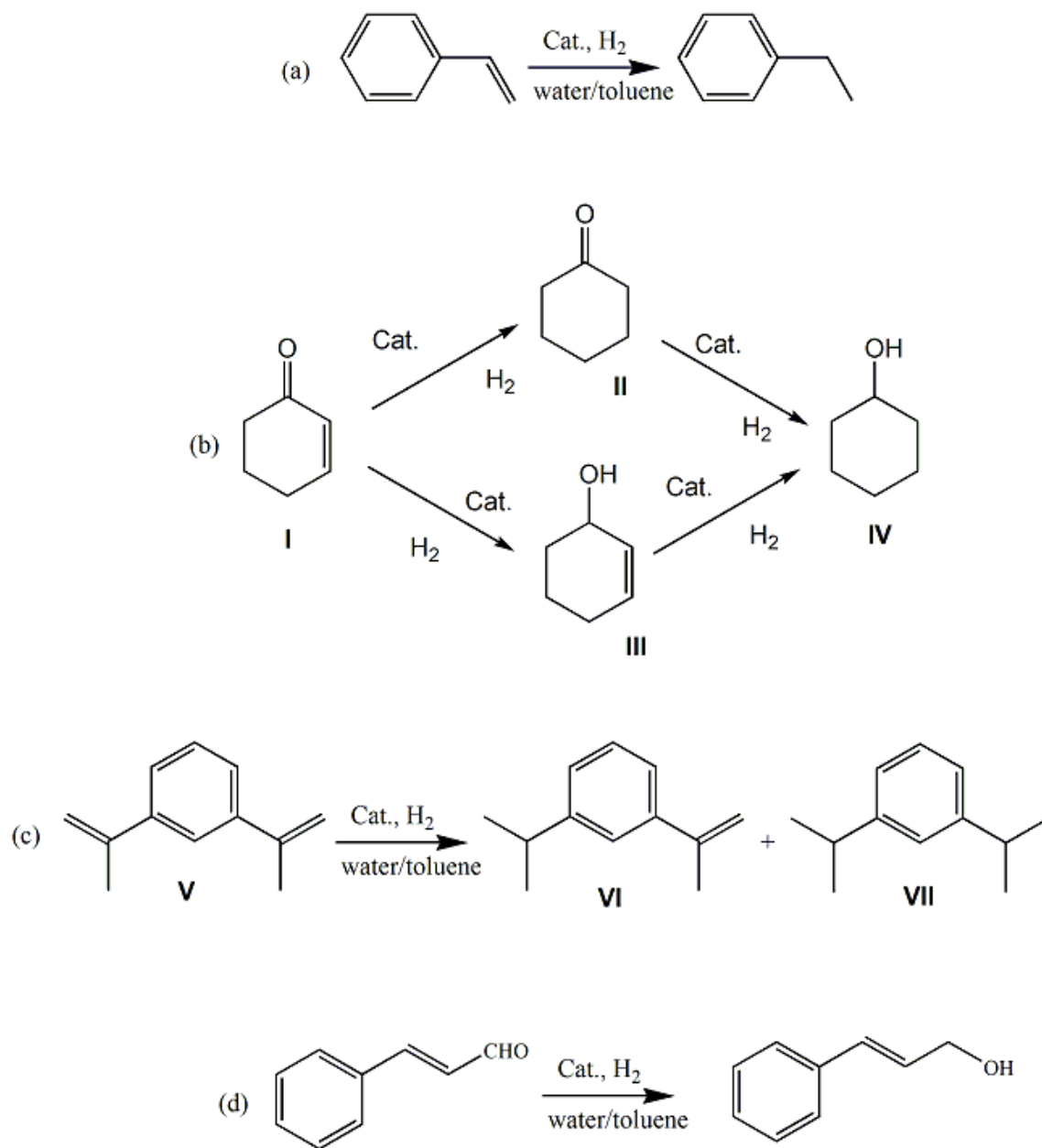
Table 4.0 List of the synthesized triazole ligands

Ligand	R	X
Pyridyl-triazole		
1.Na	2-CH ₂ Py	(CH ₂) ₂ OSO ₃ Na
2	"	(CH ₂) ₂ OH
3	"	Ph
Methyl(thio)ethyl-triazole		
4	CH ₃ S(CH ₂) ₂	(CH ₂) ₂ OH
5	"	(CH ₂) ₂ Br
6	"	(CH ₂) ₂ SO ₃ CH ₃
7.Na	"	(CH ₂) ₂ O(CH ₂) ₃ SO ₃ Na
8	"	(CH ₂) ₂ PySO ₃ CH ₃

Among the triazole ligands, ligand **1.Na** and ligand **4** are soluble in water, methanol, and DMSO. The water soluble ligands are employed in the catalysis of biphasic hydrogenation and hydroformylation of C=C and C=O double bonds. These triazole ligands have been used for the preparation of new transition metal complexes. In this Thesis, the new ruthenium complexes $[\text{RuCl}(\eta^6\text{-}p\text{-cymene})(\text{ligand } \mathbf{1})]$ (complex **1**), $[\text{RuCl}(\eta^6\text{-}p\text{-cymene})(\text{ligand } \mathbf{2})]\text{Cl}$ (complex **2**), and $[\text{RuCl}(\eta^6\text{-}p\text{-cymene})(\text{ligand } \mathbf{3})]\text{Cl}$ (complex **3**) were synthesized by stirring 1:1 equivalent of ligand and ruthenium precursor, $[\text{RuCl}_2(p\text{-cymene})]_2$ in methanol. $[\text{Co}(\text{ligand } \mathbf{1})_2(\text{H}_2\text{O})] \cdot 4\text{H}_2\text{O}$ complex was synthesized according to the same procedure as for ruthenium complexes. The synthesis of $[\text{Pd}(\eta^3\text{-C}_3\text{H}_5)(\text{ligand } \mathbf{8})\text{Cl}](\text{CH}_3\text{SO}_3)_2$ was reported. The characterization of the ligands and complexes were carried out by elemental analysis, IR, ESI-MS and NMR spectroscopy. The *in situ* iridium and rhodium complexes are prepared by simple stirring of metal precursor ($[\text{Ir}(\text{COD})\text{Cl}]_2$ or $[\text{Rh}(\text{COD})\text{Cl}]_2$) and water soluble ligand in water.

Homogenous catalysis is a powerful tool for organic synthesis but its success in industrial application is limited because of difficult catalyst separation and reuse. To overcome these issues, the use of biphasic catalysis is at present of great interest because the catalyst is confined in one of the two-phases and the product in the other phase allowing for a prompt recovery of the product and an easy recycle of the catalyst. In particular, the development of water soluble catalysts for aqueous/organic biphasic reactions is increasingly attractive.

The biphasic hydrogenations (Figure 4, **a**, **b**, **c**) of styrene, 2-cyclohexene-1-one, *m*-diisopropenylbenzene, and cinnamaldehyde using preformed $[\text{RuCl}(\eta^6\text{-}p\text{-cymene})(\text{ligand } \mathbf{1})]$ catalyst and *in situ* prepared iridium-ligand **1** catalyst have been investigated (Scheme 4.0). Both catalysts are highly active in the hydrogenations of styrene, 2-cyclohexene-1-one, and *m*-diisopropenylbenzene but inactive for cinnamaldehyde. An efficient hydroformylation of styrene was studied using a water soluble catalyst formed by the interaction between $[\text{Rh}(\text{COD})\text{Cl}]_2$ and ligand **4**. An efficient hydroformylation of styrene (Figure 4, **d**) was studied using a water soluble catalyst formed by the interaction between $[\text{Rh}(\text{COD})\text{Cl}]_2$ and ligand **4**.

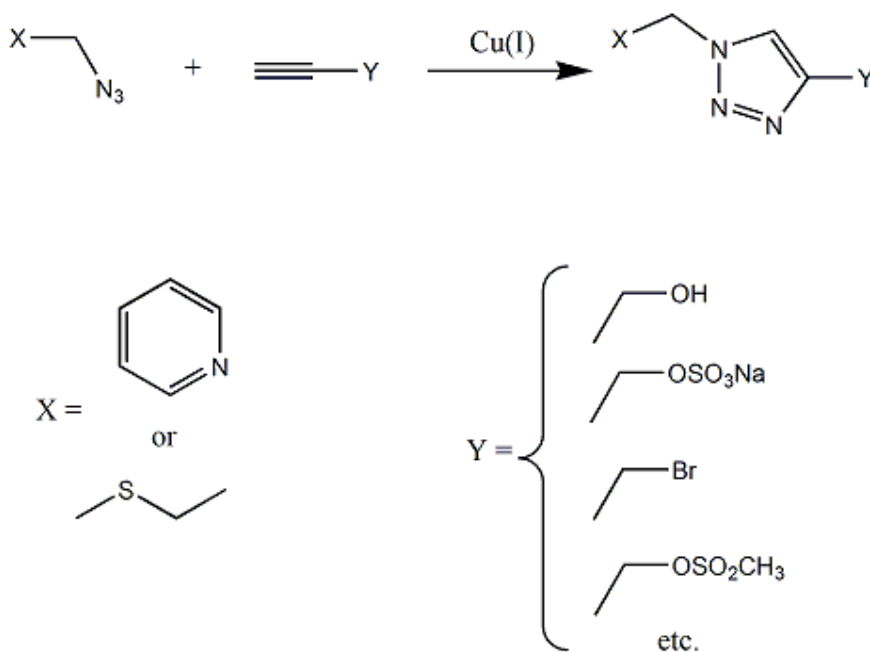


Scheme 4.0 Biphasic catalysis of C=C and C=O.

4.1 RESULTS AND DISCUSSION

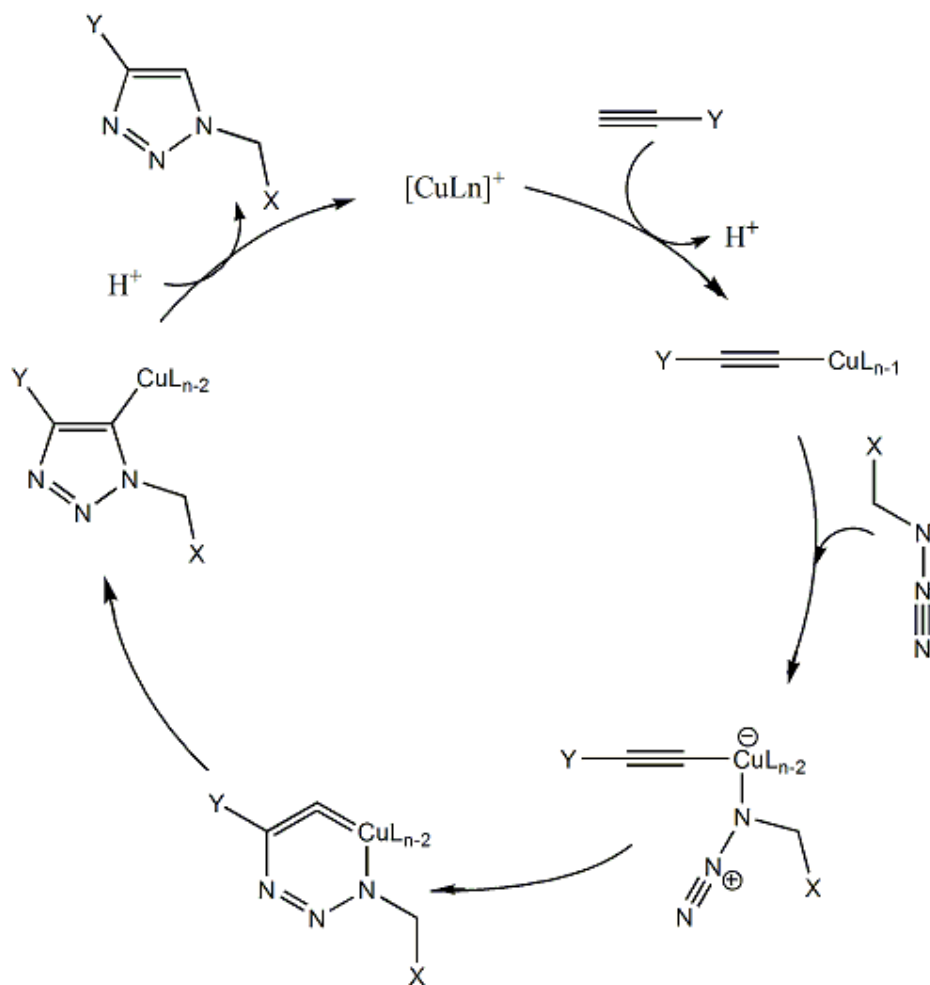
4.1.1 Synthesis and characterization of triazole ligands

Triazoles are important chemical moieties widely used as biologically active compounds [30-31]. Many attractive works have been reported on the coordination behavior of 1,2,3-triazole ligands in the presence of transition metals, their anticancer activity of ruthenium complexes [45-49], and their activity in transition-metal catalyzed homogeneous reactions [46, 62]. According to my literature review, none of the previously reported ligands are water soluble. Recently, we synthesized a water-soluble 1,2,3-triazole ligand which was successfully used in aqueous phase Suzuki-Miyaura cross-coupling reaction [63]. The triazole ligands are synthesized by click reaction which have lot of advantages such as high yield and atom efficiency, available solvents and reagents, no side reactions etc [36]. The copper(I)-catalyzed cycloaddition reaction is carried out starting from an azide and a terminal alkyne (Scheme 4.1) [35, 47].



Scheme 4.1 Copper(I)-catalyzed click reaction.

The catalyst usually used is $\text{Cu}(\text{AcO})_2 \times \text{H}_2\text{O}$ or an *in-situ* mixture of CuSO_4 and sodium ascorbate. The azide is synthesized from the corresponding halide by the reaction with sodium azide in a mixture of solvents (*tert*-butanol:water, 4:1) [104]. The alkynes are either commercially available or synthesized according to literature [105]. The well accepted mechanism of copper(I)-catalyzed azide-alkyne cycloaddition reaction is reported below (Scheme 4.2) [36].

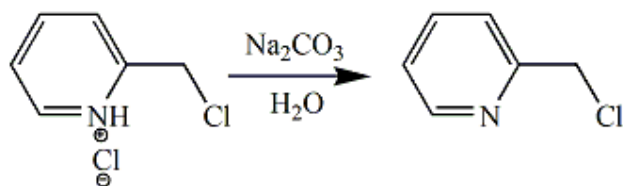


Scheme 4.2 Mechanism of Cu(I)-catalyzed azide-alkyne cycloaddition reaction.

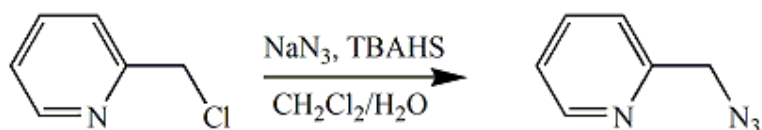
4.1.1.1 Synthesis and characterization of pyridyl-triazole ligands

The synthesis of 2-(1-((pyridine-2-yl)methyl)-1*H*-1,2,3-triazol-4-yl)ethyl sodium sulfate (ligand **1.Na**) consists of four distinct reactions (Scheme 4.3):

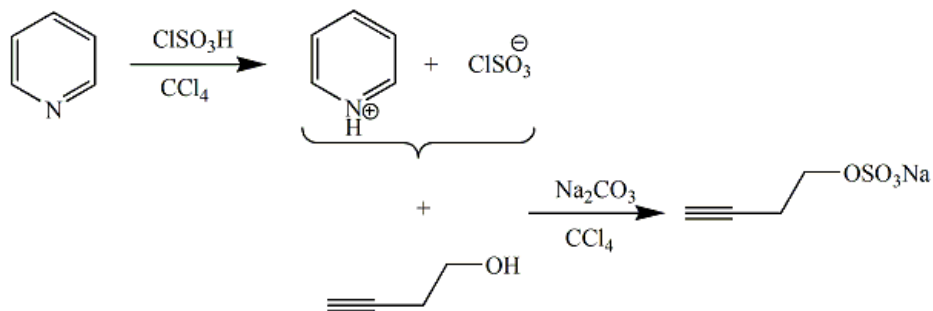
(a) deprotonation of 2-(chloromethyl)pyridine hydrochloride



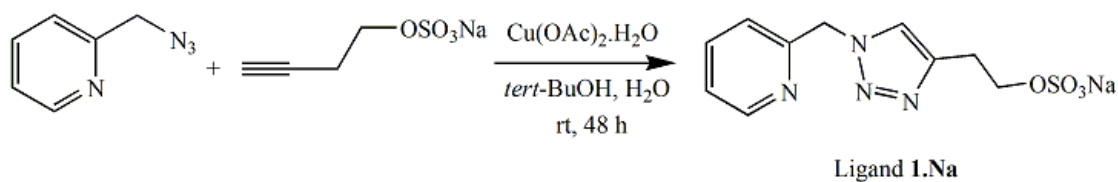
(a) Synthesis of 2-(chloromethyl)pyridine



(b) Synthesis of 2-(azidomethyl)pyridine



(c) Synthesis of sodium 3-butyn-1-sulfate



Ligand **1.Na**

(d) Synthesis of ligand **1.Na**

Scheme 4.3 Synthesis of ligand **1.Na**.

(b) preparation of 2-(azidomethyl)pyridine.

(c) preparation of sodium 3-butyn-1-sulfate

(d) synthesis of the ligand **1.Na**.

The deprotonation of 2-(chloromethyl)pyridine hydrochloride in the presence of Na_2CO_3 gives 2-(chloromethyl)pyridine.

2-(azidomethyl)pyridine was prepared by the reaction of 2-(chloromethyl)pyridine with NaN_3 in a biphasic system (dichloromethane/water) in the presence of a phase transfer agent tetrabutylammonium hydrogensulfate (TBAHS) [104]. NaN_3 is dissolved in water while 2-(chloromethyl)pyridine in dichloromethane. TBAHS allows NaN_3 to transfer from aqueous phase into the organic phase containing 2-(chloromethyl)pyridine where the substitution of Cl by N_3 occurs. The preparation requires a large excess (slight excess of 2 equivalent) of azide and 48 hours to achieve complete substitution with azide. The yield is 89 %. ^1H NMR spectrum (see experimental section 4.2.2.2) is consistent with the structure of the prepared 2-(azidomethyl)pyridine (Figure 4.1).

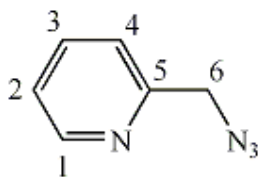


Figure 4.1 Chemical structure of 2-(azidomethyl)pyridine.

The preparation of sodium 3-butyn-1-sulfate is carried out by the treatment of 3-butyn-1-ol in the presence of chlorosulfonic acid (ClSO_3H) and pyridine [105]. The addition of chlorosulfonic acid into carbontetrachloride and pyridine at 0°C produces a mixture of pyridinium and chlorosulfonate ion (Scheme 4.3, c). The observation is the formation of white smoke. Dropwise addition of 3-butyn-1-ol into the reaction vessel and overnight stirring at room temperature produces pyridine hydrochloride and 3-butyn-1-hydrogensulfate. 3-butyn-1-hydrogensulfate is extracted with water. The combined aqueous phase is evaporated to almost half of the volume, the basification by saturated solution of Na_2CO_3 (until no CO_2 evolution, $\text{pH} \approx 9-10$) gave the desired product, sodium 3-butyn-1-sulfate (Figure 4. 2) which is recrystallized from hot EtOH (84%). The white crystal is characterized by ^1H NMR and ^{13}C NMR spectra. (see experimental section 4.2.2.3).

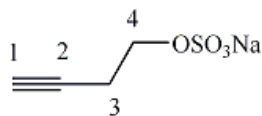


Figure 4. 2 Chemical structure of sodium 3-butyn-1-sulfate.

Finally, water-soluble 2-(1-((pyridine-2-yl)methyl)-1H-1,2,3-triazol-4-yl)ethyl sodium sulfate (ligand **1.Na**) is obtained by [3+2] cycloaddition reaction (a class of click reaction) between the previously prepared 2-(azidomethyl)pyridine and sodium 3-butyn-1-sulfate in *tert*-BuOH/water (4/1) solvents. Cu(AcO)₂·H₂O (10-15 mol %) is used as catalyst. The azide acts as a diene while the terminal alkyne as a dienophile. In this synthetic protocol, a Glaser-type reaction produces copper(I) catalytic species which permit azide-alkyne cycloaddition reaction to give 1,4-disubstituted 1,2,3-triazole product. The *tert*-BuOH itself acts as a reducing agent to generate active copper(I) species [41]. After 48 hours of stirring at room temperature, the green solid obtained was purified by column chromatography (silica gel, dichloromethane / methanol = 8/2 or tetrahydrofuran/methanol = 8/2) to give a pure white solid (ligand **1.Na**) in 79% yield (see experimental section 4.3.1.4) (Figure 4. 3).

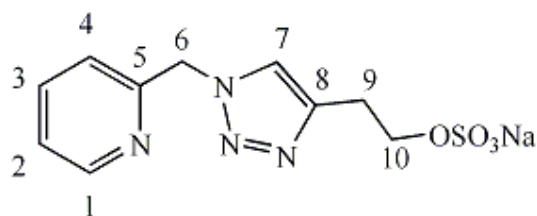


Figure 4.3 Chemical structure of 2-(1-((pyridine-2-yl)methyl)-1H-1,2,3-triazol-4-yl)ethyl sodium sulfate (ligand **1.Na**).

The bidentate nitrogen ligand **1.Na** is soluble in water, methanol, and DMSO. The composition of ligand **1.Na** was confirmed by elemental analysis, NMR spectra, and ESI-MS spectrum in the negative mode (see the experimental section 4.3.1.4). In the ¹H NMR spectrum (Figure 4.4) of ligand **1.Na** in CD₃OD, the evidence of the formation of triazole ring comes from the presence of a characteristic triazole-H(7) strong singlet at 7.97 ppm. A remarkable shift of δ value (Δδ = 1.21) for CH₂ (6) proton of 2-(azidomethyl)pyridine has been noticed upon the formation of ligand **1.Na**.

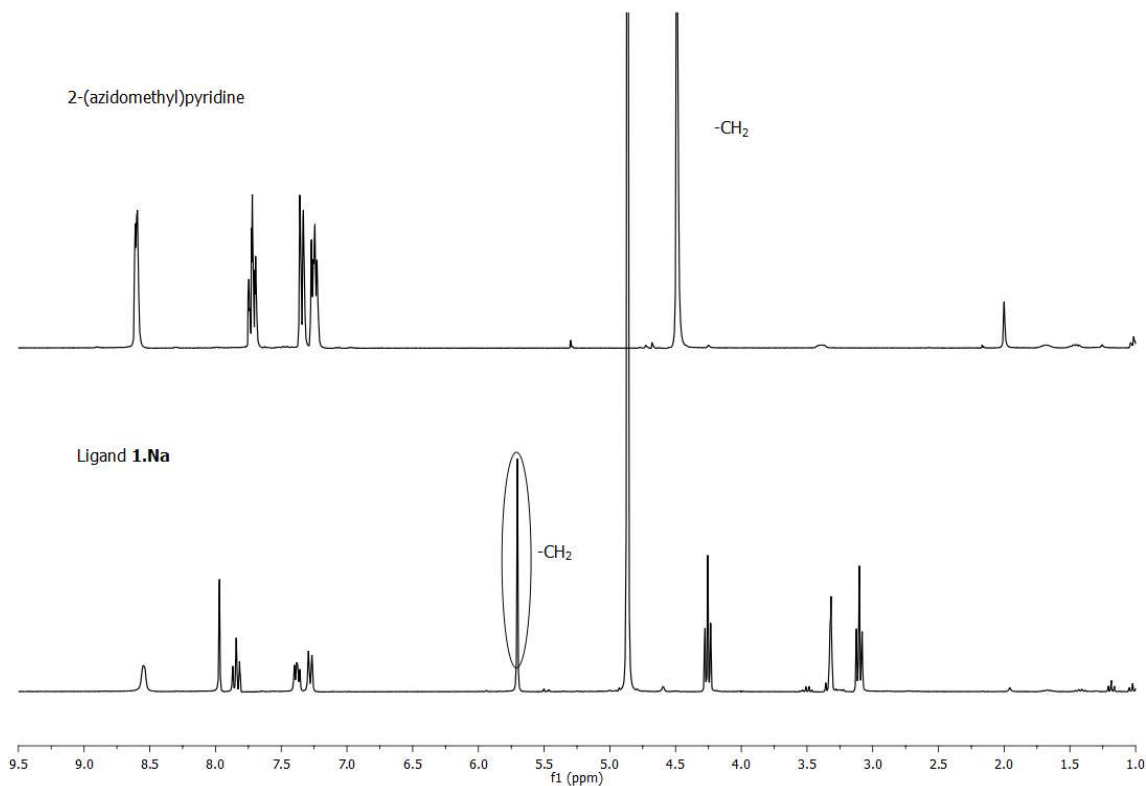
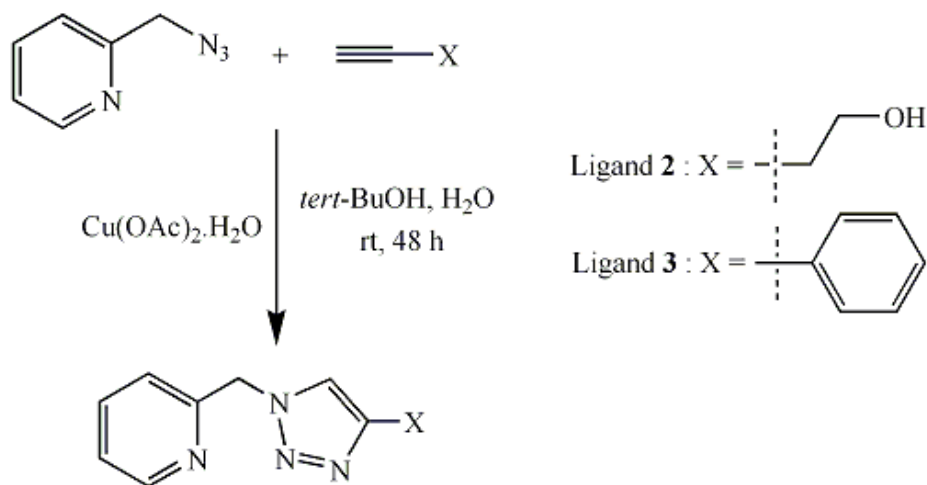


Figure 4.4 Comparison between the ^1H NMR spectra of 2-(azidomethyl)pyridine and ligand **1.Na**.

In the ^{13}C NMR spectrum, the triazole carbon (C7) which resonates at 137.90 ppm indicates the formation of ligand **1.Na**. These observations are consistent with the ^{13}C NMR spectrum of triazole ligand reported by Urankar *et al* [45].

Anal. cal. for $\text{C}_{10}\text{H}_{11}\text{N}_4\text{O}_4\text{SNa}$ (306.27): C, 39.22; H, 3.62. Found: C, 39.3; H, 3.5. The measured and calculated ESI-MS spectra are shown in Figure 4.7 (see experimental section, Figure 4.21). The data, 283.0 ($\text{C}_{10}\text{H}_{11}\text{N}_4\text{O}_4\text{S}^-$, 100%), 589 (ligand **1**+ $\text{C}_{10}\text{H}_{11}\text{N}_4\text{O}_4\text{S}^-$, 4%) are in good agreement with the formation of ligand **1.Na**.

The ligand **2** and ligand **3** were synthesized according to the same protocol as for ligand **1.Na** (Scheme 4.4). The azide used is the same as for ligand **1.Na**, whereas the alkynes (3-butyn-1-ol for ligand **2**, and phenylacetylene for ligand **3**) are different. The crude ligand **2** is a green oil which was purified by column chromatography (silica gel, dichloromethane / methanol = 9/1) to give a pure yellow oil (ligand **2**) with 87% yield.



Scheme 4.4 Synthesis of ligands (2 and 3).

The ^1H NMR and ^{13}C NMR spectra of ligand **2** (Figure 4.5) were measured in CDCl_3 (see the experimental section 4.2.2.5, Figure 4.22 & 4.23, respectively). ^1H NMR spectrum indicates the presence of triazole-singlet at 7.60 ppm and the shift of δ value for CH_2 proton of 2-(azidomethyl)pyridine from 4.5 to 5.63 ppm. These observations are fully consistent with the ^1H NMR spectrum of triazole ligand reported by Emanuele *et al.* [63]. The ^{13}C NMR spectrum is also in good agreement with the structure of ligand **2**.

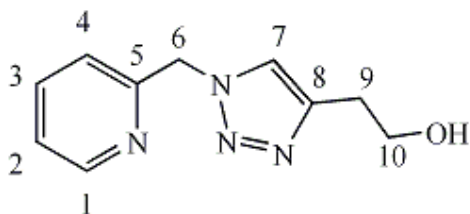


Figure 4.5 Chemical structure of ligand **2**.

The reaction crude of ligand **3** (Figure 4.6) is a white solid, purified by column chromatography (silica gel, dichloromethane / ethyl acetate = 5/5).

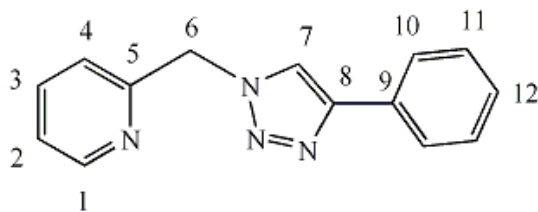


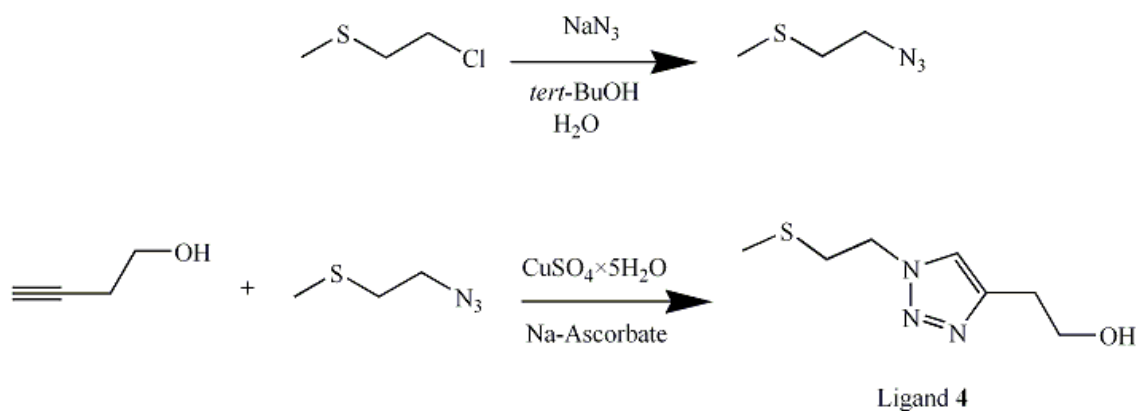
Figure 4.6 Chemical structure of ligand **3**.

The ^1H NMR and ^{13}C NMR spectra of ligand **3** (Figure 4.6) were carried out in CDCl_3 (see the experimental section 4.2.2.6, Figures 4.24 & 4.25, respectively). ^1H NMR indicates the presence of triazole-singlet H(7) at 7.95 ppm and the shift of δ value for CH_2 proton H(6) of 2-(azidomethyl)pyridine from 4.5 to 5.69 ppm. The NMR spectral data are in good agreement with reported values for similar ligands [62].

4.1.1.2 Synthesis and characterization of 1-(2-(methylthio)ethyl)-1H-1,2,3-triazole ligands

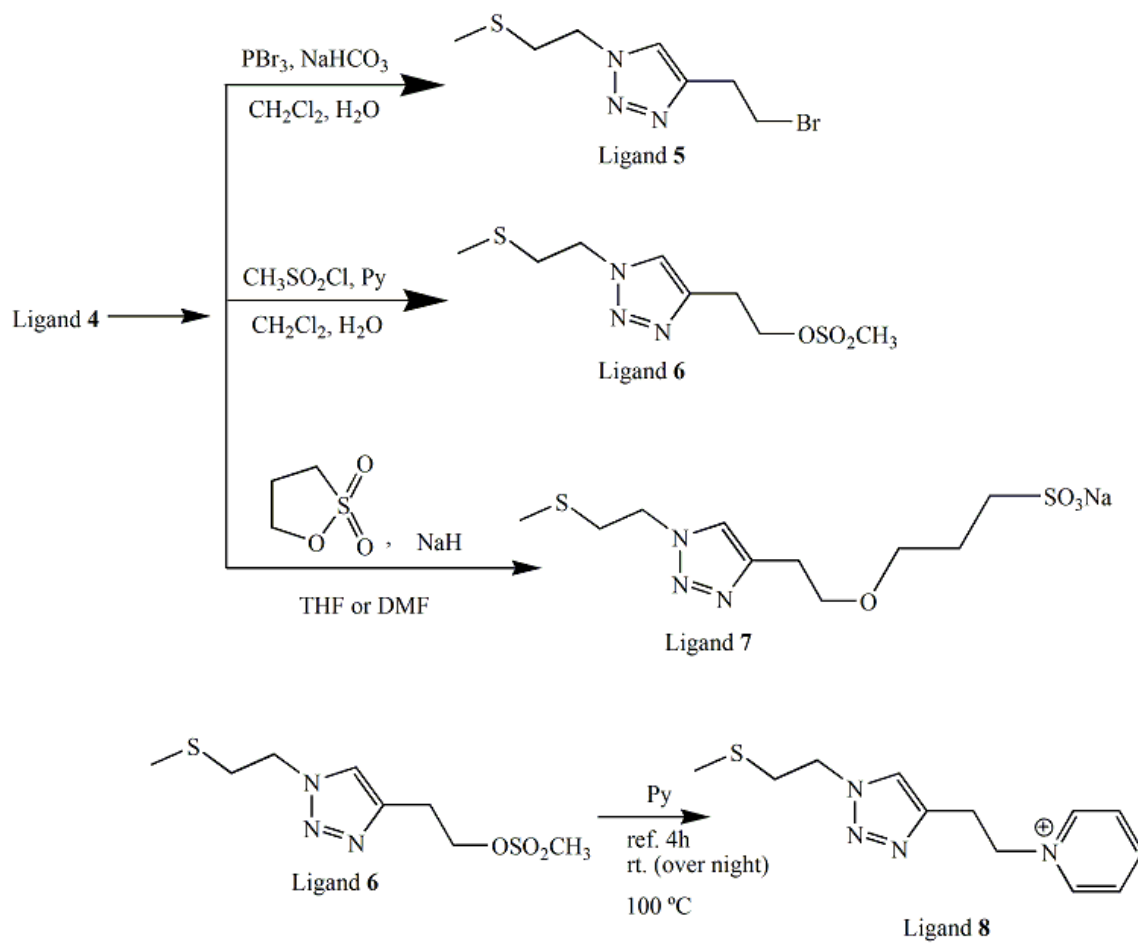
The synthesis of methyl(thio)ethyl-triazole ligand was carried according to V.V. Rostovtsev *et al.* [35]. The synthesis consists of two steps. First, the reaction of sodium azide with (2-chloroethyl)(methyl)sulfane in *tert*-BuOH/water (4:1) solvent mixture, was analyzed by GC. When the conversion was complete (monitored by GC analysis), the highly volatile (2-azidoethyl)(methyl)sulfane was collected in closed vessel. The large excess of sodium azide ensured the complete conversion of chloride into the corresponding azide.

Second, 3-buten-1-ol is added to the closed vessel followed by the addition of copper catalyst ($\text{CuSO}_4 \cdot 5\text{H}_2\text{O}$ and Na-ascorbate). After 24 hours stirring at room temperature, a pale yellow oil was obtained (Scheme 4.5). Extraction with chloroform gave a yellow oil in 85% yield. The NMR spectra is consistent with the product, ligand **4** (see the experimental section 4.2.3.1).



Scheme 4.5 Synthesis of ligand **4** (2-(1-(2-(methylthio)ethyl)-1H-1,2,3-triazol-4-yl)ethanol).

In the ^1H NMR spectrum, the strong singlet H(4) at 7.51 ppm. indicates the formation of triazole moiety. The pure ligand **4** was used as the starting material for the preparation of ligands **5**, **6**, **7**, and **8** (Scheme 4.6).

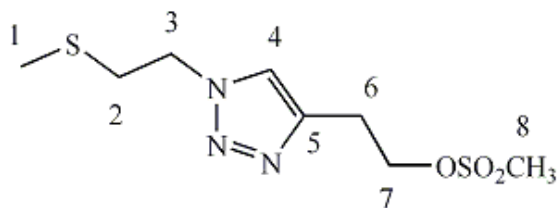


Scheme 4.6 Synthesis of the ligands **5**, **6**, **7**, and **8**.

The various attempts have been taken to the preparation of ligand **5**. One of them is the reaction of ligand **4** with bromine in dichloromethane. The method is unsuccessful to get any product. After then, we succeed to synthesis the ligand **5** in very low yield. The synthesis consists of two steps. In the first step, a dichloromethane solution of PBr_3 (1.25 eq., 25% excess) was slowly added to the dichloromethane solution of ligand **4** (1 eq.) under inert atmosphere at 0 °C. After 1.5 hours of stirring at 0 °C, the system was kept under stirring at room temperature for overnight.

In the second step, an aqueous solution of NaHCO_3 (2 eq.) was slowly (over an hour) added into the reaction mixture. After a few seconds, the solution becomes intensely red and smoke is formed. The organic layers were extracted with CH_2Cl_2 , combined together, and dried with sufficient MgSO_4 . After filtration and vacuum dried, the product is a colorless oil in 30% yield. The ^1H NMR spectrum is consistent with the structure of ligand **5**. In the ^1H NMR spectrum, the chemical shifts (7.58 ppm) of the triazole ring proton is almost unchanged with respect to the starting ligand **4**, but a small shift of δ value (0.3) compared to CH_2 (7) proton of ligand **4** has been noticed upon the formation of ligand **5** (see experimental section 4.2.3.2).

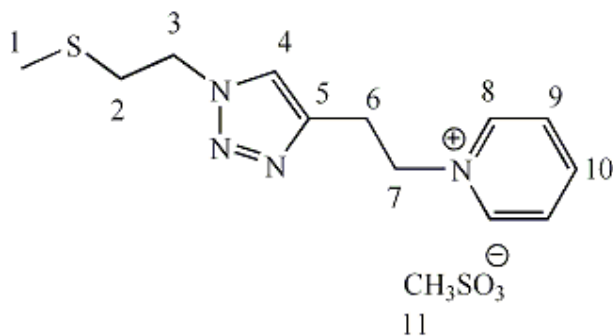
The synthesis of ligand **6** was carried out according to the literature reported by Vladimir C. Sekera *et al.* [106]. The synthesis was carried out by the reaction between ligand **4** and methane sulfonyl chloride in dichloromethane and pyridine. Pyridine acts as a *scavenger* for hydrochloric acid. To avoid the formation of by-product such as pyridinium salt containing the ester product (sulfonic acid ester) reported by J. F. *et al* [107], the addition of methane sulfonyl chloride was started at 0 °C. After return the reaction at room temperature, the reaction mixture was stirred overnight. The resulting green solution was evaporated under reduced pressure, and extracted with dichloromethane/water solvents. The extracted dichloromethane solution was dried with sufficient MgSO_4 , filtered off, and evaporated to yellow oil in 77% yield. The ^1H NMR and ^{13}C NMR (Figure 4.15 and Figure 4.16 respectively) spectral data are in good agreement with the structure of ligand **6**. In the ^1H NMR spectrum, the chemical shifts (7.55 ppm) of the triazole ring proton is almost unchanged with respect to the starting ligand **4**. The $-\text{CH}_3$ (8) proton signal overlap with $-\text{CH}_2$ (2) proton at 2.97 ppm (see the experimental section 4.2.3.3).



Ligand 6

According to the reaction scheme in the experimental section 4.2.3.4, the ligand 7 was synthesized by the nucleophilic ring opening of 1,3-propanesultone with sodium 2-(1-(2-(methylthio)ethyl)-1H-1,2,3-triazol-4-yl)ethanoate under mild condition. The synthesis was carried out according to the procedure reported by Brent C. Norris *et al.* [108]. A THF solution of 1,3-propanesultone was slowly added to the mixture of NaH and ligand 4 at 0 °C. The final reaction mixture was refluxed for 3 hours and kept overnight stirring under room temperature, filtered, and precipitated using diethyl ether. The ¹H NMR spectrum of the light yellow solid is in good agreement with the structure of ligand 7.

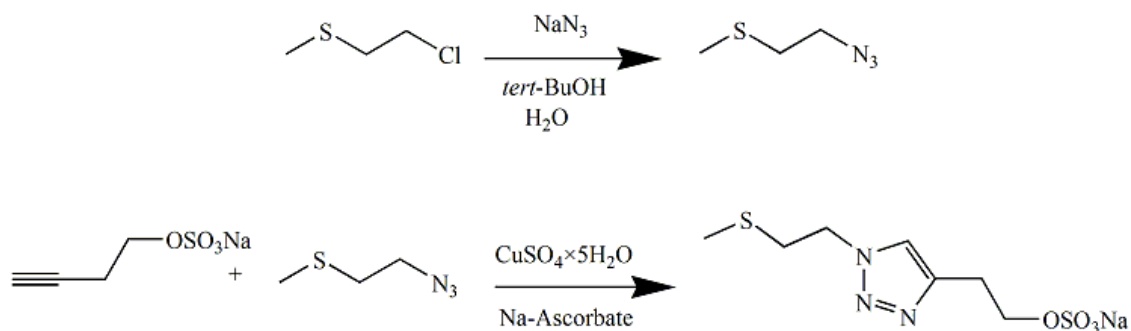
The ligand 8 was synthesized by the nucleophilic substitution of methanesulfonate with a molecule of pyridine from ligand 6 [109]. A mixture of ligand 6 and a large excess of pyridine was refluxed for 4 hours under inert atmosphere. The additional overnight stirring at room temperature gave brown solid which was washed with diethyl ether (yield 98%). The NMR spectra consistent with the structure of the ligand 8 (see the experimental section 4.2.3.5, Figure 4.32 & 4.33). In the ¹H NMR spectrum (CDCl₃), doublet at 9.31 ppm is in agreement with two protons, (H8) on α-carbon to the N-atom of pyridine. The strong singlet at 2.81 ppm corresponds to the three protons, (H11) of counter ion, methanesulfonate. The ¹³C NMR spectrum exhibits the resonance for the protons on the pyridine ring at 147.14 (C10), 146.11(C8), and 129.39 (C9), and 39.49 (C11) ppm respectively.



Ligand 8

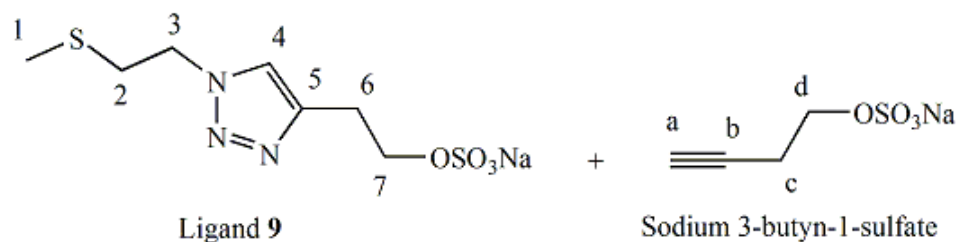
Besides the ligands 1-8, we attempted to synthesis ligand 9 and 10 for several times. The synthesis of ligand 9 was tried according to the literature method reported by V. V. Rostovtsev *et al.* [35]. The method is the same as for the preparation of ligand 4, it consists of

two steps. First step is the synthesis of (2-azidoethyl)(methyl)sulfane (see the synthesis of ligand **4**) while the second step is a copper catalyzed azide-alkyne [3+2] cycloaddition reaction (Scheme 4.7).

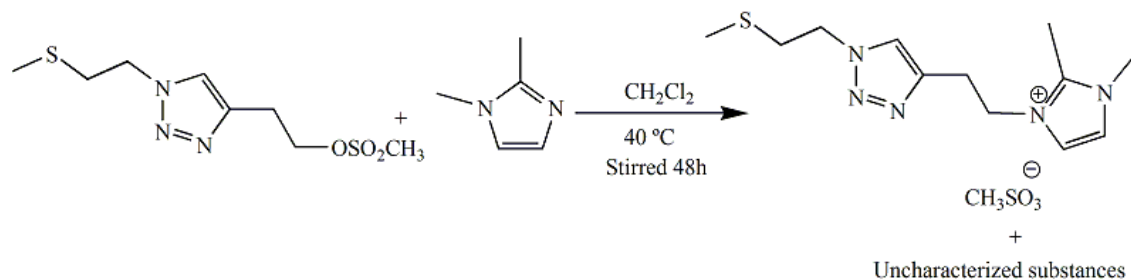


Scheme 4.7 Attempt to synthesis the ligand **9**.

The ^1H NMR spectrum indicate that the product is always a mixture of ligand **9** (65%) and the starting material sodium 3-butyn-1-sulfate (35%) (Figure 4.20, see the experimental section 4.2.3.6). Chromatographic separation does not effective for the purification of the ligand **9**.



The synthesis (Scheme 4.8) of ligand **10** was carried out according to the procedure reported by Eglinton, *et al.* [109]



Scheme 4.8 Attempt to synthesis the ligand **10**.

A mixture of ligand **6** and 1,2-dimethylimidazole was stirred in dry dichloromethane at 40 °C for 48 hours under inert atmosphere. The yellow-brown molten solid obtained was characterized by ¹H NMR spectroscopy. The product is a mixture of ligand **10** and unknown substances (Figure 4.35, see the experimental section 4.2.3.7). No further attempts were made to synthesis this ligand.

THE SYNTHESIS, CHARACTERIZATION AND STUDY OF CATALYTIC AND BIOLOGICAL ACTIVITY OF METAL COMPLEXES BEARING THE NEW LIGANDS

4.1.2 Synthesis and characterization of ruthenium-triazole complexes

4.1.2.1 Synthesis of the ruthenium-pyridyl triazole complexes

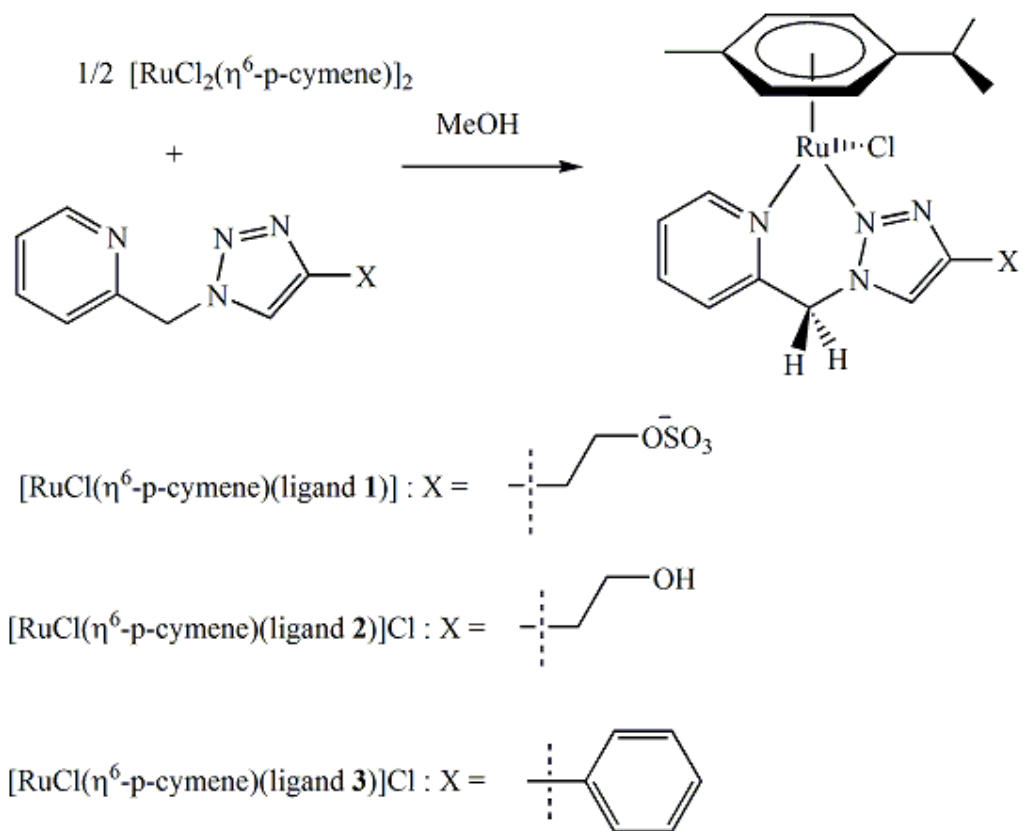
Complex **1** = [RuCl(η⁶-*p*-cymene)(ligand **1**)]

Complex **2** = [RuCl(η⁶-*p*-cymene)(ligand **2**)]Cl

Complex **3** = [RuCl(η⁶-*p*-cymene)(ligand **3**)]Cl

Synthesis of the ruthenium-pyridyl triazole complexes consists of two distinct reactions. First, the preliminary preparation of ruthenium precursor, [RuCl₂(η⁶-*p*-cymene)]₂ was carried out according to the procedure reported by M. A. Bennett *et al.* [110]. The ruthenium precursor complex [RuCl₂(η⁶-*p*-cymene)]₂ was prepared by the reaction of ruthenium trichloride trihydrate with large excess of α-phellandrene in ethanol which was characterized by melting point, FT-IR and ¹H NMR spectroscopy (see the experimental section 4.2.4). In the ¹H NMR spectrum, the presence of 4 equivalent proton indicates the formation of *p*-cymene. Again, the multiplet due to 6 methyl proton shifted 1 ppm into down field from α-phellandrene.

Second, the ruthenium-pyridyl triazole complexes (complex **1**, **2** or **3**) were prepared by stirring [RuCl₂(η⁶-*p*-cymene)]₂ with ligand **1**, **2** or **3** (Ru: ligand = 1:1) in methanol at room temperature (Scheme 4.9).



Scheme 4.9 Synthesis of ruthenium-pyridyl triazole ligand complexes.

4.1.2.2 Characterization of the $[\text{RuCl}(\eta^6\text{-p-cymene})(\text{ligand } \mathbf{1})]$ (complex **1**)

The crude complex **1**, obtained from the reaction of equivalent amount of ligand **1.Na** with $[\text{RuCl}_2(\eta^6\text{-p-cymene})]_2$ is a yellow crystalline powder. Recrystallization of the crude product from hot ethanol affords yellow-orange microcrystals which were found to be smaller aggregates unsuitable for X-ray structure determination. Therefore complex **1** was formulated on the basis of the elemental analysis, conductivity measurements, ESI-MS, and NMR spectroscopy data. Methanol or water solutions of complex **1** are nonconducting ($\Lambda_M < 1 \Omega^{-1} \text{cm}^2 \text{mol}^{-1}$ for a $1.0 \times 10^{-3} \text{ M}$ solution) in agreement with its zwitterionic nature [111-112]. In the ESI-MS spectrum of complex **1** the most intense peaks are: m/z 1685 (M_3+Na)⁺, 1131 (M_2+Na)⁺, and 577 ($\text{M}+\text{Na}$)⁺, with relative intensities 100, 40 and 28, respectively. MS/MS scans showed that from the peak at $m/z = 577$ ($\text{M}+\text{Na}$)⁺ arise peaks having $m/z = 519$ ($\text{M}-\text{Cl}$)⁺, 497 ($\text{M}-\text{SO}_3+\text{Na}$), and 439 ($\text{M}-\text{SO}_3-\text{Cl}$)⁺. NMR spectroscopy indicates that in

complex **1** the pyridyl-triazolyl ligand chelates ruthenium through the pyridyl nitrogen atom and the central nitrogen atom of the triazole ring (see Figure 4.7 for the relevant numbering scheme).

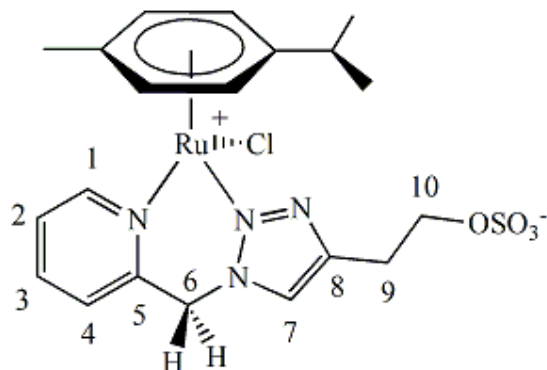


Figure 4.7 Chemical structure of complex **1**.

In fact, in the ^1H NMR spectrum (CD_3OD , 298 K) of complex **1** both the H(1) doublet and the H(7) singlet are found significantly downfield with respect to the free ligand ($\Delta\delta = 0.57$ and 0.33 ppm, respectively) as found for other pyridyl-triazole ligands when chelating to a metal centre [45-46, 62]. Definitive evidence for chelation of ligand **1** at ruthenium comes from the AB spin pattern found for the methylene bridge protons. This pattern is due to the lack of any element of symmetry in the six-membered ring which forms upon ligand chelation. Hence, the axial and the equatorial protons of the methylene moiety become non-equivalent and give two separate resonances with a geminal coupling constant of 15.8 Hz (Figure 4.8).

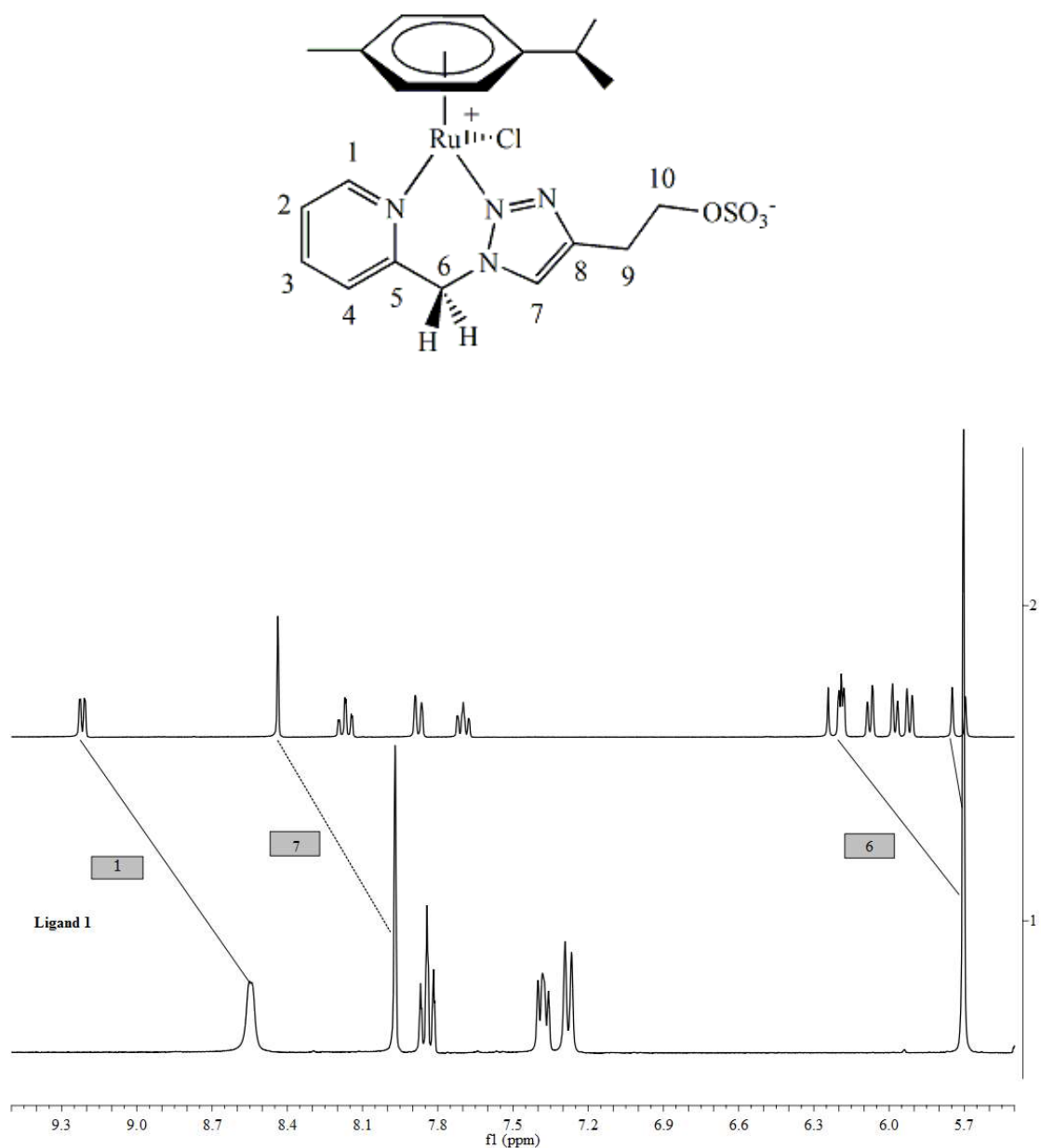


Figure 4.8 Comparison between ^1H NMR spectra of ligand **1.Na** and $[\text{RuCl}(\eta^6\text{-}p\text{-cymene})(\text{ligand } \mathbf{1})]$ in CD_3OD .

Owing to the lack of symmetry, the aromatic protons of the coordinated *p*-cymene give four separate resonances (two AB spin systems) in the 6.1–5.8 ppm range, about 1 ppm upfield with respect to the free ligand. The chemical shifts of the isopropyl and the methyl moieties are almost unchanged with respect to the starting ruthenium complex (Figure 4.9); in this connection it is worth noting that the two methyls of isopropyl moiety which are

accidentally equivalent in the ^1H NMR spectrum give two separate signals in the ^{13}C NMR spectrum.

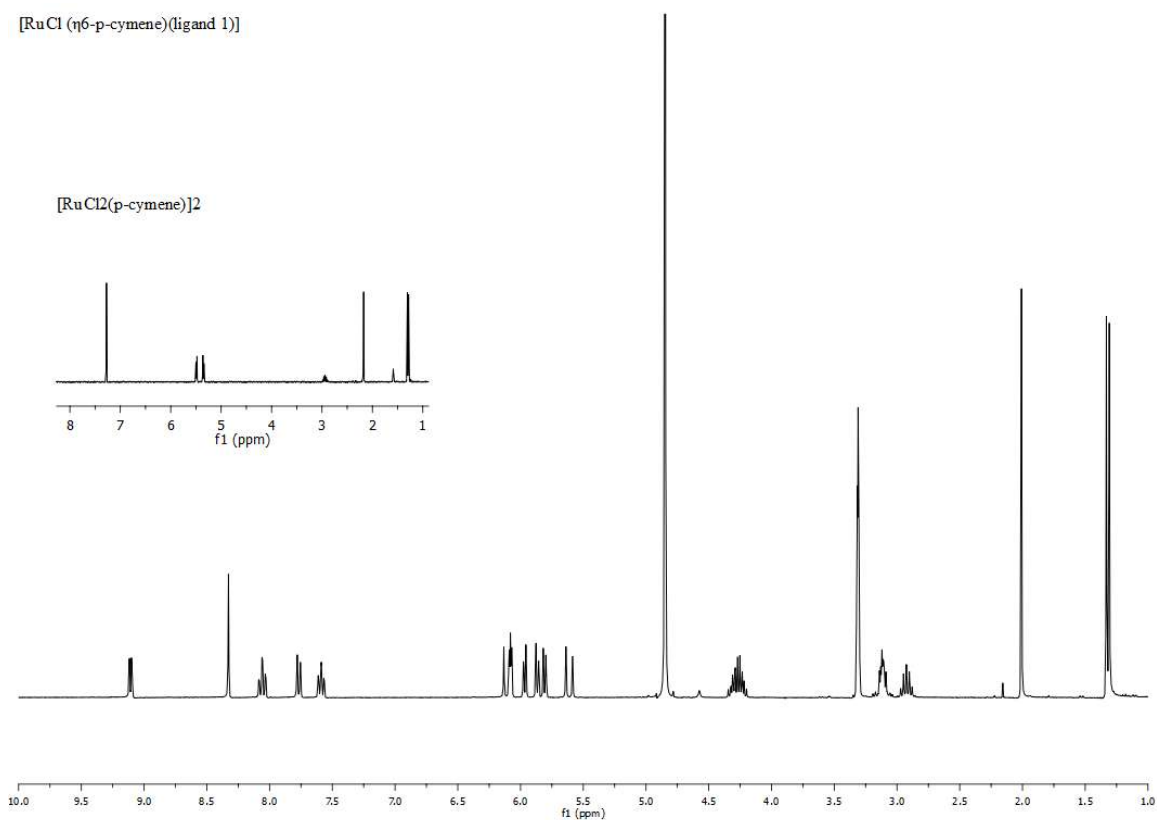
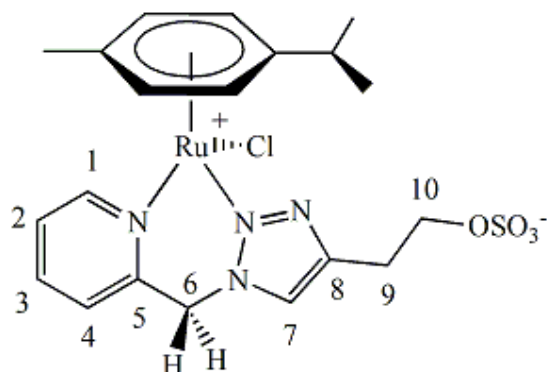


Figure 4.9 Comparison between ^1H NMR spectra of complex **1** and $[\text{RuCl}_2(\eta^6\text{-}p\text{-cymene})]_2$.

Ligand chelation is also indicated by the ^{13}C NMR spectrum in which both C(1) and C(7) resonate at lower fields with respect to free ligand **1.Na**, the $\Delta\delta$ s being 4.80 and 5.13 ppm, respectively. It is worth remarking that both the ^1H and the ^{13}C NMR spectra are in good

agreement with those reported by Kõsmrlj and co-workers for the strictly related species $[\text{RuCl}(\eta^6\text{-}p\text{-cymene})(\text{ligand } \mathbf{3})]\text{Cl}$ the structure of which has been determined by X-Ray crystallography [45, 49].

4.1.2.3 Characterization of the complex **2** and complex **3**

Complex **2** or complex **3** were prepared by simple mixing of $[\text{RuCl}_2(\eta^6\text{-}p\text{-cymene})]_2$ with ligand **2** or ligand **3** respectively in a 1:1 molar ratio. The reaction needs 2-3 days to complete. The crude complexes are yellow powders. Extraction with ethanol gave a light yellow powder in 60-70% yield. These complexes were characterized by ^1H NMR and ^{13}C NMR spectroscopy.

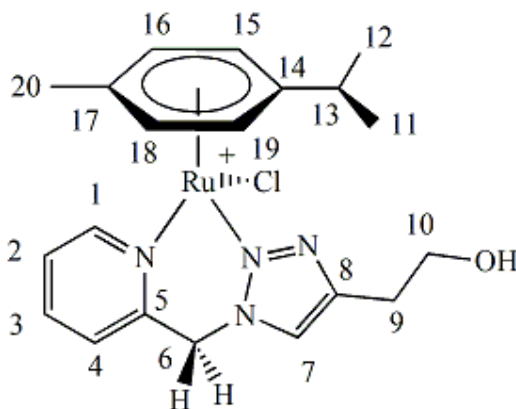


Figure 4.10 Chemical structure of complex **2**.

^1H NMR and ^{13}C NMR spectra of complex **2** indicates that ligand **2** chelates the ruthenium through pyridyl N-atom and the central N atom of the triazole ring (see Figure 4.10 for the relevant numbering scheme). The ^1H NMR spectrum (CD_3OD , 298 K) reveals that the doublet due to H(C-1) and the singlet due to H(C-7) resonate significantly downfield with respect to the free ligand ($\Delta\delta = 0.57$ and 0.33 ppm, respectively) as found for other pyridyl-triazole ligands when chelating to a metal centre [45-46, 62]. Chelation of ligand **2** at the ruthenium centre is also confirmed by the formation of AB spin pattern for the methylene bridge protons. This pattern is due to the lack of any element of symmetry in the six-membered ring which forms upon ligand chelation. Hence, the axial and the equatorial protons of the methylene moiety become non-equivalent and give two separate resonances

with a geminal coupling constant of 15.3 Hz. The chemical shifts of the isopropyl and their methyl moieties are almost unchanged with respect to the starting ruthenium complex while that of methyl group attached into the aromatic ring are shifted 0.10 ppm up field (Figure 4.11).

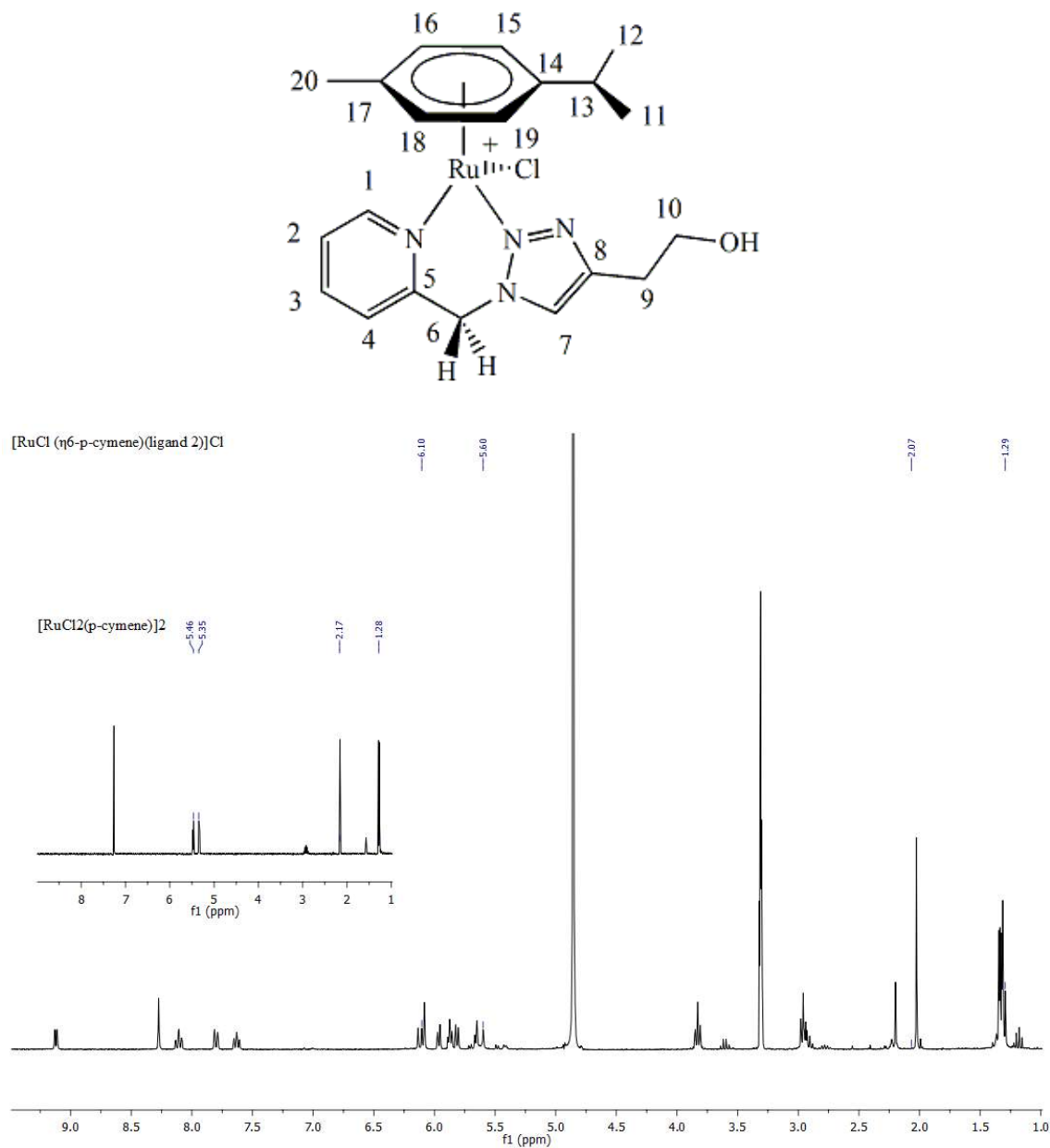


Figure 11 ^1H NMR comparison between $[\text{RuCl}_2(\eta^6\text{-}p\text{-cymene})]_2$ and complex 2.

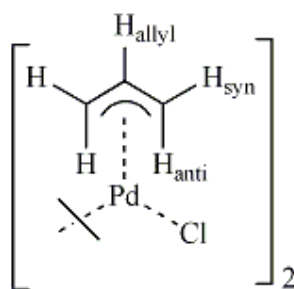
Ligand chelation is also confirmed by the ^{13}C NMR spectrum in which both C(1) and C(7) resonate at lower fields with respect to free ligand 2, the $\Delta\delta$ s being 5.01 and 4.23 ppm,

respectively (see the experimental section 4.2.4.3). It is worth remarking that both the ^1H and the ^{13}C NMR spectra are in good agreement with those reported by Kõsmrlj and co-workers for the strictly related species $[\text{RuCl}(\eta^6\text{-}p\text{-cymene})(\text{ligand } \mathbf{3})]\text{Cl}$ (complex $\mathbf{3}$) the structure of which has been determined by X-Ray crystallography [45, 49]. To test the antimetastatic properties of complex $\mathbf{3}$ against human cancer cell and compare them with that of complex $\mathbf{1}$ and complex $\mathbf{2}$, we prepared the complex $\mathbf{3}$ which characterized by FT-IR and NMR spectroscopy (see the experimental section 4.2.4.4). and are consistent with the data reported by Urankar *et al.*

4.1.3 Synthesis and characterization of Pd-triazole and Co-triazole complexes

4.1.3.1 Preparation of $[\text{Pd}(\eta^3\text{-C}_3\text{H}_5)\text{Cl}]_2$

The $[\text{Pd}(\eta^3\text{-C}_3\text{H}_5)\text{Cl}]_2$ was prepared according to the literature method reported by Hartley F.R., *et al.* [113]. The preparation consists of two steps. In first one, 4 equivalents of NaCl are reacted with PdCl_2 in water to gave a brown suspension of $\text{Na}_2[\text{PdCl}_4]$. In the second step, the allyl chloride added to the suspension, and stirred overnight under inert atmosphere. The product (yellow oil) extracted with dichloromethane/water. The organic phases are combined together, and dried with MgSO_4 . After filtration and evaporation of the solvent, the yellow solid was recrystallized from dichloromethane/diethyl ether to give 75% yield. The ^1H NMR (see the experimental section 4.2.4.5) spectra revealed the structure of title compound, $[\text{Pd}(\eta^3\text{-C}_3\text{H}_5)\text{Cl}]_2$. In the ^1H NMR spectrum, the three protons of allyl ligand are distinguished as: δ 5.53-5.40 (m, 1H_{allyl}), 4.12 (d, 2H_{syn} , $J = 6.71$ Hz), 3.04 (d, 2H_{anti} , $J = 12.17$ Hz) ppm. From the structure of the complex, the allyl ligands are in a plan that three carbon atoms are almost perpendicular into the Pd-allyl bond. In this form, two terminal protons of the allyl ligand are not chemically equivalent and defined as H_{syn} and H_{anti} .



4.1.3.2 Synthesis of $[\text{Pd}(\eta^3\text{-C}_3\text{H}_5)(\text{ligand } \mathbf{8})](\text{CH}_3\text{SO}_3)_2$

The complex $[\text{Pd}(\eta^3\text{-C}_3\text{H}_5)(\text{ligand } \mathbf{8})\text{Cl}](\text{CH}_3\text{SO}_3)_2$ was synthesized according to the procedure reported by Amadio E., *et al.* [62]. The synthesis consists of two steps. In the first *step*, a methanol solution of AgCH_3SO_3 was added to a dichloromethane solution of $[\text{Pd}(\eta^3\text{-C}_3\text{H}_5)\text{Cl}]_2$ under stirring. Immediate precipitation of AgCl (white) indicates the formation of a cationic intermediate of palladium-allyl complex in which the positive charge compensated by anion, CH_3SO_3^- . The white precipitate of AgCl was filtered off, and into the filtrate a methanol solution of ligand **8** was drop wise added at 0 °C. After 24 hours stirring under inert atmosphere, the yellow solution was vacuum evaporated. The solid obtained was recrystallized from dichloromethane/diethyl ether in 77% yield. NMR spectra revealed the structure of the title compound, $[\text{Pd}(\eta^3\text{-C}_3\text{H}_5)(\text{ligand } \mathbf{8})](\text{CH}_3\text{SO}_3)_2$.

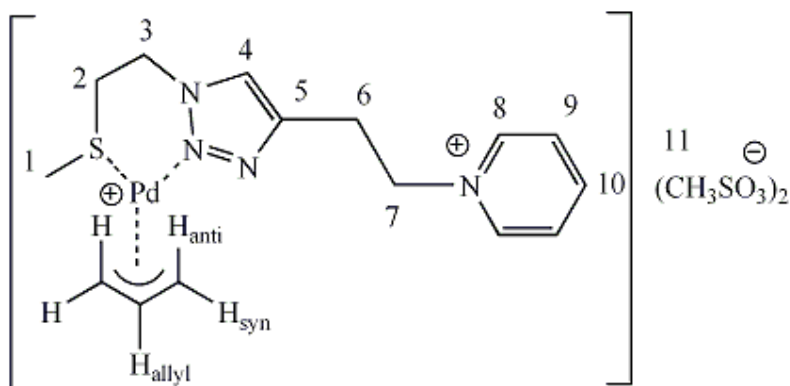


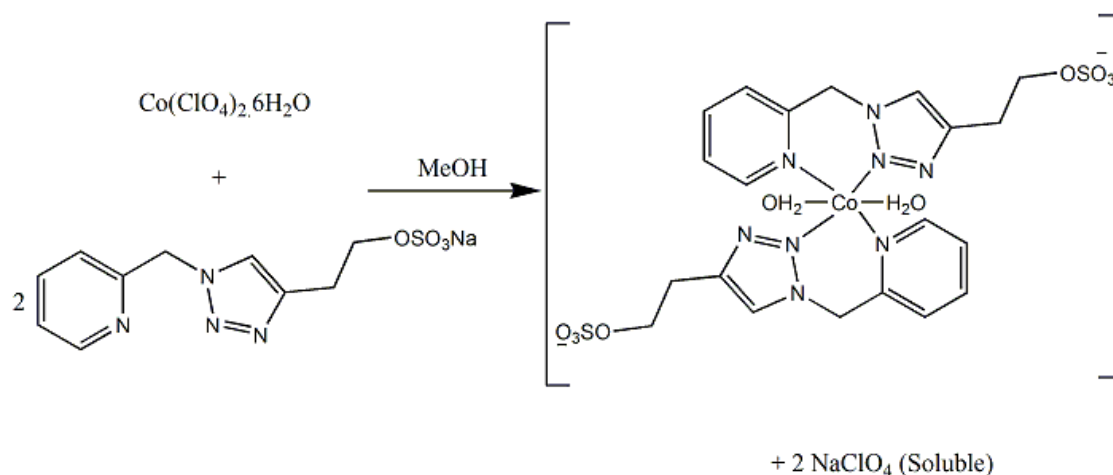
Figure 4.12 Chemical structure of $[\text{Pd}(\eta^3\text{-C}_3\text{H}_5)(\text{ligand } \mathbf{8})](\text{CH}_3\text{SO}_3)_2$.

On the basis of NMR characterizations, we assume that the triazole ligand **8** coordinates to the palladium centre through the sulfur atom and central N atom of the triazole ring (Figure 4.12). In fact, in the proton NMR spectrum both the singlet due to H(1) and H(4) are shifted downfield with respect to the free ligand ($\delta_{\text{coord.}} - \delta_{\text{free}} = 0.51$ and 0.08 ppm respectively). ^1H NMR spectrum of $[\text{Pd}(\eta^3\text{-C}_3\text{H}_5)(\text{ligand } \mathbf{8})](\text{CH}_3\text{SO}_3)_2$ (CD_3OD) confirms that the allyl moiety is coordinated to palladium in a trihapto mode. The allyl proton (H_{allyl}) give rise to a sharp multiplet at 5.80-5.93 ppm accompanied by a doublet (δ 4.33, $J = 6.7$ Hz) attributable to the anti protons and a broader doublet centered at δ 3.41 ($J = 12.6$ Hz) due to syn protons.

^{13}C NMR data also support the chelation of ligand. In the ^{13}C NMR spectrum (CD_3OD), both C(1) and C(4) resonate down field with respect to the free ligand **8**. The $\Delta\delta$ values are 6.2 and 3.73 ppm, respectively. It is worth remarking that both the ^1H and the ^{13}C NMR spectra (see the experimental section 4.2.4.6) are in good agreement with those reported by Amadio *et al.* [46].

4.1.3.3 Synthesis of cobalt(II)-triazole complex

The synthesis of cobalt(II)-triazole complex was carried out by simple mixing of the ligand **1.Na** with $\text{Co}(\text{OAc})_2 \cdot 4\text{H}_2\text{O}$ in methanol solution [43].



Before starting the synthetic reaction, the species present in the reaction solution were characterized by ESI-MS. We used three metal sources such as $\text{Co}(\text{ClO}_4)_2 \cdot 6\text{H}_2\text{O}$, $\text{CoCl}_2 \cdot 6\text{H}_2\text{O}$, and $\text{Co}(\text{OAc})_2 \cdot 4\text{H}_2\text{O}$. and obtained the same complex species identified as $[\text{Co}(\text{ligand } \mathbf{1.Na})(\text{ligand } \mathbf{1})]^+$ which corresponds to the m/z value at 648.6, $[\text{Co}(\text{ligand } \mathbf{1.Na})]^+$ at m/z 402.6 (Figure 4.13). Considering the solubility of the byproduct ($\text{NaClO}_4/\text{NaCl}/\text{Na}(\text{OAc})_2$) in methanol, we decided to use $\text{Co}(\text{ClO}_4)_2 \cdot 6\text{H}_2\text{O}$ as a metal source because NaClO_4 has higher solubility than NaCl or $\text{Na}(\text{OAc})_2$.

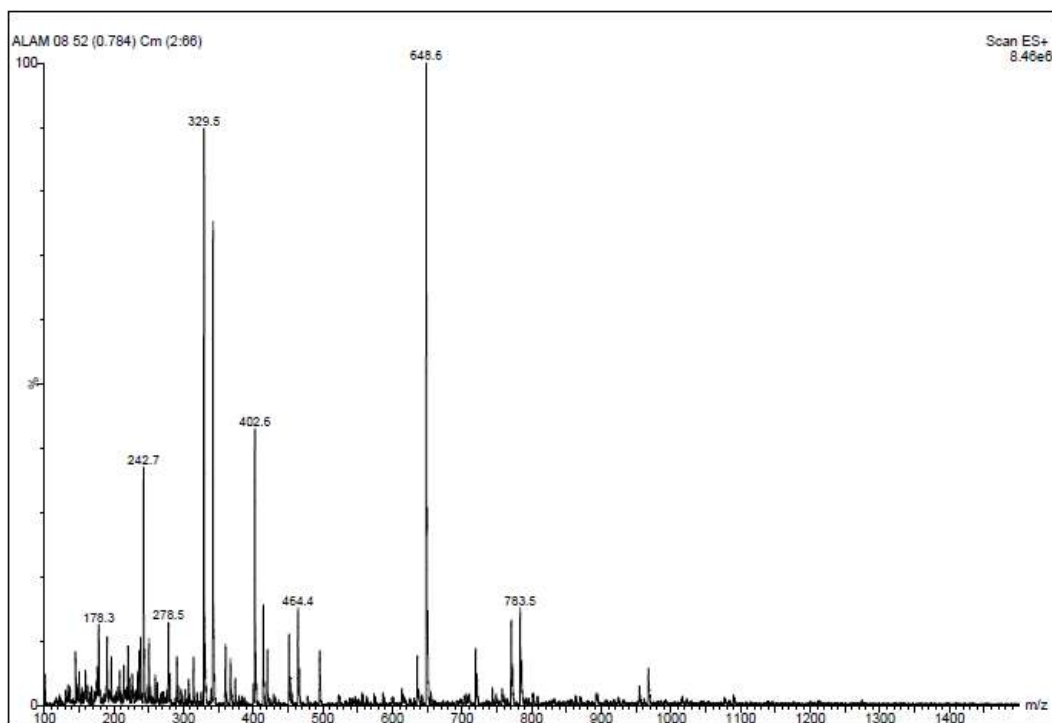


Figure 4.13 ESI-MS spectrum of $[\text{Co}(\text{ligand } 1.\text{Na})(\text{ligand } 1)]^+$ measured in MeOH.

Cobalt-triazole complex was isolated as pure block like crystals $[\text{Co}(\text{ligand } 1)_2(\text{H}_2\text{O})] \cdot 4\text{H}_2\text{O}$ which are soluble in dimethylformamide (DMF), light pink in color, fairly stable at open atmosphere and losses the lattice solvent slowly. The growth of crystals is largely depend on the concentration of the reaction mixture. From FT-IR spectrum, the absence of perchlorate as a counter ion indicates that the complex is neutral (Figure 4.14). The coordination number of the octahedral cobalt complex was satisfied by two water molecules. The CHN elemental analysis is in good agreement with four water molecules as lattice solvents.

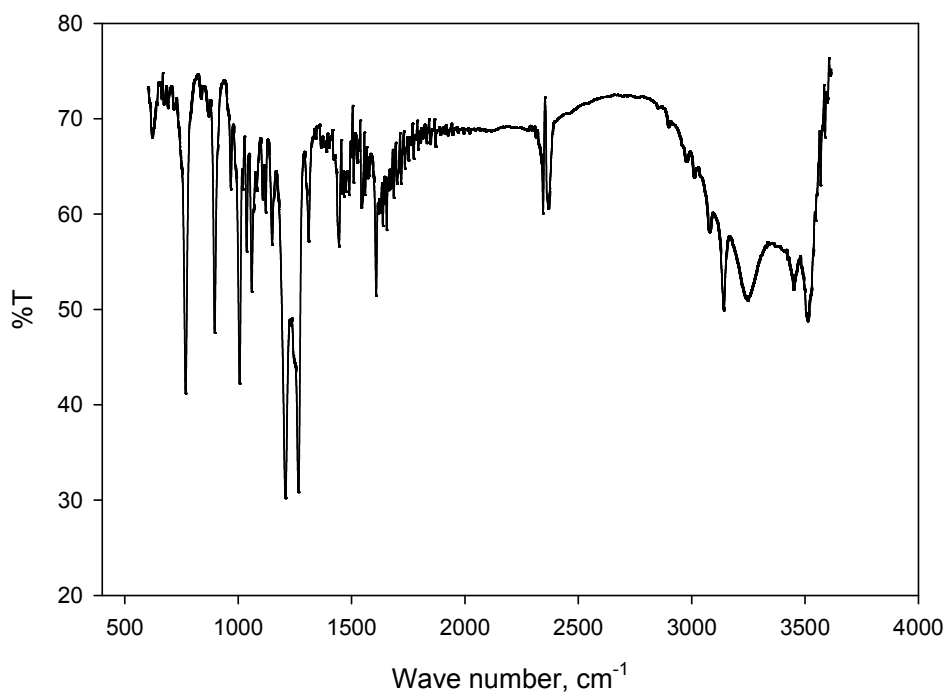
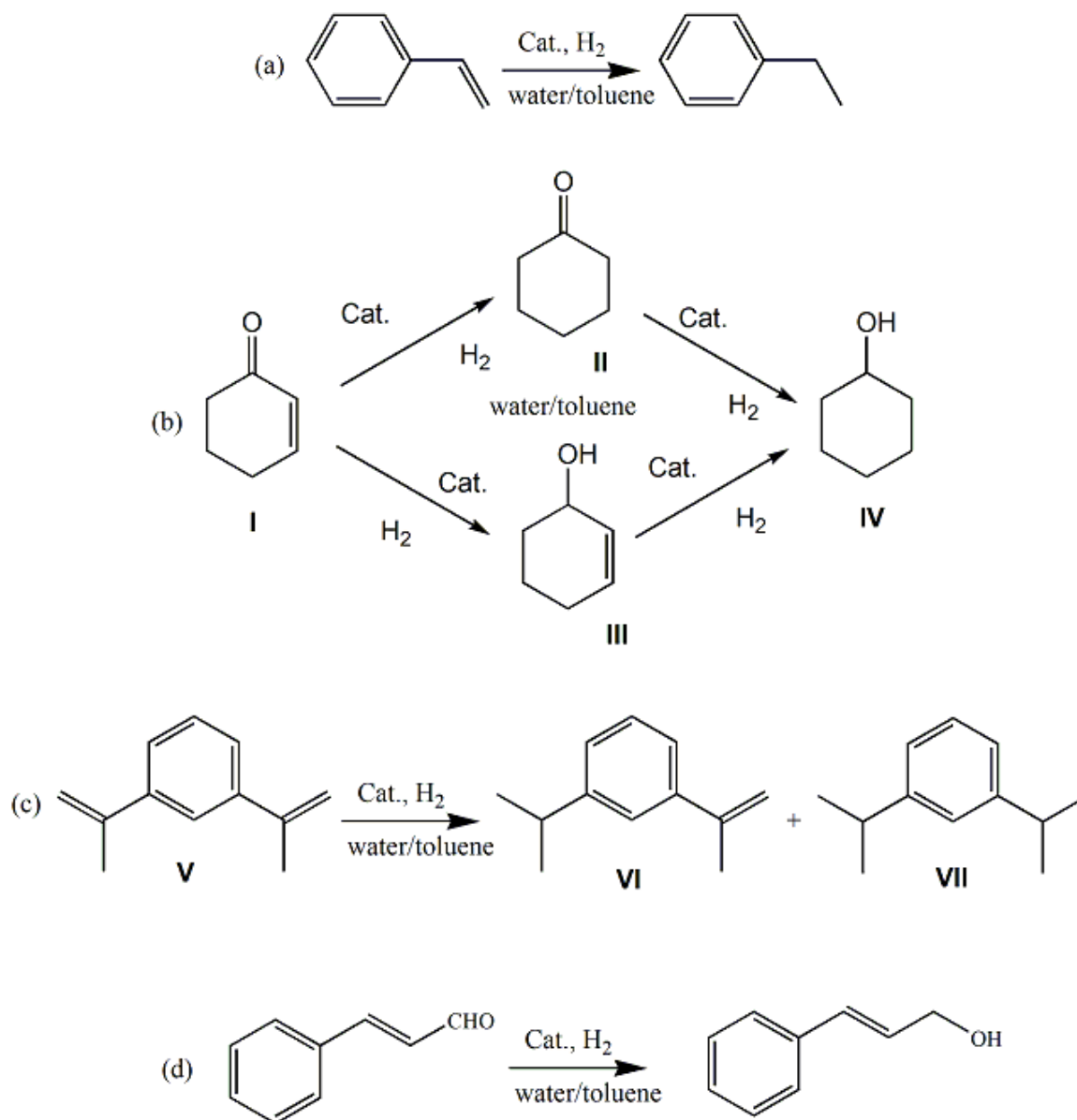


Figure 4.14 IR spectrum of $[\text{Co}(\text{ligand } \mathbf{1})_2(\text{H}_2\text{O})].4\text{H}_2\text{O}$

4.1.4 Biphasic catalysis: hydrogenations and hydroformylation

4.1.4.1 Hydrogenation of C=C and C=O bonds

The hydrogenation of C=C and C=O has been carried out according to the method reported by S. D. Dio *et al.* [74]. The catalytic activity of ruthenium preformed catalyst, $[\text{RuCl}(\eta^6\text{-}p\text{-cymene})(\text{ligand } \mathbf{1})]$ (see the preparation of catalyst, section 4.2.4) was tested in the biphasic (water/toluene) hydrogenation of styrene and 2-cyclohexen-1-one. The *in situ* prepared iridium catalyst containing water-soluble ligand **1.Na** was also tested in the biphasic (water/toluene) hydrogenation of styrene, 2-cyclohexen-1-one, *m*-diisopropenylbenzene, and cinnamaldehyde (Scheme 4.0).



Scheme 4.10 Biphasic hydrogenations (a) styrene, (b) 2-cyclohexen-1-one, (c) *m*-diisopropenylbenzene, and (d) cinnamaldehyde.

4.1.4.1.1 Catalysis with ruthenium complex **1**, [RuCl(η^6 -*p*-cymene)(ligand **1**)]

In order to investigate the usefulness of ligand **1.Na** in biphasic hydrogenation, a first set of hydrogenation experiments of model substrate styrene (see Scheme 4.11a) was carried out employing the ruthenium complex **1**. The results are summarized in Table 4.1 and graphically presented in the Figure 4.15. The reactions were carried out in a water/toluene system at 80

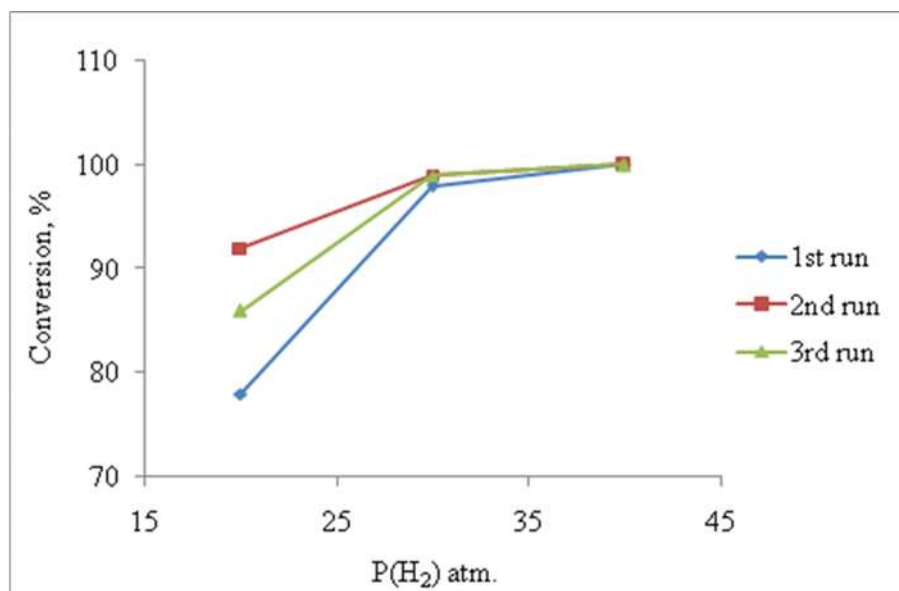
°C. A first experiment carried out at $P(\text{H}_2) = 40$ atm which showed that complex **1** has a moderately good catalytic activity as 25% of the substrate is hydrogenated to ethyl benzene in 1 hour (Entry 1). Most importantly, a recycle experiment not only shows that the recovered aqueous phase remains catalytically active, but also that its activity increases affording 67% of substrate conversion under the same conditions (column 5 in Entry 1); furthermore, this enhanced catalytic activity is maintained in a second recycle experiment.

In a second set of experiments the reaction time was increased to 3 hours; this allowed to obtain a substrate conversion of 62% in the first run and almost complete conversion in the two following recycle experiments, confirming that the catalyst becomes more active after the first catalytic run. When the reaction time is extended to 6 hours, styrene conversion is complete in the presence of both fresh and recycled catalyst (Entry 3).

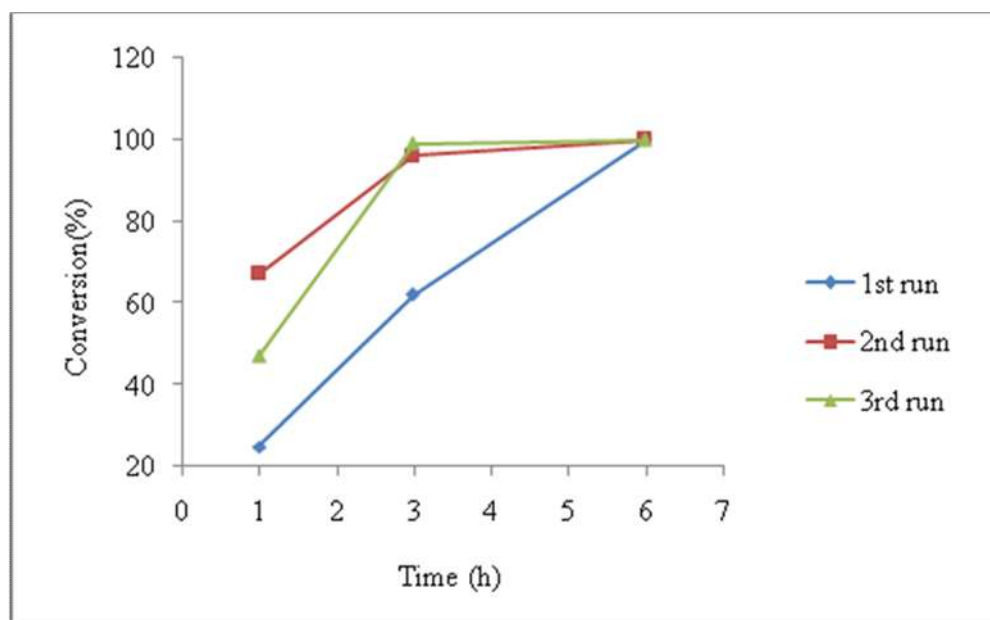
Table 4.1 Biphasic hydrogenation of styrene in the presence of $[\text{RuCl}(\eta^6\text{-}p\text{-cymene})(\text{ligand } \mathbf{1})]$

Entry	$P(\text{H}_2)$ (atm)	t (h)	%Conv. ^a (TOF ^b)		
			1 st Run	2 nd Run	3 rd Run
1	40	1	25 (125)	64 (320)	60 (300)
2	40	3	62 (103)	96 (160)	99 (165)
3	40	6	100 (83)	100 (83)	100(83)
4	30	6	98 (81)	99 (82)	99 (82)
5	20	6	78 (65)	92 (77)	88 (73)

Reaction conditions: $[\text{RuCl}(\eta^6\text{-}p\text{-cymene})(\text{ligand } \mathbf{1})] = 4.0$ mg (0.0072 mmol); styrene = 374 mg (3.59 mmol), $T = 80$ °C, $\text{H}_2\text{O} = 2.0$ mL, toluene = 2.0 mL, substrate:Ru (molar ratio) = 500:1. ^aBy GLC. ^b(Moles of substrate hydrogenated/moles of catalyst)×per hour.



(a)



(b)

Figure 4.15 Hydrogenations of styrene: (a) effect of pressure ($t = 6$ hours) and (b) effect of reaction time ($P = 40$ atm).

Owing to the good activity displayed by the catalytic system, an experiment was carried out by lowering the hydrogen pressure to 30 atm. Again, a practically complete olefin hydrogenation is obtained after 6 hours, and the recovered catalyst maintains its activity unchanged in two consecutive recycle experiments (Entry 4). A further decrease of $P(\text{H}_2)$ to 20 atm brings to a moderate decrease of the substrate conversion (78%) in the first run, but

the catalyst, when recycled, shows a remarkable increase of efficiency affording ethylbenzene in about 90% yield (Entry 5). These results are consistent with the literature reported by P.G.J. Koopma [114]. It is worth noting that in all the experiments described, no catalyst leaching was observed. As a matter of fact, the organic phase recovered after the first hydrogenation reaction (Entry 1, Table 1) was used as catalyst in the homogeneous hydrogenation of undec-1-ene in toluene, after 6 h at 80 °C and 20 atm of H₂ undecane was not formed at all. Furthermore, the toluene phases recovered from a few different experiments were analyzed by Inductively Coupled Plasma-Mass Spectrometry (ICP-MS) in order to determine the content of ruthenium: in no case the ruthenium content was found to be greater than 1 ppm.

In order to test the chemoselectivity of the catalyst we studied the hydrogenation of 2-cyclohexen-1-one (**I**, see Scheme 4.11b), the relevant data are collected in Table 4.2. In a first experiment carried out at 80 °C and p(H₂) = 20 atm the catalyst activity appeared modest as only 17% of the substrate was hydrogenated in 6 hours (Entry 1). On the other hand, the experiment showed that the catalyst is endowed with a good chemoselectivity. In fact, only small amounts of cyclohexanol (**IV**) are formed in addition to cyclohexanone (**II**) which is by far the most abundant product, while 2-cyclohexen-1-ol (**III**) does not form at all.

Table 4.2 Biphasic hydrogenation of 2-cyclohexen-1-one (**I**) in the presence of the [RuCl(*p*-cymene)(ligand **1**)].

Entry	p(H ₂) (atm)	t (h)	Run	%Conv. ^a (TOF ^b)	%Selectivity ^c	
					II	IV
1	20	6	1st	17 (15)	94	6
2	20	24	1st	100 (21)	96	4
3	20	24	2nd	100 (21)	95	5
4	20	24	3rd	100 (21)	95	5

Reaction conditions. [RuCl(η⁶-*p*-cymene)(ligand **1**)] = 4.0 mg (0.0072 mmol), 2-cyclohexen-1-one = 345 mg (3.59 mmol), T= 80 °C, H₂O = 2.0 mL, toluene = 2.0 mL, substrate:Ru (molar ratio) = 500:1. ^aBy GLC. ^b(Moles of substrate hydrogenated/moles of catalyst) × per hour. ^cFormation of **III** was never observed.

When the reaction time is increased to 24 h, complete substrate hydrogenation is obtained. This result can be explained only by admitting that the catalyst undergoes an activation

process during the reaction. Once the catalyst has been activated it maintains its activity for at least two recycle experiments (Entries 3 and 4 of Table 2). In this connection it is worth noting that activation process does not change the chemoselectivity of the catalyst.

4.1.4.1.2 Catalytic hydrogenations with the *in situ* prepared system $[\text{Ir}(\eta^4\text{-COD})\text{Cl}]_2$ /ligand **1.Na**

4.1.4.1.2.1 Hydrogenation of styrene and 2-cyclohexen-1-one [Scheme 4.11a & b]

To further explore the scope of our ligand **1.Na** in aqueous biphasic hydrogenation, we studied the catalytic activity of a system prepared by combining *in situ* ligand **1.Na** with $[\text{Ir}(\eta^4\text{-COD})\text{Cl}]_2$ (COD: 1,5-cyclooctadiene) which is a commercially available iridium precursor widely used in hydrogenation reactions [115-116]. For sake of comparison the efficiency of the system was tested with the same substrates employed with ruthenium.

Simple stirring of ligand **1.Na** with the iridium precursor in deaerated water at room temperature affords in about 30 minutes a clear catalytically active solution. Preliminary experiments showed that the catalytic activity depends on the ligand to iridium ratio, the best results being obtained using 4 moles of ligand for mole of $[\text{Ir}(\eta^4\text{-COD})\text{Cl}]_2$ (ligand **1.Na**/Ir = 2/1), therefore such ratio was used in all the hydrogenation experiments. The most significant results obtained in styrene hydrogenation are reported in Table 4.3.

Table 4.3 Styrene hydrogenation in water/toluene mixture using the Iridium-ligand **1.Na** system.

Entry (recycle)	P(H ₂) (atm)	T (°C)	t (h)	%Conv ^a . (TOF ^b)
1	10	40	3	26 (43)
2	40	60	1	100 (500)
2a (1 st)	40	60	1	98 (490)
2b (2 nd)	40	60	1	96 (480)
2c (3 rd)	40	60	1	95 (475)
2d (4 th)	40	60	1	93 (465)

Reaction conditions. $[\text{Ir}(\eta^4\text{-COD})\text{Cl}]_2$ = 3.2 mg (0.0048 mmol), styrene = 500 mg (4.8 mmol), T= 80 °C, H₂O = 2.0 mL, toluene = 2.0 mL, ligand **1.Na** = 5.9 mg (0.019 mmol),

substrate:Ir (molar ratio) = 500:1.^aBy GLC.^b(Moles of substrate hydrogenated/moles of catalyst) × per hour.

A first experiment carried out under mild conditions affords a modest ethylbenzene yield (26%, Entry 1), but when the temperature is increased to 60 °C and the hydrogen pressure to 40 atm. complete substrate conversion is obtained in only 1 hour. Most importantly, the recovered aqueous phase can be reused four times (Entries 2a-d, Table 4.3). ICP-MS analyses indicates that the organic phases recovered after the hydrogenation reaction contain small amounts of iridium (about 8 ppm). According to these results it may be concluded that the iridium/ligand **1.Na** system is significantly more active than the ruthenium catalyst (complex **1**), while this latter appears more robust.

To shed some light on the ligand's role, an hydrogenation experiment (not reported in Table 4.3) was carried out under the conditions of Entry 2 in the absence of ligand **1.Na**. The iridium precursor remains confined in the organic phase and although styrene is completely hydrogenated, extensive decomposition of $[\text{Ir}(\eta^4\text{-COD})\text{Cl}]_2$ to iridium black occurs, indicating the key role played by the ligand which not only confines the metal in the water phase, but also stabilizes it against reduction to metal. The results of 2-cyclohexen-1-one hydrogenation (Scheme 4.13b) are collected in Table 4.4.

Table 4.4 Hydrogenation of 2-Cyclohexen-1-one in water/toluene using the Iridium-ligand **1** system

Entry (recycle)	P(H ₂)(atm)	T (°C)	t (h)	%Conv ^a . (TOF ^b)	Selectivity ^a	
					II	IV
1	40	60	21	100 (47)	4	96
2	40	60	1	100 (500)	80	20
2a (1 st)	40	60	1	100 (500)	81	19
2b (2 nd)	40	60	1	100 (500)	83	17
3	5	40	6	100 (83)	100	0
3a (1 st)	5	40	6	100 (83)	95	5
3b (2 nd)	5	40	6	100 (83)	97	3

Reaction conditions. $[\text{Ir}(\eta^4\text{-COD})\text{Cl}]_2$ = 3.2 mg (0.0048 mmol), 2-Cyclohexen-1-one = 461 mg (4.8 mmol), T= 80 °C, H₂O = 2.0 mL, toluene = 2.0 mL, ligand **1.Na** = 5.9 mg (0.019 mmol), substrate:Ir (molar ratio) = 500:1. ^aBy GLC. ^bMoles of substrate hydrogenated/moles of catalyst) × per hour.

Under the same reaction conditions employed for styrene hydrogenation (60 °C and $P(\text{H}_2) = 40$ atm), complete substrate conversion is achieved by 21h leading to a mixture of IV and II in 96/4 molar ratio (Entry 1). Accordingly, the reaction time was reduced to 1h in order to understand through which reaction sequence the final products form (i.e. if the reaction path is $\text{I} \rightarrow \text{II} \rightarrow \text{IV}$, or if $\text{I} \rightarrow \text{III} \rightarrow \text{IV}$, Scheme 4.10b). The experiment showed that the actual reaction sequence is the former, and that the hydrogenation of the endocyclic C=C is much faster than C=O hydrogenation resulting in a moderate selectivity towards the formation of cyclohexanone. The aqueous phase remains catalytically active and may be reused two times without loss of efficiency. Complete chemoselectivity towards cyclohexanone was finally obtained by further decreasing the temperature to 40 °C and the $p(\text{H}_2)$ to 5 atm. Under these very mild conditions, complete C=C double bond hydrogenation is achieved by 6 hours, cyclohexanone being the only product observed; moreover, it is possible to recycle at least two times the aqueous phase with only a negligible loss of chemoselectivity.

4.1.4.1.3 Hydrogenation of *m*-diisopropenylbenzene and cinnamaldehyde [Scheme 4.10 c & d].

To widen the application of our ligand **1.Na**, we studied the catalytic activity of a system prepared by combining *in situ* ligand **1.Na** with $[\text{Ir}(\eta^4\text{-COD})\text{Cl}]_2$ in biphasic hydrogenation of *m*-diisopropenyl benzene and cinnamaldehyde.

The catalyst was prepared by simple stirring of ligand **1.Na** with the iridium precursor in deaerated water at room temperature. After stirring for 30 minutes, a clear catalytically active solution was obtained. Preliminary experiments showed that the catalytic activity depends on the ligand to iridium ratio, the best results being obtained (for *m*-diisopropenylbenzene) using ligand **1.Na**/Ir = 1/4, therefore such ratio was used in the hydrogenation of *m*-diisopropenylbenzene. The most significant results obtained in the hydrogenation of *m*-diisopropenylbenzene are reported in Table 4.5.

Table 4.5 *m*-Diisopropenylbenzene hydrogenation in water/toluene using the Iridium-ligand **1** system

Entry (recycle)	PH ₂ (atm)	T (°C)	t (h)	%Conv ^a . (TOF ^b)	Selectivity ^b	
					VI	VII
1	40	60	3	99	19	81
2	10	40	6	72	61	39
3	5	40	6	71	65	35
5	10	40	4	70	74	26

Reaction conditions. [Ir(η^4 -COD)Cl]₂ = 3.2 mg (0.0048 mmol), *m*-diisopropenylbenzene = 760 mg (4.8 mmol); T= 80 °C; H₂O = 2.0 mL; toluene = 2.0 mL, ligand **1** = 11.8 mg (0.038 mmol); Ir/ligand **1** = 1/4; substrate:Ir (molar ratio) = 500:1.^aBy GLC. ^b(Moles of substrate hydrogenated/moles of catalyst) × per hour.

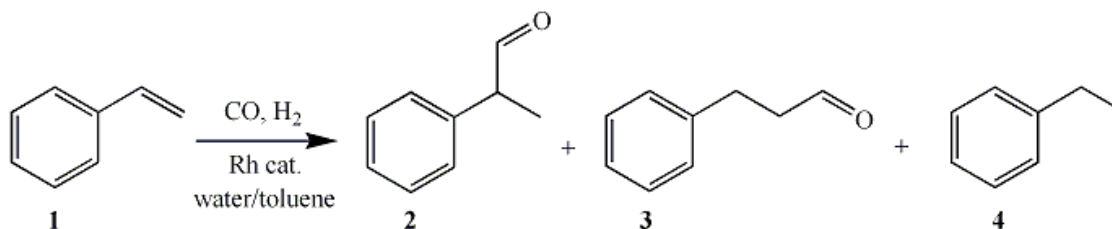
A first experiment carried out at P(H₂) = 40 atm showed that catalyst has a good catalytic activity as 99% of the substrate is hydrogenated to 1-isopropyl-3-(prop-1-en-2-yl)benzene (VI) and 1,3-diisopropylbenzene (VII) in a 19/81 ratio in 3 hours at 60 °C. Aiming to synthesized partially hydrogenated product (VI), we carried out the reaction in milder conditions. The conversion decreases (in Entry 2), upon lowering pressure (from 40 to 10 atm) and temperature (60 to 40 °C) despite longer reaction time. The relative ratio of partially hydrogenated product (VI) is increased to 61%. A further decrease of pressure into 5 atm brings little influence on the result. The best result obtained from the entry 4 (with 10 atm, 40 °C, and 4 hours). For all the reactions, the recycle experiments gave conversions ranging from 8 to 22%.

Using the same catalyst (*in situ* prepared ligand **1.Na-Ir**), we studied the biphasic hydrogenation of cinnamaldehyde. The iridium *in situ* catalyst is inactive (for both metal/ligand = 1/4 and 1/2 molar ratio), gaving maximum 1% of conversion.

4.1.4.2 Hydroformylation of styrene

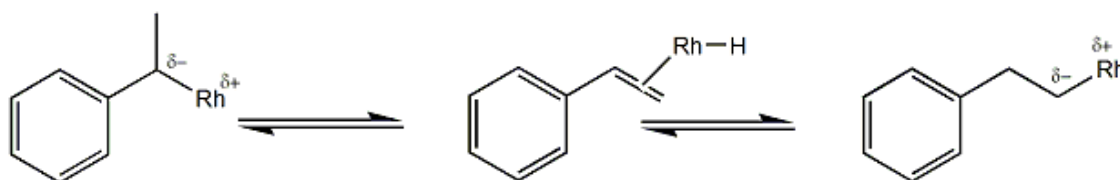
Styrene is an important model substrate frequently used to test the catalytic activity of new catalyst and ligands in the hydroformylation reaction. The use of styrene does not have a great industrial important but it is still used as a standard substance because it is a less volatile liquid.

The main products which were formed by the hydroformylation of styrene (Scheme 4.11) are 2-phenylpropanal (2) and 3-phenylpropanal (3). The first isomer is a branched aldehyde (2), comes from the attack of -CHO group into the 2 position of the double bond of styrene while the second one is a linear aldehyde (3), derived from the attack of -CHO group into the 1 position of the double bond of styrene. The third possible product is ethyl benzene (4) which comes from the partial hydrogenation of styrene.



Scheme 4.11 Hydroformylation of styrene.

Generally, the hydroformylation of an unsaturated substrate produced linear product as the major product. Instead, in our case the hydroformylation of styrene gave the reverse result, the branched aldehyde (2) is the major product. This peculiarity can be explained by observing the expected intermediate formations (Scheme 4.12). The branched intermediate is more stable compared to linear intermediate because in the branched intermediate the partial negative charge on the carbon atom adjacent to the rhodium centre is delocalized onto the aromatic ring.



Scheme 4.12 Formation of intermediates via coordination of rhodium into styrene

The catalytic hydroformylation of styrene in aqueous biphasic system was carried out according to the procedure reported by S. Paganelli *et al.* [85, 89]. The precursor used is either $[\text{Rh}(\text{CO})_2(\text{acac})]$ or $[\text{RhCl}(\text{COD})]_2$. Although both precursors are commercially

available, we prepared $[\text{RhCl}(\text{COD})]_2$ in our laboratory (see the experimental section 4.2.6.1). The ligand used is a water-soluble methyl(thio)ethyl-triazole ligand (Figure 4.16).

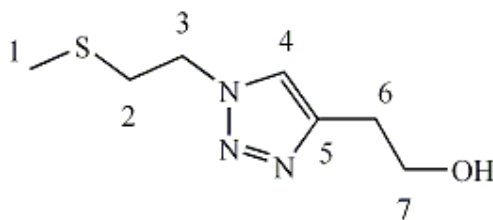


Figure 4.16 Chemical structure of the ligand **4**.

The simple stirring of $[\text{Rh}(\text{COD})\text{Cl}]_2$ and ligand **4** in deaerated water at room temperature in about 10 minutes provides a clear orange-yellow solution. Before start this reaction, we carried out several experiments to understand the activity of two different precursors $[\text{Rh}(\text{COD})\text{Cl}]_2$, and $[\text{Rh}(\text{CO})_2(\text{acac})]$ in combination with water-soluble ligand **4**. We found both of them have same catalytic activity (see the Table 4.6) under same condition. The precursor $[\text{Rh}(\text{COD})\text{Cl}]_2$ has comparatively better solubility in water than $[\text{Rh}(\text{CO})_2(\text{acac})]$, therefore $[\text{Rh}(\text{COD})\text{Cl}]_2$ was used in all the hydroformylation experiments.

Table 4.6 Biphasic hydroformylation of styrene catalyzed by Rh/ligand **4** *in-situ* catalytic system.

Entry	Precursor	Rh/ligand 4	P(CO+H ₂) atm	t(h)	^a Conv. (%)	(2) ^a	(3) ^a	(4) ^a
1	$[\text{Rh}(\text{COD})\text{Cl}]_2$	¼	80	18	100	81	19	0
2	$[\text{Rh}(\text{CO})_2(\text{acac})]$	¼	80	18	100	79	21	0
3	$[\text{Rh}(\text{COD})\text{Cl}]_2$	¼	20	5	17	53	45	2
4	$[\text{Rh}(\text{CO})_2(\text{acac})]$	¼	20	5	13	48	50	2

Reaction conditions. Styrene/Rh = 1000; styrene = 9.62 mmol; $[\text{Rh}(\text{COD})\text{Cl}]_2 = 4.81 \times 10^{-3}$ mmol (2.40 mg); $[\text{Rh}(\text{CO})_2(\text{acac})] = 9.62 \times 10^{-3}$ mmol (2.49 mg); T = 80°C; H₂O = 2.0 mL; toluene = 2.0 mL. ^a By GLC.

Preliminary experiments revealed that the catalytic activity depends on the ligand to rhodium ratio, the best results being obtained using 8 moles of ligand for mole of $[\text{Rh}(\text{COD})\text{Cl}]_2$ (Rh/ligand **4** = 1/4), therefore such ratio was used in all the hydroformylation experiments. The most significant results obtained for styrene hydroformylation (Scheme 4.13) are reported in Table 4.7.

Table 4.7 Biphasic hydroformylation of styrene catalyzed by Rh/ligand **4** *in-situ* catalytic system.

Entry	t(h)	P(CO+H ₂) atm	Conv.(%) ^a	2 ^a	3 ^a	4 ^a	B/L(2/3)
1	18	80	100	81	19	0	4
2	5	80	100	75	24	traces	3
2a (1 st)	"	"	99	81	19	0	4
2b (2 nd)	"	"	84	81	19	0	4
2c (3 rd)	"	"	40	82	18	0	4
3	5	20	17	53	45	2	1

Reaction conditions, Styrene/Rh = 1000; styrene = 9.62 mmol; $[\text{Rh}(\text{COD})\text{Cl}]_2 = 4.81 \times 10^{-3}$ mmol (2.40 mg); ligand **4** = 7.2 mg (0.039 mmol); Rh/ligand = 1/4; T = 80 °C; H₂O = 2.0 mL; Toluene = 2.0 mL. ^a By GLC (2a) 1st recycle; (2b) 2nd recycle; (2c) 3rd recycle experiment.

The first reaction was carried out at 80 atm (CO/H₂ = 1/1) in 18 hours provides complete conversion of the reactants and the products obtained from the organic phase are 81% of 2-phenylpropanal (2) and 19% of 3-phenylpropanal (3). The branched to linear ratio (B/L) is 3. Upon lowering of reaction time to 5 hours (Entry 2), the conversion remains 100% with an increase of branched/linear (B/L) ratio into 4. Recycle experiments (Entry 2a) were carried out in condition of entry 2 affords 99% conversion with a modest enlargement in the selectivity towards branched product. Further recycling experiment shows gradual decreases in conversion 84% (Entry 2b), and 40% (Entry 2c). Interestingly, all the recycle experiments maintain the same B/L ratio and in all cases no ethyl benzene is formed. The retainence of selectivity shown by the catalyst during recycle experiments is an indication that homogeneous and not heterogeneous catalyst is the active species.

Further decrease of pressure from 80 atm to 20 atm in 5 hours affords only 17% of conversation with 1/1 B/L ratio.

4.2 EXPERIMENTAL SECTION

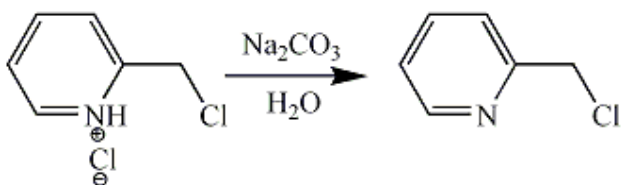
4.2.1 General methods

The reagents and solvents with high degree of purity were purchased directly from the market and used without further purification. In case where it is necessary to handle the reaction in absence of oxygen and water, solvents and reagents were distilled and dried according to the procedure reported in the literature [103].

Column chromatography was performed using ICN Silica gel supplied by ICN ECOCHROM, Germany. Thinlayer chromatography (TLC) was performed on EM reagents 0.25 mm silica 60-F plates. ^1H NMR, ^{13}C NMR and ^{31}P NMR spectra were measured on Bruker Avance-300 spectrometer. Infrared spectra were recorded on a Perkin Elmer Spectrum One FT-IR in KBr pellet in the range of 4000-400 cm^{-1} . Gas chromatographic analysis were performed on a Agilent Technologies 6850 gas chromatograph fitted with an HP-5 column (30m \times 0.32 μm \times 0.25 μm).

4.2.2 Synthesis of pyridyl-triazole ligands

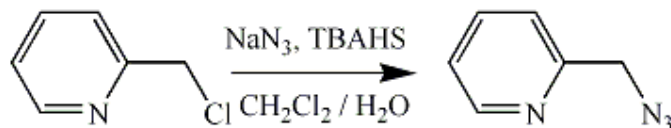
4.2.2.1 Synthesis of 2-(chloromethyl)pyridine



In a 50.0 mL round bottom flask, 2-(chloromethyl)pyridine hydrochloride (1.30 g, 8.1 mmol) was dissolved in 8.0 mL of H₂O. A saturated solution of Na₂CO₃ was added until pH 10-11, under gentle stirring. The reaction mixture was extracted with CH₂Cl₂ (3 x 8 mL). The combined organic layers were dried with MgSO₄, filtered off, and the solvent evaporation under vacuum to give 0.80 g (77%) of a light yellow oil which was characterized by gaschromatography (t_r = 9.34 mins.) and ^1H NMR spectrum.

^1H NMR (200 MHz, CDCl₃, 298 K): δ 8.52 (br d, 1H(1)), 7.64 (t, 1H(3), J = 7.0 Hz), 7.5-7.35 (m, 1H(4)), 7.25-7.1 (m, 1H(2)), 4.44 (br s, 2H(6)) ppm.

4.2.2.2 Synthesis of 2-(azidomethyl)pyridine



The synthesis of 2-(azidomethyl)pyridine was carried out according to the procedure reported by Golas P. *et al.* [104]. In a 50.0 mL round bottom flask, 2-(chloromethyl)pyridine (0.80 g, 6.3 mmol) was dissolved in 5.0 mL of CH₂Cl₂. A 5.0 mL aqueous solution of NaN₃ (0.97 g, 14.9 mmol) and tetrabutylammonium hydrogensulfate (0.082 g, 0.24 mmol) were added dropwise to the solution of 2-(chloromethyl)pyridine under inert atmosphere and stirring. The reaction was monitored by gaschromatography to verify the complete conversion of 2-(chloromethyl)pyridine. The reaction mixture was extracted with CH₂Cl₂ (3 x 6 mL), the combined organic layers were dried with MgSO₄. Complete evaporation of solvent under vacuum gave 0.75 g (89 %) of a light yellow oil which was characterized by gaschromatography (*t_r* = 11.22 mins.), and ¹H NMR spectrum (Figure 4.17).

2-(azidomethyl)pyridine

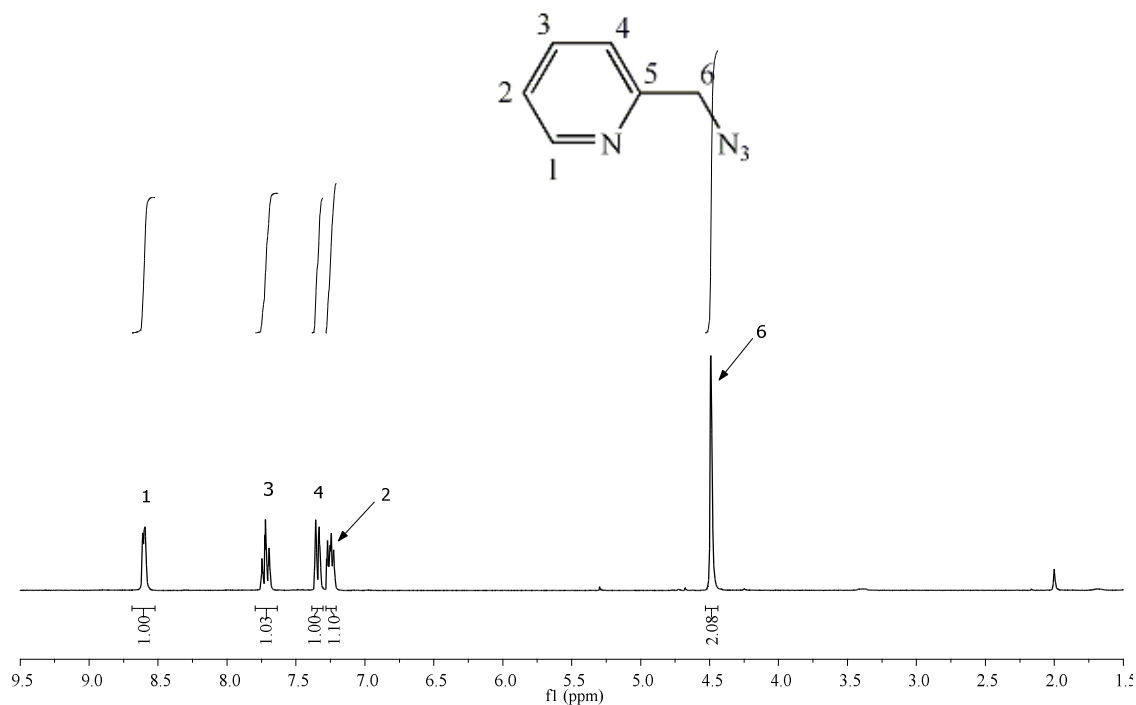
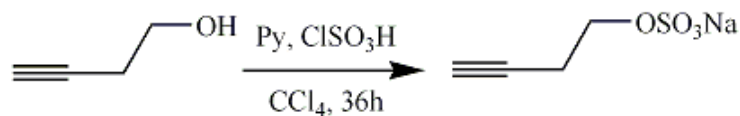


Figure 4.17 ^1H NMR spectrum of 2-(azidomethyl)pyridine in CDCl_3 .

^1H NMR (300 MHz, CDCl_3 , 298 K): δ 8.59 (d, 1H(1), $J = 4.7$ Hz), 7.72 (t, 1H(3), $J = 7.7$ Hz), 7.35 (d, 1H(4), $J = 7.7$ Hz), 7.24 (m, 1H(2)), 4.49 (s, 2H(6)) ppm.

4.2.2.3 Synthesis of sodium 3-butyne-1-sulfate



The synthesis of sodium 3-butyne-1-sulfate was carried out according to the procedure reported by Sousa-Herves, A. *et al.* [105]. In a 50.0 mL two-neck round bottom flask, ClSO_3H (0.47 mL, 7.13 mmol) was added dropwise to a solution of pyridine (1.3 mL, 16.0 mmol) in CCl_4 (7.0 mL) at 0 °C. After 30 minutes of stirring, 3-butyne-1-ol (0.57 mL, 7.13 mmol) was slowly added, and reaction mixture kept at 0 °C for 4 hours. Then the reaction was allowed to reach room temperature, and after overnight stirring, extracted with H_2O (2x15 mL). The combined aqueous phase was evaporated to almost half volume, and then a

saturated solution of Na_2CO_3 added until no CO_2 evolution ($\text{pH} \approx 9\text{-}10$) was observed. The resulting mixture was evaporated to dryness under vacuum, and recrystallized from hot EtOH (80.0 mL) to give 0.95 g (84%) of white crystals which was characterized by ^1H NMR (Figure 4.18) and ^{13}C NMR (Figure 4.19) spectra.

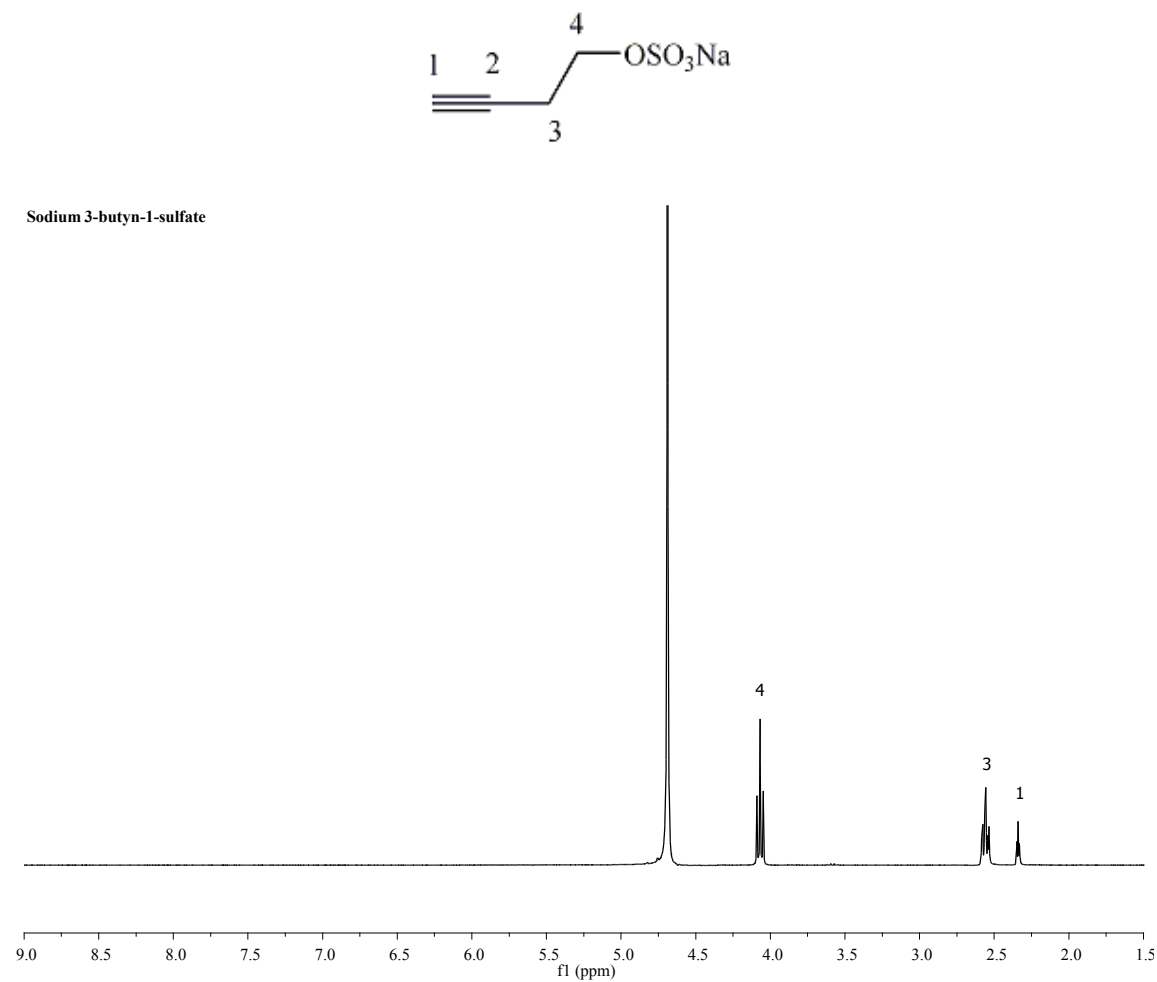


Figure 4.18 ^1H NMR spectrum of sodium 3-butyn-1-sulfate in D_2O .

^1H NMR (300 MHz, D_2O , 298 K): δ 4.06 (t, 2H(4), $J = 6.4$ Hz), 2.55 (td, 2H(3), $J = 6.3$ Hz, $J = 2.2$ Hz), 2.33 (t, 1H(1), $J = 2.2$ Hz) ppm.

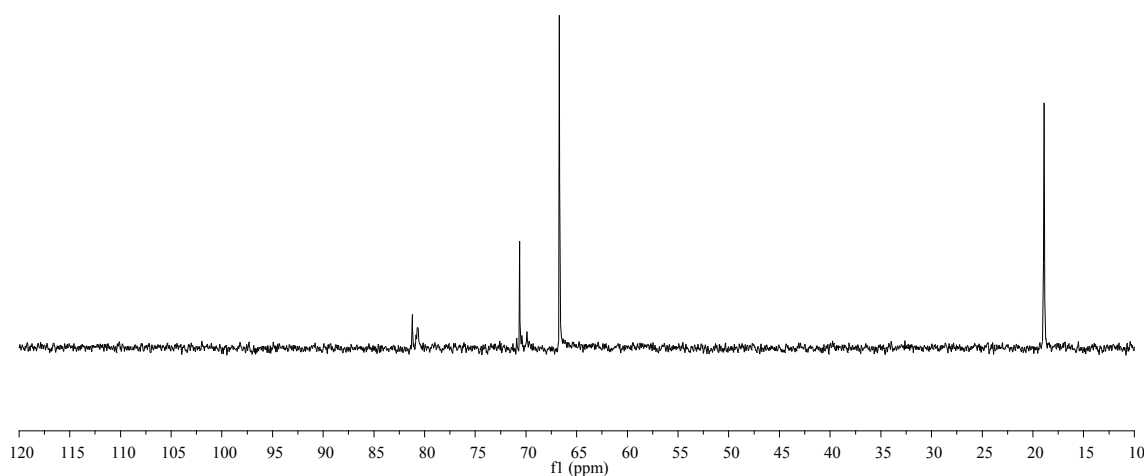
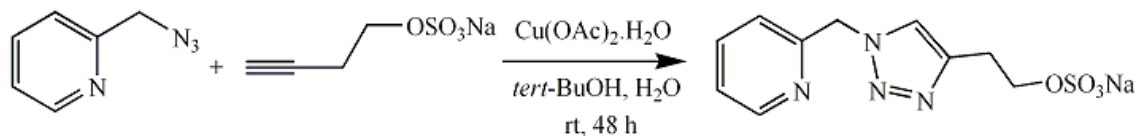


Figure 4.19 ^{13}C NMR spectrum of sodium 3-butyne-1-sulfate in D_2O .

^{13}C NMR (300 MHz, D_2O , 298 K): δ 81.22, 70.72, 66.72, 18.91 ppm.

4.2.2.4 Synthesis of ligand **1.Na**

Ligand **1.Na** = 2-(1-((pyridine-2-yl)methyl)-1H-1,2,3-triazol-4-yl)ethyl sodium sulfate



The synthesis of ligand **1.Na** was carried out according to the procedure reported by Brotherton, W.S. *et al.* [41]. In a 50.0 mL two-neck round bottom flask, a *tert*-butanol solution (6.0 mL) of 2-(azidomethyl)pyridine (0.48 g, 3.57 mmol) was added to a *tert*-butanol solution (17.0 mL) of sodium 3-butyne-1-sulfate (0.61 g, 3.57 mmol) under inert atmosphere. Additional 2.0 mL of water were added to dissolve all the reactants. The slow addition of 1.0

mL aqueous solution of cupric acetate monohydrate (0.036 g, 0.18 mmol) to the reaction vessel result in an immediate color change from light yellow to green. After 48 hours of stirring, the solution was evaporated to dryness under vacuum. The green solid obtained was purified by column chromatography (silica gel, dichloromethane/methanol = 8/2) to give the title compound as a white solid in 79% (0.86 g) yield which were characterized by ^1H NMR (Figure 4.20), ^{13}C NMR (Figure 4.21) and ESI-MS (Figure 4.22) spectroscopy.

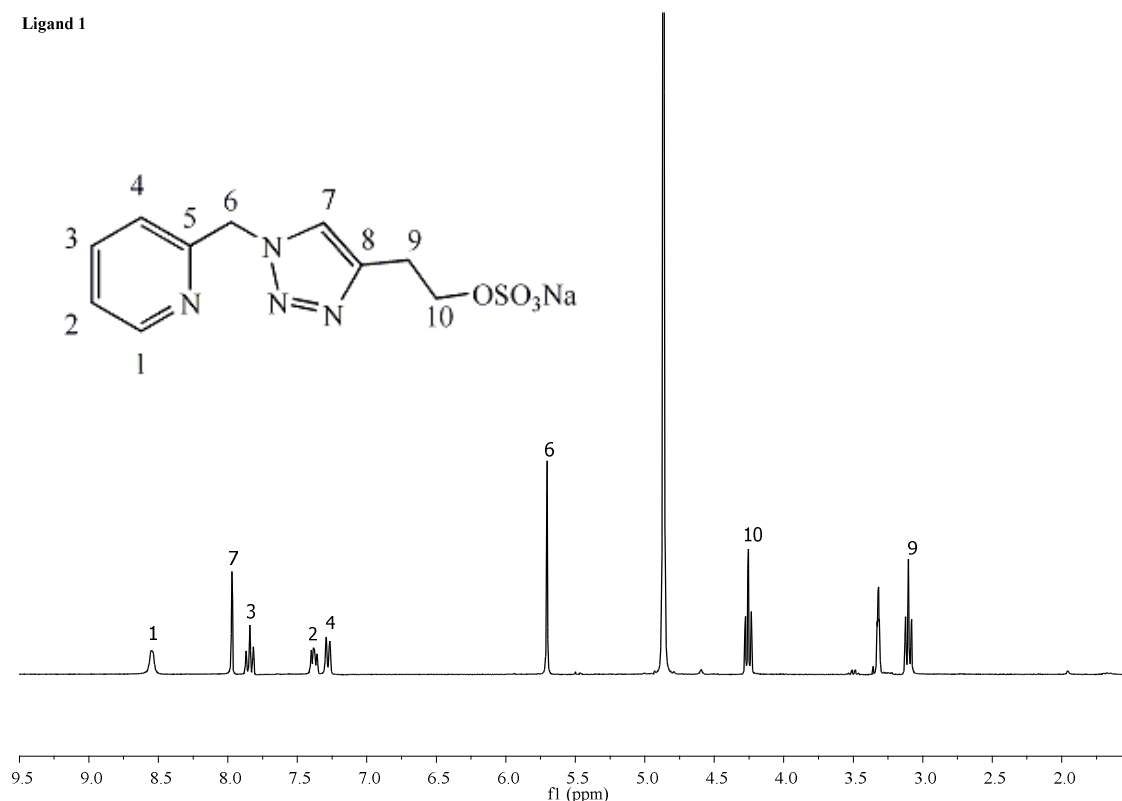


Figure 4.20 ^1H NMR spectrum of 2-(1-((pyridine-2-yl)methyl)-1*H*-1,2,3-triazol-4-yl)ethyl sodium sulfate (ligand **1.Na**) in CD_3OD .

$^1\text{HNMR}$ (300 MHz, CD_3OD , 298 K): δ 8.55 (br s, 1H(1)), 7.97 (s, 1H(7)), 7.84 (t, 1H(3), J = 7.7 Hz), 7.38 (br, m, 1H(2)), 7.28 (d, 1H(4), J = 7.9 Hz), 5.70 (s, 2H(6)), 4.26 (m, 2H(10)), 3.10 (t, 2H(9), J = 6.4 Hz) ppm.

Ligand 1

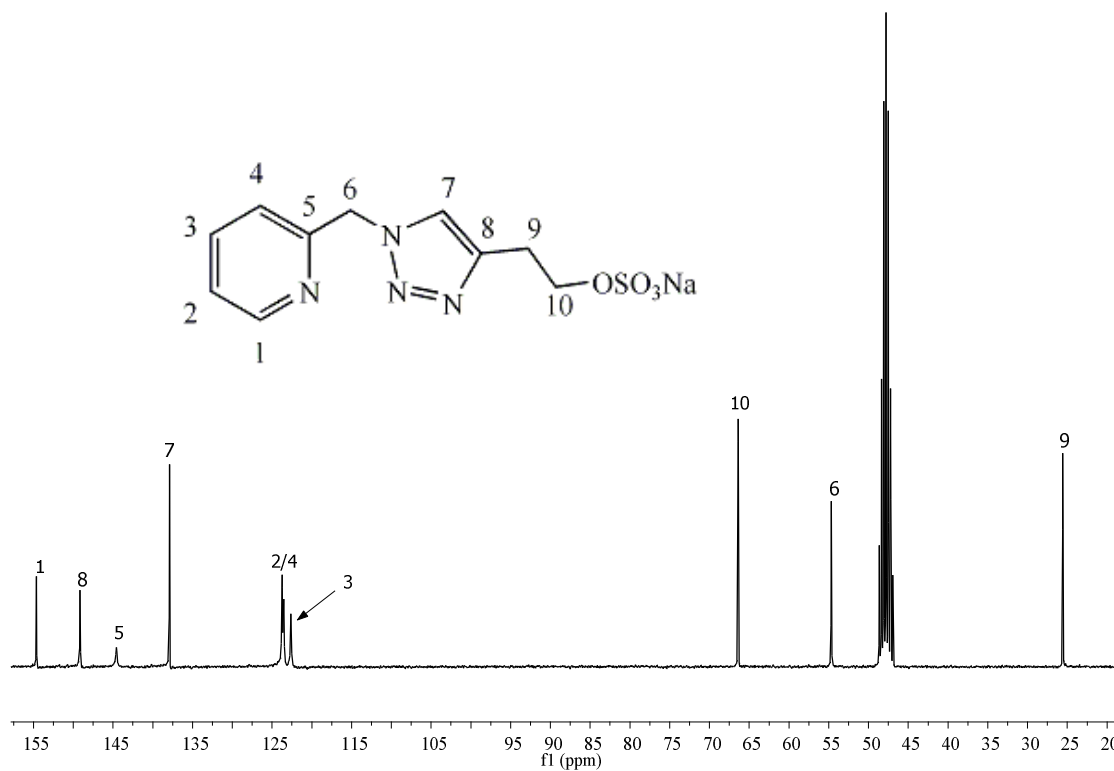
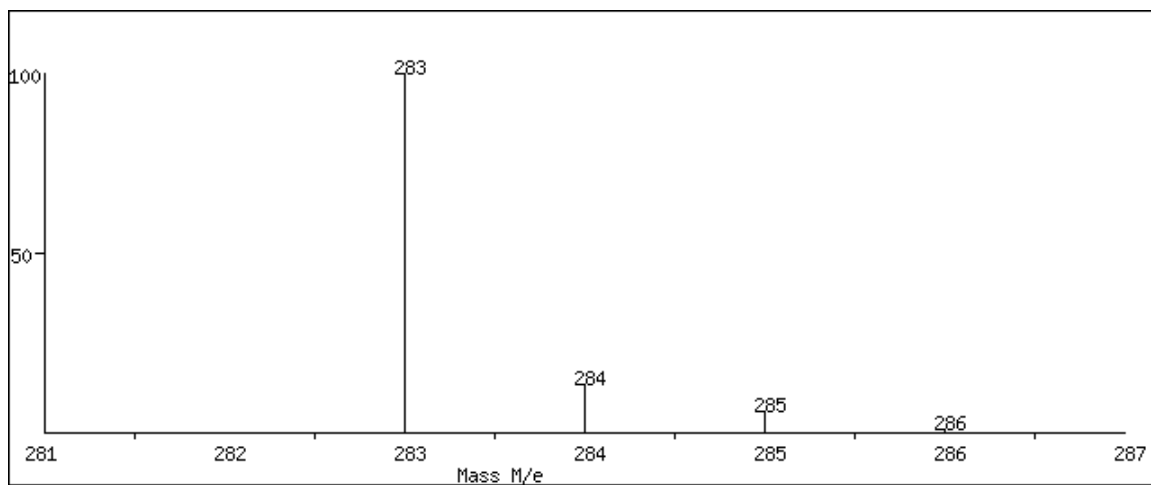
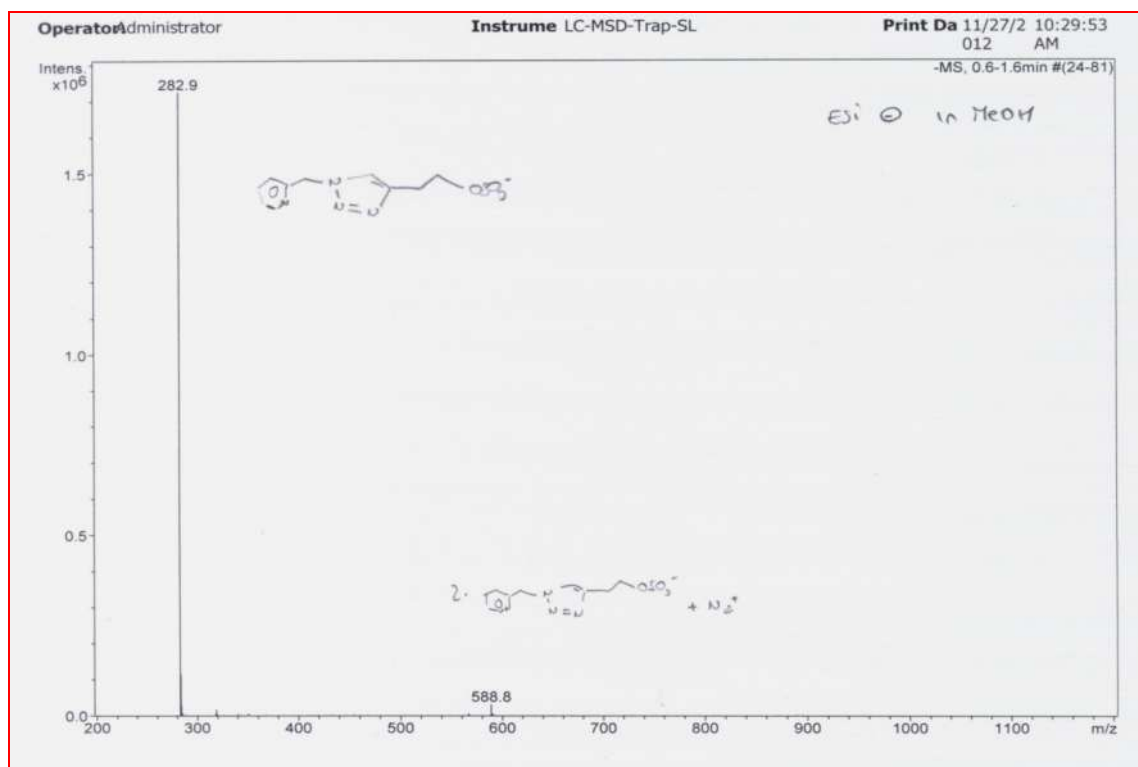


Figure 4.21 ¹³C NMR spectrum of 2-(1-((pyridine-2-yl)methyl)-1H-1,2,3-triazol-4-yl)ethyl sodium sulfate (ligand 1.Na) in CD₃OD.

¹³C NMR (300 MHz, CD₃OD, 298 K): δ 154.62 (C1), 149.14 (C8), 144.55 (C5), 137.90 (C7), 123.73 (C2/4), 122.62 (C3), 66.39 (C10), 54.67 (C6), 25.58 (C9) ppm.



(a) Calculated

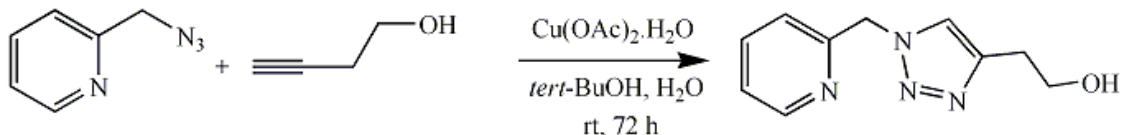


(b) Measured

Figure 4.22 ESI-MS spectra of 2-((1-((pyridine-2-yl)methyl)-1H-1,2,3-triazol-4-yl)ethyl)sulfate sodium sulfate (ligand **1.Na**) in MeOH. (a) calculated, and (b) measured.

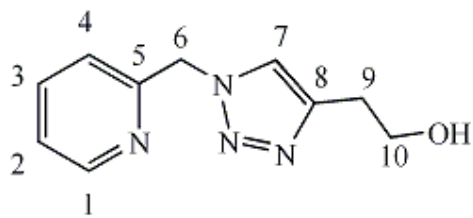
4.2.2.5 Synthesis of ligand 2

Ligand 2 = 2-(1-((pyridin-2-yl)methyl)-1H-1,2,3-triazol-4-yl)ethanol



The synthesis of ligand 2 was carried out according to the procedure reported by Brotherton, W.S. *et al.* [41].

In a 50.0 mL two-neck round bottom flask, a *tert*-butanol solution (7.0 mL) of 2-(azidomethyl)pyridine (0.52 g, 3.9 mmol) was added to a *tert*-butanol solution (5.0 mL) of 3-butyn-1-ol (0.45 mL, 0.41 g, 3.90 × 1.50 mmol) under inert atmosphere. Additional 1.0 mL of water was added to dissolve all the reactants. Then, 1.0 mL aqueous solution of cupric acetate monohydrate (0.039 g, 0.20 mmol) was slowly added to the reaction vessel, result in an immediate color change from light yellow to green. After 72 hours of stirring, the solution was evaporated to dryness under vacuum. The green oil obtained was purified by column chromatography (silica gel, dichloromethane/methanol = 9/1) to give the title compound in 87% (0.86 g) yield, which was characterized by ¹H NMR (Figure 4.23) and ¹³C NMR (Figure 4.24) spectra.



Ligand 2

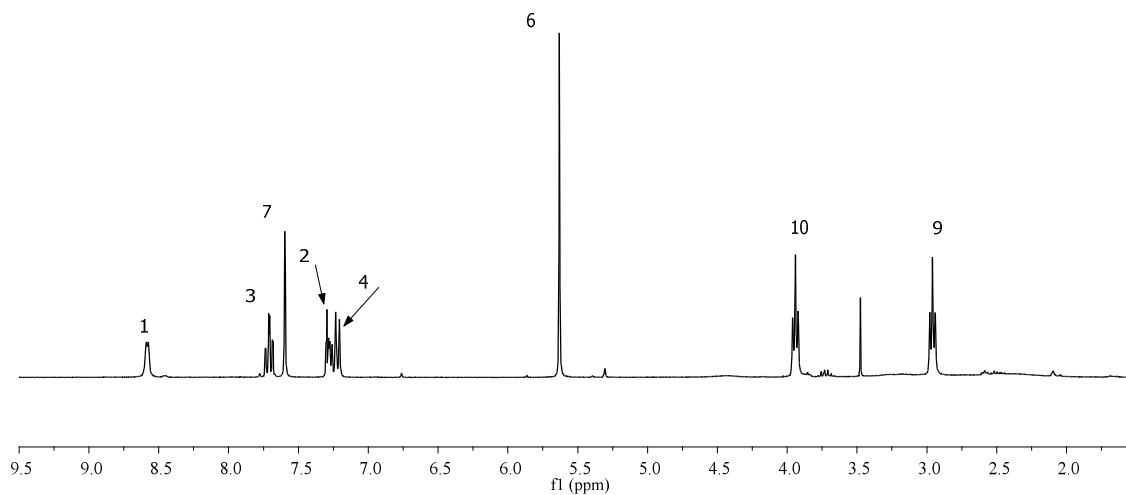
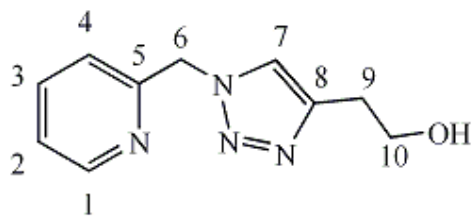


Figure 4.23 ^1H NMR spectrum of ligand **2** in CDCl_3 .

^1H NMR (300 MHz, CDCl_3 , 298 K): δ 8.59 (d, 1H(1), $J = 4.0$ Hz), 7.71 (t, 1H(3), $J = 7.7$ Hz), 7.60 (s, 1H(7)), 7.30 (br, m, 1H(2)), 7.22 (d, 1H(4), $J = 7.8$ Hz), 5.63 (s, 2H(6)), 3.94 (t, 2H(10), $J = 5.9$ Hz), 2.96 (t, 2H(9), $J = 5.9$ Hz) ppm.



Ligand 2

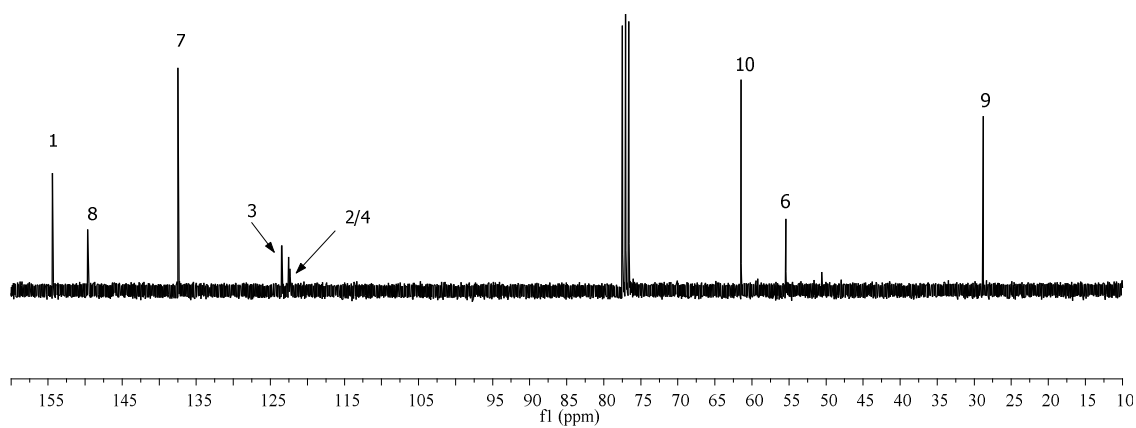
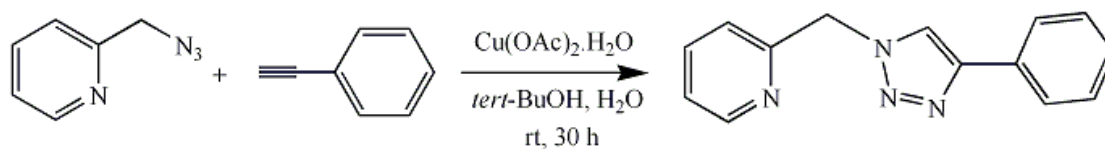


Figure 4.24 ^{13}C NMR spectrum of ligand 2 in CDCl_3 .

^{13}C NMR (300 MHz, CDCl_3 , 298 K): δ 154.56 (C1), 149.85 (C8), 137.59 (C7), 123.60 (C3), 122.60 (C2/4), 61.55 (C10), 55.54 (C6), 28.88 (C9) ppm.

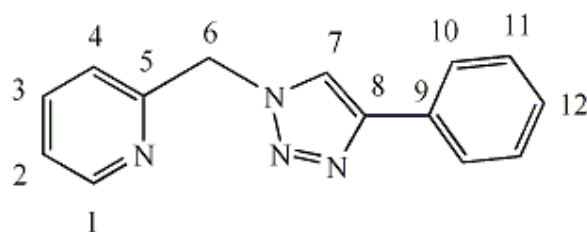
4.2.2.6 Synthesis of ligand 3

Ligand 3 = 2-((4-phenyl-1H-1,2,3-triazol-1-yl)methyl)pyridine



The synthesis of ligand **3** was carried out according to the procedure reported by Amadio, E. *et al.* [62].

In a 50.0 mL two-neck round bottom flask, *tert*-butanol solution (5.0 mL) of 2-(azidomethyl)pyridine (0.70 g, 5.2 mmol) was added to a *tert*-butanol solution (5.0 mL) of phenylacetylene (0.64 g, 5.2 mmol, slight excess) under inert atmosphere. Then, 1.0 mL aqueous solution of cupric acetate monohydrate (0.052 g, 0.26 mmol) was slowly added to the reaction vessel. After 30 hours of stirring, the solution was evaporated to dryness under vacuum. The white solid obtained was purified by column chromatography (silica gel, dichloromethane/ethyl acetate = 5/5), and characterized by ^1H NMR (Figure 4.25) and ^{13}C NMR (Figure 4.26) spectroscopy.



Ligand **3**

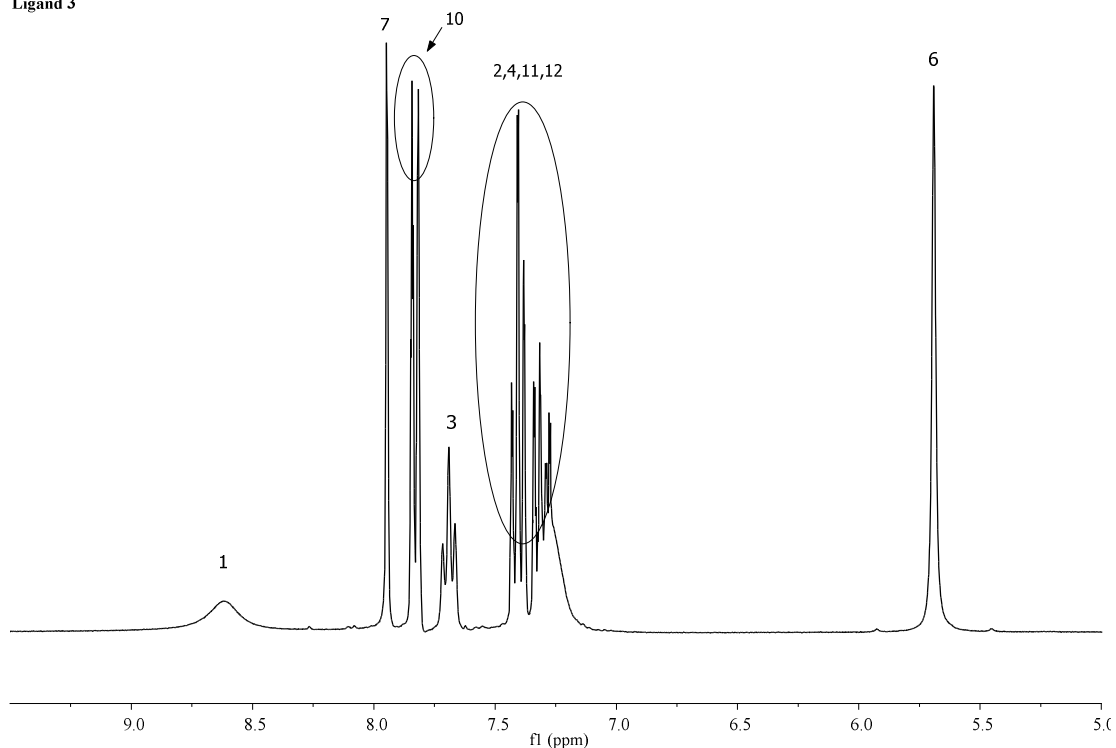


Figure 4.25 ^1H NMR spectrum of ligand **3** in CDCl_3 .

^1H NMR (300 MHz, CDCl_3 , 298 K): δ 8.62 (d, 1H(1)), 7.95 (s, 1H(7)), 7.83 (d, 2H(10)), 7.69 (t, 1H(3), $J = 7.6$ Hz), 7.40 (td, 2H(2/11)), 7.34-7.27 (m, 2H(4/10)), 5.69 (s, 2H(6)) ppm.

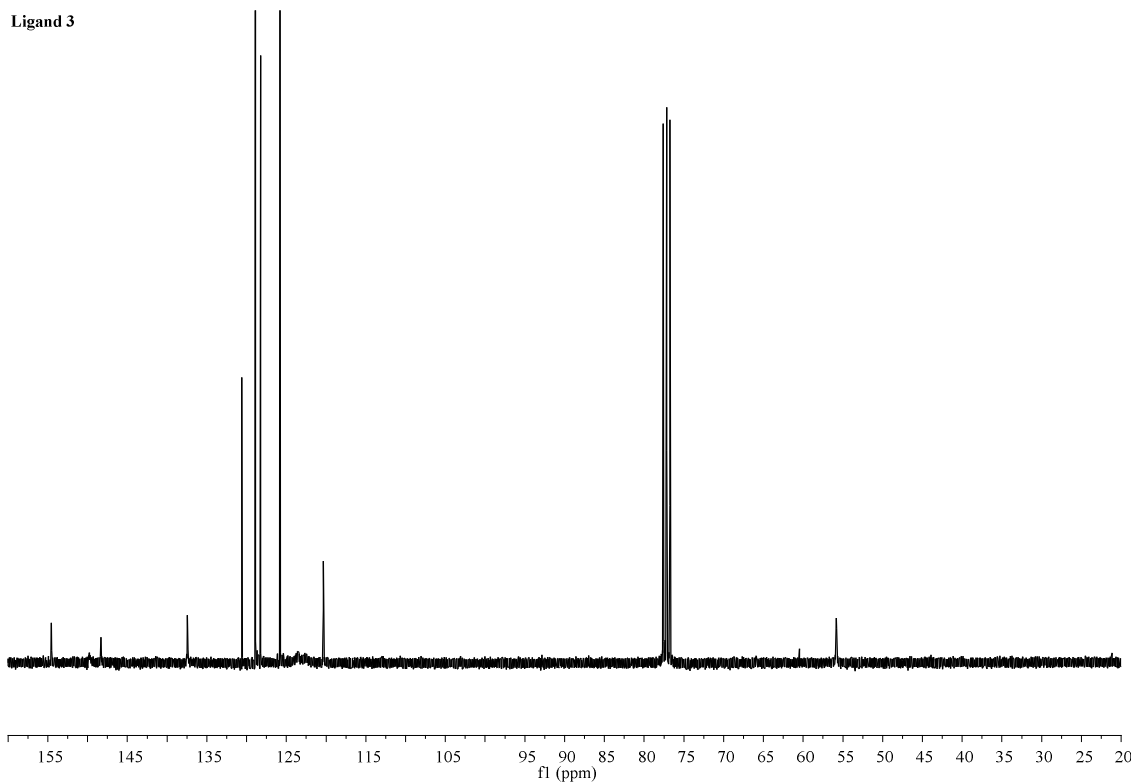


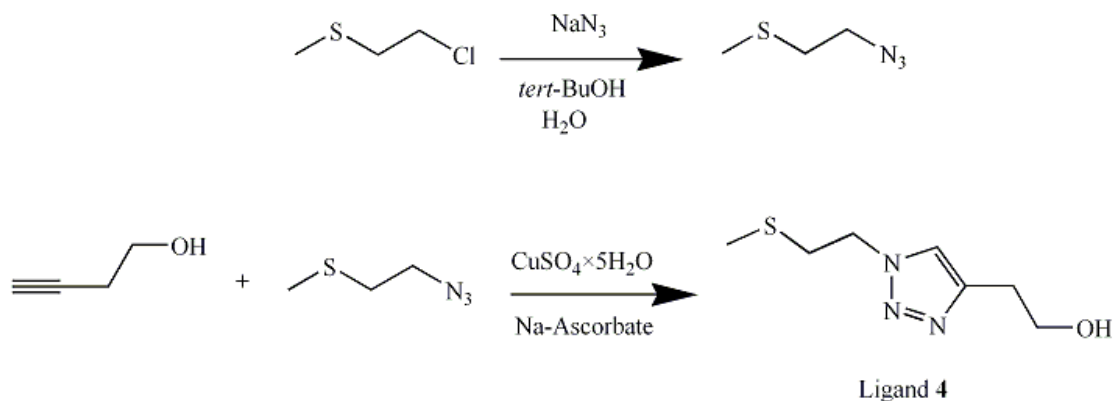
Figure 4.26 ^{13}C NMR spectrum of ligand **3** in CDCl_3 .

^{13}C NMR (300 MHz, CDCl_3 , 298 K): δ 154.55, 148.34, 137.43, 130.56, 128.86, 128.25, 125.76, 120.30, 55.74 ppm.

4.2.3 Synthesis of methyl(thio)ethyl-triazole ligands

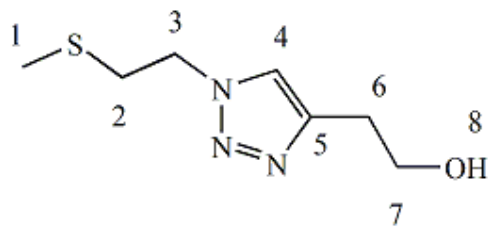
4.2.3.1 Synthesis of ligand 4

Ligand **4** = (2-(1-(2-(methylthio)ethyl)-1*H*-1,2,3-triazol-4-yl)ethanol).



The synthesis of ligand 4 was carried out according to the procedure reported by Rostovtsev, V.V. *et al.* [35].

In a 50.0 mL round bottom flask, sodium azide (0.54 g, 8.35 mmol) was dissolved in a mixture of 16.0 mL of *tert*-BuOH and 4.0 mL of water. (2-chloroethyl)(methyl)sulfane (0.42 mL, 4.17 mmol) was slowly added to the reaction vessel under N₂ atmosphere. After overnight stirring, (2-azidoethyl)(methyl)sulfane was collected into a N₂ refrigerated vessel by high vacuum pump. When the system returned to r.t., 3-butyn-1-ol (0.158 mL, 2.086 mmol) was added to the azido solution. Then, 1.0 mL aqueous solution of a mixture of CuSO₄·5H₂O (0.2086 mmol) and Na-ascorbate (0.4172 mmol) was added to the reaction vessel. The mixture was left for additional 24 hours under stirring. After filtration and vacuum evaporation to dryness, a pale yellow oil was obtained. Extraction with CHCl₃ (5 mL x 2) and dried over vacuum gave a yellow oil (85%) which was characterized by ¹H-NMR (Figure 4.27) and ¹³C-NMR (Figure 4.28) in CDCl₃.



Ligand 4

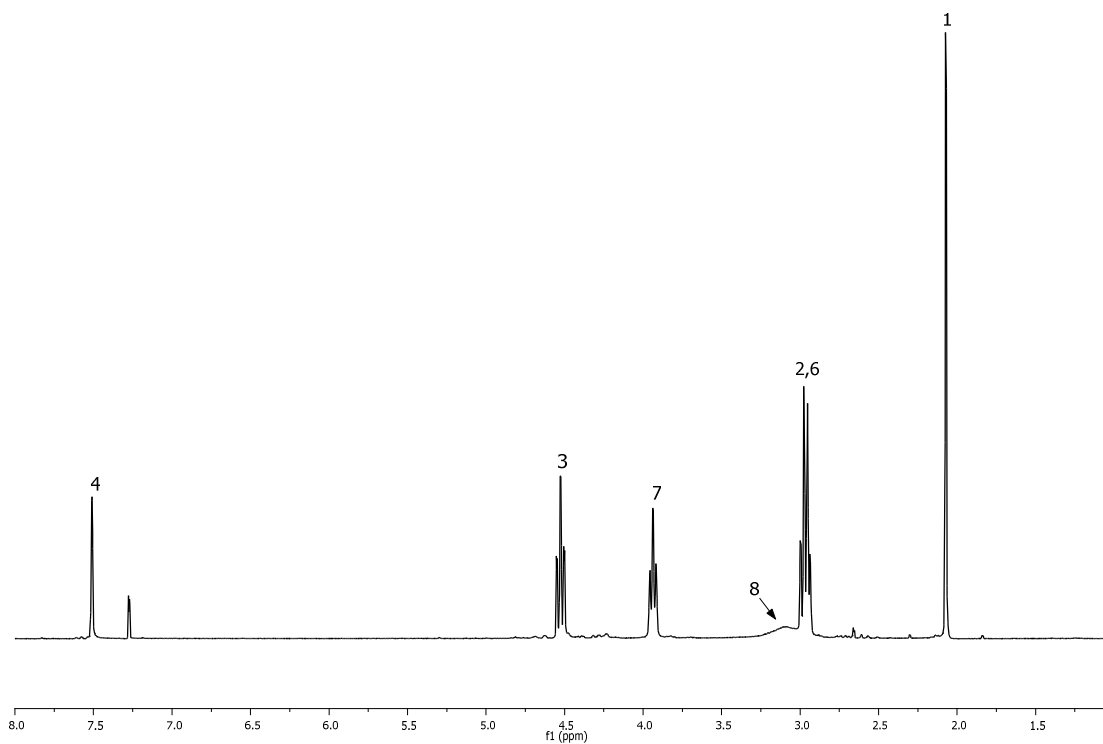


Figure 4.27 ^1H NMR spectrum of ligand 4 in CDCl_3 .

^1H NMR (300 MHz, CDCl_3 , 298 K): δ 7.51(s, 1H(4)), 4.52 (t, 2H(3), $J = 7.0$ Hz), 3.93 (t, 2H(7), $J = 5.9$ Hz), 3.15 (br, s, 1H(8)), 2.96 (m, 4H(2,6)), 2.07 (s, 3H(1)) ppm.

Ligand 4

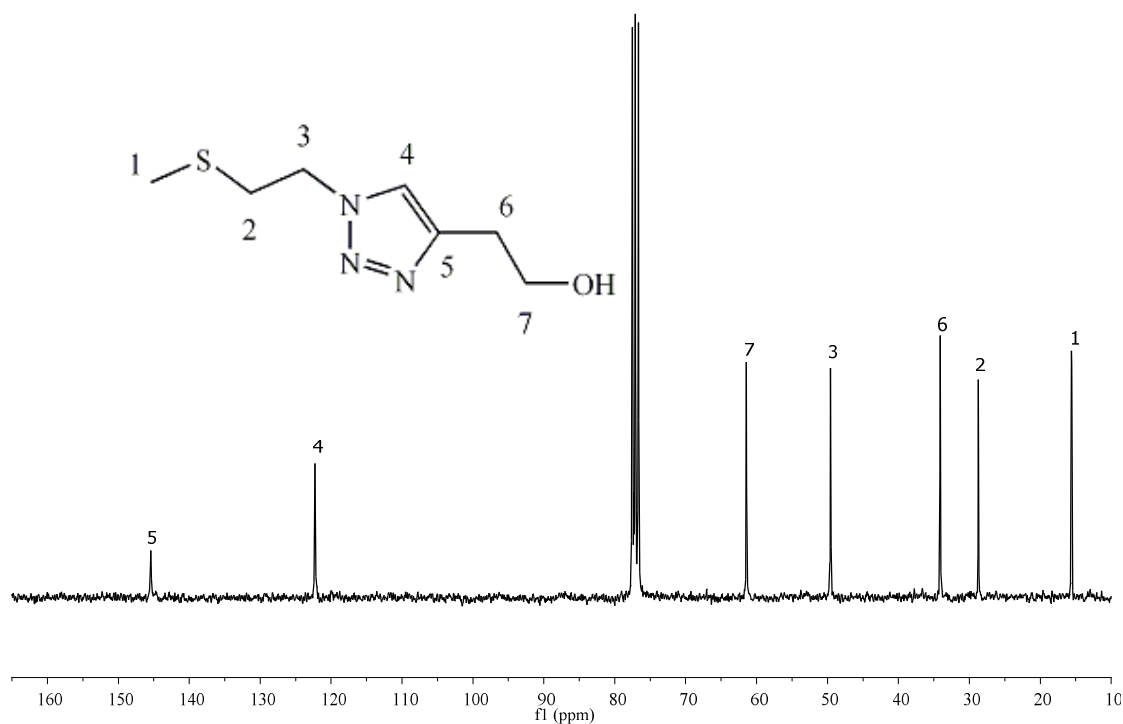
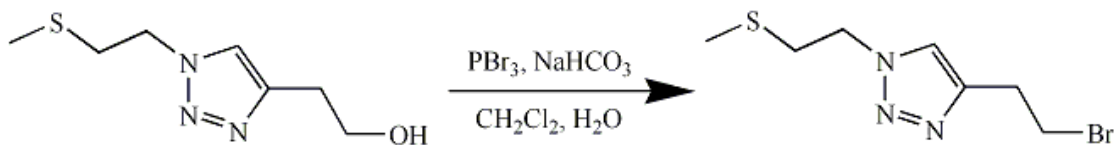


Figure 4.28 ¹³C NMR spectrum of ligand 4 in CDCl₃.

¹³C NMR (300 MHz, CDCl₃, 298 K): δ 145.45 (C5), 122.30 (C4), 61.44 (C7), 49.57 (C3), 34.11 (C6), 28.72 (C2), 15.59 (C1) ppm.

4.2.3.2 Synthesis of ligand 5

Ligand 5 = (4-(2-bromoethyl)-1-(2-(methylthio)ethyl)-1H-1,2,3-triazole).



In a 50 mL round bottom flask, ligand 4 (0.21 g, 1.12 mmol) was dissolved in 2.5 mL of dry CH₂Cl₂. 2.5 mL CH₂Cl₂ solution of PBr₃ (132.0 μL) were added to the reaction vessel under inert atmosphere at 0 °C. After 1 hour of stirring at 0 °C, the stirring was continued overnight at room temperature. 3.5 mL of aqueous solution of NaHCO₃ (0.20 g, 2.25 mmol) were slowly (over an hour) added to the reaction mixture. An intense red color was appeared with

huge smoke. The organic layers were extracted with CH_2Cl_2 , (2.5×3 mL) combined together, dried with sufficient MgSO_4 and filtered. The solvent of the filtrate was removed in vacuo to give a pale yellow ligand **5** in 30 % yield. The ligand **5** was characterized by ^1H NMR spectroscopy (Figure 4.29).

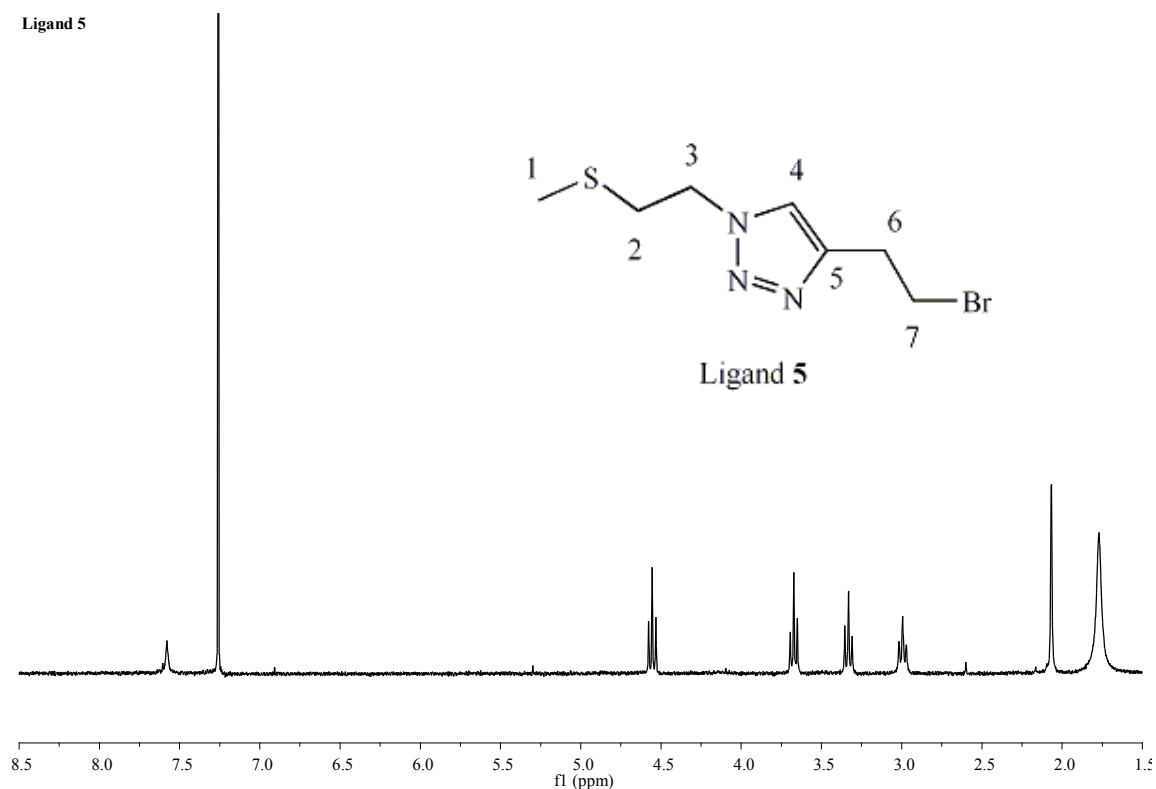
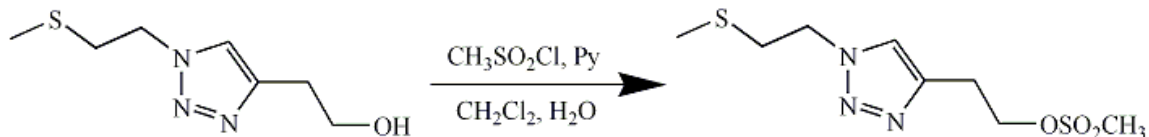


Figure 4.29 ^1H NMR spectrum of ligand **5** in CDCl_3 .

^1H NMR (300 MHz, CDCl_3 , 298 K): δ 7.58(s, 1H(4)), 4.55 (t, 2H(3), $J = 6.8$ Hz), 3.67 (t, 2H(7), $J = 6.7$ Hz), 3.33 (t, 2H(6), $J = 6.8$ Hz), 2.99 (t, 2H(2), $J = 7.0$ Hz) 2.07 (s, 3H(1)) ppm.

4.2.3.3 Synthesis of Ligand 6

Ligand 6 = (2-(1-(2-(methylthio)ethyl)-1*H*-1,2,3-triazol-4-yl)ethyl methanesulfonate)



The synthesis of ligand 6 was carried out according to the procedure reported by Vladimir C. Sekera *et al.* [106]. In a 50 mL round bottom flask, ligand 4 (1.39 g, 7.4 mmol) was completely dissolved in a mixture of 3.0 mL of dry pyridine and 7.0 mL of CH_2Cl_2 . A yellow solution was obtained. At 0 °C and inert atmosphere, 0.67 mL (8.7 mmol, slight excess of ligand 4) of distilled methane sulfonyl chloride was dropwise added to the yellow solution. The reaction mixture was kept stirring under inert atmosphere for 1.5 hours at 0 °C. After overnight stirring at room temperature, the resulting green solution was evaporated under reduced pressure and then 15.0 mL of CH_2Cl_2 was added, filtered, and extracted with 30.0 mL of water. The extracted CH_2Cl_2 solution was dried with sufficient MgSO_4 , filtered, and evaporated to yellow oil which was characterized by ^1H NMR (Figure 4.30) and ^{13}C NMR (Figure 4.31), spectroscopy. Yield = 77% (1.52 g).

Ligand 6

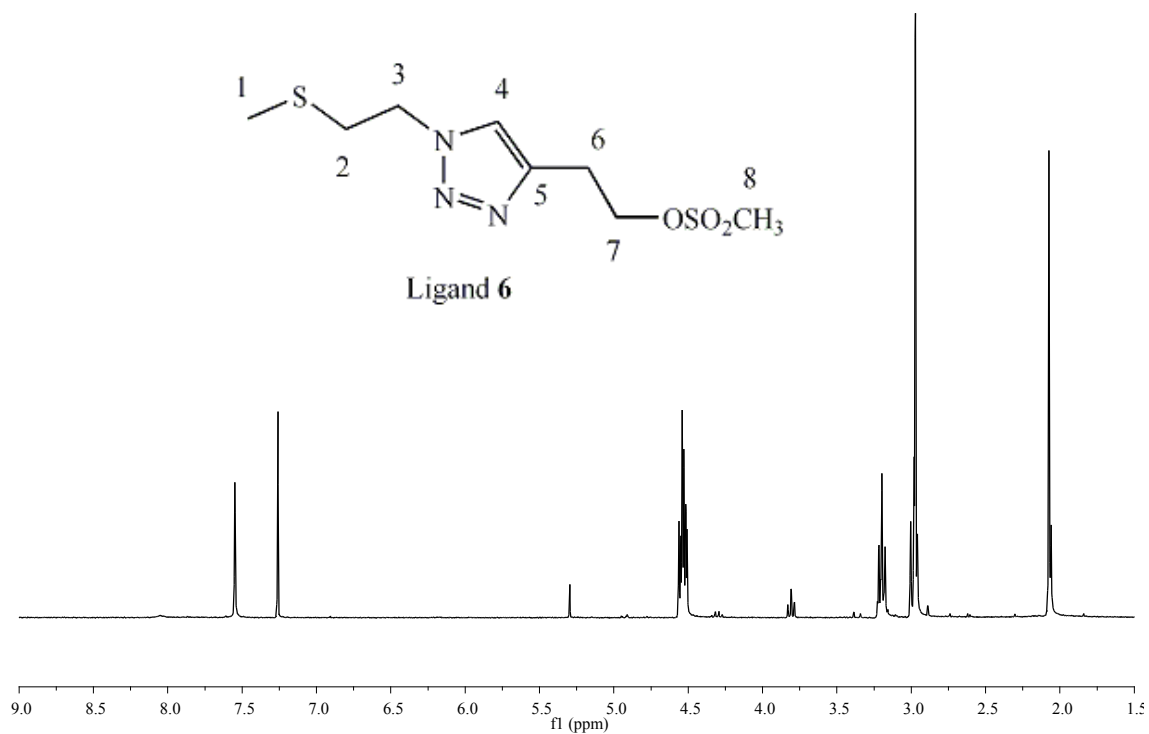
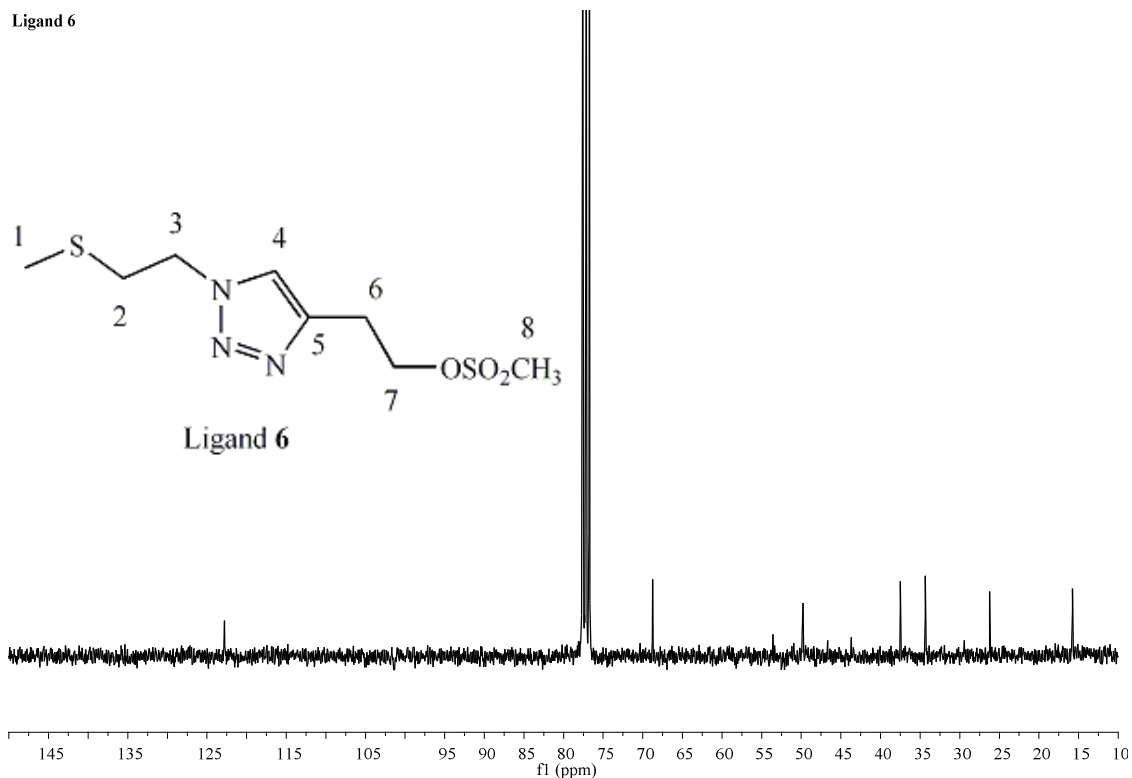


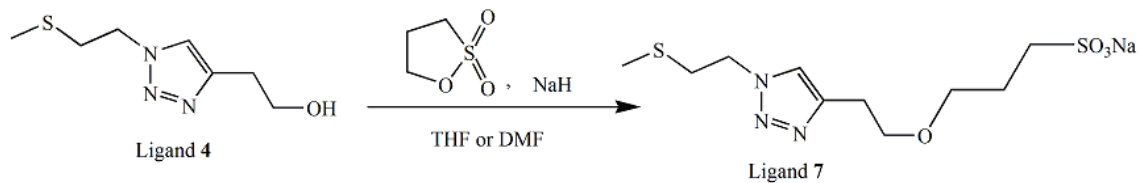
Figure 4.30 ¹H NMR spectrum of ligand **6** in CDCl₃.

¹H NMR (300 MHz, CDCl₃, 298 K): δ 7.55 (s, 1H(4)), 4.56-4.51 (m, 4H(3,7)), 3.20 (t, 2H(6), *J* = 6.4 Hz), 3.00-2.97 (m, 5H(2,8)), 2.07 (s, 3H(1)) ppm.



^{13}C NMR (300 MHz, CDCl_3 , 298 K): 122.88, 68.77, 49.91, 37.50, 34.35, 26.14, 15.76 ppm.

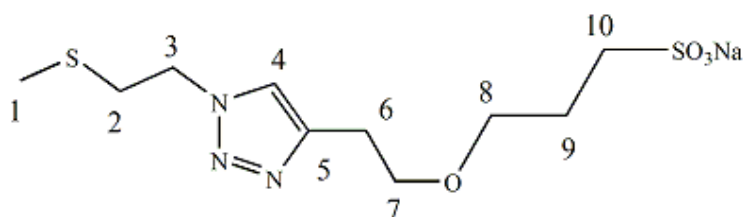
4.2.3.4 Synthesis of ligand 7



Synthesis of ligand 7 was carried out according to the procedure reported by Brent C. Norris *et al.* [108]

In a 50.0 mL round bottom flask, 0.039 g (1.61 mmol) of NaH was taken in 5.0 mL of dry THF. A 5.0 mL THF solution of ligand 4 (0.30 g, 1.61 mmol) was slowly (over 10 minutes) added to the flask under stirring at 0 °C. Then, a 10.0 mL THF solution of 1,3-propanesultone

(0.20 g, 1.61 mmol) was added slowly. The reaction mixture was stirred 10 minutes at 0 °C, refluxed for additional 4 hours. After filtration, the volume was concentrated into half by rotary evaporator and precipitation by diethyl ether afford the title compound, ligand **7** which was characterized by ¹H NMR spectroscopy (Figure 4.32).



Ligand **7**

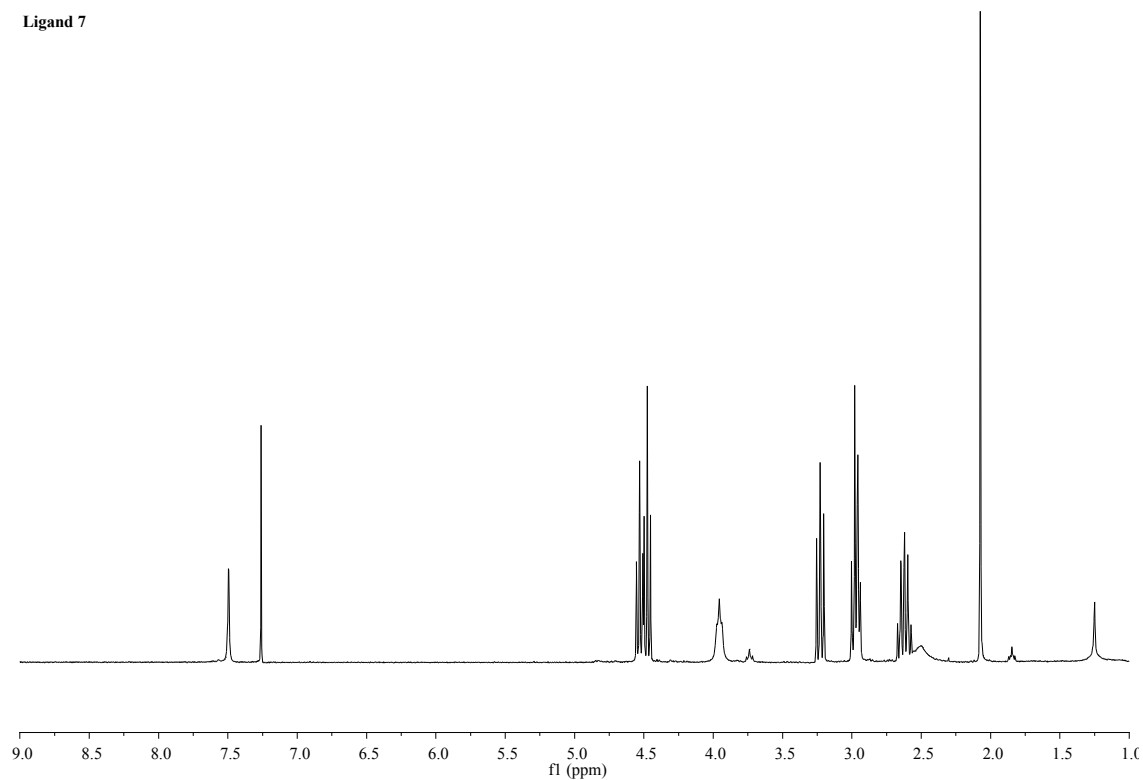
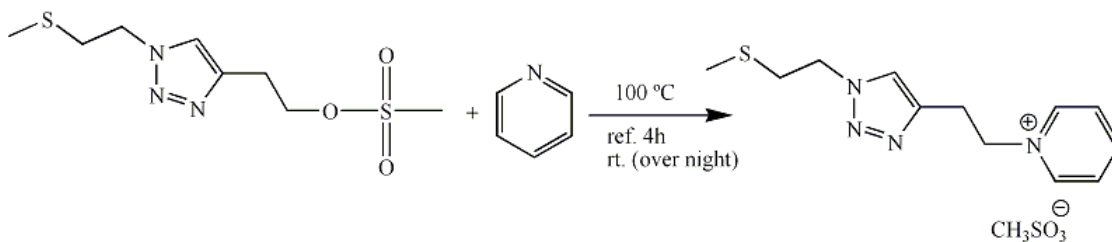


Figure 4.32 ¹H NMR spectrum of ligand **7** in CDCl₃.

¹H NMR (300 MHz, CDCl₃, 298 K): δ 7.50 (s, 1H(4)), 4.55-4.45 (m, 4H(3,7)), 3.23 (t, 2H(6), *J* = 6.4 Hz), 3.96 (m, 2H(9)), 3.00-2.94 (m, 4H(2,8)), 2.67-2.57 (m, 2H (10)), 2.07 (s, 3H(1)) ppm.

4.2.3.5 Synthesis of ligand **8**

Ligand **8** = (4-(ethyl-2-pyridinium methanesulfonate)-1-(2-(methylthio)ethyl)-1H-1,2,3-triazole)



The synthesis of ligand **8** was carried out according to the procedure reported by Eglinton, *et al.* [109]. A mixture of (0.28 g, 1.0 mmol) of ligand **6** and 1.5 mL (16.4x1.0 mmol) of dry pyridine was refluxed at 100 °C for 4 hours under inert atmosphere, then it was kept stirring overnight at room temperature. After vacuum evaporation to dryness and washed with diethyl ether afford a brown solid which was characterized by ¹H NMR (Figure 4.33) and ¹³C NMR spectroscopy (Figure 4.34).

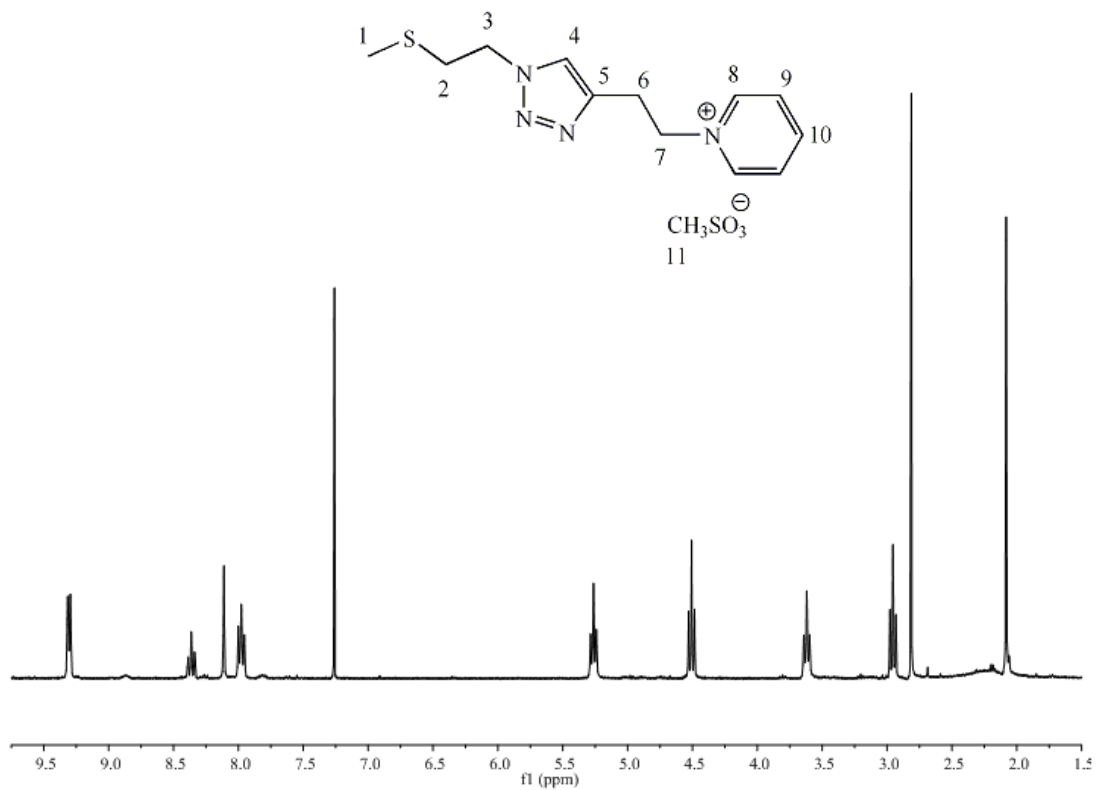


Figure 4.33 ^1H NMR spectrum of ligand **8** in CDCl_3 .

^1H NMR (300 MHz, CDCl_3 , 298 K): δ 9.31(d, 2H(8), $J = 7.6$ Hz), 8.36 (t, 1H(10), $J = 7.6$ Hz), 8.11 (s, 1H(4)), 7.98 (t, 2H(9) $J = 7.1$ Hz), 5.26 (t, 2H(2), $J = 6.7$ Hz), 4.51 (t, 2H(3), $J = 6.9$ Hz), 3.62 (t, 2H(6), $J = 6.7$ Hz), 2.96 (t, 2H(2), $J = 6.8$ Hz), 2.81 (s, 3H(11)), 2.08 (s, 3H(1)) ppm.

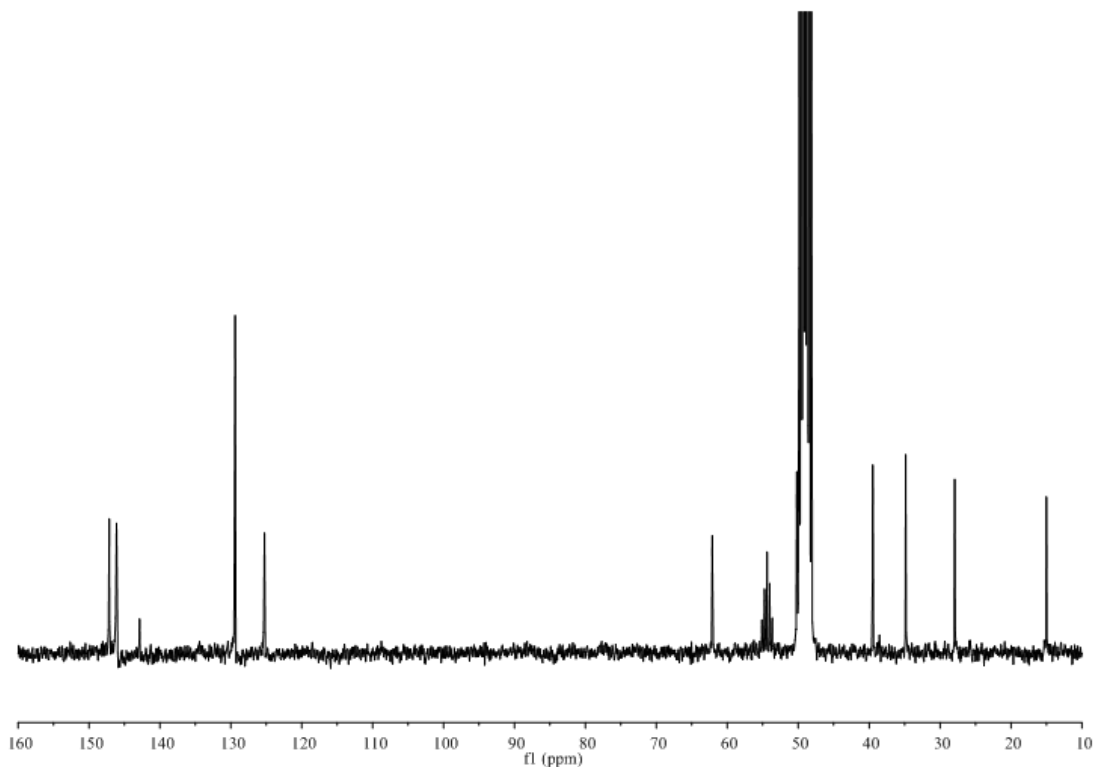
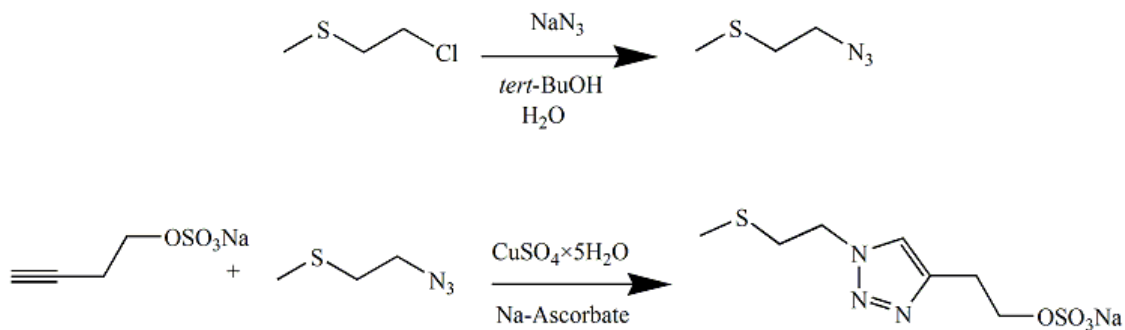


Figure 4.34 ^{13}C NMR spectrum of ligand **8** in CD_3OD .

^{13}C NMR (300 MHz, CD_3OD , 298 K): 147.14 (C10), 146.11 (C8), 142.85 (C5), 129.39 (C9), 125.25 (C4), 62.12 (C7), 50.20 (C3), 39.49 (C11), 34.85 (C2), 27.93 (C6), 15.01 (C1) ppm.

4.2.3.6 Synthesis of ligand **9**



The attempt to synthesis of ligand **9** was carried out according to the procedure reported by Rostovtsev, V. V. *et al.* [35]. In a 50.0 mL round bottom flask, sodium azide (0.54 g, 8.35

mmol) was dissolved in a mixture of 16.0 mL of *tert*-BuOH and 4.0 mL of water. (2-chloroethyl)(methyl)sulfane (0.42 mL, 4.17 mmol) was slowly added to the reaction vessel under N₂ atmosphere. After overnight stirring, (2-azidoethyl)(methyl)sulfane was collected into a N₂ refrigerated vessel by high vacuum pump. Sodium 3-butyn-1-sulfate (0.36 g, 2.086 mmol) was added to the azido solution. Then, 1.0 mL aqueous solution of mixture of CuSO₄·5H₂O (0.2086 mmol, 10%) and Na-ascorbate (0.42 mmol, 20%) was added to the reaction vessel under stirring. The reaction mixture was left under stirring for additional 24 hours. After filtration and vacuum evaporation to dryness afford a solid which was characterized by ¹H-NMR (Figure 4.35) spectrum.

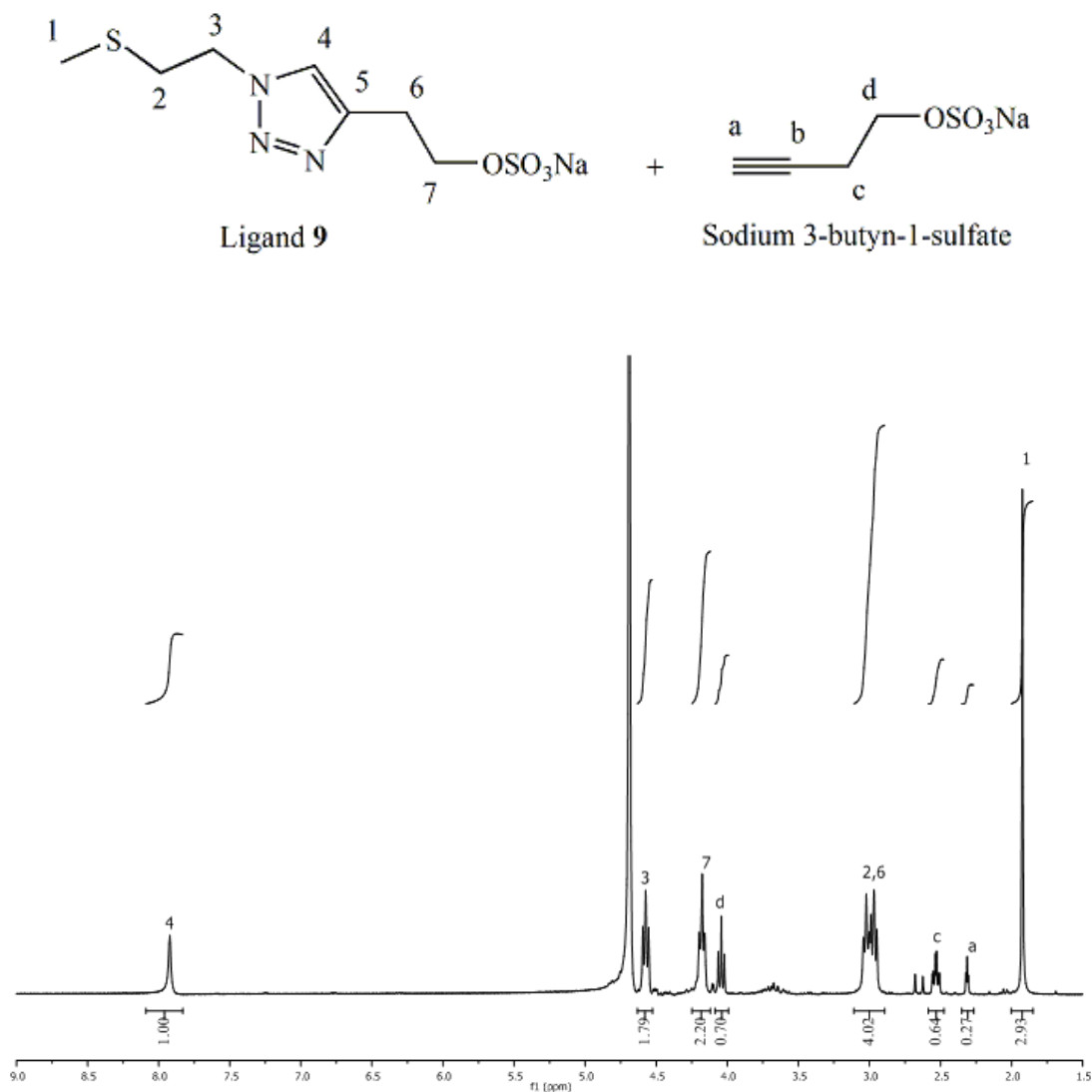
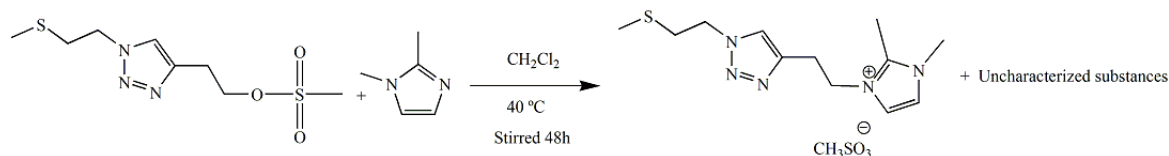
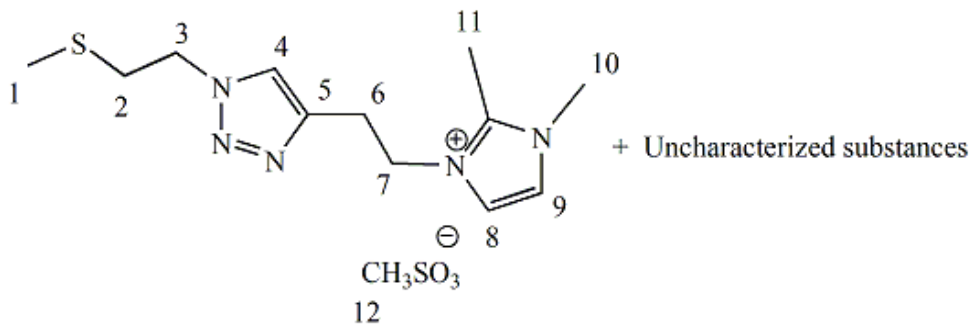


Figure 4.35 ¹H NMR spectrum of product from the reaction of synthesis of ligand 9 in D₂O.

4.2.3.7 Synthesis of ligand **10**



The attempt to the synthesis of ligand **10** was carried out according to the procedure reported by Eglinton, *et al.* [109]. A mixture of (0.22 g, 0.82 mmol) of ligand **6** and of 1,2-dimethylimidazole (0.079.0 g, 0.82 mmol) in 2.0 mL anhydrous dichloromethane was stirred at $40\text{ }^\circ\text{C}$ for 48 hours under inert atmosphere. A yellow-brown molten obtained was characterized by ^1H NMR (Figure 4.36) spectroscopy. The product is a mixture of ligand **10** and unknown substances.



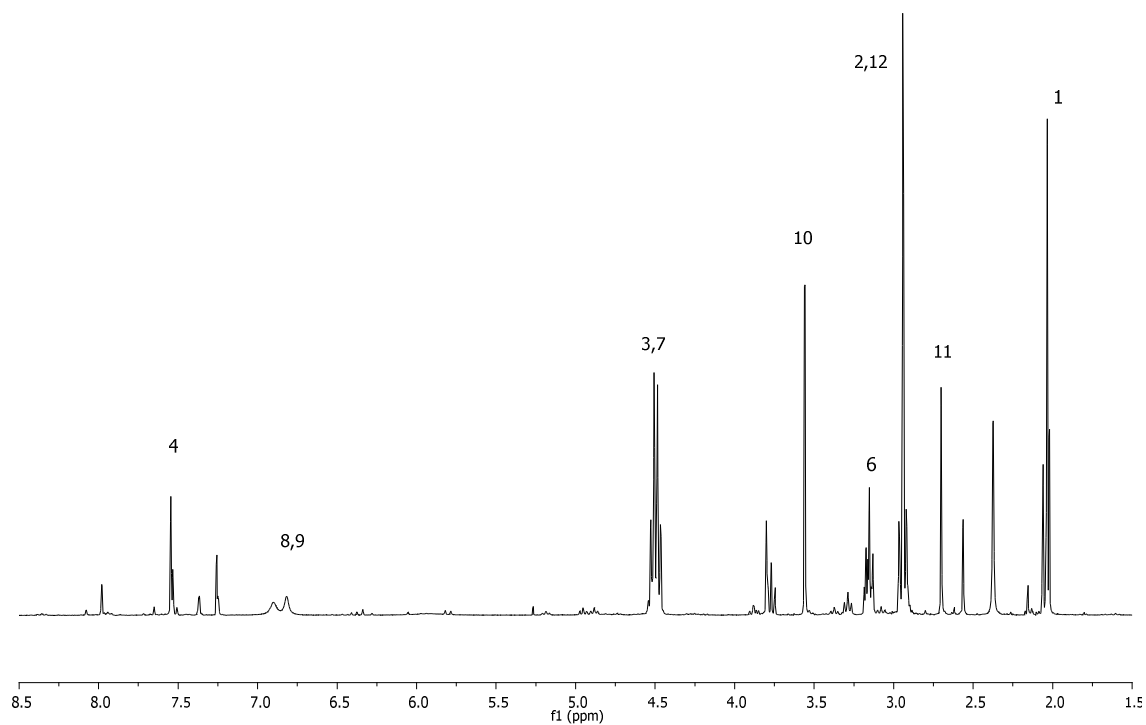
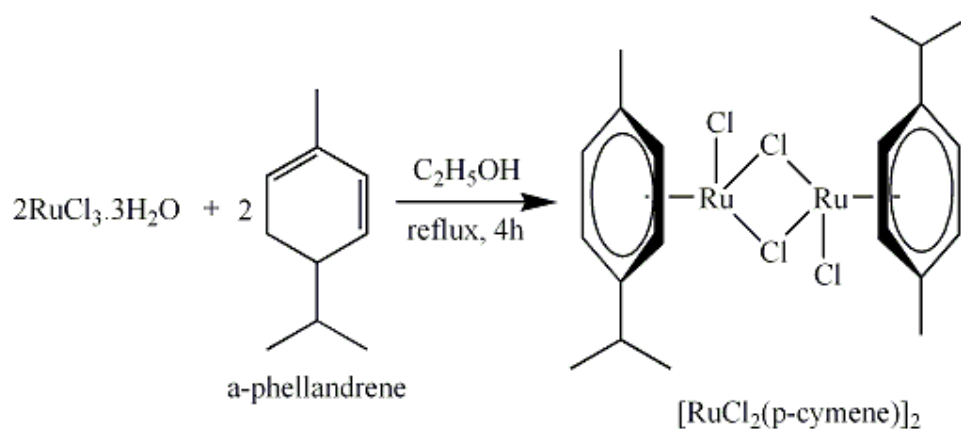


Figure 4.36 ^1H NMR spectrum of product from the reaction of synthesis of ligand **10** in CDCl_3 .

4.2.4 Synthesis of metal-triazole complexes

4.2.4.1 Synthesis of $[\text{RuCl}_2(\eta^6\text{-}p\text{-cymene})]_2$ precursor complex



The synthesis of $[\text{RuCl}_2(\eta^6\text{-}p\text{-cymene})]_2$ complex was carried out according to the procedure reported by Bennett, M. A. *et al.* [110]. In a 100.0 mL round bottom flask, 7.0 mL of α -

phellandrene was added to an ethanol solution (50.0 mL) of $\text{RuCl}_3 \cdot 3\text{H}_2\text{O}$ (1.03 g, 3.94 mmol). A nitrogen atmosphere can be used but is not strictly necessary. The reaction mixture was refluxed for 4 hours, the solution was allowed to cool at room temperature, a red-brown, crystalline product precipitates. After filtration, additional product is obtained by evaporating the filtrate under reduced pressure to approximately half-volume and refrigerating overnight. After drying in vacuum, the overall yield is 0.98 g (81%). The complex was characterized by melting point (208-212°C), FT-IR (Figure 4.37) and ^1H NMR (Figure 4.38) spectroscopy.

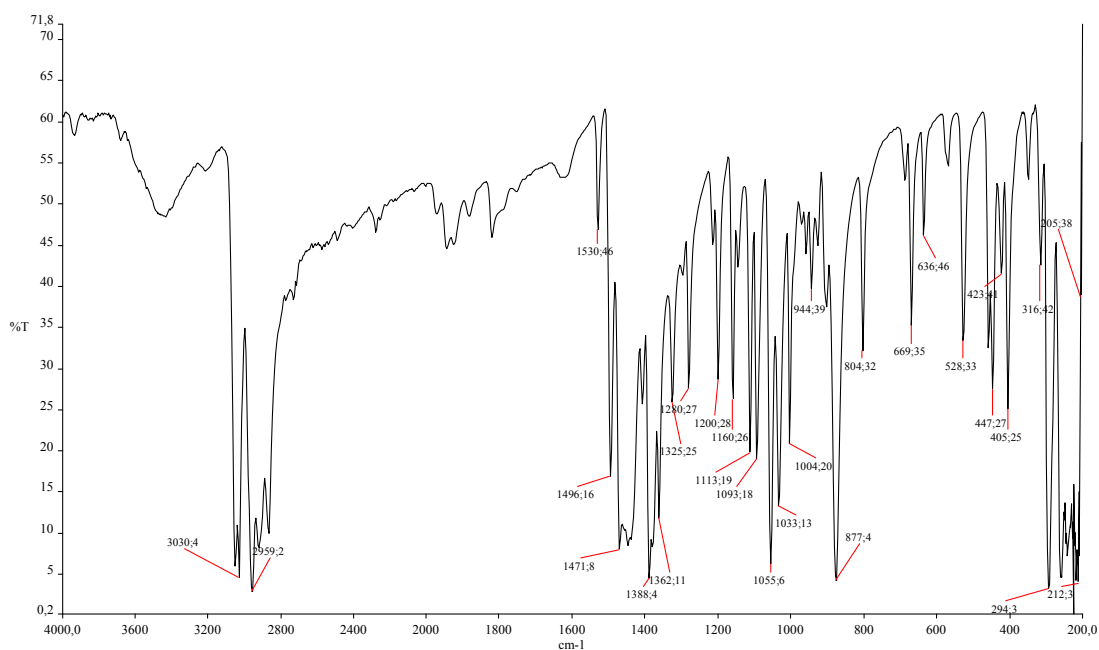
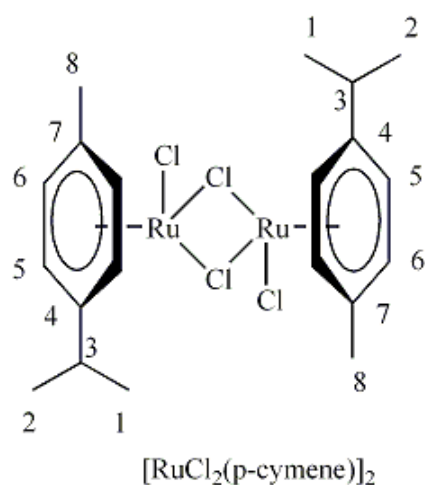


Figure 4.37 IR spectrum of $[\text{RuCl}_2(\eta^6\text{-p-cymene})]_2$ in KBr.

IR (KBr pellet) ν_{\max} : 3030 (p-cym, =C-H stretching), 2959 (Me, C-H stretching), 1530 (p-cym, C=C), 1496 (p-cym, C=C stretching), 1471 (Me, C-H bending), 1362 (Me, C-H bending), 1055 (=C-H bending), 877, 669, 528, 447, 405 294, 212. cm^{-1} .

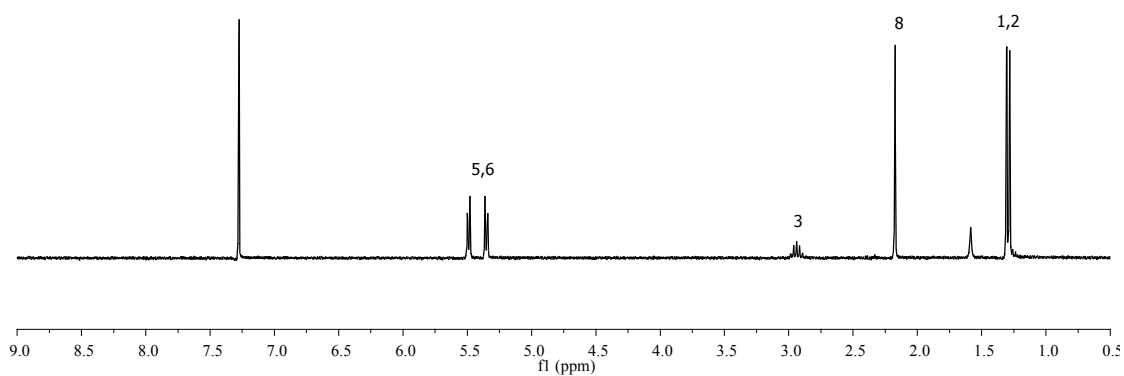
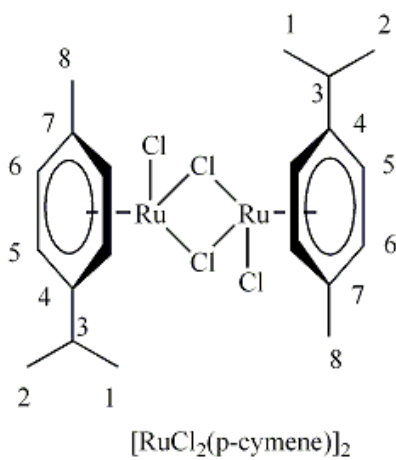
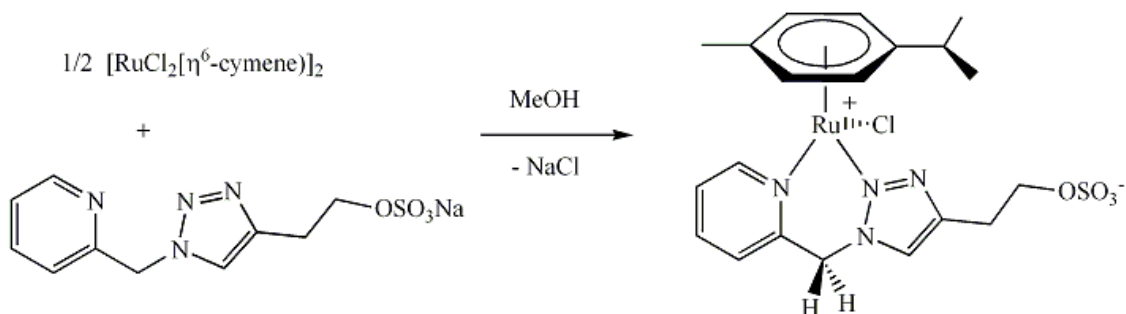


Figure 4.38 ^1H NMR spectrum of $[\text{RuCl}_2(\eta^6\text{-}p\text{-cymene})]_2$ in CDCl_3 .

^1H NMR (300 MHz, CDCl_3 , 298 K): δ 5.34-5.50 (dd, 4H(5,6), $J = 6.1$ Hz), 2.94 (m, 1H(3)), 2.17 (s, 3H(8)), 1.30 (d, 6H(1,2), $J = 6.9$ Hz) ppm.

4.2.4.2 Synthesis of Complex **1**, ([RuCl(η^6 -*p*-cymene)(ligand **1**)] complex)



The synthesis of $[\text{RuCl}(\eta^6\text{-}p\text{-cymene})(\text{ligand } \mathbf{1})]$ complex was carried out according to the procedure reported by Uranker, D. *et al.* [45]. In a 50.0 mL two-neck round bottom flask, a mixture of ligand **1.Na** (0.12 g, 0.39 mmol) and $[\text{RuCl}_2(\eta^6\text{-}p\text{-cymene})]_2$ (0.12 g, 0.20 mmol) was stirred in methanol (20.0 mL) at room temperature for 3 days. The mixture was filtered, and filtrate were evaporated by vacuum to give $[\text{RuCl}(p\text{-cymene})(\text{ligand } \mathbf{1})]$ as yellow crystalline powder. The product was dissolved in boiling EtOH (10.0 mL), and the resulting solution was left to stand at room temperature overnight. Yellow-orange microcrystals were collected and characterized by elemental analysis, FT-IR, ^1H NMR, ^{13}C NMR, and ESI-MS spectroscopy (Figure 39, 40, 41 and 42 respectively). Anal. Calc. for $\text{C}_{20}\text{H}_{25}\text{ClN}_4\text{O}_4\text{RuS}$ (554.0): C, 43.36; H, 4.55; N, 10.11; Cl, 6.40%. Found: C, 43.12; H, 4.54; N, 9.88; Cl, 6.15%.

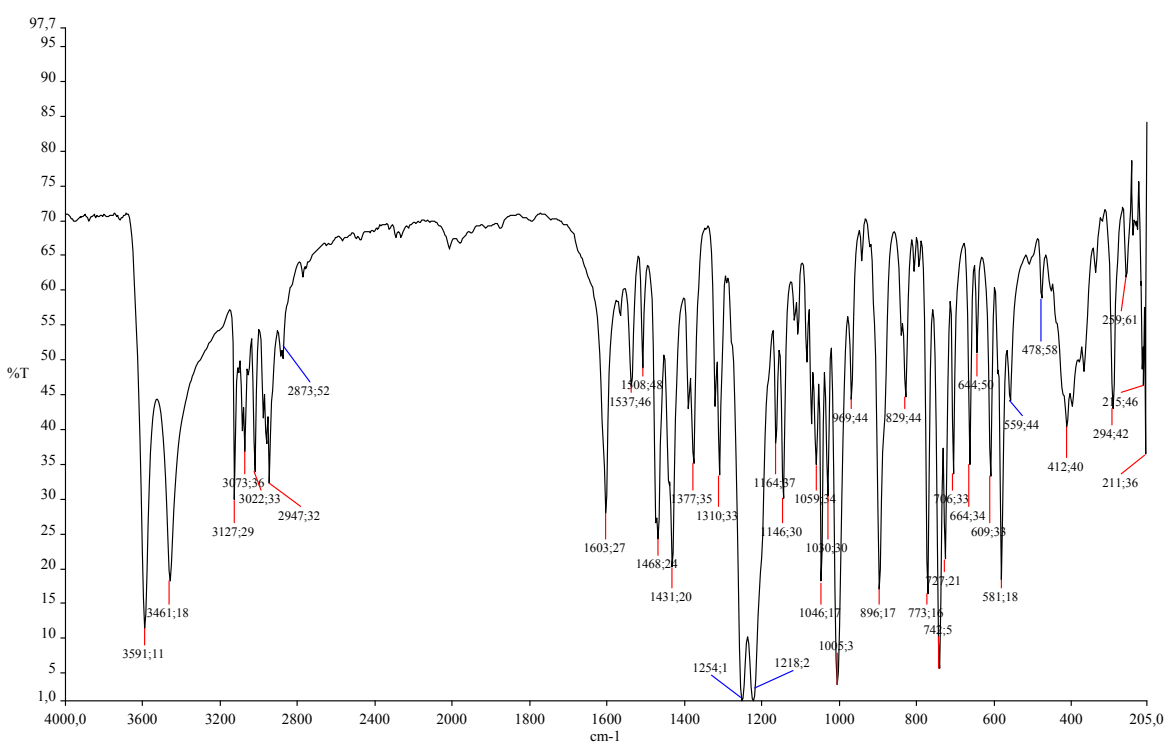
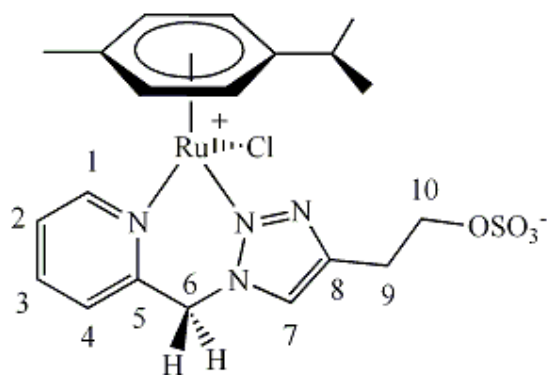


Figure 4.39 IR spectrum of $[\text{RuCl}(\eta^6\text{-}p\text{-cymene})(\text{ligand } 1)]$ in KBr.

IR (KBr pellet) ν_{max} : 3591(H_2O stretching), 3461(H_2O stretching), 3127($p\text{-cym}$, =C-H stretching), 3073($p\text{-cym}$, =C-H stretching), 3022($p\text{-cym}$, =C-H stretching), 2947($p\text{-cym}$, -C-H stretching), 1603(Py C=N stretching), 1468, 1431, 1254, 1218, 1005(C-N stretching), 896, 773, 742, 581 cm^{-1} .

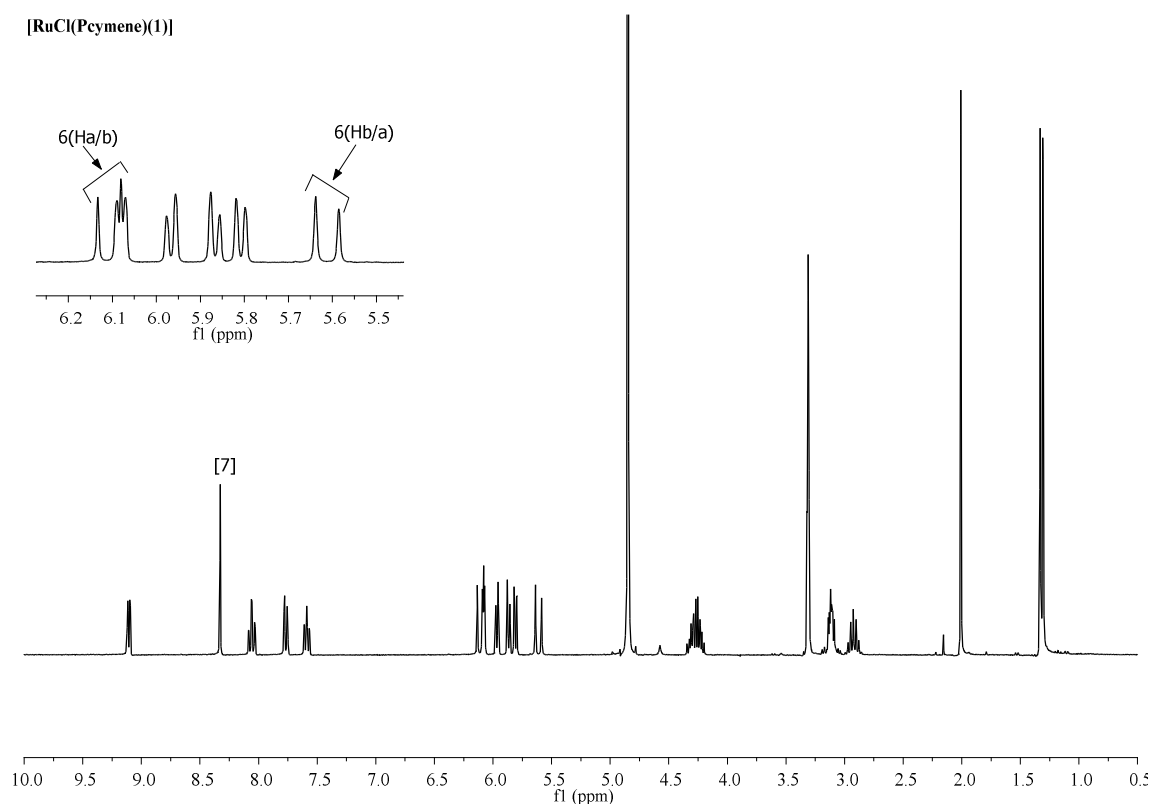
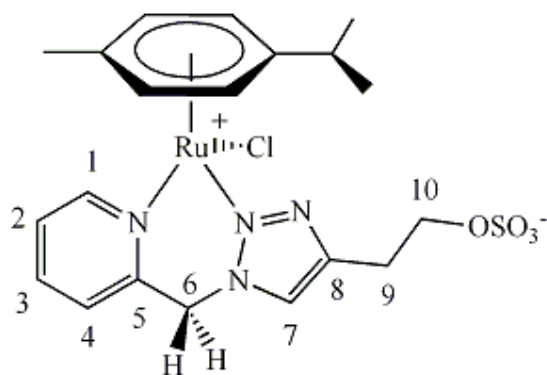


Figure 4.40 ^1H NMR spectrum of $[\text{RuCl}(\eta^6\text{-}p\text{-cymene})(\text{ligand } 1)]$ in CD_3OD .

^1H NMR (300 MHz, CD_3OD , 298 K): δ 9.11 (d, 1H(1), $J = 5.0$ Hz), 8.33 (s, 1H(7)), 8.06 (td, 1H(3), $J = 7.7, 1.25$ Hz), 7.77 (d, 1H(4), $J = 7.3$ Hz), 7.59 (t, 1H(2), $J = 6.7$ Hz), 6.13-6.07 (m, CH^a/CH Ar, 2H), 5.97 (d, 1H Ar, $J = 6.0$ Hz), 5.87 (d, 1H Ar, $J = 6.1$ Hz), 5.81 (d, 1H Ar, $J = 6.2$ Hz), 5.62 (d, 1H^b, $J = 15.8$ Hz), 4.34-4.20 (m, 2H(10)), 3.19-3.04 (m, 2H(9)), 2.97-2.88 (m, 1H(13)), 2.01 (s, 3H(18)), 1.32 (d, 6H(11,12), $J = 6.9$ Hz) ppm.

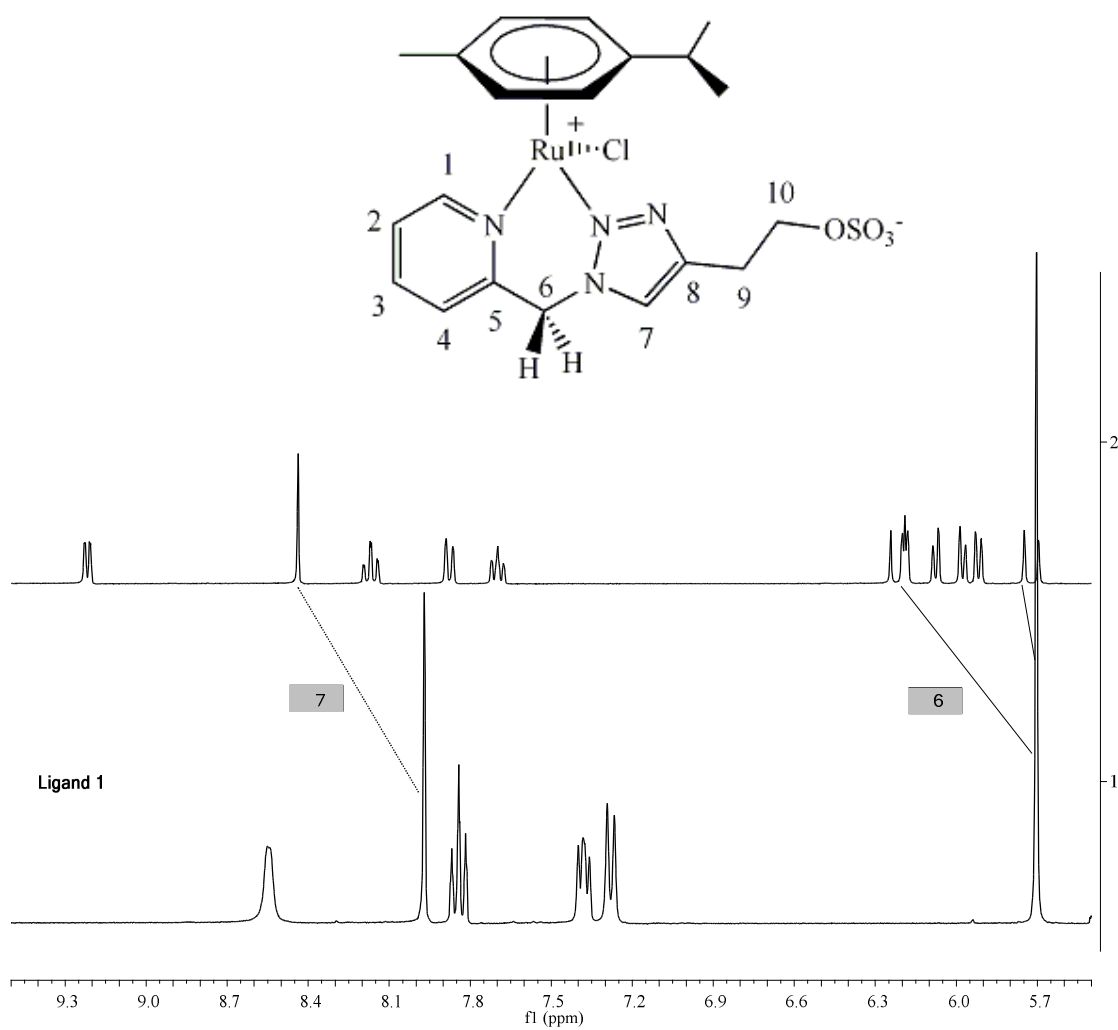


Figure 4.40(1) Comparison between ^1H NMR spectra of ligand **1**.Na and $[\text{RuCl}(\eta^6\text{-}p\text{-cymene})(\text{ligand } \mathbf{1})]$ in CD_3OD .

[RuCl(*p*-cymene)(**1**)]

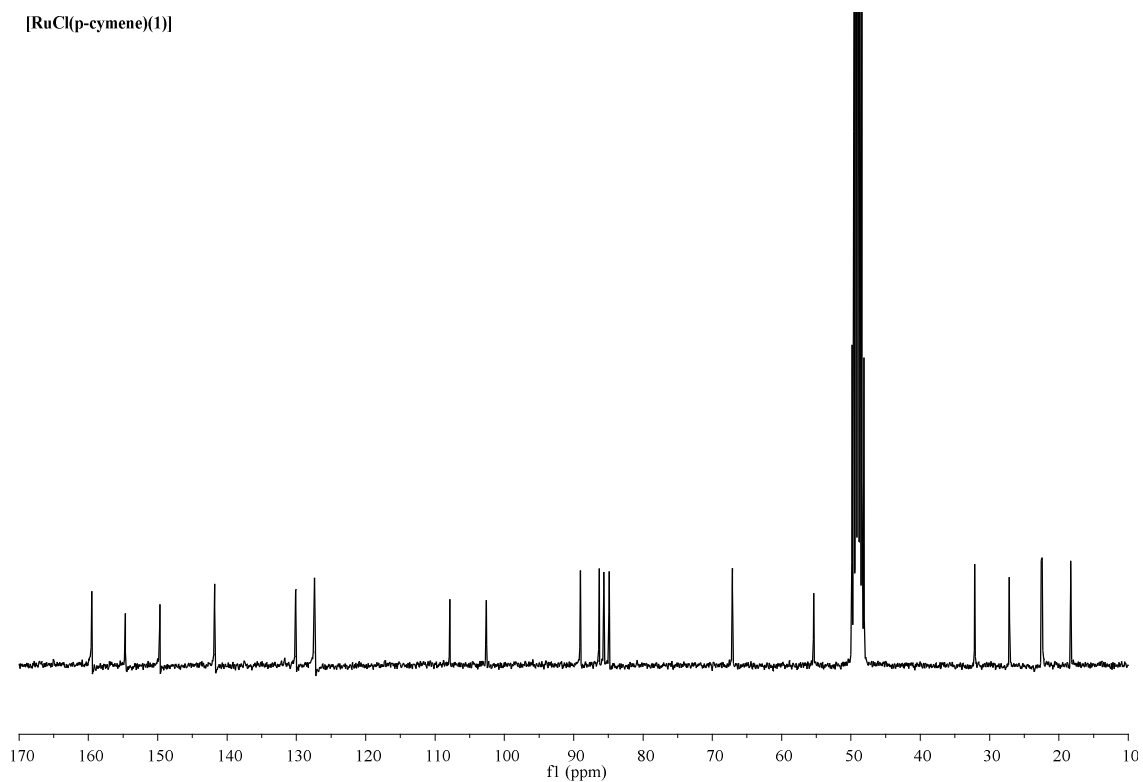


Figure 4.41 ¹³C NMR spectrum of [RuCl(η^6 -*p*-cymene)(ligand **1**)] in CD₃OD.

¹³C NMR (300 MHz, CD₃OD, 298 K): δ 159.48 (C-1), 154.66 (C-5), 149.68 (C-7), 141.78 (C-3), 130.10 (C-4), 127.39 (C-8 or C-2), 127.28 (C-8 or C-2), 107.87 (*p*-cym), 102.59 (*p*-cym), 89.02 (*p*-cym), 86.32 (*p*-cym), 85.64 (*p*-cym), 84.88 (*p*-cym), 67.11 (C-10), 55.38 (C-6), 32.18 (*p*-cymCH), 27.16 (C-9), 22.57 (CHCH₃), 22.43 (CHCH₃), 18.30 (*p*cymCH₃) ppm.

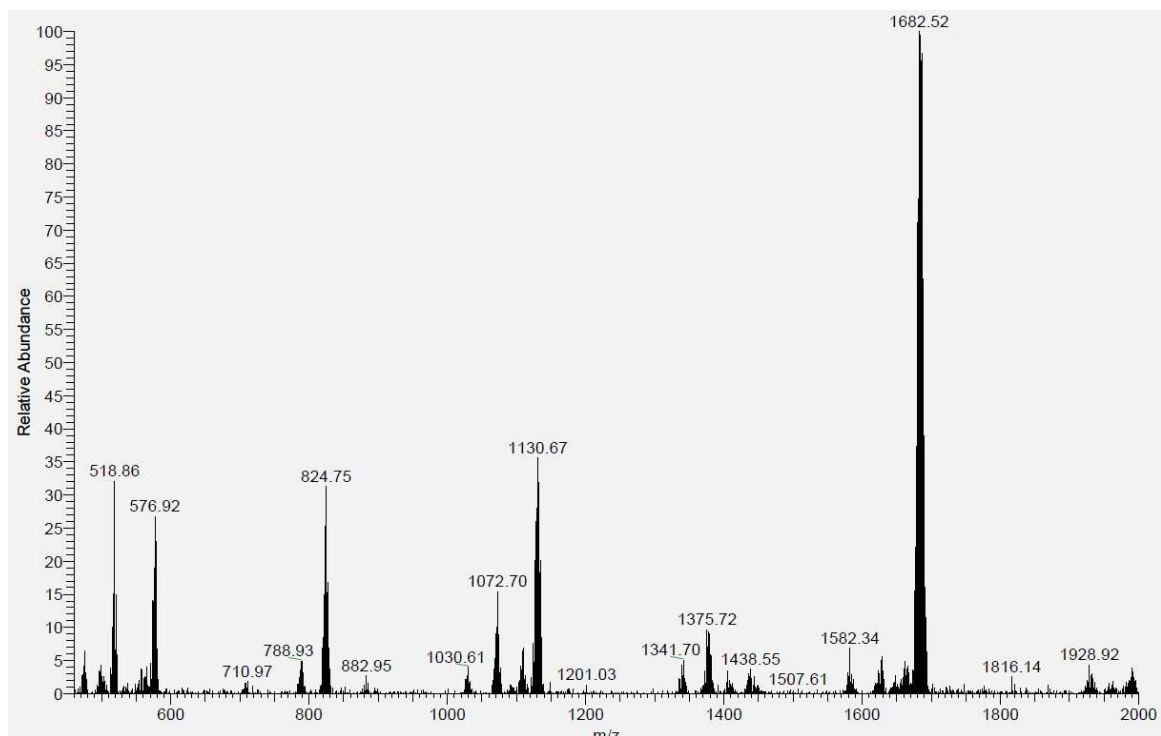
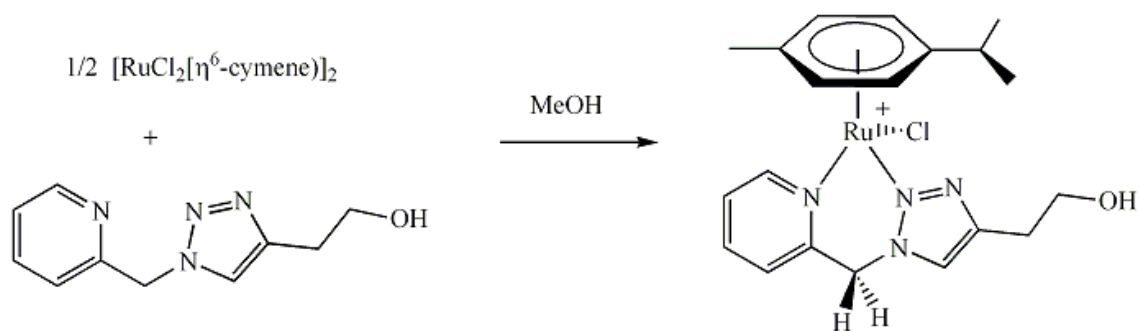


Figure 4.42 ESI-MS spectrum of $[\text{RuCl}(\eta^6\text{-}p\text{-cymene})(\text{ligand } 1)]$ in MeOH.

ESI-MS (m/z): 1685 (M_3+Na)⁺, 1131 (M_2+Na)⁺, 577 ($\text{M}+\text{Na}$)⁺, 519 ($\text{M}-\text{Cl}$)⁺, 497 ($\text{M}-\text{SO}_3+\text{Na}$), and 439 ($\text{M}-\text{SO}_3-\text{Cl}$)⁺.

4.2.4.3 Synthesis of Complex 2, ($[\text{RuCl}(\eta^6\text{-}p\text{-cymene})(\text{ligand } 2)]\text{Cl}$ complex)



The synthesis of $[\text{RuCl}(\eta^6\text{-}p\text{-cymene})(\text{ligand } 2)]\text{Cl}$ complex was carried out according to the procedure reported by Uranker, D. *et al.* [45]. In a 50.0 mL two-neck round bottom flask, a mixture of ligand **2** (0.07 g, 0.34 mmol) and $[\text{RuCl}_2(\eta^6\text{-}p\text{-cymene})]_2$ (0.10 g, 0.17 mmol) was

stirred in methanol (10.0 mL) at room temperature for 3 days. The mixture was filtered, and then filtrate were evaporated by vacuum to give yellow powder. The product was extracted from EtOH (10.0 mL), and the resulting solution was evaporated by vacuum to give $[\text{RuCl}(\eta^6\text{-}p\text{-cymene})(\text{ligand } \mathbf{2})]\text{Cl}$ as yellow crystalline powder which characterized by FT-IR (Figure 4.43), ^1H NMR (Figure 4.44), and ^{13}C NMR (Figure 4.45) spectroscopy.

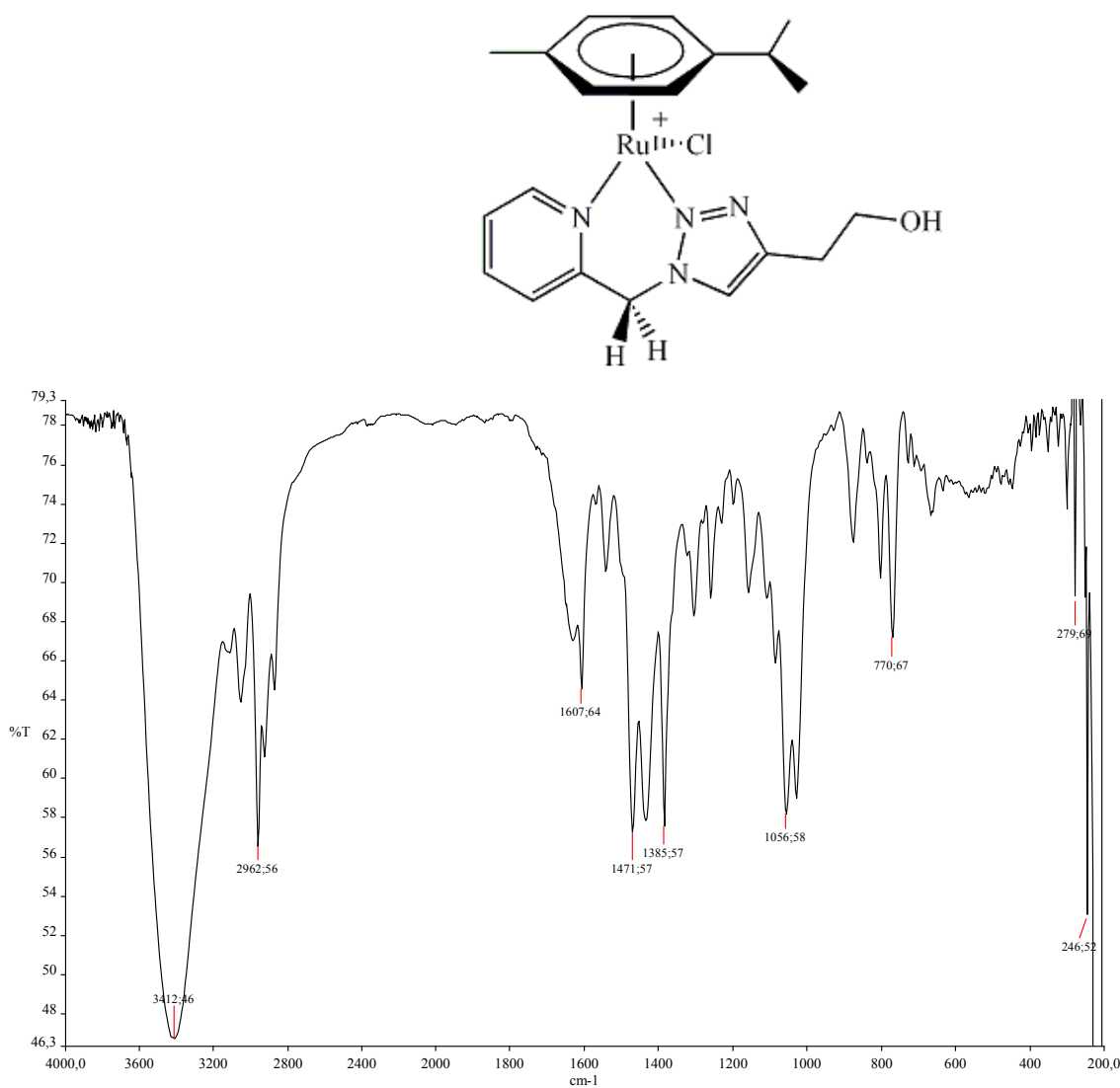
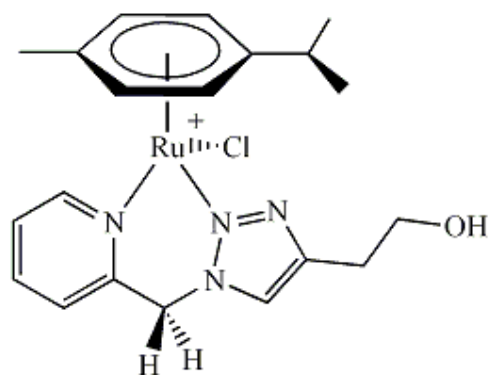


Figure 4.43 IR spectrum of $[\text{RuCl}(\eta^6\text{-}p\text{-cymene})(\text{ligand } \mathbf{2})]\text{Cl}$ in KBr.

IR (KBr pellet) ν_{max} : 3412(H_2O stretching), 2963($p\text{-cym}$, $-\text{C-H}$ stretching), 1608(Py C=N, stretching), 1472, 1386, 1057, 771, 280, 247 cm^{-1} .



[RuCl(Peymene)(2)] complex

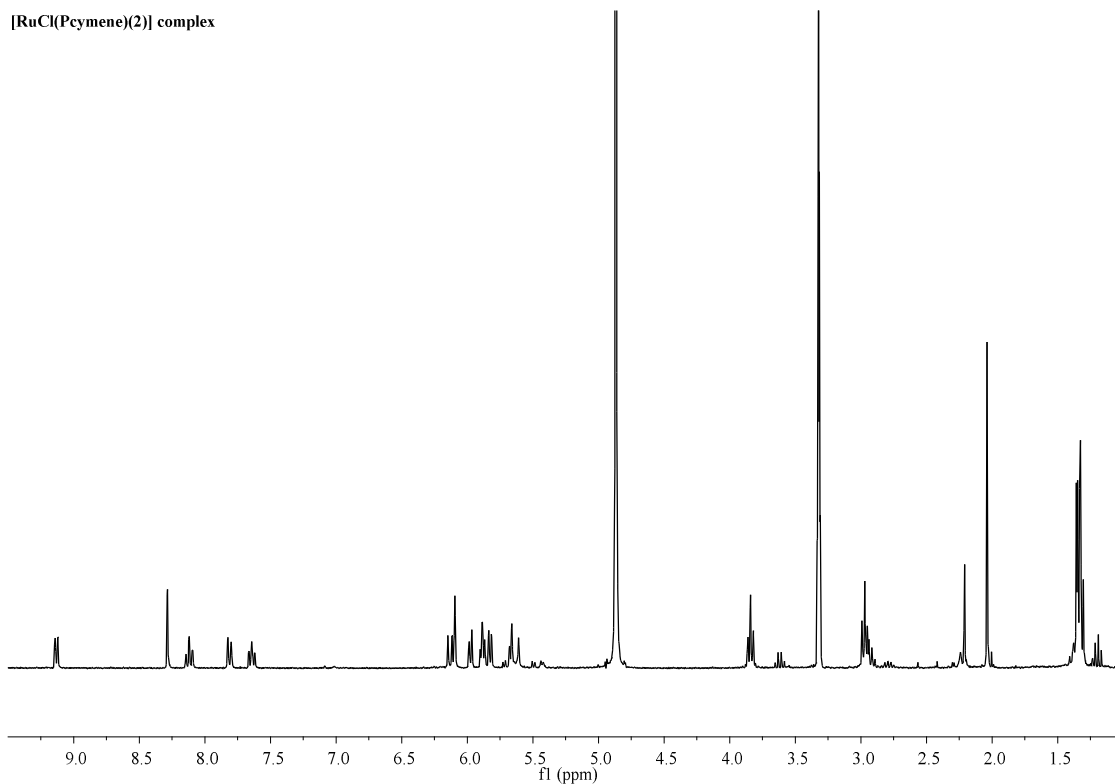


Figure 4.44 ^1H NMR spectrum of $[\text{RuCl}(\eta^6\text{-}p\text{-cymene})(\text{ligand } \mathbf{2})]\text{Cl}$ in CD_3OD .

^1H NMR (300 MHz, CD_3OD , 298 K): δ 9.12 (d, 1H, $J = 5.6$ Hz), 8.27 (s, 1H), 8.11 (td, $J = 7.8$, 1H, 1.25 Hz), 7.80 (d, 1H, $J = 7.7$ Hz), 7.63 (t, 1H, $J = 6.4$ Hz), 6.14-6.08 (m, CH^a/CH Ar, 2H), 5.96 (d, 1H Ar, $J = 5.9$ Hz), 5.87 (t, 1H Ar, $J = 5.8$ Hz), 5.81 (d, 1H Ar, $J = 5.9$ Hz), 5.66 (d, 1H^b , $J = 15.3$ Hz), 3.83 (t, 2H, $J = 6.2$ Hz), 2.98-2.88 (m, 3H), 2.03 (s, 3H), 1.35-1.30 (m, 6H) ppm.

[Ru(Pcymene)(2)Cl] complex

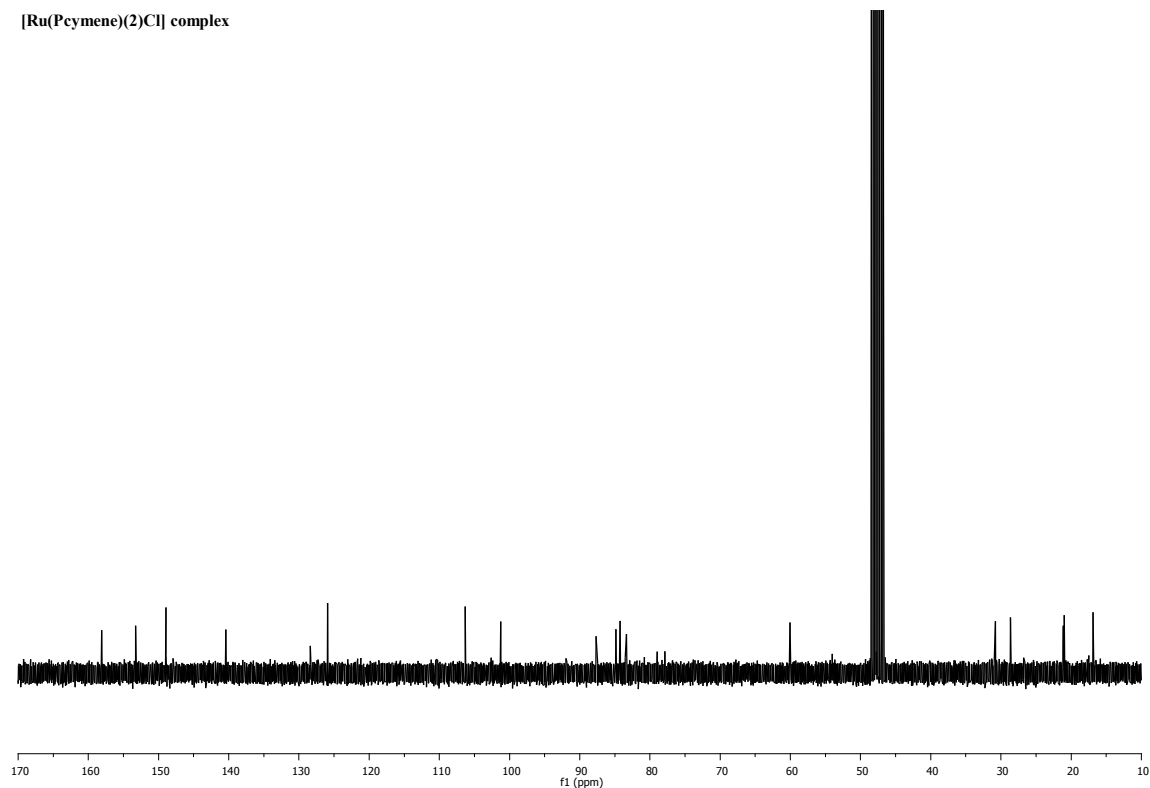
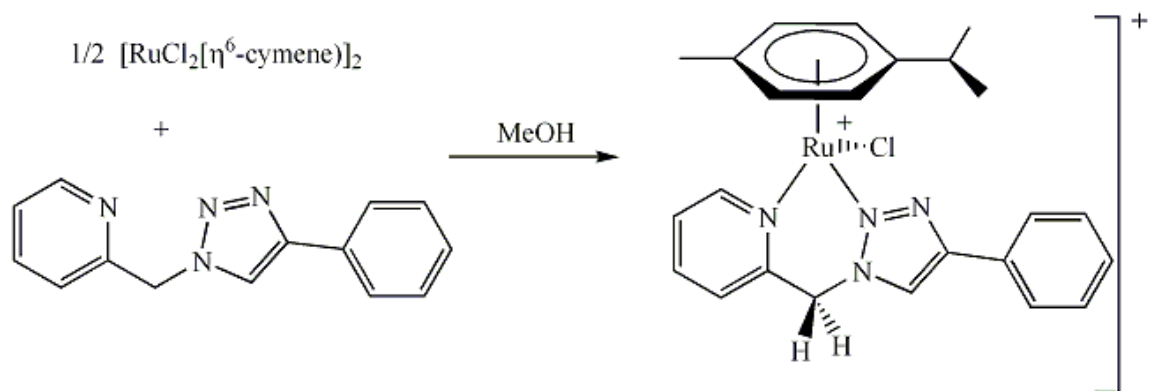


Figure 4.45 ^{13}C NMR spectrum of $[\text{RuCl}(\eta^6\text{-}p\text{-cymene})(\text{ligand } 2)]\text{Cl}$ in CD_3OD .

^{13}C NMR (300 MHz, CD_3OD , 298 K): δ 159.57, 154.69, 150.34, 141.82, 129.77, 127.27, 107.71, 102.69, 89.15, 86.25, 85.67, 84.78, 61.46, 32.23, 30.05, 22.56, 22.38, 18.32 ppm.

4.2.4.4 Synthesis of Complex 3, ($[\text{RuCl}(\eta^6\text{-}p\text{-cymene})(\text{ligand } 3)]\text{Cl}$) complex



The synthesis of $[\text{RuCl}(\eta^6\text{-}p\text{-cymene})(\text{ligand } \mathbf{3})]\text{Cl}$ complex was carried out according to the procedure reported by Uranker, D. *et al.* [45]. In a 50.0 mL two-neck round bottom flask, a mixture of ligand **3** (0.08 g, 0.34 mmol) and $[\text{RuCl}_2(\eta^6\text{-}p\text{-cymene})]_2$ (0.10 g, 0.17 mmol) was stirred in methanol (10.0 mL) at room temperature for 24 hours. The evaporation of solution by vacuum gave yellow crystalline solid. The product was extracted from EtOH (5.0 mL), and recrystallization from diethylether gave the title complex, $[\text{RuCl}(\eta^6\text{-}p\text{-cymene})(\text{ligand } \mathbf{3})]\text{Cl}$ as yellow crystalline powder which was characterized by IR (Figure 4.46), and ^1H NMR (Figure 4.47) spectroscopy.

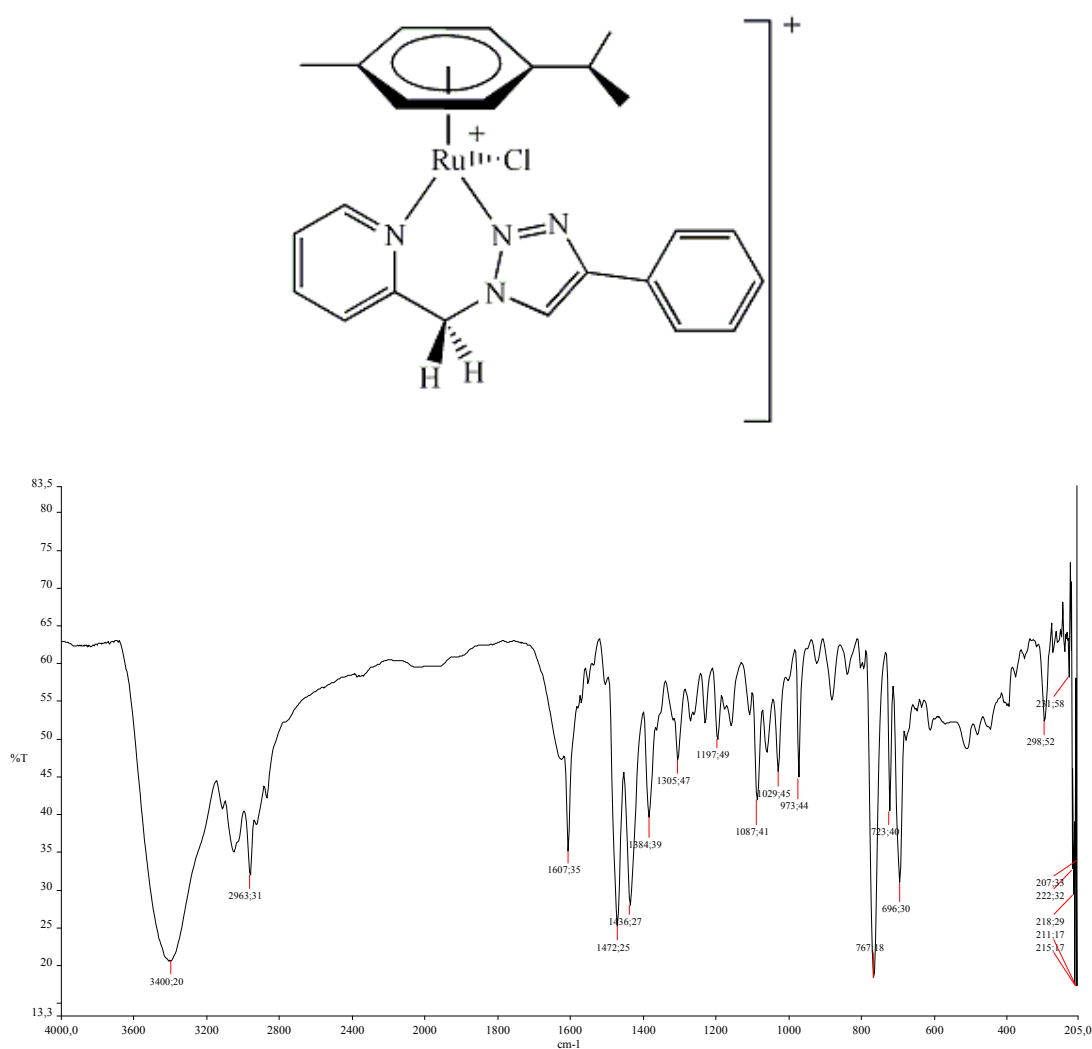


Figure 4.46 IR spectrum of $[\text{RuCl}(\eta^6\text{-}p\text{-cymene})(\text{ligand } \mathbf{3})]\text{Cl}$ complex in KBr.

IR (KBr pellet) ν_{\max} : 3400(H₂O stretching), 2963(p-cym, -C-H stretching), 1607 (Py C=N, stretching), 1472, 1434, 1384, 1305, 1087, 767, 696, 298 cm⁻¹.

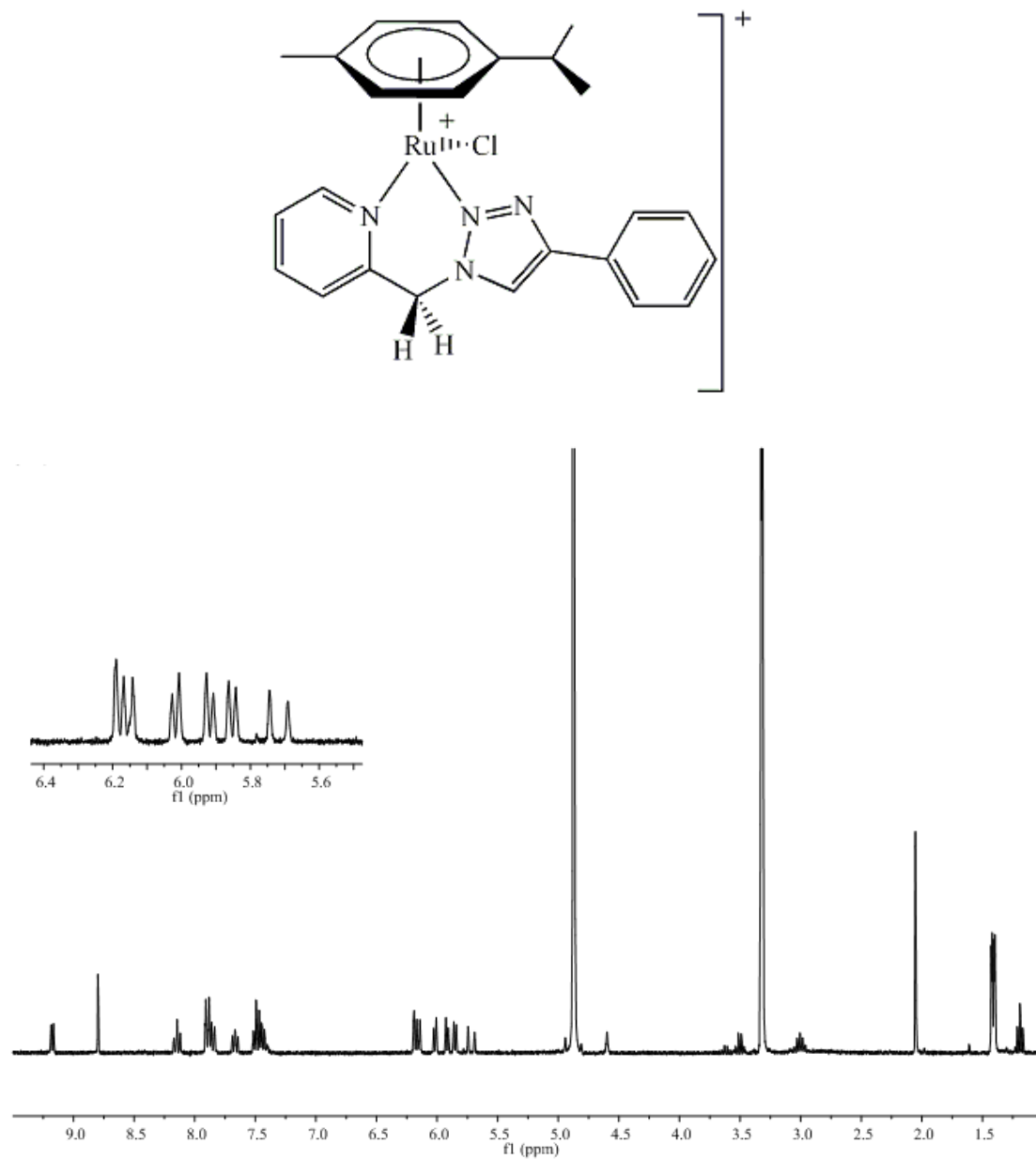
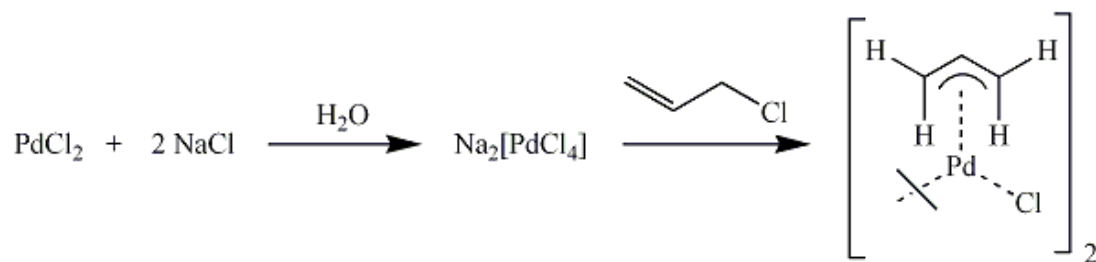


Figure 4.47 ¹H NMR spectrum of [RuCl(η⁶-p-cymene)(ligand 3)]Cl complex in CD₃OD.

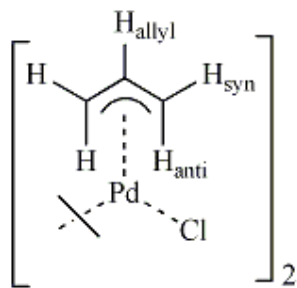
¹H NMR (300 MHz, CD₃OD, 298 K): δ 9.16 (d, 1H, *J* = 5.9 Hz), 8.79 (s, 1H), 8.13 (td, 1H, *J* = 7.8), 7.90 (t, 1H, *J* = 7.3 Hz), 7.88-7.82 (m, 2H), 7.66 (t, 1H, *J* = 7.4 Hz), 7.51-7.38 (m, 3H), 6.18-6.13 (m, 2H), 6.01 (d, 1H, *J* = 6.0 Hz), 5.91 (d, 1H, *J* = 6.1 Hz), 5.84 (d, 1H, *J* = 6.5 Hz), 5.70 (d, 1H, *J* = 15.8 Hz), 3.04-2.95 (m, 1H), 2.04 (s, 3H), 1.41 (dd, 6H, *J* = 6.9 Hz) ppm.

4.2.4.5 Synthesis of [Pd(η³-C₃H₅)Cl]₂ complex



The synthesis of precursor complex, [Pd(η³-C₃H₅)Cl]₂ was carried out according to the procedure reported by Hartley F.R., *et al.* [113].

In a one-neck 100.0 mL round bottom flask, NaCl (0.66 g, 22.3 mmol) and PdCl₂ (1.0 g, 5.61 mmol) are mixed in 20.0 mL H₂O. After overnight stirring, a brown suspension was obtained. 15.0 mL (184.3 mmol) of allyl chloride were added to the reaction vessel and kept the stirring overnight under inert atmosphere. The resulting yellow oil was extracted with (25×4) mL CH₂Cl₂, washed with 15.0 mL de-ionized water, and dried with appropriate amount of MgSO₄. After filtration and evaporation of all the CH₂Cl₂, the yellow solid was dissolved in CH₂Cl₂ and recrystallied from diethyl ether. Yield = 75%. The title product was characterized by ¹H NMR spectroscopy (Figure 4.48).



^1H NMR of Pd-allyl complex

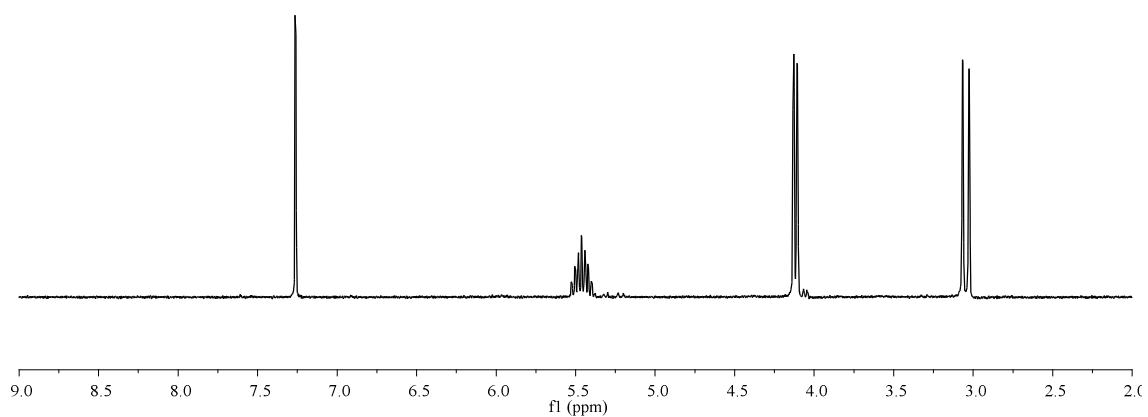
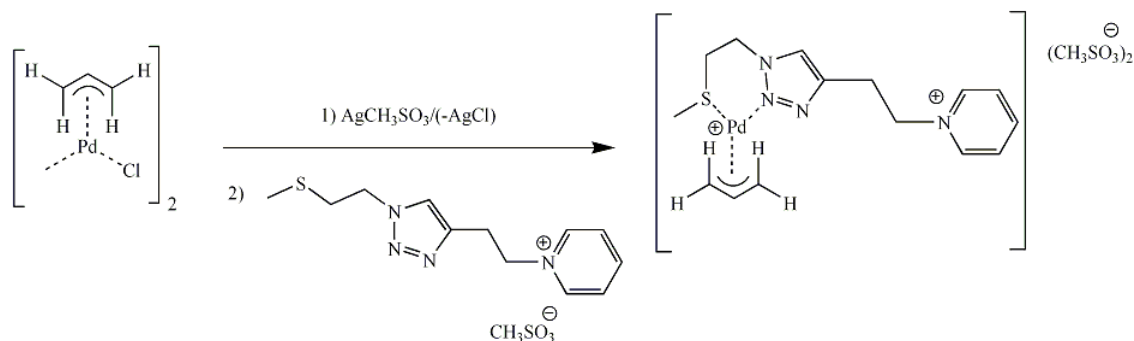


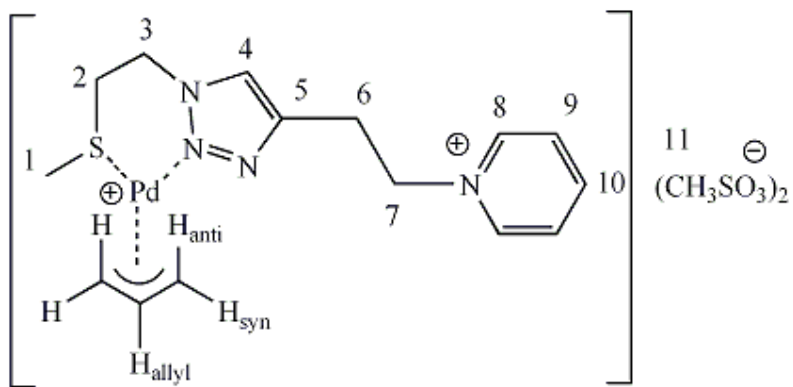
Figure 4.48 ^1H NMR spectrum of $[\text{Pd}(\eta^3\text{-C}_3\text{H}_5)\text{Cl}]_2$ complex in CDCl_3 .

^1H NMR (300 MHz, CDCl_3 , 298 K): δ 5.53-5.40 (m, 1H_{allyl}), 4.12 (d, 2H_{syn} , $J = 6.71$ Hz), 3.04 (d, 2H_{anti} , $J = 12.17$ Hz) ppm.

4.2.4.6 Synthesis of Complex 4, $[\text{Pd}(\eta^3\text{-C}_3\text{H}_5)(\text{ligand } \mathbf{8})](\text{CH}_3\text{SO}_3)_2$ complex)



The complex **4**, $[\text{Pd}(\eta^3\text{-C}_3\text{H}_5)(\text{ligand } \mathbf{8})\text{Cl}](\text{CH}_3\text{SO}_3)_2$ was prepared according to the procedure reported by Amadio E., *et al.* [62]. In a two-neck 100.0 mL round bottom flask, a methanol solution (10.0 mL) of AgCH_3SO_3 (0.18 g, 0.88 mmol) was added to a dichloromethane solution (20.0 mL) of $[\text{Pd}(\eta^3\text{-C}_3\text{H}_5)\text{Cl}]_2$ (0.16 g, 0.44 mmol) under stirring. The suspension was stirred for two hours at room temperature. The white precipitate of AgCl was filtered off through celite, and then to the filtrate a methanol solution (10.0 mL) of ligand **8** (0.30 g, 0.88 mmol) was dropwise added at 0 °C. The yellow solution is left under stirring at room temperature under inert atmosphere for 24 hours. At the end of the reaction, a light yellow solution was evaporated by vacuum. The solid obtained (77.3%) was recrystallized from dichloromethane/diethyl ether and characterized by ^1H NMR (Figure 4.49) and ^{13}C NMR (Figure 4.50) spectroscopy.



[Pd(C₃H₅)(ligand 8)](CH₃SO₃)₂ complex

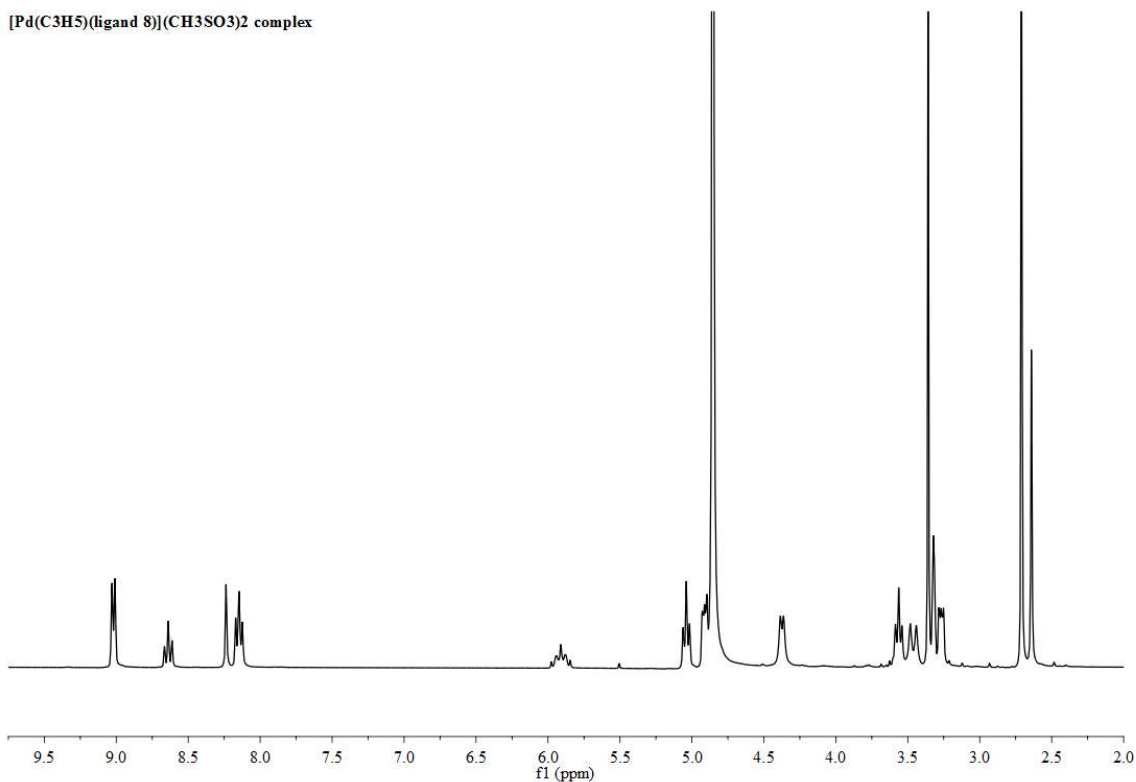


Figure 4.49 ¹H NMR spectrum of [Pd(η³-C₃H₅)(ligand 8)](CH₃SO₃)₂ complex in CD₃OD.

¹H NMR (300 MHz, CDCl₃, 298 K): δ 8.97 (d, 2H(8), *J* = 6.1 Hz), 8.59 (t, 1H(10), *J* = 7.7 Hz), 8.19 (s, 1H(4)), 8.10 (t, 2H(9) *J* = 6.9 Hz), 5.93-5.80 (m, 1H(H_{allyl})), 4.99 (t, 2H(7) *J* = 6.7 Hz), 4.89-4.86 (m, 2H (3)), 4.33 (d, 2H(H_{syn}) *J* = 6.7 Hz), 3.51 (t, 2H(6) *J* = 6.7 Hz), 3.41 (d, 3H(H_{anti}), *J* = 12.6 Hz), 3.24-3.20 (m, 2H(2)), 2.66 (s, 6H(11)), 2.59 (s, 3H (1) ppm).

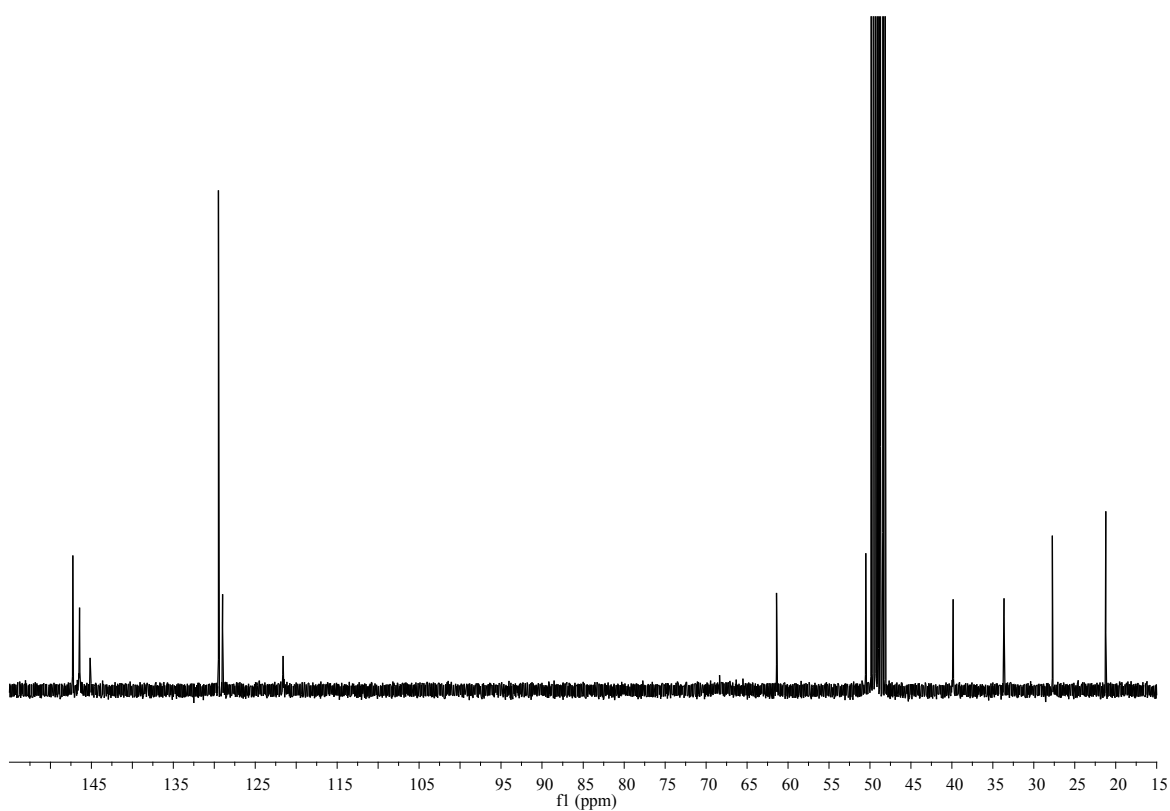
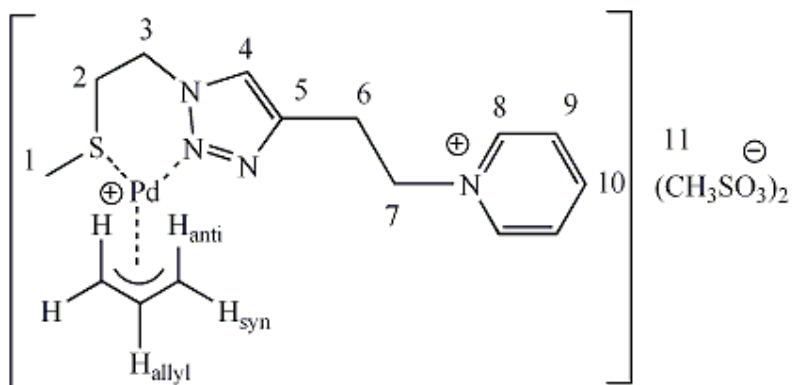


Figure 4.50 ^{13}C NMR spectrum of $[\text{Pd}(\eta^3\text{-C}_3\text{H}_5)(\text{ligand } \mathbf{8})](\text{CH}_3\text{SO}_3)_2$ complex in CD_3OD .

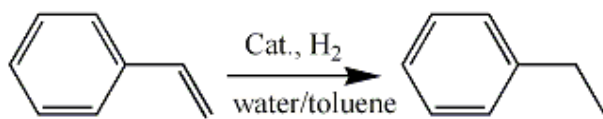
^{13}C NMR (300 MHz, CDCl_3 , 298 K): δ 147.28 (C10), 146.45(C8), 145.15 (C5), 129.48 (C9), 128.98 (C4), 121.56 (C_{anti}), 61.38 (C7), 50.51 (C3), 39.86 (C11), 33.65 (C2), 27.73 (C6), 21.21 (C1) ppm.

4.2.4.7 Synthesis of cobalt(II)-triazole complex

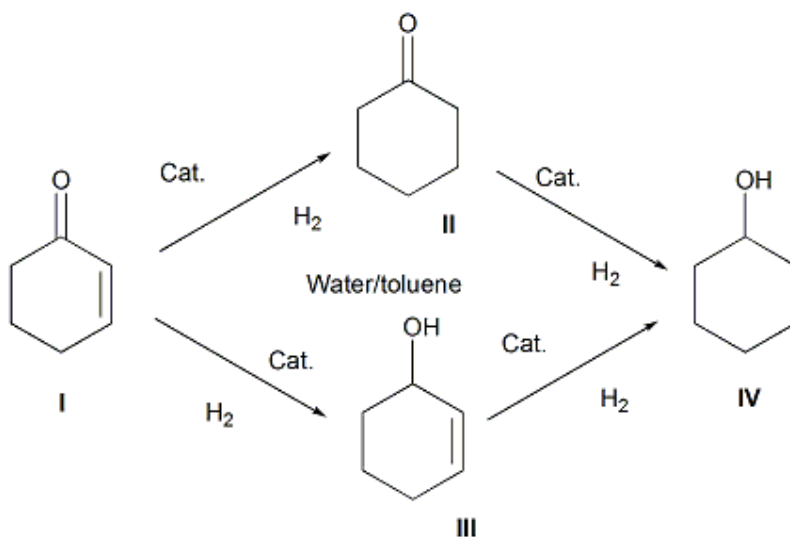
In a 25 mL one-neck round bottom flask, into a 3 mL of methanol solution of 133 mg (0.43 mmol) ligand **1**, 2 mL of methanol solution containing 79.4 mg (0.217 mmol) of Cobalt(II) perchlorate hexahydrate ($\text{Co}(\text{ClO}_4)_2 \cdot 6\text{H}_2\text{O}$) was slowly added without stirring. The reaction mixture kept for several days to form a very good crystals of title compound. The complex was characterized by IR and elemental analysis. IR (KBr): ν 3511, 3449, 3247, 3141, 1608, 1444, 1265, 1208, 1059, 1006, 895, 768, 588 cm^{-1} . Anal. Calcd for $\text{C}_{20}\text{H}_{34}\text{CoN}_8\text{O}_{14}\text{S}_2$: C, 32.74; H, 4.67; N, 15.27. Found: C, 32.86, H, 4.26; N, 15.18.

4.2.5 Biphasi hydrogenation of C=C and C=O double bonds

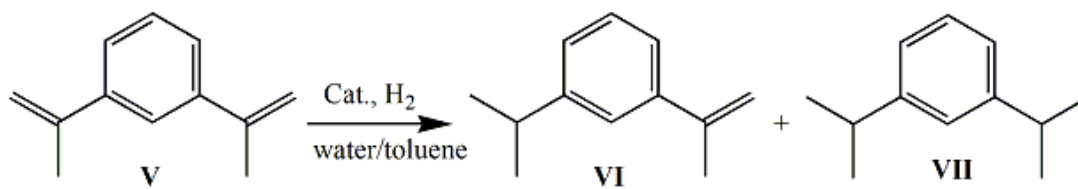
The catalysis of aqueous biphasic hydrogenation of C=C and C=O double bonds (scheme 13) were carried out according to the procedure reported by M. Marchetti *et al.* [84, 117]. The hydrogenation reactions have been carried out by using either ruthenium preformed catalyst, $[\text{RuCl}(\eta^6\text{-}p\text{-cymene})(\text{ligand } \mathbf{1})]$ or *in situ* prepared iridium (by mixing $[\text{Ir}(\eta^4\text{-COD})\text{Cl}]_2$ and ligand **1.Na** in water) catalyst.



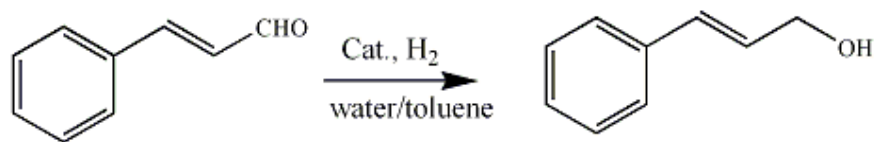
(a)



(b)



(c)



(d)

Scheme 4.13 Catalytic hydrogenation of (a) styrene, (b) 2-cyclohexen-1-one, (c) m-diisopropenylbenzene, and (d) cinnamaldehyde.

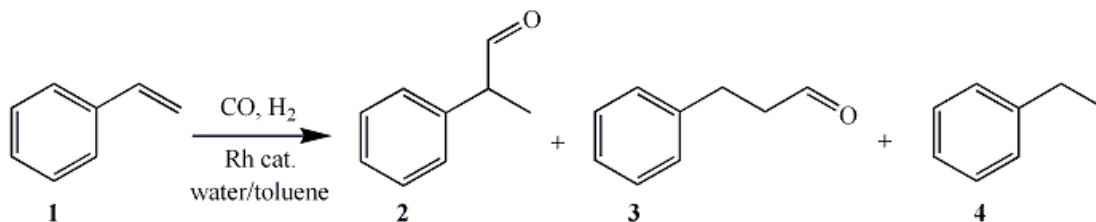
4.2.5.1 Biphasic hydrogenation experiments with preformed catalyst, [RuCl(η^6 -*p*-cymene)(ligand **1**)]

As an example the experimental details relevant to Entry 3 in Table 4.1 (see the results & discussion section 4.3.1.1) are reported. In a Schlenk tube, 0.004 g (0.0072 mmol) of [RuCl(η^6 -*p*-cymene)(ligand **1**)] was stirred under nitrogen in 2.0 mL of deaerated water until complete dissolution of complex. A 2.0 mL solution of styrene (0.50 g, 4.8 mmol) in toluene was then added to the aqueous phase. The Schlenk tube was then transferred into a 150 mL stainless steel auto clave under nitrogen, pressurized with 4.0 MPa (for styrene) or 2.0 MPa (for 2-cyclohexen-1-one) of H₂ and magnetically stirred for 6 or 24 hours at 80 °C respectively. The reactor then cooled to room temperature and the residual gases released. The organic phase was separated (extracted with Et₂O), dried on MgSO₄, and analyzed by GC (HP5 column 30 m × 0.32 mm × 0.25 μm). The catalytic aqueous phase was recycled for further experiments.

4.2.5.2 Biphasic hydrogenation experiments with *in situ* prepared iridium catalyst

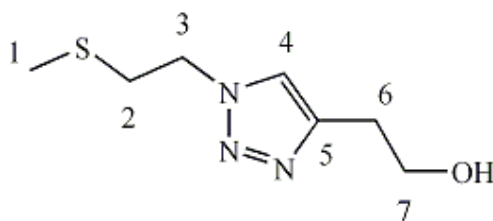
As an example the experimental details relevant to Entry 3 in Table 4.4 (see the results & discussion section) are reported. In a Schlenk tube, 3.2 mg (0.0048 mmol) of [Ir(η^4 -COD)Cl]₂ and 5.9 mg (0.019 mmol) of ligand **1** (5.9 mg for metal/ligand = 1/2) were stirred under nitrogen in 2.0 mL of deaerated water until complete dissolution of complex. A 2.0 mL solution of 461 mg (4.8 mmol) of 2-cyclohexen-1-one in toluene was then added to the aqueous phase. The Schlenk tube was then transferred into a 150 mL stainless steel auto clave under nitrogen, pressurized with 0.5 MPa. of H₂ and magnetically stirred for 1 hours at 60 °C. The reactor then cooled to room temperature and the residual gases released. The organic phase was separated (extracted with Et₂O), dried on MgSO₄, and analyzed (HP5 column 30 m × 0.32 mm × 0.25 μm). The catalytic aqueous phase was recycled for further experiments.

4.2.6 Biphasic hydrofomylation of styrene



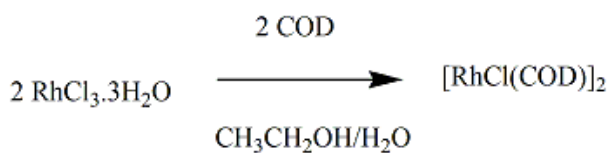
Scheme 4.14 Biphasic hydrofomylation of styrene.

In biphasic hydroformylation of styrene (Scheme 4.14), Rh(CO)₂(acac) and [RhCl(COD)]₂ were used as precursor. Both of them are commercially available but we prepared [RhCl(COD)]₂ in our laboratory. The *in situ* prepared rhodium catalyst (a clear solution of a mixture of [RhCl(COD)]₂ and ligand **4**) has been employed. The ligand used is a water-soluble methyl(thio)ethyl-triazole ligand. The structure of the ligand **4** is as follows



Ligand **4**

4.2.6.1 Preparation of [RhCl(COD)]₂ precursor complex



The precursor complex, [RhCl(COD)]₂ was prepared according to the procedure reported by Giordano G. *et al.* [118]. In a 100.0 mL two-neck round bottom flask, 2.00 g (7.6 mmol) of rhodium trichloride trihydrate were dissolved in 20.0 mL mixture (5:1) of ethanol-water. After addition of 3.0 mL of cyclooctadiene, the mixture was reflux for overnight, precipitates

a yellow-orange solid. The mixture was cooled and immediately filtered. The product was washed with pentane and then with methanol-water (1:5) until the washing no longer contained chloride ion. Yield 90%. The product was characterized by ^1H NMR (Figure 4.51) spectroscopy.

[RhCl(COD)]₂ complex

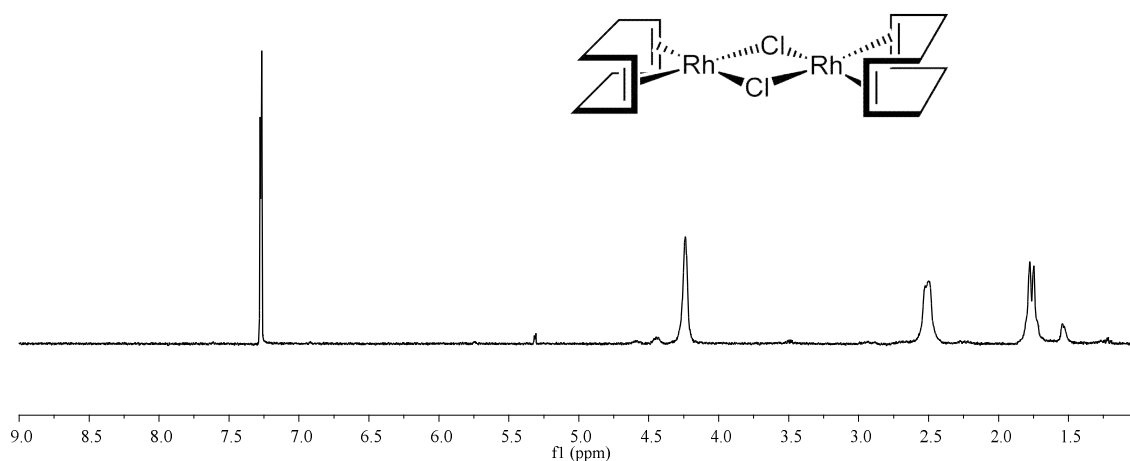


Figure 4.51 ^1H NMR spectrum of $[\text{RhCl}(1,5\text{-C}_8\text{H}_{12})]_2$ complex in CDCl_3 .

^1H NMR (300 MHz, CDCl_3 , 298 K): δ 4.24 (s, 1H), 4.12 (br,m, 2H), 1.75 (d, 2H, $J = 8.6$ Hz) ppm.

4.2.6.2 Hydroformylation experiments with *in situ* prepared rhodium-ligand **4** catalyst

The catalysis of aqueous biphasic hydroformylation was carried out according to the procedure reported by S. Paganelli *et al.* [85]. As an example the experimental details relevant to Entry 2 in Table 4.7 (see the results & discussion section 4.2.4.2) are reported. In a Schlenk tube, 2.4 mg (4.81×10^{-3} mmol) of $[\text{Rh}(\text{COD})\text{Cl}]_2$ and 7.2 mg (0.039 mmol) of ligand **4** (according to the table) were stirred under nitrogen in 2.0 mL of deaerated water

until complete dissolution of the complex (about 30 min). A solution of styrene (1.0 g, 9.62 mmol) in 2.0 mL of toluene was then added to the aqueous phase. The Schlenk tube was then transferred into a 150.0 mL stainless steel autoclave under nitrogen, pressurized with syngas (according to the table, CO/H₂ = 1) and magnetically stirred for 5 hours at 80 °C. The reactor was then cooled to room temperature and the residual gas vented off. The organic phase was separated (extracted with Et₂O), dried on MgSO₄ and analyzed by GC (HP5 column 30 m × 0.32 mm × 0.25 μm).

4.3 Conclusion

The new ligands, namely pyridyl-triazole (1-3) and methyl(thio)ethyl-triazole ligands (4-8) using CuAAC reaction were synthesized. They were employed as chelating ligands to prepare Ru(II), Pd(II), and Co(II) complexes. The pyridyl-triazole ligands reacts with [RuCl₂(p-cymene)]₂ giving complex 1-3. [Co(ligand **1**)₂(H₂O)].4H₂O complex was prepared by the reaction ligand **1.Na** with Co(ClO₄)₂.6H₂O. The synthesis of [Pd(η³-C₃H₅)(ligand **8**)Cl](CH₃SO₃)₂ was carried out by the reaction of ligand **8** with [Pd(η³-C₃H₅)Cl]₂. Ligands and metal complexes were characterized by analytical data, ESI-MS, ¹H and ¹³C NMR spectroscopy.

The catalytic activities of complex **1** and an iridium system containing water soluble pyridyl-triazolyl ligand (sodium 2-(1-((pyridin-2-yl)methyl)-1*H*-1,2,3-triazol-4-yl)ethyl sulfate) were studied in water/toluene biphasic catalytic hydrogenation of C=C and C=O double bonds. Both catalytic systems are highly active for the hydrogenation of styrene and 2-cyclohexene-1-one, moderately active for the hydrogenation of *m*-diisopropenylbenzene, and inactive for the hydrogenation of cinnamaldehyde. The water soluble 2-(1-(2-(methylthio)ethyl)-1*H*-1,2,3-triazol-4-yl)ethanol ligand in combination with [RhCl(COD)]₂ gives a system displaying good activity in olefin hydroformylation.

APPLICATION OF RUTHENIUM-PYRIDYL TRIAZOLE COMPLEXES AS ANTIMETASTATIC AND ANTICANCER AGENTS AGAINST HUMAN CANCER CELL

Since the discovery of cisplatin, thousands of other metal complexes have been synthesized and screened for antitumor activity. However, only other 2 complexes reached the clinical approval, namely oxaliplatin and carboplatin. Although these heavy metal agents are active against a variety

of cancers, their use is associated with severe side effects and is limited by primary and acquired resistance to this agent. This has led to an ongoing quest for the discovery of non-platinum metals that may extend the spectrum of activity of metal-based drugs. Among these, ruthenium (Ru) appears to be the most promising. Indeed, in recent years ruthenium-based molecules have emerged as promising antitumor and antimetastatic agents with potential uses in platinum-resistant tumors or as alternatives to platinum. Ruthenium compounds possess unique biochemical features thus allowing them to accumulate preferentially in neoplastic cells and to convert to their active state only after entering tumor cells. The first property seems to correlate with its ability to interact with transferrin. It has been proposed that transferrin–ruthenium complexes are actively transported into neoplastic tissues containing high transferrin receptor densities. The latter, conversely, depends on its ability to be selectively reduced where there is a lower oxygen content and higher acidity compared to normal tissues, such as in hypoxic tumors. Interestingly, many ruthenium agents show significant activity against cancer metastases but have minimal effects on primary tumors. This antimetastatic effect is likely mediated by inhibition of tumor cell detachment, invasion/migration, and re-adhesion to a new growth substrate. Chapter 5 outlined the anticancer and antimetastatic activity of ruthenium-triazole complexes against human cancer cell. The target cell lines are A375, A431, BxPC3, A549, HCT-15, and HEK-293.

5.1 Results and discussion

The in vitro antitumor activity of $[\text{RuCl}(\eta^6\text{-}p\text{-cymene})(\text{ligand } \mathbf{1})]$ (complex **1**) was evaluated versus several human cancer cell lines derived from solid tumors by the MTT test. The cytotoxicity parameters, in terms of IC_{50} (the median growth inhibitory concentration calculated from dose–survival curves) obtained after 72 h exposure, are listed in Table 5 1.

Table 5.1. Cytotoxic activity in terms of $IC_{50}(\mu M) \pm S. D$ of the tested compounds at 72 h on the human cancer cell lines A375, A431, BxPC3, A549 and HCT-15.

Compound	$IC_{50}(\mu M) \pm S. D.$				
	A375	A431	BxPC3	A549	HCT-15
Complex 1	32.98±4.22	113.42±6.11	49.43±3.13	126.76±5.99	35.65±2.38
Cisplatin	3.11±0.98	1.65±0.51	11.13±2.36	9.98±2.86	11.32±1.51

Table 5.2 Cytotoxic activity against human nontumor cell line (human embryonic kidney HEK293)

Compound	$IC_{50}(\mu M) \pm S. D. (HEK293)$	S. I.
Complex 1	456.22±3.23	6.1
Cisplatin	21.11±2.17	2.8

Conditions: Cells ($3-8 \times 10^4 \text{ mL}^{-1}$) were treated for 72 h with increasing concentrations of tested compounds dissolved in PEG400. Cytotoxicity was assessed by MTT test. IC_{50} values were calculated by 4-PL model ($P < 0.05$). SD = standard deviation. S.I. = average IC_{50} normal cells / average IC_{50} malignant cells

Cell lines representative of cervical (A431), pancreatic (BxPC3), lung (A549) and colon (HCT-15) cancers, along with melanoma (A375), have been included. For comparison purposes, cytotoxicity of cisplatin was assessed under the same experimental conditions. The tested complex showed a limited in vitro antitumor activity, with IC_{50} values up to one order of magnitude higher than those recorded with cisplatin. Cytotoxicity of the complex was also evaluated against a human nontumor cell line. As reported in Table 2, the IC_{50} value calculated for complex **1** against human embryonic kidney HEK293 cells (human noncancerous cells in rapid proliferation) was 200 times lower than that recorded after cisplatin treatment. Interestingly, the selectivity index value (SI = quotient of the average IC_{50} toward normal cells divided by the average IC_{50} for the malignant cells) of the complex was significantly higher (about 2 times) to that calculated with cisplatin.

Complex **1** was also tested against human colon cancer LoVo cells, endowed with a high metastatic potential. As depicted in Figure 5.1.

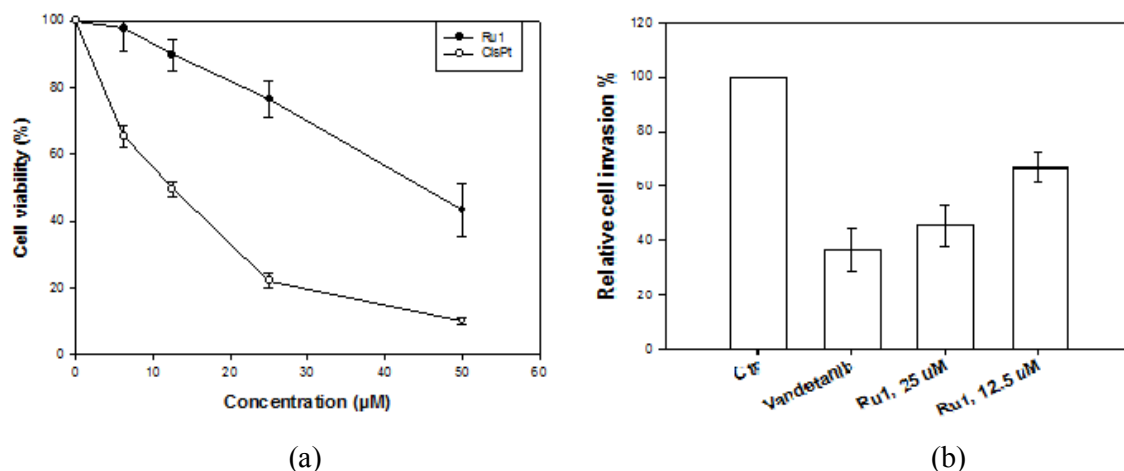


Figure 5.1. Cytotoxicity (a) and (b) antimetastatic potential against LoVo cells. Cells (5×10^4) were treated for 72 h with increasing concentrations of tested compounds. The cytotoxicity was assessed by MTT test. IC_{50} values were calculated by 4-PL ($P < 0.05$). Error bars represent standard deviation. Where, Ru1 = Complex **1**, CisPt = Cisplatin.

Complex **1** elicited a dose-dependent cytotoxicity that was, however, lower than that of cisplatin. Based on the dose-response curve, 25 and 12.5 μM were selected as non toxic doses to be employed to assess tumor cell invasion ability (Figure 5.1, b). Vandetanib, a well tyrosine kinase inhibitor endowed with a significant antimetastatic potential, has been used as positive control.

The invasion potential of LoVo treated and untreated cells was assayed through the matrigel-barrier in transwell inserts test. The addition of Complex **1** significantly reduced the invasion potential of LoVo cells in a dose dependent manner. Notably, at 25 μM Ru1 (complex **1**) determined a cell invasion inhibition that was rather similar to that obtained with Vandetanib (5 μM).

5.2 Experimental section

5.2.1 Material and Methods

5.2.1.1 Experiments with Cultured Human Cells

Complex **1** was dissolved in DMSO just before the experiment, and a calculated amount of drug solution was added to the cell growth medium to a final solvent concentration of 0.5%, which had no detectable effect on cell killing. Cisplatin was dissolved in 0.9% sodium chloride solution. MTT (3-(4,5-dimethylthiazol-2-yl)-2,5-diphenyltetrazolium bromide) and cisplatin were obtained from Sigma Chemical Co, St. Louis, USA.

5.2.1.2 Cell Cultures

Human lung (A549), pancreatic (BxPC3), and colon (HCT-15) carcinoma cell lines along with melanoma (A375) were obtained from American Type Culture Collection (ATCC, Rockville, MD). Human nontumor embryonic kidney HEK293 cells were obtained from European Collection of Cell Cultures (ECACC, Salisbury, UK). Human cervical carcinoma cells A431 were kindly provided by Prof. F. Zunino (Division of Experimental Oncology B, Istituto Nazionale dei Tumori, Milan, Italy). LoVo human colon-carcinoma cell line was kindly provided by Prof. F. Majone (Department of Biology of Padova University, Italy). Cell lines were maintained in the logarithmic phase at 37 °C in a 5% carbon dioxide atmosphere using the following culture media containing 10% fetal calf serum (Euroclone, Milan, Italy), antibiotics (50 units/mL penicillin and 50 µg/mL streptomycin), and 2 mM L-glutamine: (i) RPMI-1640 medium (Euroclone) for A431, HCT-15, and BxPC3 cells; (ii) F-12 HAM'S (Sigma Chemical Co.) for LoVo and A549 cells; and (iii) DMEM for A375 cells.

5.2.1.3 MTT Assay

The growth inhibitory effect toward tumor cells was evaluated by means of MTT assay.⁴⁹ Briefly, $(3-8) \times 10^3$ cells/well, dependent upon the growth characteristics of the cell line, were seeded in 96-well microplates in growth medium (100 µL). After 24 h, the medium was removed and replaced with fresh media containing the compound to be studied at the appropriate concentration. Triplicate cultures were established for each treatment. After 72 h,

each well was treated with 10 μ L of a 5 mg/mL MTT saline solution, and following 5 h of incubation, 100 μ L of a sodium dodecylsulfate (SDS) solution in HCl 0.01 M was added. After an overnight incubation, cell growth inhibition was detected by measuring the absorbance of each well at 570 nm using a Bio-Rad 680 microplate reader. Mean absorbance for each drug dose was expressed as a percentage of the control untreated well absorbance and plotted vs drug concentration. IC_{50} values, the drug concentrations that reduce the mean absorbance at 570 nm to 50% of those in the untreated control wells, were calculated by four parameter logistic (4-PL) model. Evaluation was based on means from at least four independent experiments (Figure 5.2).

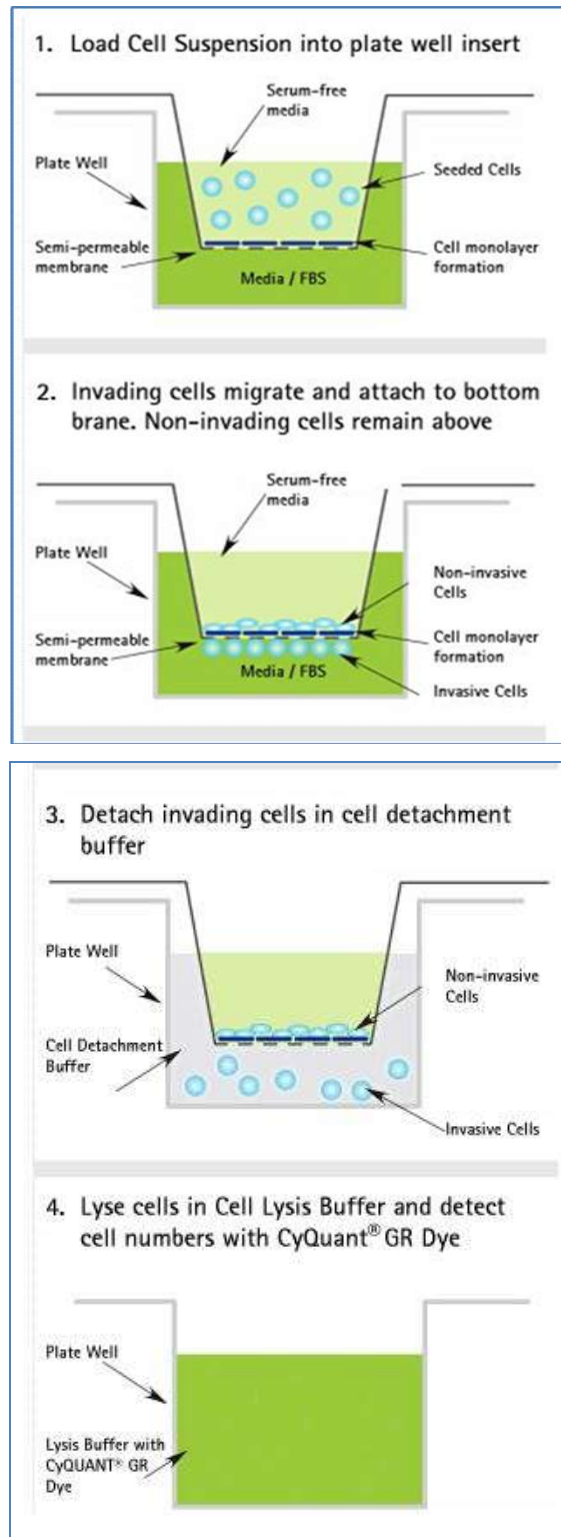


Figure 5.2 Four experiments (MTT assay methods).

5.2.1.4 Tumor cell invasion assays

Transwell inserts with 8- μ m pores (Corning) were coated with 100 μ l Matrigel (Becton Dickinson), which was diluted 1:4 in ice-cold F-12 HAM'S, and allowed to gel at 37°C. LoVo cells were starved in a medium without fetal bovine serum overnight, and then 1×10^5 cells resuspended in 100 μ L of serum-free medium, containing the compound to be tested at the appropriate concentration, were added to the upper chamber and cultured for 24 h. Removed the nonmigratory cells on the upper surface of the membrane, the cells were stained in 0.1% crystal violet and counted..

5.3 Conclusions

These preliminary data suggest for Complex **1** an antimetastatic potential. Further studies are ongoing in order to confirm and to deeply investigate its ability to interfere with metastatic and angiogenic processes.

ACKNOWLEDEMENTS

I sincerely thank my Ph.D. supervisor Dr. ssa Beghetto Valentina for her guidance, encouragement, and inspiration for chemistry throughout my Ph.D. career. I appreciate the freedom she gave me to pursue my research ideas and the direction she provided in achieving my research goals. I would also like to thank my co-supervisor Professor Alberto Scrivanti and Professor Stefano Paganelli for their time and valuable discussions.

I want to thank the past and present Matteoli's group members as well, for providing a pleasant and friendly working environment. In particular, I am very grateful to Dr. Matteo Bertoldini and Dr. Manuela Aversa for their generous help and suggestions. I am grateful to MIUR for financial support of my Ph.D. course.

Finally and most importantly, this dissertation is dedicated to my parents for their endless love and support.

Md. Mahbulul Alam

References

- (1) J. Hagen, *Industrial Catalysis: a practical approach*, 2nd edition Wiley VCH, Weinheim, **2006**.
- (2) Z. Z. Zhou, F. S. Liu, D. S. Shen, C. Tan, L. Y. Luo, *Inorganic Chemistry Communications*, **2011**, 14, 659-662.
- (3) A. Scrivanti, M. Bertoldini, U. Matteoli, V. Beghetto, S. Antonaroli, A. Marini, B. Crociani, *Journal of Molecular Catalysis A: Chemical*, **2005**, 235, 12-16.
- (4) P. Pollak, *Fine Chemicals: The Industry and the business*, John Wiley & Sons, Ltd., **2007**.
- (5) A. Sheldon, H. Van Bekkum (Eds.), *Fine chemicals through Heterogeneous catalysis*, Wiley-VCH, Weinheim, **2001**.
- (6) P. T. Anastas, J. C. Warnar (Eds), *Green Chemistry: Theory and Practice*, Oxford University Press, New York, **1998**.
- (7) S. B. Soloway, *Environmental Health Perspectives*, **1976**, 14, 109-117.
- (8) S. Li, S. F. Zhu, J. H. Xie, S. Song, C. M. Zhang, and Q. L. Zhou, *J. Am. Chem. Soc.*, **2010**, 132, 1172-1179.
- (9) N. Kurihara, J. Miyamoto, G. D. Paulson, B. Zeeh, M. W. Skidmores, R. M. Hollingworth, and H. A. Kuiper, *Pure & Appl. Chem.*, **1997**, 69, 1335-1348.
- (10) J. A. Turner and D. J. Pernich, *J. Agric. Food Chem.*, **2002**, 50, 4554-4566.
- (11) W. Liu and M. Tang, *Herbicides -Mechanisms and Mode of Action* , **2011**, 4, 65-80.
- (12) C. J. Sih, Q. M. Gu, X. Holdgrun and K. Harris, *Chirality*, **1992**, 4, 91-97.
- (13) S. Fukui, T. Kawamoto, K. Sonomoto and A. Tanaka, *Appl. Microbiol. Biotechnol.*, **1990** 34, 330-334.
- (14) G. M. Gauchi, R. Teissier, *US 20060014976A1*, **2006**.
- (15) A. Grala, J. Ejfler, L. B. S. P. Jerzykiewicz, *Dalton Trans.* **2011**, 40, 4042-4044.
- (16) (a) R. Noyori, M. Kitamura In *Modern Synthetic Methods*, R. Scheffold Ed.; *Springer: Berlin*, **1989**, 5, 115-198. (b) H. Takaya, T. Ohta, R. Noyori In *Catalytic Asymmetric Synthesis*, I. Ojima, Ed., *VCH: New York*, **1993**, 1.
- (17) W. S. Knowles, Asymmetric hydrogenations, *Angew. Chem. Int. Ed.*, **2002**, 41, 1998-2007.
- (18) R. Noyori, Asymmetric Catalysis: Science and Opportunities, *Angew. Chem. Int. Ed.*, **2002**, 41, 2008-2022.
- (19) S. F. Zhu, Y. B. Yu, S. Li, L. X. Wang, and Q. L. Zhou, *Angew. Chem. Int. Ed.*, **2012**, 51, 8872-8875.

- (20) P. E. Maligres, S. W. Krska, and G. R. Humphrey, *Organic Letters*, **2004**, 6, 3147-3150.
- (21) (a) S. Jayasree, A. Seayad, S.P. Gupte, and R.V. Chaudhari, *Catalysis Letters*, **1999**, 58, 213–216, (b) O. N. Temkin and L. G. Bruk, *Kinetics and Catalysis*, **2003**, 44, 601–617.
- (22) E. Drent, P. Arnoldy and P. H. M. Budzelaar, *Journal of Organometallic Chemistry*, **1993**, 455, 247-253.
- (23) (a) T. H. Chan, P. W. K. Lau, and W. Mychajlowskij, *Tetrahedron Letters*, **1977**, 38, 3317-3320, (b) R. B. Miller, and T. Reichenbach, *Tetrahedron Letters*, **1974**, 6, 543-546.
- (24) V. Rosanti, A. Saba, and A. Salimbeni, *Tetrahedron Letters*, **1981**, 22, 167-168.
- (25) A. Scrivanti, U. Matteoli, *Tetrahedron Letters*, **1995**, 36, 9015-9018
- (26) U. Matteoli, V. Beghetto, A. Srivinti, M. Aversa, M. Bertoldini, AND S. Bovo, *CHIRALITY*, **2011**, 23, 779–783.
- (27) A. Scrivanti, V. Beghetto, E. Campagna, M. Zanato, and U. Matteoli, *Organometallics*, **1998**, 17, 630-635.
- (28) L. Crawford, D. J. C. Hamilton, and M. Buhl, *Organometallics*, **2015**, 34, 438-449.
- (29) S. Haider, M. S. Alam, H. Hamid, *Inflammation & Cell Signalling*, **2014**, 1:e95.
- (30) M J Soltis, K. A. Cole, N. Whittaker, R. P. Wersto, and E. C. Kohn, *Drug Metab Dispos* **1996**, 24, 799-806.
- (31) C. Sheng and W. Zhang, *Current Medicinal Chemistry*, **2011**, 18, 733-766.
- (32) R. Kumar, M. S. Yar, S. Chaturvedi, A. Srivastava, *International Journal of PharmTech Research*, **2013**, 5, 1844-1869.
- (33) S. Haider, M. S. Alam, H. Hamid, S. Shafi, A. Nargotra, P. Mahajan, S. Nazreen, A. M. Kalle, C. Kharbanda, Y. Ali, A. Alam, A. K. Panda, *European Journal of Medicinal Chemistry*, **2013**, 70, 579-588.
- (34) S. Shafi, M. M. Alam, N. Mulakayala, C. Mulakayala, G. Vanaja, A. M. Kalle, R. Pallu, M. S. Alam, *European Journal of Medicinal Chemistry*, **2012**, 49, 324-333.
- (35) V. V. Rostovtsev, L. G. Green, V. V. Fokin, K. B. Sharpless, *Angew. Chem. Int. Ed.*, **2002**, 41, 2596-2599.
- (36) F. Himo, T. Lovell, R. Hilgraf, V. V. Rostovtsev, L. Noodleman, K. B. Sharpless, V. V. Fokin, *J. Am. Chem. Soc.*, **2005**, 127, 210-216.
- (37) B. C. Boren, S. Narayan, L. K. Rasmussen, L. Zhang, H. Zhao, Z. Lin, G. Jia, V. V. Fokin, *J. Am. Chem. Soc.*, **2008**, 130, 8923-8930.
- (38) R. Huisgen, R. Grashey, J. Sauer, Chemistry of Alkenes, *Interscience*, New York, **1964**, 806-877.
- (39) C. D. Hein, X. M. Liu, and D. Wang, *Pharm Res*. **2008**, 25, 2216-2230.

- (40) (a) V.D. Bock, H. Hiemstra, J.H. van Maarseveen, *Eur. J. Org. Chem.*, **2006**, 51-68, (b) M. Meldal, C.W. Tornøe, *Chem. Rev.*, **2008**, 108, 2952-3015.
- (41) W.S. Brotherton, H. A. Michaels, J. T. Simmons, L. Zhu, *Organic Letters*, **2009**, 11, 4954-4957.
- (42) Y. Jiang, C. Kuang, Q. Yang, *SYNLETT*, **2009**, 19, 3163-3166.
- (43) J. Barluenga, C. Valdés, G. Beltrán, M. Escribano, F. Aznar, *Angew. Chem. Int. Ed.*, **2006**, 45, 6893-6896.
- (44) 217th American Chemical Society Annual Meeting, **1999**.
- (45) D. Urankar, B. Pinter, A. Pevec, F. D. Proft, I. Turel, and J. Kosmrlj, *Inorg. Chem.* **2010**, 49, 4820-4829.
- (46) E. Amadio, A. Scrivanti, G. Chessa, U. Matteoli, V. Beghetto, M. Bertoldini, M. Rancan, A. Dolmella, A. Venzo, R. Bertani, *Journal of Organometallic Chemistry*, **2012**, 716, 193-200.
- (47) C.W. Tornøe, C. Christensen, M. Meldal, *J. Org. Chem.*, **2002**, 67, 3057-3064.
- (48) H. Struthers, T.L. Mindt, R. Schibli, *Dalton Trans.*, **2010**, 39, 675-696.
- (49) I. Bratsos, D. Urankar, E. Zangrando, P. G. Kalou, J. Kosmrlj, E. Alessio, and I. Turel, *Dalton Trans.*, **2011**, 40, 5188-5199.
- (50) R. J. Detz, S. A. Heras, R. de Gelder, P. W. N. M. van Leeuwen, H. Hiemstra, J. N. H. Reek, and J. H. van Maarseveen, *Organic Letters*, **2006**, 8, 3227-3230.
- (51) J. Hassan, M. Sévignon, C. Gozzi, E. Schulz, M. Lemaire, *Acc. Chem. Res.*, **2007**, 40, 676-684.
- (52) R. Martin, S.L. Buchwald, *Acc. Chem. Res.*, **2008**, 41, 1461-1473.
- (53) G.A. Molander, B. Canturk, *Angew. Chem. Int. Ed.*, **2009**, 48, 9240-9261.
- (54) F. Hanasaka,† K. Fujita, and R. Yamaguchi, *Organometallics*, **2004**, 23, 1490-1492.
- (55) M. J. Schultz, S. S. Hamilton, D. R. Jensen, and M. S. Sigman, *J. Org. Chem.*, **2005**, 70, 3343-3352.
- (56) K. Muniz, *Adv. Synth. Catal.*, **2004**, 346, 1425-1428.
- (57) M. Poyatos, J. A. Mata, E. Falomir, R. H. Crabtree, and E. Peris, *Organometallics*, **2003**, 22, 1110-1114.
- (58) M. Muehlhofer, T. Strassner, and W. A. Herrmann, *Angew. Chem. Int. Ed.*, **2002**, 41, 1745-1747.
- (59) W. A. Herrmann, M. Elison, J. Fischer, C. Kocher, and G. R. J. Artus, *Angw. Chem. Int. Ed.*, **1995**, 34, 2371-2374.
- (60) H. M. Lee and S. P. Nolan, *Organic Letters*, **2000**, 2, 2053-2055.

- (61) Y. Sato, T. Yoshino, and M. Mori, *Organic Letters*, **2003**, 5, 31-33.
- (62) E. Amadio, M. Bertoldini, A. Scrivanti, G. Chessa, V. Beghetto, U. Matteoli, R. Bertani, A. Dolmella, *Inorganica Chimica Acta*, **2011**, 370, 388-393.
- (63) E. Amadio, A. Scrivanti, V. Beghetto, M. Bertoldini, Md. M. Alam and U. Matteoli, *RSC Advances*, **2013**, 3, 21636-21640.
- (64) Shriver and Atkins' *Inorganic Chemistry*, W.H. Freeman & Co., 5th Ed., **2010**.
- (65) R. H Crabtree, *Acc. Chem. Res*, **1979**, 12, 331-337.
- (66) B. R. James, *Homogeneous Hydrogenation*, John Wiley & Sons, New York, **1973**.
- (67) R. Noyori, T. Ohkuma, M. Kitamura, H. Takaya, N. Sayo, H. Kumobayashi, S. Akutagawa, *J. Am. Chem. Soc.*, **1987**, 109, 5856-5858.
- (68) B. Štefane and F. Požgan, Asymmetric Hydrogenation and Transfer Hydrogenation of Ketones, *Hydrogenation*, **2012**, 2.
- (69) B. Cornils, W. A. Herrmann, I. T. Horvath, W. Leitner, S. Mecking, H. Olivier-Bourbigou, Vogt (Eds.) *D. Multiphase Homogeneous Catalysis*, Wiley-VCH, Weinheim, **2005**.
- (70) F. Joo, *Aqueous Organometallic Catalysis*, Kluwer Acad. Publ. Dordrecht, **2001**.
- (71) B. Cornils, E.G. Kuntz, *Journal of Organometallic Chemistry*, **1995**, 502, 177-186.
- (72) D. J. Cole-Hamilton, R. P. Tooze, *Catalyst Separation, Recovery and Recycling*, Springer, Dordrecht, **2006**.
- (73) P. H. Dixneuf, V. Cadierno, *Metal-Catalyzed Reactions in Water*, Wiley-VCH, Weinheim, **2013**.
- (74) S. D. Dio, M. Marchetti, S. Paganelli, O. Piccolo, *Applied Catalysis A: General*, **2011**, 399, 205-210.
- (75) A. Fukuoka, W. Kosugi, F. Morishita, M. Hirano, L. McCaffrey, W. Henderson and S. Komiya, *Chem. Commun.*, **1999**, 489-490.
- (76) M. T. Musser, "Cyclohexanol and Cyclohexanone" in *Ullmann's Encyclopedia of Industrial Chemistry*, Wiley-VCH, Weinheim, **2005**.
- (77) I. Ojima, C. Y. Tsai, M. Tzamarioudaki, D. Bonafoux, *Org. React.* **2000**, 56, 1.
- (78) O. Roelen, *German patent* DE 849548, 1938/1952.
- (79) O. Roelen, *Chem. Abstr.*, **1944**, 38, 3631.
- (80) D. S. Breslow and R. F. Heck, *Chem. Ind. (London)*, **1960**, 467.
- (81) R. F. Heck and D. S. Breslow, *J. Am. Chem. Soc.*, **1961**, 83, 4023-4027.
- (82) D. Evans, J. A. Osborn, G. Wilkinson, *J. Chem. Soc.*, **1968**, 3133-3142.

- (83) J. A. Osborn, F. H. Jardine, J. F. Young, G. Wilkinson, *J. Chem. Soc. A*, **1966**, 1711-1732.
- (84) M. Marchetti, G. Mangano, S. Paganelli and C. Botteghi, *Tetrahedron Letters*, **2000** 41, 3717-3720.
- (85) S. Paganelli, M. Marchetti, M. Bianchin, C. Bertucci, *Journal of Molecular Catalysis A: Chemical*, **2007**, 269, 234-239.
- (86) L. G. Melean, M. Rodriguez, M. Romero, M. L. Alvarado, M. Rosales, P. J. Baricelli, *Applied Catalysis A: General*, **2011** 394, 117-123.
- (87) S. Paganelli, A. Ciappa, M. Marchetti, A. Scrivanti, U. Matteoli, *Journal of Molecular Catalysis A: Chemical*, **2006**, 247, 138-144.
- (88) T. Borrmann, H. W. Roesky, U. Ritter, *Journal of Molecular Catalysis A: Chemical*, **2000**, 153, 31-48.
- (89) S. Paganelli, O. Piccolo, P. Pontini, R. Tassini, V. D. Rathod, *Catalysis Today*, **2015**, 247, 64-69.
- (90) S. Paganelli, Md. M. Alam, V. Beghetto, A. Scrivanti, E. Amaio, M. Bertoldini and U. Matteoli, *Applied Catalysis A: General* (In press)
- (91) B. S. Howerton, D. K. Heidary, and E. C. Glazer, *J. Am. Chem. Soc.*, **2012**, 134, 8324-8327.
- (92) A. Levina, A. Mitra and P. A. Lay, *Metallomics*, **2009**, 1, 458-470.
- (93) Y. K. Yan, M. Melchart, A. Habtemariam and P. J. Sadler, *Chem. Commun.*, **2005**, 4764-4776.
- (94) E. Drent, P. Arnoldy and P.H.M. Budzelaar, *Journal of Organometallic Chemistry*, **1994**, 475, 57-63.
- (95) L. Piovesan, *Master's Thesis of Industrial Chemistry*, Ca' Foscari University of Venice, **1996-97**.
- (96) D. Zargarian, H. Alper, *Organometallics*, **1993**, 12, 712-724.
- (97) J. Tsuji, *Acc. Chem. Res.*, **1969**, 2, 144-152.
- (98) V. V. Grushin, *Chem. Rev.*, **1996**, 96, 2011-2034.
- (99) A. Scrivanti, B. Valentina, E. Campagna, U. Matteoli, *Journal of Molecular Catalysis A: Chemical*, **2001**, 168, 75-80.
- (100) European Patent 0441447A1.
- (101) K. E. Koenig, P. Weber, *Tetrahedron Letters*, **1973**, 27, 2533-2536.
- (102) A. G. Brook, J. M. Duff, *Journal of Organometallic Chemistry*, **1976**, 121, 293-306.

- (103) W. L. F. Armarego, D. D. Perrin, *Purification of Laboratory Chemicals*, 3rd ed., Pergamon Press, **1988**.
- (104) P. L. Golas, N. V. Tsarevsky, *Macromol. Rapid Commun.*, **2008**, 29, 1167-1171.
- (105) A. S. Herves, E. F. Megia and R. Riguera *Chem. Commun.*, **2008**, 3136-3138.
- (106) V. C. Sekera and C. S. Marvel, *J. Am. Chem. Soc.* **1933**, 55, 345-349.
- (107) J. Ferns and A. Lapworth, *J. Chem. Soc., Trans.*, **1912**, 101, 273-287.
- (108) B. C. Norris, W. Li, E. Lee, A. Manthiram, C. W. Bielawski, *Polymer*, **2010**, 51, 5352-5358.
- (109) G. Eglinton and M. C. Whiting, *J. Chem. Soc.*, **1950**, 3650-3656.
- (110) M. A. Bennett, K. Smith, *Dalton Trans.*, **1974**, 233-241.
- (111) R. R. Schrock, J. A. Osborn, *Inorg. Chem.*, **1970**, 9, 2339-2343.
- (112) H. J. Nolte, G. Gafner, L. M. Haines, *J. Chem. Soc.: Chem. Commun.* **1969**, 1406.
- (113) F. R. Hartley, S. R. Jones, *Journal of Organometallic Chemistry*, **1974**, 66, 465-473.
- (114) P.G.J. Koopma, *Ruthenium Hydrogenation Catalyst: Activation, Characterization and Application*.
- (115) G. H. Hou, J. H. Xie, P. C. Yan, Q. L. Zhou, *J. Am. Chem. Soc.*, **2009**, 131, 1366-1367.
- (116) G. Hou, R. Tao, Y. Sun, X. Zhang, F. Gosselin, *J. Am. Chem. Soc.* **2010**, 132, 2124-2125.
- (117) M. Marchetti, F. Minello, S. Paganelli, O. Piccolo, *Applied Catalysis A: General*, **2010**, 373, 76-80.
- (118) G. Giordano and R. H. Crabtree, *Inorganic Synthesis*, **1990**, 28, 88-90.
- (119) R. Romagnoli, P. G. Baraldi, M. K. Salvador, M. E. Camacho, J. Balzarini, J. Bermejo, F. Estévez, *European Journal of Medicinal Chemistry*, **2013**, 63, 544-57.
- (120) B.S. Sekhon, *Journal of Pesticide Science*, **2009**, 34, 1-12.
- (121) R. Amoroso, G. Bettoni, M. L. Tricca, F. Loiodice, S. Ferorelli, *Il Farmaco* **1998**, 53, 73-79.
- (122) D. R. Feller, V. S. Kamanna, H. A. I. Newman, K. J Romstedt, D. T Witiak, G. Bettoni, S. H. Bryant, D. Conte- Camerino, F. Loiodice, V. Tortorella, *J. Med. Chem.* **1987**, 30, 1265-1270.

ABSTRACT OF THE THESIS

SYNTHESIS AND CHARACTERIZATION OF NOVEL LIGANDS AND APPLICATION OF THEIR TRANSITION METAL COMPLEXES AS CATALYSTS OR ANTICANCER AGENTS

By

MD. MAHBUBUL ALAM

Supervisor: Dr. ssa Valentina Beghetto

Co-supervisor: Professor Alberto Scrivanti

In this Thesis work, we report an innovative approach for the synthesis of 2-bromoacrylic acid and its ester derivatives that are the key intermediates in the synthesis of chiral aryloxypropionic acid an important class of herbicides. The synthesis of the bromo substituted acrylics was carried out *via* carbonylation of (trimethylsilyl)acetylene using as catalytic system $\text{Pd}(\text{OCOCH}_3)_2$ in combination with $\text{CH}_3\text{SO}_3\text{H}$ and 2-(6-methyl)(diphenylphosphine)pyridine. When the reaction is carried out in methanol, methyl 2-(trimethylsilyl)acrylate was obtained in good yields with a branched/linear ratio 95/5. On the other hand, hydroxycarbonylation reactions give 2-(trimethylsilyl)acrylic acid with lower conversions and selectivities (ca. 53%, and 93/7 respectively). The effects of phosphine/palladium, acid/palladium, reaction time, temperature, and CO pressure on the substrate conversion and selectivity towards branched isomer have been investigated. The bromodesilylation of methyl 2-(trimethylsilyl)acrylate in the presence of an excess of base gives 2-bromoacrylic acid in good yield (ca. 90%). The intermediate product methyl 2,3-dibromo-2-(trimethylsilyl)propanoate is easily prepared by reaction of methyl 2-(trimethylsilyl)acrylate with bromine in dry dichloromethane.

A series of triazole ligands were synthesized by the CuAAC reaction. They were employed as chelating ligands to prepare Ru(II), Pd(II), and Co(II) complexes. Ligands and metal complexes have been characterized by analytical data, ESI-MS and ^1H and ^{13}C NMR spectroscopy.

The water soluble sodium 2-(1-((pyridin-2-yl)methyl)-1H-1,2,3-triazol-4-yl)ethyl sulfate ligand has been employed as ligand in biphasic water/organic solvent catalysis. A preformed

ruthenium complex and an iridium system containing this water soluble pyridyl-triazolyl ligand were successfully employed in water/toluene biphasic catalytic hydrogenation of C=C and C=O double bonds. The hydrogenation of styrene, 2-cyclohexene-1-one, *m*-diisopropenylbenzene, and cinnamaldehyde has been investigated. The same ligand in combination with [RhCl(COD)]₂ gives a system displaying good activity in olefin hydroformylation.

The above water soluble [RuCl(η⁶-*p*-cymene)(sulphated ligand)] complex has been tested *in vitro* against several human cancer cell lines (A375, A431, BxPC3, A549 and HCT-15.) derived from solid tumors by the MTT test. Preliminary results indicate that the ruthenium complex is less cytotoxic than cisplatin but has a potential as antimetastatic agent.

ABSTRACT

SINTESI E CARATTERIZZAZIONE DI NUOVI LIGANTI E L'APPLICAZIONE DELLA LORO DI TRANSIZIONE COMPLESSI METALLICI COME CATALIZZATORI O AGENTI ANTITUMORALI

MD. MAHBUBUL ALAM

Supervisore: Dr. ssa Valentina Beghetto

Co-supervisore: Professor Alberto Scrivanti

Nel presente lavoro di Tesi si riporta un approccio innovativo per la sintesi dell'acido 2-bromoacrilico e dei suoi derivati esterei, intermedi chiave per la sintesi degli acidi arilossipropionici chirali, un'importante classe di erbicidi. La sintesi di tali substrati acrilici bromurati è stata effettuata mediante una reazione di carbonilazione condotta sul (trimetilsilil)acetilene, utilizzando come sistema catalitico $\text{Pd}(\text{OCOCH}_3)_2$ in combinazione con $\text{CH}_3\text{SO}_3\text{H}$ e 2-(6-metil)(difenilfosfino)piridina. Quando la reazione è condotta in metanolo, 2-(trimetilsilil)acrilato viene ottenuto in buone rese con un rapporto lineare/ramificato pari a 95/5. Mediante le reazioni di idrossicarbonilazione è stato inoltre possibile sintetizzare l'acido 2-(trimetilsilil)acrilico con conversioni e selettività inferiori (circa 53% e 93/7, rispettivamente). Uno studio più approfondito ha esaminato gli effetti dei rapporti fosfina/palladio ed acido/palladio, del tempo di reazione, della temperatura e della pressione di CO sulla conversione del substrato e sulla selettività nei confronti dell'isomero ramificato.

Il metil-2,3-dibromo-2-(trimetilsilil)propanoato è stato preparato con facilità per reazione tra il 2-(trimetilsilil)acrilato ed il bromo, in diclorometano anidro. La successiva reazione di bromodesililazione di metil 2-(trimetilsilil)acrilato, condotta in presenza di un eccesso di base, porta alla formazione di acido 2-bromoacrilico con buone rese (circa 90%).

Una serie di leganti triazolici sono stati sintetizzati mediante la reazione CuAAC. Questi ultimi sono stati impiegati come chelanti per preparare i corrispondenti complessi a base di

Ru(II), Pd(II) e Co(II). I leganti ed i complessi metallici sintetizzati sono stati caratterizzati mediante ESI-MS e spettroscopia ^1H e ^{13}C NMR.

Il 2-(1-((piridin-2-il)metil)-1H-1,2,3-triazolo-4-il)-etilolfato di sodio, specie solubile in acqua, è stato impiegato come legante in catalisi bifasica acqua/solvente organico. Un complesso di rutenio preformato ed un sistema catalitico a base di iridio, entrambi contenenti il legante idrosolubile piridil-triazolico, sono stati impiegati con successo nell'idrogenazione catalitica di doppi legami C=C e C=O in un sistema bifasico acqua/toluene.

Sono state esaminate le reazioni di idrogenazione dello stirene, del 2-cicloesen-1-one, del *m*-diisopropenylbenzene e della cinnamaldeide; il legante descritto, in combinazione con $[\text{RhCl}(\text{COD})]_2$, fornisce un sistema dotato di buona attività nei confronti della idroformilazione delle suddette olefine.

Il $[\text{RuCl}(\eta^6\text{-}p\text{-cimene})(\text{legante solfonato})]$, complesso solubile in acqua, è stato testato in vitro contro diverse linee cellulari tumorali umane (A375, A431, BxPC3, A549 e HCT-15.), derivanti da tumori, sottoposti in precedenza al saggio MTT. I risultati preliminari indicano che il complesso di rutenio è meno citotossico del cisplatino, ma presenta comunque potenzialità come agente antimetastasi.

CURRICULUM VITAE

Education Background

2012-present: Ph.D. in Chemical Sciences, Department of Molecular Sciences and Nanosystems, Ca' Foscari University of Venice, Venice, Italy.

Research Supervisor: Dr. ssa Beghetto Valentina

2008-2010: M.Sc. in Chemistry, Department of chemistry, biology, and marine science, University of the Ruykuys, Nishihara, Okinawa, Japan.

Research Advisor: Prof. Eiji Asato

List of Publications

- (1) S. Paganelli; **Md. M. Alam**; V. Beghetto; A. Scrivanti; E. Amadio; M. Bertoldini; U. Matteoli *A pyridyl-triazole ligand for Ruthenium and Iridium catalyzed C=C and C=O hydrogenations in water/organic solvent biphasic systems*, **Applied Catalysis A: General**, Volume 503, 25 August **2015**, Pages 20–25.
- (2) **Md. M. Alam**; V. Beghetto; A. Scrivanti; M. Bertoldini; U. Matteoli; A. Zancanaro *Stereoselective synthesis of 2-substituted acrylic derivatives via carbonylation reaction*, **XXV Congress of Italian Chemical Society-SCI 2014**, University of Calabria, 7-12 September, 2014, (*Abstract in Atti di convegno*).
- (3) **Md. M. Alam**; S. Paganelli; V. Beghetto; A. Scrivanti; E. Amadio; M. Bertoldini; U. Matteoli, *Synthesis of Water-soluble Triazole Ligands and Application of Their Metal Complexes in Biphasic Hydrogenations of C=C and C=O*, **International Conference on Materials Chemistry, ICMC-2014**, Sylhet, 6-8 December, 2014 (*Abstract in Atti di convegno*).
- (4) Ramkrishna Saha; Faisal Ahmed; **Md. Mahbubul Alam**; and S. M. Saiful Islam, *Synthesis, Characterization and Antibacterial Activity on Dinuclear Schiff-base Macrocyclic Metal Complexes*, **International Conference on Materials Chemistry, ICMC-2014**, Sylhet, 6-8 December, 2014 (*Abstract in Atti di convegno*).
- (5) Emanuele Amadio; Alberto Scrivanti; Valentina Beghetto; Matteo Bertoldini; **Md. Mahbubul Alam**; Ugo Matteoli, *A water-soluble pyridyl-triazole ligand for aqueous phase palladium catalyzed Suzuki–Miyaura coupling*, **RSC ADVANCES**, 2013, 3, 21636-21640.
- (6) **Md. M. Alam**; S. Paganelli; V. Beghetto; A. Scrivanti; U. Matteoli, *Catalytic hydrogenation using a water soluble pyridine-triazole ligand*, **9th International School of Organometallic Chemistry**, 30 August-3 September, 2013 (*Abstract in Atti di convegno*).
- (7) **Md. Mahbubul Alam***, Valentina Beghetto, Alberto Scrivanti, Matteo Bertoldini, Ugo Matteoli, and Lodovico Agostinis, *Stereoselective synthesis of fine chemical intermediates by palladium catalyzed carbonylation of terminal alkynes*, **16th Asian Chemical Congress (16ACC)**, 18-21 November, 2015 Dhaka, Bangladesh.